Mössbauer Hyperfine Interaction Studies of Fe^{2+} Tutton Salts, Alkali Dithioferrates and EFG Tensor Calculations

Thesis submitted to the
University of Roorkee
for the award of the
Degree of Doctor of Philosophy
in
Physics

by

DEO RAJ

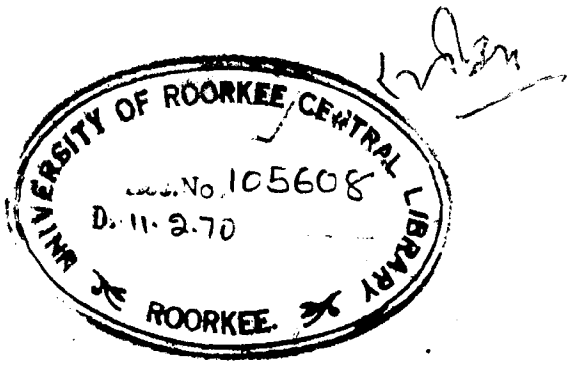

DEPARTMENT OF PHYSICS
UNIVERSITY OF ROORKEE
ROORKEE (INDIA)
1969

Mossbauer Effect

C E R T I F I C A T E

Certified that the thesis entitled " MÖSSBAUER HYPERFINE INTERACTION STUDIES OF Fe^{2+} TUTTON SALTS, ALKALI DITHIOFERRATES (III) AND EFG TENSOR CALCULATIONS " which is being submitted by Shri Dee Raj in fulfilment for the award of the Degree of Doctor of Philosophy in Physics of University of Roorkee, Roorkee is a record of his own work carried-out by him under my supervision and guidance from Jan. 1964 to June 1969.

The matter embodied in this thesis has not been submitted for the award of any other Degree.

S. P. Puri

(S.P. Puri)
Department of Physics
University of Roorkee
ROORKEE (INDIA)

Dated August 20'69

ACKNOWLEDGEMENTS

It is a privilege and a matter of great pleasure to express my deep sense of gratitude to Dr.S.P.Puri, Reader in Physics, University of Roorkee, Roorkee, for the inspiration, encouragement and valuable guidance throughout this work. In fact, it is virtually impossible to thank him suitably for all the help he rendered.

Thanks are due to Dr. K.C.Mittal, my colleague whose active collaboration made the experimentation a success. I am also thankful to all the members of 'Nonlinear Group' for extending me full cooperation and a helping hand throughout this work.

I am also grateful to Prof. S.K.Joshi, Head of the Physics Department, for his interest and encouragement in the progress of this work and providing the laboratory facilities.

I also take this opportunity to express my sincere thanks to all the staff members and research scholars of the Department for cooperation and useful discussions throughout the period of the work, especially to Sarvsri V.K.Garg, V.K. Agarwal, Vishwa Mitra and Nar Singh Dass for the assistance in the final stages of the thesis. The cooperation from the ministerial and laboratory staff is also highly appreciated.

The help from S.R.C., Roorkee and T.I.F.R., Bombay, Computer Centres is deeply acknowledged.

I am also thankful to Sarvsri Ramesh Babu and Raj B.Lal for typing the manuscript.

Last, but not the least, the financial help from Council of Scientific and Industrial Research, New Delhi (India) in the form of J.R.F. and from Department of Atomic Energy (India) as S.R.F.(A) is thankfully acknowledged.

(DEO RAJ)

Dated August 20,1969.

R E S U M E

The recoilless resonant absorption of γ-rays i.e. the Mössbauer effect technique has been applied to study the hyperfine interactions in Fe^{2+} Tutton salts, Chalcopyrite ($CuFeS_2$) and Alkali Dithioferrates(III), using the 14.4 keV γ-rays from Co^{57}. Point charge-point dipole model is discussed and used to compute the electric field gradient tensor (EFG) on the Fe site in the trivalent iron compounds and the value of $Q(Fe^{57m})$ is estimated.

A mechanical velocity drive arrangement employing a constant velocity cam and capable of giving continuously variable speed from 0.0025 cm/sec. to 5.0 cm/sec. has been constructed for use as a Doppler tuning device. 1 mm thick NaI(Tl) crystal in conjuction with a linear amplifier and a single channel analyzer is used and a reproducible resolution of 45-50% for the Mössbauer transition is attained.

The Mössbauer spectra of Fe^{2+} Tutton salts, which form an isomorphous series of hexahydrated double sulphates having the general formula $Fe(MSO_4)_2.6H_2O$, with M = NH_4^+, K^+, Rb^+ and Cs^+ have been studied over a temperature range from 77^0- 300^0K. The data is analysed to assign the characteristic temperatures of the t_{2g} levels and find the splittings. It is concluded that the ground state wave function is singlet, $|xy\rangle$ in all these cases. Furthermore the effect of varying electronegativity has negligible effect on I.S.

Chalcopyrite, $CuFeS_2$, is a well known semiconducting antiferromagnetic copper mineral with Neel temperature 550^0C. All the Mössbauer spectra at three different observation

temperatures 300, 373, 448°K show a six fingered magnetic hyperfine split pattern with small, temperature independent quadrupole splittings. The magnitude and sign of the magnetic field at these temperatures is estimated and is accounted to originate primarily through the Fermi contact interaction, H_c; both the H_{dip} and H_{orb} contributions being zero. These features are explained by assuming that Fe atom is in a spin free trivalent state in a weak crystal field configuration. The existing literature on Mössbauer studies of this compound is discussed with a special reference to the investigations of Aramu et al.[30]

The alkali dithioferrates(III) studied include a series of tetrahedrally coordinated (sp^3) compounds with general formula $AFeS_2$ where A = Na, K, Rb and Cs. The Mössbauer spectra and molar susceptibilities were taken over a temperature range of 77-300°K. The values of the quadrupole splitting, ΔE_Q in all these compounds are temperature independent and imply that the levels are far apart to permit any change in Boltzmann distribution over this range of temperature.

Total s-electron density and 4s-character have been evaluated using the observed I.S. values. In view of the I.S. values and the total s-electron densities the pairing of d-electrons is speculated and the μ_{eff} values computed from molar susceptibilities provide the number of unpaired d-electrons. In these compounds the effect of electronegativity on I.S. is explained qualitatively and is opposite to the mechanism put forward in the case of octahedrally bonded (d^2sp^3) compounds. It is remarked that the WMJ plot can be used in the case of (sp^3) tetrahedrally bonded compounds in contrast to the

octahedral case (d^2sp^3) where d-electrons take part in bonding.

The five independent components of the symmetric, traceless tensor of EFG, have been computed on a point charge-point dipole model for three trivalent compounds, $CuFeO_2$, $ZnFe_2O_4$ and α-Fe_2O_3. A brief review of the existing literature on the value of $Q(Fe^{57m})$ is made and its value is re-evaluated using the computed values of EFG tensor and the experimentally determined values of $\triangle E_Q$. The values so obtained are quite divergent and so inconclusive for a definite assignment. In view of the lack of precision X-ray data, dipolar and quadrupolar polarizabilities, exact assignment of effective charges and covalency factors, we conjecture that the point charge-point dipole model is inadequate for such an assignment.

LIST OF PUBLICATIONS *

1. Mössbauer Studies of Ferro - and Ferricyanide super-complexes with 3d Transition Elements.
   K.Chandra, Deo Raj and S.P.Puri
   J.Chem. Phys. 46 (1967)1466

2. Crystal Field Splitting in Fe^{2+} Tutton salts from Mössbauer studies.
   Deo Raj, K.Chandra and S.P.Puri
   J.Phys. Soc.Japan 24, 35 (1968)38

3. Mössbauer Studies of Chalcopyrite
   Deo Raj, K.Chandra and S.P.Puri
   J.Phys. Soc. Japan, 24 (1968) 39

4. Nuclear Quadrupole Moment of 14.4 KeV State of Fe^{57m} from Mössbauer data in trivalent iron salts
   Deo Raj andS.P.Puri
   Proc. Nucl. Phys. and Solid State Phys.Symposium Madras (1968)Pob. p 218

5. Mössbauer Spectra of Tetrahedral Alkali dithioforrate (III)
   Deo Raj and S.P.Puri
   J.Chem.Phys. 50 (1969) 3184

6. On the Mössbauer Effect of Chalcopyrite (Critique)
   Deo Raj and S.P.Puri
   Nuovo Cimento 60 B (1969) 201

7. Recoilless Fraction and Thermal shift for 29.4 KeV transition in Reaction produced K^{40}.
   Deo Raj and S.P.Puri
   Phys.Status Solidi 34 (1969) 1st. July

8. Recoilless Fraction/Factor and Thermal shift of W^{182} and W^{183}
   Deo Raj and S.P.Puri
   Phys. Letters Vol.30A(1969) July 5th

9. Mössbauer Fraction and Thermal shift for 67.4 KeV gamma-rays in Ni^{61}
   Deo Raj and S.P.Puri
   J.Phys. Soc.Japan Vol.27(1969)

10. Evidence of Force Constant Changes of Sn^{119} in Vanadium
    Deo Raj and S.P.Puri
    Phys. Letters (Communicated)

* Appended in the end.

TABLE OF CONTENTS

-000-

CHAPTER I

PRELIMINARIES AND STATEMENT OF THE PROBLEM

1.1(A) INTRODUCTION

'You mean that, despite thermal vibrations of approximately 10^5 cm/sec., you expect me to believe γ-ray absorption can be changed by applying 10^{-2} cm/sec to the source??!!'

Circa Fall(1959)

In fact, the Mössbauer Effect[1] has a very dramatic and historical entry in the realm of physics. Not only its appearance perturbed the discoverer himself but it was also first recognised with a bet of 'is' and 'is not' when after an unnoticed period of one year, two research teams of Argonne National and Los Alamos Labs. of United States established its existence. Scientists soon realised that they had at hand a new and beautiful tool-simple in its basic ideas, requiring only a minimum equipment, and allowing ingenious applications not only in Nuclear Physics, Relativity and Solid State Physics, but also in Chemistry, Biophysics, Metallurgy, Mineralogy and Technology. In certain cases it has come out as a unique tool, e.g., in the interpretation of Twin Paradox, a test of the equivalence principle for rotating systems, in determination of gravitational red shift, in study of the motion of the fluid of the inner ear, and in determination of the electric and magnetic moments of the excited states of nuclei and electron density at the nucleus in a direct and simple manner. The impact of this

realisation has yielded several hundred papers[2,3] (both experimental and theoretical), review articles[4-18]° (ranging from an introductory to a sophisticated level), international conferences[19-22], and books[23-31] dealing its principles and applications. It is gratifying that the importance of Mössbauer's work was recognised by the award of the 1961 Nobel Prize in Physics. The Mössbauer Effect is a hot field of research activities and its scope is encompassing several other disciplines of natural sciences and engineering, making feasible a host of hitherto unknown new applications. In a period of one decade, the Mössbauer experiments are being carried out routinely in many student laboratories.

(B) NUCLEAR RESONANCE FLUORESCENCE BEFORE MÖSSBAUER'S DISCOVERY

When a nucleus of a free atom de-excites by emitting a γ-ray of energy E_γ it recoils with an energy $R(= \frac{E_\gamma^2}{2Mc^2})$ in conformity with the principle of conservation of linear momentum. Here M is the mass of the nucleus and c, the velocity of light. The conservation of energy, then reduces the gamma-ray energy from E_0 to $E_\gamma - R$ where E_0 is the transition energy between the two levels. If we neglect the thermal motion of the nucleus, the gamma radiation emission spectrum $V(E)$ will be a Lorentz distribution with width $\Gamma = \hbar/\tau$, and centred about $E = E_0 - R$

$$V(E) = \frac{(\Gamma/2)^2}{(E-E_0+R)^2 + (\Gamma/2)^2}$$

° These are only few typical examples, in fact many more can be included in the list.

where τ is the life time of the excited state. Similarly, the absorption spectrum will be of the same form but centred about the energy, $E_0 + R$; since the gamma ray must have surplus energy to excite the absorbing nucleus and also supply it with the recoil energy R. Now for resonance absorption to take place, the two spectra should overlap and this leads to a condition $\Gamma \geq 2R$, which is usually not satisfied in nuclear Physics, since the life times τ correspond to $\Gamma \ll R$ in most cases.

Fortunately the nuclei are always in some kind of thermal motion which leads to Doppler broadening of the gamma radiation. In case of gas for instance, one can use the Maxwell distribution and this leads to a Doppler width, $\Delta = 2\sqrt{RkT}$, to the radiation spectrum. Here k is the Boltzmann constant and T is the absolute temperature. The energy distribution remains centred about the energy, $E = E_0 \pm R$, but becomes Gaussian, Fig.1(a). This treatment is strictly valid for a gas, and in addition holds only when the natural line-width is much smaller than the Doppler width, $\Gamma \ll \Delta$. The condition for resonance therefore becomes: $\Delta \gg 2R$. This requirement is always satisfied in atomic cases, where one usually finds $R \leq \Gamma < \Delta$. On the other hand, in nuclear processes, we have $R \geq \Delta \gg \Gamma$. Thus, while Doppler broadening insures atomic resonance fluorescence, it renders it feasible only in limited number of nuclear cases. This is the reason why the phenomenon of resonance fluorescence in atomic systems[32] has been known for many years and in the nuclear system, Moon[33] could observe it in 1961, when its possible existence had been predicted by Kuhn[34], a couple of decades earlier. He used the ultracentrifuge device to compensate the

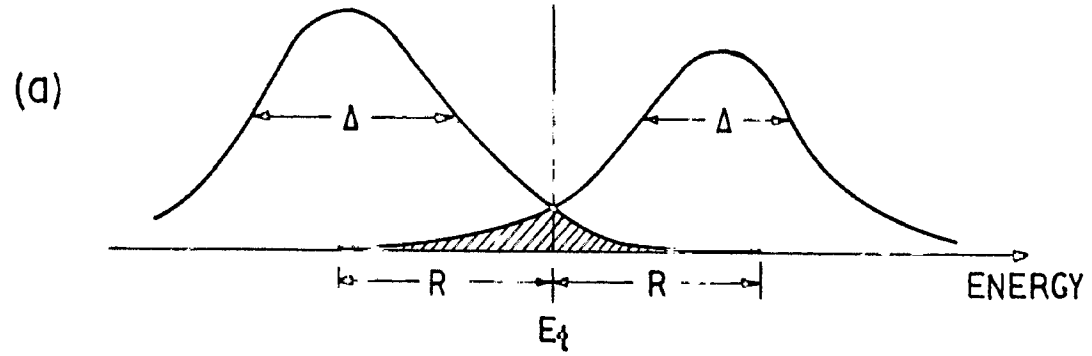

FIG. 1·1(a) EMISSION AND ABSORPTION SPECTRA IN A GAS OF FREE ATOMS. E_e, E_g, E_t AND R ARE THE EXCITED STATE, GROUND STATE, TRANSITION AND RECOIL ENERGIES RESPECTIVELY. Δ IS THE THERMAL DOPPLER SHIFT.

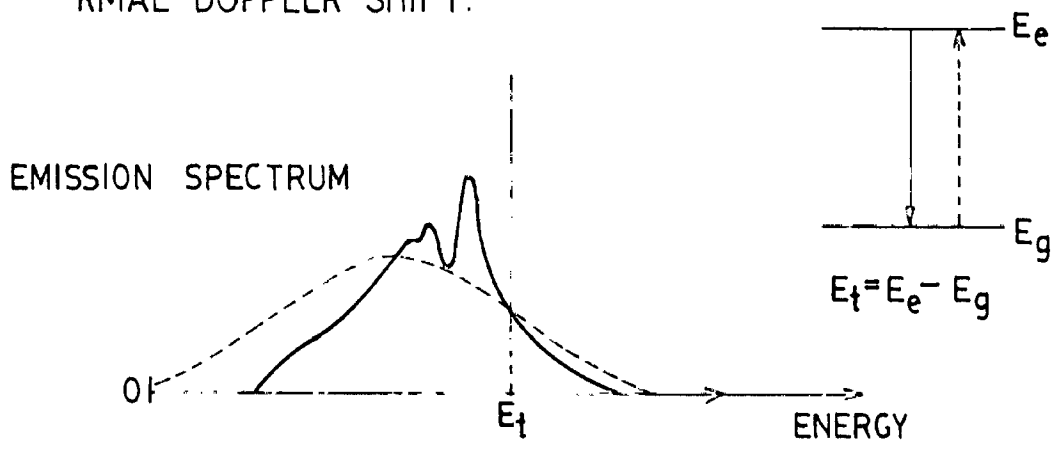

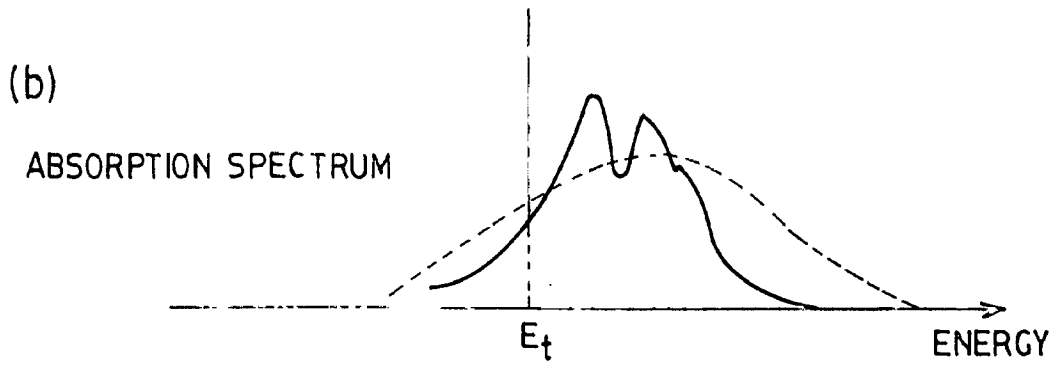

FIG. 1·1(b) STRUCTURE OF GAMMA EMISSION AND ABSORPTION LINES OF NUCLEI BOUND IN SOLIDS (AFTER MÖSSBAUER REF. 28)

(i) THE CASE OF VERY HIGH RECOIL ENERGY WHERE MULTIPHONON PROCESSES DOMINATE (DASHED LINE)

(ii) THE CASE OF VERY LOW RECOIL ENERGY WHERE FEW PHONONS PARTICIPATE (SOLID LINE) AND

(iii) THE VERTICAL LINE IS THE ZERO PHONON LINE & HAS THE NATURAL LINE WIDTH DETERMINED BY THE NUCLEAR LIFE TIME.

recoil energy by imparting the source a Doppler velocity of 10^3 cm/sec. Others were successful, by increasing the width by employing thermal excitation method[35] and by previous recoil in the proper direction[30]. For detailed discussion of resonant scattering experiments prior to Mössbauer's discovery, one can refer to the articles of Metzger[37] and Malmfors[38]. The common drawback of these techniques is their inability to restore the natural width of the lines from their recoil broadened state. This limits their use to measuring short mean life times only, as small changes in the energy levels cannot be detected.

(C) MÖSSBAUER'S DISCOVERY

While studying the scattering of 129-keV gamma rays of Ir^{191} by Ir and Pt, R.L. Mössbauer found an unexpected increase in scattering in Ir at low temperatures. The startling result was that inspite of the fact that the calculated line width of the 129-keV gamma ray, $\Gamma \sim 8 \times 10^{-3}$ eV, was much less than the recoil energy of the Ir^{191} nucleus, $R \sim 0.05$eV, Mössbauer obtained a significant amount of resonance absorption without cooling the source[33] or employing any of the other methods[35,36] to compensate the missing energy due to recoil. In fact, cooling and not the heating[35] increased the effect. Furthermore by imparting modest velocities of the order of few cm/sec, he obtained an absorption line of width (H.W.H.M.) nearly 2Γcm/sec which is double of the natural line-width. This is in agreement with the picture of recoilless emission and absorption. The factor of 2 arises because the observed absorption is the result

of folding an emission spectrum together with an absorption spectrum, each with a width Γ [8].

The essential mechanism underlying Mössbauer discovery and explanation of recoilless emission and absorption of γ-rays was well known in the theories of X-ray crystallography[39] and neutron scattering[40]. A somewhat similar mechanism was studied by Dicke[41] in connection with the problem of collision narrowing of emission lines in a dense gas. It was in fact Lamb's paper[40] on 'Capture of Neutrons by Atoms in a Crystal' which led Mössbauer to the interpretation of his unexpected and remarkable results. The detailed theoretical papers giving classical and or quantum mechanical description of mechanism have been put forward by the discoverer[1,9,14] and others[4,23,25,42-46]. Our aim is not to reproduce the whole theory here, but simply to mention the salient features of the phenomenon of recoilless emission and absorption of γ-rays.

When an atom is bound in a solid the situation is quite different than that of a free atom as the atom is not free to recoil. In fact the recoil momentum is taken up by the crystal as a whole. The expression for recoil energy R has now a mass M of the whole crystal as denominator and thus reduces to a negligible value. Further in the lattice, the atoms are vibrating with energy quantization, i.e., an atom is free to emit zero, one, or many phonons, but is unable to recoil with an arbitrary energy. Because of this quantization of allowed energy shifts upon recoil, there will be a certain probability that no phonon will be emitted (and hence no energy shift due to recoil, Fig.1b). Further discussion on this topic will be done in the next section

which deals with Mössbauer fraction. It may be remarked that the term 'recoilless' refers to the transfer of recoil energy only and is not connected with the transfer of recoil momentum whatsoever. A momentum transfer without simultaneous energy transfer does not at all constitute a new phenomenon. This process was in fact well known for decades to other domains of physics such as the coherent scattering of X-rays (Rayleigh scattering and Bragg Scattering) and the coherent scattering of slow neutrons from crystals. Lipkin[4] gives two illuminating discussions of energy and momentum conservation in the Mössbauer Effect. Feinberg[6] has also discussed energy, momentum and time conservation.

1.2 GENERAL PARAMETERS OF A MÖSSBAUER SPECTRUM

A Mössbauer spectrum consists of a plot of transmission (or scattered) gamma-beam intensity versus the Doppler velocity (Chapter II). To study the electrostatic and magnetic interactions, relaxation effects, lattice dynamical aspects, effect of temperature and pressure variation, and other nuclear and atomic properties, a well planned Mössbauer experiment must seek the numerical estimates of one or more of the following observables[17,10]

(i) line positions (or shifts)

(ii) line width

(iii) line intensity, and

(iv) line shape

Mössbauer[20] in his article has further divided the line intensity into (a) line depth and (b) the line area.

Goldanskii and Makarov[31], on the other hand, have classified these into three classes: Dynamical parameters; Electromagnetic and the combined parameters. This classification is by no way a rigid one and has been done only to facilitate the task of general enumeration of the Mössbauer parameters.

We will enumerate some important Mössbauer parameters which can be had from these observables and will discuss in some details the hyperfine interaction studies which is the main topic pertinent to our proposed research work. In principle there are about thirteen[19] Mössbauer parameters which can be derived from a well planned experiment and one must seek chemical and physical factors which influence their numerical magnitudes.

(1) LINE POSITION

It is the most concerned observable to the experimentor and corresponds to energy difference between the levels of source and absorber. A Mössbauer spectrum may be a singlelined, doublet, a six-fingered or a complex one according to the shifting and or splitting of the nuclear levels in the source/absorber excited and ground states due to electric monopole, quadrupole and magnetic interactions. The presence of different lines may also be because of more than one valence state or inequivalent sites. The line position obtained will give the well known Mössbauer parameters: Isomeric shift, quadrupole splitting, Zeeman splitting, temperature shift, pressure shift and or gravitational red shift. The definition, origin and information which one can have from their (of the first three only) numerical estimates will be given in detail when we will discuss the

hyperfine interactions.

(ii) LINE WIDTH

The overwhelming beauty of the Mössbauer Effect is that it makes available an electromagnetic radiation with an extremely well defined energy. A fractional line width of 1 part in 10^{18} may be ultimately available. In fact it is this excellent tuning which permits the measurements of small changes in the position of the resonance caused by the hyperfine interactions and gravitation effects. The latter, the famous red shift of photons, was determined in a terrestrial laboratory, an expt. hitherto considered impossible.

In an ideal case the Mössbauer line should display a natural line width given by uncertainty principle, but it happens very rarely as there may be many sources of broadening and narrowing. We will just casually mention those effects and suggest to see the actual references for complete information. The possible sources of line broadening can be one of the following two types:

(a) of experimental origin

(b) of fundamental character (e.g. solid state effects)

The experimental effects include the extraneous(mechanical) vibrations, finite solid angle, velocity resolution and finite absorber thickness. These are of little significance in the sense that in a carefully designed experiment either their effect may be avoided or can be corrected. The broadening of the absorption line due to finite absorber thickness was first treated by Visscher[23] who assuming the line shapes of emission

and absorption spectra as Lorentzian with width Γ, deduced the following relations for the apparent width Γ_{app} and effective absorber thickness T:

$$\begin{aligned} \Gamma_{app}/\Gamma &= 2.00 + 0.27T && 0 \leq T \leq 0 \\ \Gamma_{app}/\Gamma &= 2.02 + 0.29T - 0.008T^2 && 0 \leq T \leq 10 \end{aligned} \qquad (1.1)$$

The effective absorber thickness T is given by

$$T = f' n a_0 t \qquad (1.2)$$

where f' is the fraction of gamma rays absorbed without energy loss (section 1.3); n, the number of atoms per cubic centimeter; a_0 the fractional abundance of the resonantly absorbing atoms; t, the absorber thickness, and σ_0 the maximum absorption cross section at resonance, given by

$$\sigma_0 = \frac{1}{2\pi} \frac{2I_0 + 1}{2I_g + 1} \lambda^2 \frac{1}{1+\alpha} \qquad (1.3)$$

I_0 and I_g are the spin of the excited and ground state respectively; λ the wave length of the gamma ray, and α is the internal conversion coefficient of the gamma transition. Margulies and Ehrmann[37], extended the work of Visscher who calculated the relative line broadening Γ_{app}/Γ for different absorber thicknesses and line shapes. Roberts[43] has also recently calculated the line widths for various absorber thicknesses. A line broadening due to solid angle effects has been estimated by Northrop[40] and is given as proportional to $\frac{vD^2}{10d^2}$, where v is the velocity of the source, D is the diameter of the detector and d is the distance between source and detector. Hence if the outer lines of an Fe^{57} metal spectrum

are to be broadened by no more than 0.1 of the natural width the source-detector distance must be atleast four time the detector diameter.

The solid state effects are of extreme importance and give microscopic information about the solid. The possible mechanism which lead to line broadening are (a) partially relaxed hyperfine structure (spin flip processes, super-paramagnetism, fluctuation near critical temperature and paramagnetic relaxation phenomena) (b) anharmonic lattice behaviour (c) atomic motion due to diffusion[48] and Brownian motion of atoms or molecules and (d) association of Mössbauer source and or absorber atom with various kind of defects, e.g. the Mössbauer atom may not be uniformly incorporated in the crystal lattice leading to a blurring of δ and ε (e) very low lattice vibrations may cause a change in the field gradient, which are not averaged as they are of higher frequencies (f) the presence of local modes and (g) the inhomogeneous hyperfine interaction e.g., the broadened line of Fe^{57} in stainless steel may be attributed to the wide range of nearest neighbour environment in these alloys which can produce inhomogeneous isomeric shift broadening. Vignali[50] has discussed some of these effects in detail and has also given a good bibliography. Wickman and Wertheim[51] and Blume[52] and his coworkers while discussing the relaxation mechanisms, have also given due consideration to the line broadening and line shape. The line broadening in the Zeeman pattern is closely connected to the motional narrowing[53] in the NMR. The study of line width

thus given information about the life-time of the excited states, relaxation times (spin-lattice and spin-spin), diffusion coefficient and lattice defects etc.

In special cases, the line can be even narrower than the natural line width, for instance, by increasing the effective half-life with a selective delay coincidence technique[83] or as a result of a thermal spike by the foregoing decay[84]. In the latter case the recoil-free fraction becomes an increasing function of the time, the excited state has existed and therefore the nuclei which contributed to the Mössbauer Effect line have an apparent larger mean life time. Recently Harris[88] has given a quantum mechanical model for the Mössbauer line narrowing. This model includes both radiation and relaxation processes in the lowest order to have a quantum mechanical solution and describes an initially excited nucleus in an excited lattice. It is found that under certain conditions, Mössbauer lines result which are narrower than the natural line width, although line broadening is the more usual effect of lattice relaxation. The maximum narrowing in this approximation never exceeds 36% of the natural width. Anomalous narrowing of Mössbauer lines of some paramagnetic Fe^{3+} compounds has been observed[86] when transverse or longitudinal magnetic fields are applied. A longitudinal field has a stronger effect than the transverse field. Pluck[12] has given some typical values of line width for different charge states of iron as 0.31, 0.24, 0.23 and 0.22 cm/sec for Fe^{3+}, Fe^{2+} states, Fe complexes and for metallic iron respectively.

(iii) LINE INTENSITY

Different absorption lines will have different depths and areas. It is the area which one should consider when comparing the intensities of the lines and not merely the depths as there may be line shape distortion and line broadening which may lead to wrong interpretations if only depths were considered. Of course, in a well defined unbroadened lines of Lorentzian shape, only the line depth consideration can give acceptable accuracy. There are many factors which contribute to the line intensity difference in Mössbauer Effect. We will just mention the much obvious reasons.

One of the most trivial reasons is the relative transition probabilities (Clebsch-Gordan coefficients) which are different for various hyperfine components. Another reason is the angular dependence of radiation intensity which is different for different hyperfine components. These have been exemplified in the case of hyperfine interaction of Fe^{57} in the section 1.5. The consequence of this angular dependence is evident when one uses a single crystal absorber where the intensities of the spectrum peaks will depend on the angle between the emitted quantum and the crystal axes in the source, the angle between the emitted quantum and the crystal axes in the absorber, etc. In a polycrystalline sample these angular dependent intensities get averaged and this will be discussed in detail. The intensities may also be affected by the inequivalent sites of Mössbauer source or absorber leading to different absorption spectrum which when superimposed give different line intensities and shapes. The Mössbauer fraction

(discussed in the next section) which is responsible for the area and the depth of the absorption line in general, will not add to the intensity difference in the lines if it is isotropic. In case of anisotropic f-factors, the line intensities may be different even for a polycrystalline sample[87]. This is called the Goldanskii-Karyagin effect and was first observed in a quadrupole split spectra and has its origin in the anisotropy of the binding of the Mössbauer atom to the neighbours. Another possible reason for the difference in line intensity is the relaxation effects[82]. Recently the Goldanskii-Karyagin effect has been studied in detail in the case of Sn compounds by Stöcklor et al.[88]

(iv) LINE SHAPE

The Mössbauer absorption experiment makes it possible to measure not only the line width but also the line shape of the gamma ray, i.e., its spectral energy distribution or frequency spectrum, $I(\omega)$. A Mössbauer γ-ray emitting nucleus may be considered a damped oscillator[28] and its equation of motion is

$$\ddot{x} = -\omega_0^2 x - \gamma \dot{x} \qquad (1.4)$$

ω_0 is in fact the frequency of the undamped oscillator and γ represents the damping constant (radiation reaction). The solution of Eq.(1.4) when $\gamma \ll \omega_0$, is

$$\begin{aligned} x(t) &= x_0\, e^{-\gamma t/2}\, e^{i\omega_0 t} && \text{for } t > 0 \\ &= 0 && \text{for } t < 0 \end{aligned} \qquad (1.5)$$

γ is the reciprocal of the mean life of the excited state. From its Fourier transform we get the frequency spectrum of this damped oscillator as

$$I(\omega) = \frac{\gamma}{2\pi} \frac{\hbar\omega}{(\omega-\omega_0)^2 + 1/4\gamma^2} \qquad (1.6)$$

For $\omega \approx \omega_0$, the frequency dependence is well approximated by

$$\frac{1}{(\omega-\omega_0)^2 + \frac{1}{4}\gamma^2} \sim \frac{1}{(E-E_0)^2 + \frac{1}{4}\Gamma^2}$$

where $\hbar\omega = E$ and $\hbar\gamma = \Gamma$. This is called a Lorentzian (or Breit-Wigner) line shape. The energy dependence of the resonance absorption cross section is

$$\sigma(E) = \sigma_0 \frac{(\Gamma_a/2)^2}{(E-E_0)^2 + (\Gamma_a/2)^2} \quad f'a \qquad (1.7)$$

where Γ_a is the full width at half maximum of the absorption line, σ_0 is given by Eqn.(1.8), f' is the fraction of the gamma rays absorbed without recoil and a is the natural abundance of the absorbing nuclei. The experimentally observed line shape is the superposition of the emission and absorption lines according to the Eq.

$$\sigma_{expt.}(E) = \int_{-\infty}^{\infty} \omega(o)\sigma(E-o)do \qquad (1.8)$$

where $\omega(o)$ is the spectral line shape of the emitted gamma ray:

$$\omega(o) = \frac{(\Gamma_s/2)^2}{(o-E_0)^2 + (\Gamma_s/2)^2} \quad fa$$

This reduces to

$$\sigma_{expt.}(E) = \sigma_0 \frac{(\Gamma_s+\Gamma_a)^2/4}{(E-E_0)^2 + (\Gamma_s+\Gamma_a)^2/4} ff'a^2 \quad (1.0)$$

This shows that the resonance line is also Lorentzian with width given by $(\Gamma_s+\Gamma_a)$, and indicates that the line widths of source and absorber are additive. If natural line width is realised both in emission and absorption, the observed experimental line width will be just twice the natural line width. This situation is rarely attained in practice and the experimental lines have a shape intermediate between Lorentzian and Gaussian. Determination of exact line shape is a complicated but important subject and has been treated extensively in literature[59]. The study of the line shape can give the lattice properties of source and absorber. The background of non-resonant gamma rays, noise, hyperfine interactions, lack of complete homogeneity in the sample, self absorption, finite thickness of the source and absorber and instrumental limitations are some of the causes which distort the resultant line shape. The effect of radiofrequency resonance on natural line shape has been studied independently by Hack and Hamermesh as well as Ruby and Bolef[60].

1.8 MÖSSBAUER FRACTION

When an emitting atom is embedded in a solid, there is a definite probability that the gamma-ray emitted has the full transition energy E_0 and the lattice remains in its initial state. That is there is no excitation of lattice vibrations (phonons) and thus the process is called a zero phonon process.

This probability is called the Mössbauer fraction f. Its value is obviously zero for a free atom and increases with the increase of lattice rigidity, becoming unity for a completely rigid lattice. Lipkin's[4] two sum rules to explain the existence and magnitude of Mössbauer fraction, have been explained very clearly by Lustig[5]. On the average, the energy transferred to the lattice is just R(the energy which the individual nucleus could have if it recoiled freely). The first sum rule[4] allows an appreciable probability for no energy transfer to the lattice (zero phonon process), provided there is an appreciable probability for an energy transfer greater than R. Under harmonic potential approximation, both classically as well as quantum mechanically,[4] the following expression for f can be derived

$$f = \exp\left(-K^2 \langle x^2 \rangle\right) \qquad (1.10)$$

where $K = 2\pi/\lambda$ denotes the wave vector of the photon (λ = wavelength), $\langle x^2 \rangle$ is the mean square displacement of the emitting nucleus (measured along the direction of propagation of the γ-ray) at temperature T. It is ordinarily expressed as $f = e^{-2W}$, where 2W is the Debye-Waller factor. To estimate the value of f one must know precisely the value of $\langle x^2 \rangle$ which accounts for the dynamical aspect of the lattice. In fact it is not very simple to calculate this value for all type of structures and has been calculated only in a few simple cases, with simplifying assumptions. In an harmonic approximation for a cubic monatomic crystal matrix the expression for $\langle x^2 \rangle$ can be written as[26]

$$\langle n^2 \rangle = \frac{\hbar}{3Nm} \int_0^{\omega_{max.}} \left\{ \frac{1}{2} + \frac{1}{\exp(\hbar\omega/kT) - 1} \right\} \frac{g(\omega)}{\omega} \, d\omega \qquad (1.11)$$

or alternatively

$$\langle n^2 \rangle = \frac{\hbar}{3Nm} \int_0^{\omega_{max.}} \coth\left(\frac{\hbar\omega}{2kT}\right) \frac{g(\omega)}{\omega} \, d\omega \qquad (1.11a)$$

where $3N$ is the normalising constant and $g(\omega)$ is the density of vibrational states, k the Boltzmann constant and T the absolute temperature. The expression for 'f' becomes therefore

$$f = \exp - \left[\frac{2E_\gamma^2}{2mc^2 \hbar 3N} \int_0^{\omega_{max.}} \left\{ \frac{1}{2} + \frac{1}{\exp(\hbar\omega/kT) - 1} \right\} \frac{g(\omega)}{\omega} \, d\omega \right]$$

or (1.12)

$$f = \exp - \left[\frac{2R}{3Nh} \int_0^{\omega_{max.}} \left\{ \frac{1}{2} + \frac{1}{\exp(\hbar\omega/kT) - 1} \right\} \frac{g(\omega)}{\omega} \, d\omega \right]$$

In absence of $g(\omega)$ for a real crystals or in a first approximation, a Debye model is used for the lattice which leads to an expression of f as

$$f = \exp - \left[\frac{9}{8} \frac{6R}{k\theta_D} \left\{ \frac{1}{4} + \frac{T}{\theta_D} \int_0^{\theta_D/T} \frac{x\,dx}{e^x - 1} \right\} \right] \qquad (1.13)$$

where θ_D is the Debye temperature of the solid.

For optical modes contribution to 'f', the Einstein model may be used for which

$$g(\omega) = 3N\delta \, (\omega - \omega_E) \qquad (1.14)$$

and yields

$$f = \exp - \left[\# \frac{R}{\hbar\omega_E} \coth \left(\frac{\hbar\omega_E}{2kT} \right) \right] \qquad (1.15)$$

We will use the expressions for f while laying down the requirement of a good Mössbauer isotope.

1.4 CHOICE OF A MÖSSBAUER ISOTOPE

We are working with Co^{57} isotope which has several of the properties of a good Mössbauer isotope e.g. low lying gamma ray level, convenient line width, long lived parent nuclei (Co^{57}), large Mössbauer fraction f even at higher temperatures, low internal conversion coefficient, high resonant absorption cross section etc. In addition, iron is one of the transition metals (with partially filled 3d shell) which plays the principal role in a number of incompletely understood phenomena concerned with magnetic ordering in solids. Moreover, the excited state has a spin 3/2 and ground state spin is 1/2, thus there is no quadrupole moment associated with the ground state and the quadrupole and Zeeman split spectra are not unduly complicated. The important physical parameters of interest[3] are tabulated in Table 1.1 and the decay scheme of the isotope providing 14.4 keV Mössbauer gamma ray is given in Fig.1.2

1.5 HYPERFINE INTERACTIONS

By far the largest applications[3,12,16,18-31] of the Mössbauer Effect have been to the study of interactions between electrons and the nucleus, called hyperfine interaction. This is the narrowness of the line width, made available due to recoilless resonance absorption, which renders

TABLE 1.1: IMPORTANT PHYSICAL PARAMETERS OF 14.4 keV GAMMA-RAY MOSSBAUER TRANSITION [5]

(i) Measured Properties

Half life of the excited state, $T_{1/2}$	0.97×10^{-8} sec.
Total internal conversion coefficient, α_T	9.00
Natural isotope abundance, IA	2.19%
Spin and parity of ground state, I_G	$1/2^-$
Spin and parity of excited state, I_e	$3/2^-$
Magnetic moment of the ground state, μ_g	+ 0.09024 nm
Magnetic moment of the excited state, μ_e	- 0.1547 nm
Quadrupole moment of the ground state, Q_G	0.0
Quadrupole moment of the excited state, Q	0.20b (See Reference in Chapter VI)
Maximum Resonance cross section, σ_0	2.56×10^{-18} cm^2
Atomic scattering cross section, σ_{at}	3.8×10^{-21} cm^2

(ii) Derived Parameters

Natural line width, Γ	4.6697×10^{-12} keV (0.090 mm/sec.)
Observable width, v_0	0.10427 mm/sec.
Recoil energy, R	1.9567×10^{-3} eV
Resonance cross section, σ_0	2.3554×10^{-18} cm^2
Debye temperature, θ_D	420°K
Recoilless fraction, f with θ_D= 420°K	f(90°K) = 0.02 f(300°K) = 0.79

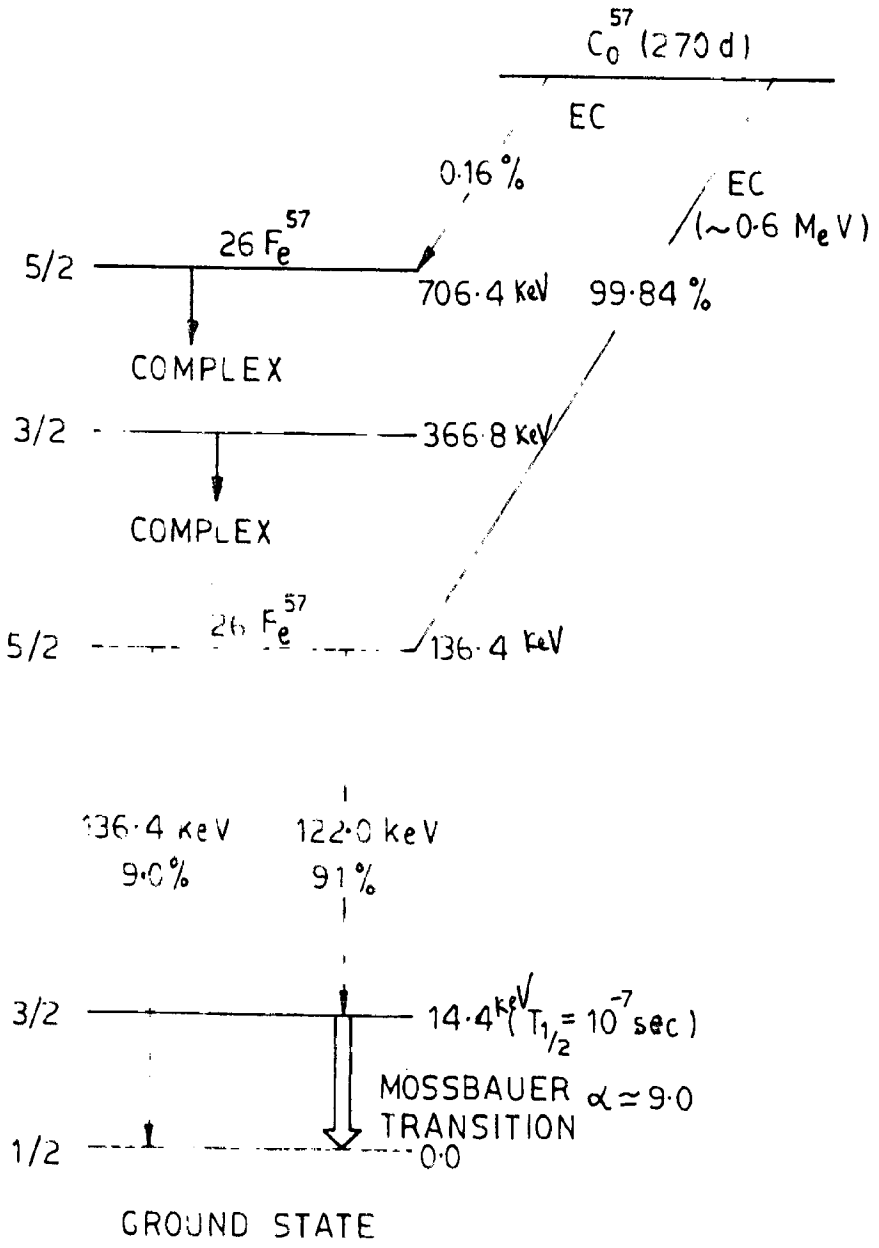

FIG. 1·2 DECAY SCHEME OF C_0^{57} SHOWING THE 14 4 k_eV MOSSBAUER TRANSITION

feasible the study of such small interactions. The nature of the interaction involves both the atomic and nuclear parameters and thus form a bridge between the two otherwise separated disciplines called solid state physics and nuclear physics. Such measurements provide the basis[91] for the determination of the electronic charge and spin distribution, magnetisation and nuclear electric and magnetic moments, ionicities (or valences), electron configuration in metals and alloys, crystal field parameters and splitting of crystal field states, ordering mechanism in alloys, magnetic (and crystallographic) transitions and magnetic ordering processes, magnetic impurities, and spin structure etc. The exploration of these atomic and nuclear properties in turn helps one to investigate and understand the basic microscopic picture of matter.

Although the theory of hyperfine interactions as manifested in Mössbauer spectroscopy has been treated by a number of authors[18-31,91], its relevance to the problem of this work justifies a brief discussion here.

The hyperfine interactions comprise of two types of interactions having origin from the static and dynamic (current) charge distribution of the nuclear and atomic electrons. These are the electrostatic and magnetic interactions. In any typical case one or both may be present and we will discuss these cases separately.

(A) <u>ELECTROSTATIC INTERACTION</u>

The electrostatic interaction[92] H_0, can be expressed

as an integral over the nuclear volume given by

$$H_0 = \int d^3x\, \rho(x)\, V(\bar{x}) \qquad (1.16)$$

where $\rho(\bar{x})$ is the nuclear charge density and $V(\bar{x})$ is the electrostatic potential arising from all extra nuclear charges. The $\bar{x}$ dependence of the potential can be treated by expanding $V(\bar{x})$ in a Taylor series about the nuclear centre of mass. This leads to

$$H_0 = \int d^3x\, \rho(x)\left\{V_0 + \sum_j \left(\frac{\partial V}{\partial x_j}\right)_0 x_j + \frac{1}{2}\sum_{j,k}\left(\frac{\partial^2 V}{\partial x_j \partial x_k}\right)_0 x_j x_k + \cdots\right\} \qquad (1.17)$$

The first term in the sum represents the electrostatic energy for a point nucleus. The dipole and octupole terms vanish because the integrand is an odd function. The magnitude of the hexadecapole term is of the order of 10^{-6} that of the quadrupole term and is observable very rarely and thus we will only consider the first and the 3rd terms.

MONOPOLE INTERACTION (Isomeric Shift)

The first term in the Eq.(1.17) which gives the electrostatic energy of a point nucleus is an over simplification of the real picture of a finite nucleus and requires a correction term which will account for the nuclear size. To simplify the calculations the nucleus is assumed to be a uniformly charged sphere with radius R. The electrostatic potential for the point nucleus and for one having a radius R are given by

$$V_{pt} = \frac{Z_0}{r} \tag{1.18}$$

$$V_{lin} = \frac{Z_0}{R}\left[\frac{3}{2} - \frac{r^2}{2R^2}\right] \qquad \text{for } r \leq R \tag{1.19a}$$

$$\text{and} \quad = \frac{Z_0}{r} \qquad \text{for } r \geq R \tag{1.19b}$$

Thus the correction term δE, the difference of E_{lin} and E_{pt}, is given by

$$\delta E = \int_0^\infty (-e|\psi(r)|^2)(V_{lin} - V_{pt})\, 4\pi r^2\, dr \tag{1.20}$$

where $-e|\psi(r)|^2$ is the electronic charge density and in the vicinity of the nucleus is given by[33].

$$-e|\psi(r)|^2 = -e\, C\, r^{2\ell-2} \tag{1.21}$$

$$\text{with} \quad C = \frac{\Gamma(\ell+1)}{\left(\Gamma(2\ell+1)\right)^2}(2Z)^{2\ell-2}\,|\phi(0)|^2 \tag{1.22}$$

where $\ell = \sqrt{(1-\alpha^2 Z^2)}$, α is the fine structure constant, and $|\phi(0)|^2$ is the nonrelativistic electron density. This electron density is mainly of the s-electrons as the contribution from p, d, and f electrons is very small[76]. The equation (1.20) becomes

$$\delta E = -\int_0^R \frac{Z_0^2}{R}\left(\frac{3}{2} - \frac{r^2}{2R^2} - \frac{R}{r}\right) C\; r^{2\ell-2} 4\pi r^2 dr \tag{1.23a}$$

$$= \frac{4\pi Z_0^2 C}{R}\left[-\frac{3R^{2\ell+1}}{2(2\ell+1)} + \frac{R^{2\ell+1}}{2(2\ell+3)} + \frac{R^{2\ell+1}}{2\ell}\right] \tag{1.23b}$$

$$= \frac{6\pi Z_0^2 C R^{2\ell}}{\ell(2\ell+1)(2\ell+3)} \tag{1.23c}$$

The total interaction for a finite nucleus is given by

$$E_{nonopole} = E_{point} + \frac{6\pi Z_0^2 C R^{2\ell}}{\ell(2\ell+1)(2\ell+3)} \tag{1.24}$$

The effect of this interaction is to shift all the nuclear energy levels, and is shown in Fig.1.3. As this interaction depends on R(the radius of the nucleus) and C(the electron charge density at the nucleus) δE will be different for excited and ground state of the nucleus and also for different materials (source and absorber in our case). Defining the energy differences of the excited and the ground states as have:

for the source

$$E_S = E_0 + \delta E_{0,S} - \delta E_{G,S} \qquad (1.28)$$

for the absorber

$$E_A = E_0 + \delta E_{0,A} - \delta E_{G,A} \qquad (1.29)$$

Thus the value of E_S and E_A will differ in general and the centroid of the spectrum will be displaced from zero velocity. This shift, usually denoted by δ, was first reported by Kistner and Sunyar[94] and is called the Isomeric shift (I.S.) (analogous to isotopic shift in nuclear physics) or chemical shift (C.S.). From Eqs.(1.24), (1.25) and (1.26) we get

$$I.S. = \frac{4\pi Ze^2}{\ell(2\ell+1)(2\ell+3)}(R_0^{2\ell} - R_G^{2\ell})\left[C_A - C_S\right] \qquad (1.27)$$

$$= \frac{4\pi Ze^2(\ell+1)(2\ell)^{2\ell-2}}{\ell(2\ell+1)(2\ell+3)\Gamma(2\ell+1)}(R_0^{2\ell} - R_G^{2\ell}) \times$$

$$\left[|\psi_A(0)|^2 - |\psi_S(0)|^2\right] - - - - \qquad (1.30)$$

It is important to note that the factor in parenthesis is a

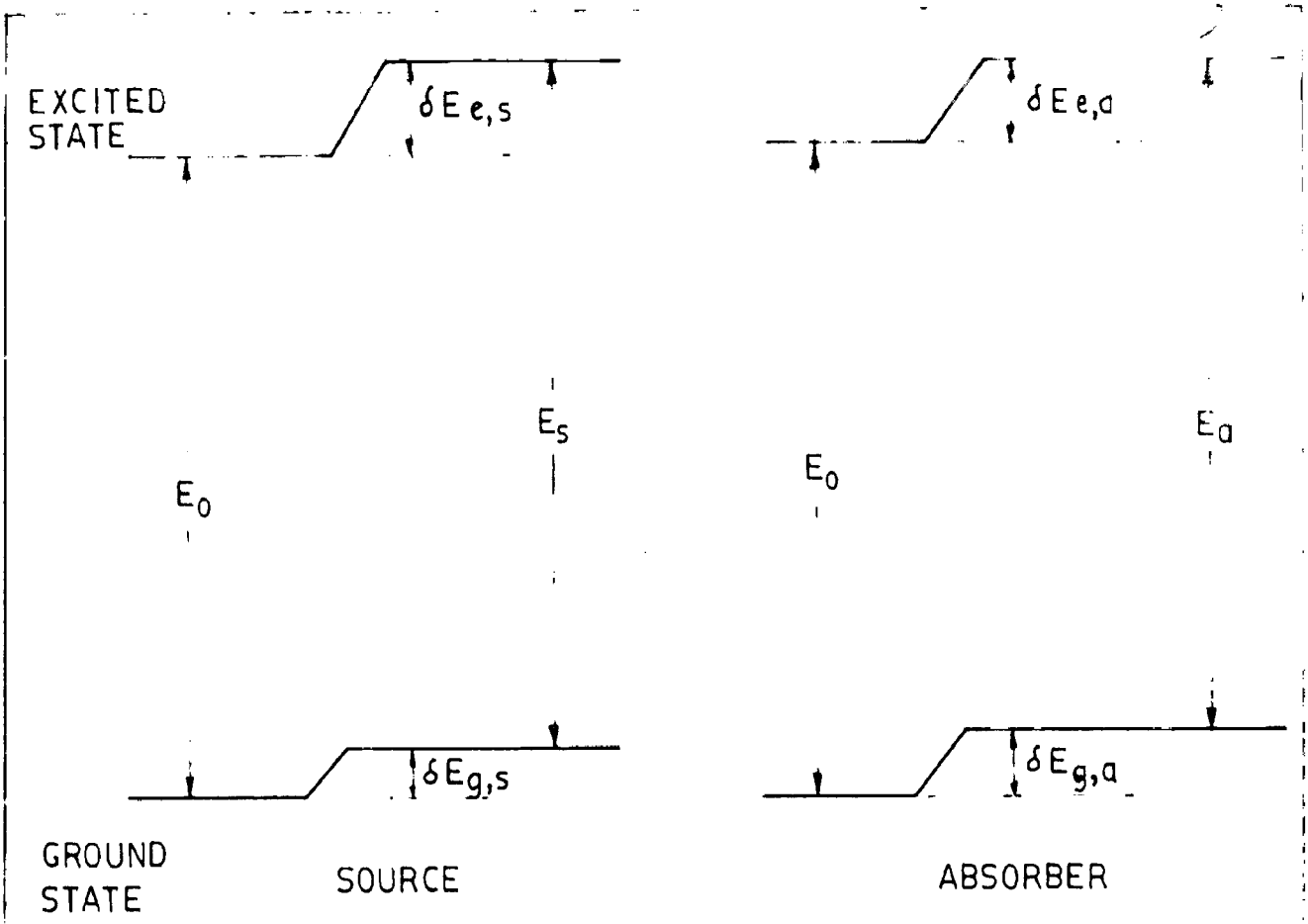

FIG. 1·3 (a) SHIFT OF THE NUCLEAR LEVELS DUE TO THE MONOPOLE COULOMBIC INTERACTION BETWEEN THE NUCLEAR AND ELECTRONIC CHARGES INSIDE THE NUCLEUS

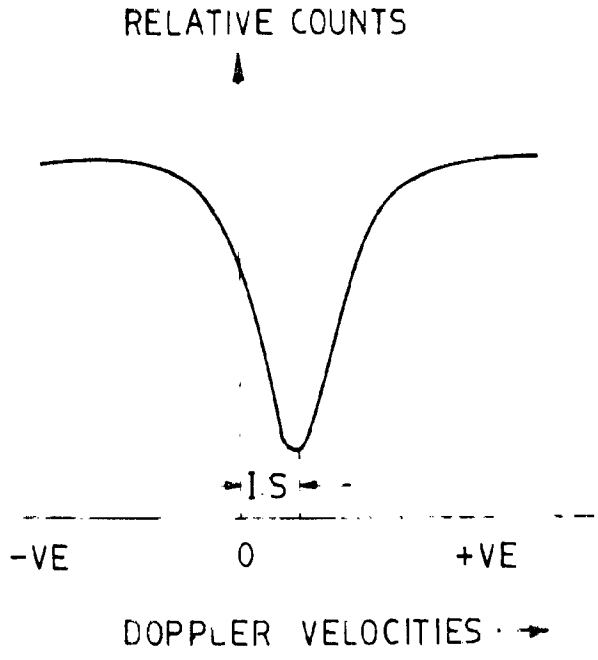

FIG 1·3(b) THEORETICAL MÖSSBAUER SPECTRUM FOR THE FIG (a) ABOVE ($I.S = E_a - E_s$)

nuclear parameter and the term in brackets is atomic in nature, reflecting the electronic configurations of the atom in the source and absorber. Shirley[66] has also given a similar relativistic expression and has calculated the relativistic correction factors for all elements. For a non-relativistic case the value of ρ tends to unity and $|\phi(0)|^2$ becomes $|\psi(0)|^2$ and the expression (1.28) becomes

$$\text{I.S.} = \frac{2\pi}{3} Ze^2(R_e^2 - R_g^2)\left[|\psi_a(0)|^2 - |\psi_s(0)|^2\right] \qquad (1.29)$$

$$\text{or} \qquad \text{I.S.} = \frac{4\pi}{3} Ze^2R^2\left(\frac{\delta R}{R}\right)\left[|\psi_a(0)|^2 - |\psi_s(0)|^2\right]$$

(Nuclear factor) (atomic factor)

where $\delta R = R_e - R_g$. This tallies with the expression given by Porthein[25].

It may be remarked that the experimental shifts are actually not the true isomeric shifts values rather it is a composite sum of the isomeric shift, 2nd order Doppler shift[66] due to thermal motion of the atom (there will be no first order effect as the average value of the velocity of an atom within the nuclear level life-time is zero because of the high frequency 10^{13} sec^{-1} vibrations) and the shift due to mass change of the nucleus on emission of the γ-ray[67]. It has been recently pointed out by Bohm[68] that the thermal and mass shifts are not identical. The temperature shift depends on the angle between the velocity v of the source and the direction of emission of γ-ray and its value in the case of polycrystalline sample is $-\frac{1}{2}\langle v^2\rangle/c^2$ while the mass change shift has no such

The statement is challenged again & the previous arguments for SOD = ± 5/2 as such stand.

angular dependence and has the value $-\frac{1}{5}\langle r^2\rangle/a^2$. Thus the total of non-chemical shifts in a polycrystalline sample is $-\frac{6}{5}\langle r^2\rangle/a^2$ and not $-\frac{1}{2}\langle r^2\rangle/a^2$ only. In most recoilless gamma-ray resonance experiments the magnetic-dipole and electric quadrupole hyperfine interaction (discussed in the next sections) do not cause any shift of the centre of gravity of the velocity spectrum. This is usually related to the fact that the trace of the hyperfine interaction Hamiltonian is zero. Nevertheless a large shift can be caused under proper conditions by a magnetic hyperfine interaction in second order, the so called pseudoquadrupole interaction[69].

SOME GENERAL FEATURES OF ISOMER SHIFTS

As seen from Eqn.(1.29), the I.S. depends on the nuclear as well as atomic factors and so one of these has to be either calculated or determined from some other technique with a view to isolate the effects of the other. As isomeric shift depends on the finite size of the nucleus it is also called the nuclear volume effect[70]. The value of δR for Fe^{57} turns out to be negative[71] and implies that the excited state radius is smaller than the ground state. This result, however, is in disagreement with the shell model. We infer therefore that the value of I.S. for an absorber increases as the s-electron density decreases (ofcourse, for the same source). It is a common practice to express the I.S. values relative either to iron or $Na_2[Fe(CN)_5NO].2H_2O$[72]. A number of systematics of I.S. correlations have been attempted. As a result the

following order has been established with regard to the magnitude of I.S. values in case of spin free (ionic) and spin-paired (covalent) iron compounds

$$Fe^{2+}(ionic) > Fe^{3+}(ionic) > Fe^{2+}(cov) > Fe^{3+}(cov);$$

For ionic divalent and trivalent compounds, I.S. values are characteristic of the valence state and are used to identify the charge state of the ion; on the other hand the corresponding values of the spin paired (covalent) compounds overlap[13]. Walker et al. studied the ionic divalent and trivalent compounds and the 3d group metals and computed the total s-electron density from the Watson's[73] free ion wave functions and Fermi-Segre-Goudsmit formula[74] (for 4s contribution) and plotted a graph between total s-electron density as a function of the percentage of 4s character for various 3d electron configurations (now onward called WWJ plot). 4s character studied in this way gives the electronic configuration of iron metal as $[Ar]3d^{6}4s^{1}$. Danon[75] studied the bonding of transition metal complexes taking into account the covalency, electronegativity and delocalization of 4 electrons due to bonding and modified the WWJ plot. The case of covalent complexes is relatively more complex. Recently Erickson[76] has reviewed the existing literature on the isomeric shift values and their interpretations. According to him the lack of generality in the interpretations of all the iron compounds can be attributed to the inherent deficiencies in the theories which largely use quantities which depend on energy differences. He has

reported a 'relative covalency' scale which is apparently valid for all octahedral ferrous or ferric compounds.

The I.S. values have been used to determine electron configuration in metals and alloys, to study the ordering mechanisms in alloys, to distinguish valence states, and to measure covalencies etc. The dependence of I.S. on volume expansion and pressure has been extensively studied[23,77] and many interesting results have come out. It is generally supposed that I.S. (after taking other contributions out) is temperature independent. Recently Housley and Hess[78] have inconclusively tried to show a temperature dependence of I.S. on the effect is of the order of experimental uncertainties.

In the end it may be pointed out that the measurement of I.S. gives some rather unique information about electron densities obtainable only by Mössbauer Effect.

QUADRUPOLE INTERACTION

The theory of quadrupole interaction has been known since long and is worked out in much detail[79]. The second non-zero term in electrostatic interaction between the nuclear charge distribution and the extra nuclear charge distribution in Eq.(1.17) is the quadrupole interaction given by

$$H_Q = \frac{1}{2} \int d^3x \rho(\bar{x}) \sum_{j,k} \left(\frac{\partial^2 V}{\partial x_j \partial x_k} \right)_0 x_j x_k \qquad (1.30)$$

or

$$H_Q = \frac{1}{6} \sum_{j,k} Q'_{jk} V_{jk} \qquad (1.30a)$$

with $Q'_{jk} = \int d^3x \rho(\bar{x}) x_j x_k$ and $V_{jk} = \left(\frac{\partial^2 V}{\partial x_j \partial x_k} \right)_0$

q'_{jk} and V_{jk} are second rank tensors symmetric by their respective definitions. Due to symmetry, V_{jk} has only six independent components. By appropriate choice of coordinates (usually called principal axes transformation) we can reduce these to three, viz., V_{XX}, V_{YY}, and V_{ZZ}. Further, we know that the s-electrons are spherically distributed and hence do not contribute to the electric field gradient tensor (EFG) and that p,d etc electrons have a negligible probability of being at the nucleus, so we can apply the Laplace's Eq.

$$V_{XX} + V_{YY} + V_{ZZ} = 0 \qquad (1.31)$$

This reduces the number of independent components to only two. It is a general practice to redefine these into two new parameters q, the z-component of EFG and η, the asymmetry parameter which measures the departure from axial symmetry.

$$q = \frac{V_{ZZ}}{e} = \left(\frac{\partial^2 V}{\partial Z^2} \right)_0 \qquad (1.32)$$

and

$$\eta = \frac{V_{XX} - V_{YY}}{V_{ZZ}}$$

The values of V_{XX}, V_{YY} and V_{ZZ} are taken in such a way that

$$|V_{ZZ}| \geq |V_{YY}| \geq |V_{XX}|$$

so that one gets $0 \leq \eta \leq 1$

The origin of EFG will be discussed in detail in the chapter IV and VI. Nevertheless, it may be stated that the two fundamental sources are the charges on distant ions

(if their symmetry is lower than cubic) and the electrons in incompletely filled shells of the atom itself. In the former case many of the properties of the EFG can be deduced from the symmetry properties of the crystal, e.g., if the crystal has a four-fold axis then choosing this axis as the z-axis, leaves the $V_{xx} = V_{yy}$ and then $\eta = 0$, i.e., there is an axially symmetric field gradient. It can be readily shown that a three-fold axis (120° rotation) also suffices to insure an axially symmetric field gradient, and that the two mutually perpendicular axes of three-fold or higher symmetry result in a vanishing field gradient.

From the symmetry of the time average of the nuclear charge distribution about the spin axis, the electric quadrupole moment tensor components

$$Q'_{ij} = \int d^3x \rho(\bar{x})\, x_i x_j \tag{1.33}$$

reduce to one independent component

$$Q_{zz} = \int d^3x \rho(\bar{x})\, (3z^2 - r^2) \tag{1.34}$$

The quadrupole moment Q of the nucleus is defined by $Q = Q_{zz}/e$, e being the protonic charge. The classical expression for the quadrupole interaction then becomes[79]

$$E_Q = \frac{e^2qQ}{4} \left[1 - \frac{1}{3}\,\eta \right] \tag{1.35}$$

where terms which are independent of nuclear orientation have been neglected. The quantum mechanical analogue of Eq.(1.33) is

$$H_Q = \frac{e^2qQ}{4I(2I-1)} \left[3\hat{I}_z^2 - \hat{I}(\hat{I}+1) + \frac{\eta}{2} (\hat{I}_+^2 + \hat{I}_-^2) \right] \tag{1.36}$$

where $\hat{I}_\alpha$ is the α component of the nuclear spin operator $\hat{I}$ and $\hat{I}_+$ and $\hat{I}_-$ are raising and lowering operators defined as $\hat{I}_\pm = \hat{I}_x \pm i\hat{I}_y$. Now to determine the eigenvalues and eigenvectors of the Hamiltonian we have to determine the matrix elements

$$\langle \hat{I}\ \alpha|H_Q|\ \hat{I}\ \alpha'\rangle \tag{1.37}$$

Now for Pa^{37}, the excited state spin $I_0 = 3/2$ and thus α and α' have the values $3/2$, $1/2$, $-1/2$ and $-3/2$. Calling $\frac{e^2qQ}{4I(2I-1)} = \frac{e^2qQ}{12} = P$, the operator equivalent technique gives[30]

$$\langle \tfrac{3}{2}\ \alpha|H_Q|\tfrac{3}{2}\ \alpha'\rangle =$$

α \ α'	3/2	1/2	-1/2	-3/2
3/2	3P	0	$\sqrt{3}P$	0
1/2	0	-3P	0	$\sqrt{3}P$
-1/2	$\sqrt{3}P$	0	-3P	0
-3/2	0	$\sqrt{3}P$	0	3P

(1.38)

The secular Eq. for the eigenvalue is

$$E_Q^2 - \left(\frac{e^2qQ}{12}\right)^2 (9+3\eta^2) = 0 \tag{1.39}$$

Therefore the eigenvalues of H_Q are

$$E_Q = \pm \frac{e^2qQ}{4}\left(1+\frac{1}{3}\eta^2\right)^{1/2} \tag{1.40}$$

Thus the excited state is split into two sublevels with energies given by Eq.(1.40). Then the following wave functions are easily found from perturbation theory:

$$E_1 = \frac{e^2qQ}{4}\sqrt{(1+\frac{1}{3}\eta^2)}$$

and

$$E_2 = -\frac{e^2qQ}{4}\sqrt{(1+\frac{1}{3}\eta^2)}.$$

$$\begin{aligned} |+\rangle &= \lambda(|3/2,3/2\rangle + A|3/2,-1/2\rangle) \\ |+\rangle' &= \lambda(|3/2,-3/2\rangle + A|3/2,1/2\rangle) \\ |-\rangle &= \lambda(|3/2,1/2\rangle - A|3/2,-3/2\rangle) \\ |-\rangle' &= \lambda(|3/2,-1/2\rangle - A|3/2,3/2\rangle) \end{aligned} \qquad (1.41)$$

$$\text{with } A = \eta/\sqrt{3}\{1+\sqrt{(1+\eta^2/3)}\} \qquad (1.42)$$

where λ is a normalising factor.

This shows that the split sublevels do not have definite values of I_z. Each degenerate state of a sublevel is a superposition of states with definite values of the spin projections. Since the ground state of Fe^{57} has no quadrupole moment, the ground level is not affected, and the ground state wave functions may be assigned the most convenient spatial axes without loss of generality. Thus ground state is doubly degenerate with wave functions $|1/2,1/2\rangle$ and $|1/2,-1/2\rangle$. In Fig.1.4 these levels and the possible Mössbauer transitions have been shown. As we know the quadrupole moment Q for Fe^{57} is positive so the quadrupole coupling constant e^2qQ/h will be positive or negative according as q, the z-component of EFG, is positive or negative. These two possible situations are demonstrated in Fig. 1.4 where the excited state sublevels interchange. The Mössbauer gamma-line is doublet with a separation of components, ΔE_Q, (sometimes denoted as ϵ) equal to

$$\Delta E_Q = \frac{1}{2} e^2qQ\,(1+\frac{1}{3}\eta^2)^{1/2} \qquad (1.43)$$

It is obvious that the measurement by the Mössbauer Effect of just one such separation (ΔE_Q) cannot determine all the parameters and the orientation of the principal axes of

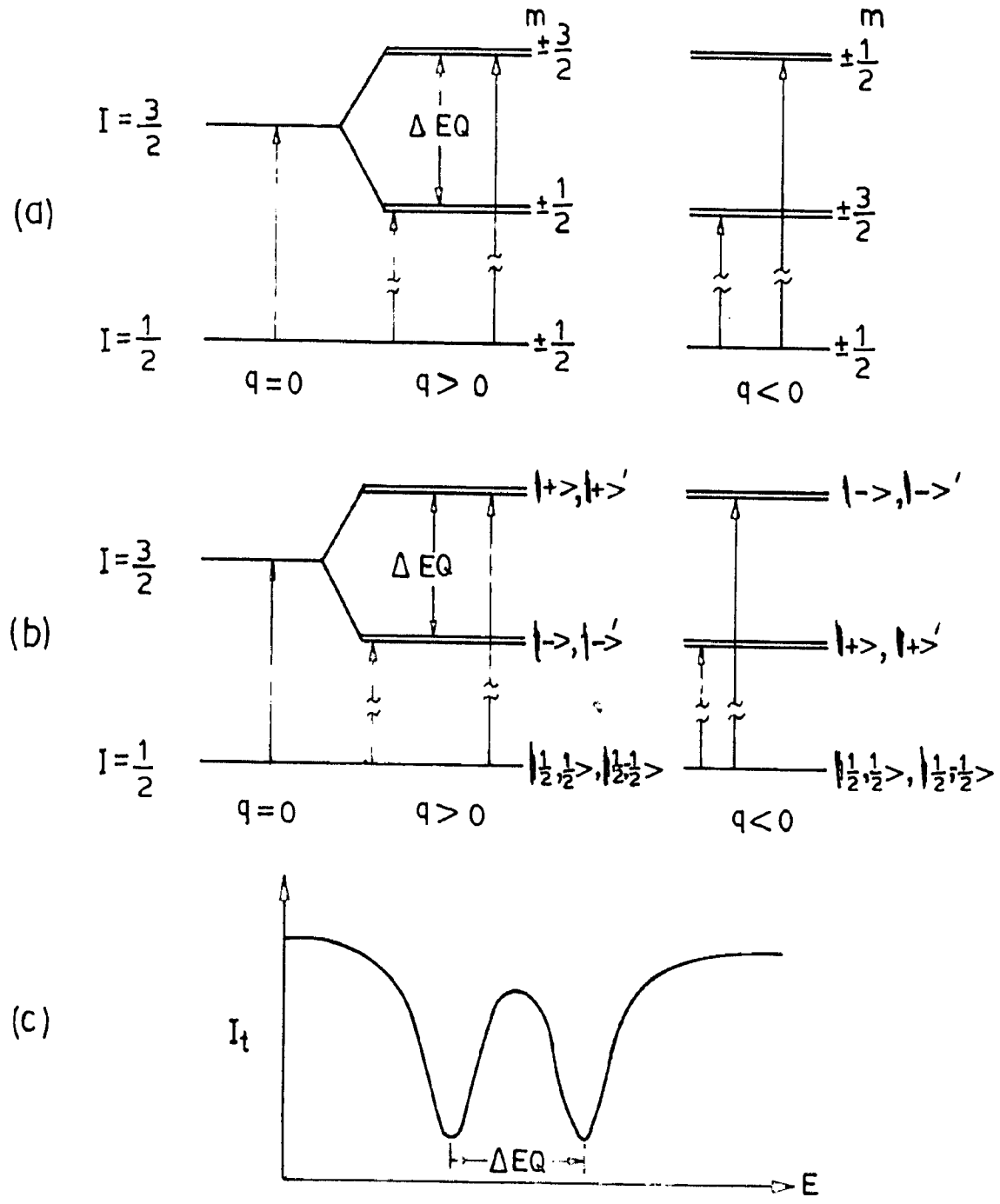

FIG. 1.4 : (a) AXIALLY SYMMETRIC FIELD GRADIENT ($\eta=0$)
(b) ASYMMETRY PARAMETER (η) NOT ZERO
(c) THEORETICAL MÖSSBAUER SPECTRUM

the EFG even if the value of Q is known from other techniques. This has been achieved by comparison of line intensities in the case of single crystal absorption spectra. If θ and ϕ are the spherical angles of the photon vector in the principal axes system of the EFG, the ratio of the intensities of the two transitions becomes[81]

$$\frac{P_+}{P_-} = \frac{(1+\Delta^2/3)(1+\cos^2\theta) + \frac{4}{3}\Delta^2\sin^2\theta + \frac{2\Delta}{\sqrt{3}}\sin^2\theta\cos 2\phi}{(1/3+\Delta^2)(1+\cos^2\theta) + \frac{4}{3}\sin^2\theta - \frac{2\Delta}{\sqrt{3}}\sin^2\theta\cos 2\phi} \qquad (1.44)$$

where Δ is defined by (1.42)

As a special case of this when field gradient is axially symmetric i.e., $\eta = 0$, we see that the whole procedure becomes very simple. The Hamiltonian of Eq.(1.30) reduces to

$$H_Q = \frac{e^2qQ}{4I(2I-1)}\left[3\hat{I}_z^2 - \hat{I}(\hat{I}+1)\right] \qquad (1.45)$$

with eigenvalues given by

$$E_Q = \frac{e^2qQ}{4I(2I-1)}\left[3m_I^2 - I(I+1)\right] \qquad (1.46)$$

which for Fe^{57} ($I = 3/2$) becomes $E_Q = \pm\frac{e^2qQ}{4}$ (1.47)

The resulting sublevels are doubly degenerate and are characterized by definite values of I_z. ($\Delta = 0$ and $\lambda = 1$ in Eq.(1.41)). The line intensity ratio simplifies to

$$\frac{P_+}{P_-} = \frac{1+\cos^2\theta}{\frac{8}{3} - \cos^2\theta} \qquad (1.48)$$

It is obvious from a comparison of Eqs.(1.44) and

(1.46) that η influences the angular dependence of the absorption cross sections of the doublet components.

It may be pointed out very clearly that the Eq.(1.44) and (1.46) do not include the effect of vibrational anisotropy (Goldanskii-Karyagin effect) and thus for any meaningful interpretation one should give proper consideration while comparing intensities. Further it is interesting to note that for a polycrystalline sample both (1.44) and (1.46) yield the intensity ratio as unity. Thus the presence or absence of any asymmetry parameter is not evident from any ordinary Mössbauer spectrum of a powdered sample. All the five quantities viz., q_{zz}, η, α, β and γ (the latter three are the Eulerian angles) which are necessary to specify the EFG tensor completely can be determined by single crystal measurements[62].

SOME GENERAL FEATURES OF THE MÖSSBAUER QUADRUPOLE INTERACTION

Like I.S. the first observed quadrupole interaction in a Mössbauer spectrum was also reported by Kistner and Sunyar[44]. Further it may also be emphasised that in the case of Fe^{57} Mössbauer Effect presents some unique information about the nuclear quadrupole interaction, because conventional methods fail since there are no suitable isotopes of iron with a ground state spin $I_g > \frac{1}{2}$. Like isomeric shift values, the quadrupole splitting (ΔE_Q) values are also characteristic of ferrous and ferric compounds with further differentiation of low spin and high spin[3,17,26]. For iron coordination compounds one finds the maximum quadrupole splitting in a high spin d^6 configuration of iron with the low spin d^5 next,

this is due to the contribution of one unccompensated electron out side a spherical half filled shell in the former case and a positive hole in the latter case. (Chapter IV and VI).

Because of the temperature dependence of occupation probabilities of this uncompensated d electron (for d^0 configuration) and positive hole (for d^8 configuration) these compounds show a temperature dependent ΔE_Q. On the other hand, the high spin d^5 and low spin d^6, having spherically symmetric d electron distribution, produce very small ΔE_Q with few exceptions (e.g., $Na_2[Fe^{II}(CN)_5NO].2H_2O$).

If there is asymmetry in the crystal which could cause an electric quadrupole splitting, the application of pressure will alter this splitting. Shear forces could be used to indicate the orientation of this asymmetry with the crystal axis. The method is exceptionally sensitive and can detect asymmetries[10] which are not measurable by X-ray diffraction. It is suggested that a preponderance of unpaired electron spins in d level can influence the gradient through spin-spin coupling. A relationship between the magnetic susceptibility and electric quadrupole splitting for iron compounds has been found[13]. Even if the site symmetry is crystallographically cubic below transition temperature, an electric field gradient can be induced due to the on set of internal or external magnetic field[24]. The presence of static Jahn-Teller distortion can also produce a non-vanishing electric field gradient[25].

The I.S. and Q.S. values have been successfully used to interpret several hitherto unsolved problems[12,13,24-28,29,30] of structural chemistry, valence state and bonding. Some very

interesting and useful empirical or otherwise intuitive correlations have been reported in literature, e.g., in I.S. vs ΔE_Q[13,83,87]; I.S. vs electronegativity[88]; I.S. vs Nephalauxetic effect[89]; magnetic susceptibility χ vs ΔE_Q[13,89]; optical parameter Dq vs ΔE_Q and I.S.[85]; proton magnetic resonance chemical shift vs I.S.[90]; Knight shift in NMR vs s-electron density[91]; I.S. vs spin-spin coupling constant J in NMR[92]; electron spin resonance parameters D and E vs ΔE_Q[83] etc.

The sign of the quadrupole coupling constant can be determined in a single crystal by studying the angular variation of area ratios[82] or by magnetic perturbation technique in case of powdered sample[92].

(B) MAGNETIC INTERACTIONS

The Hamiltonian operator for the magnetic interaction of nuclear level with spin angular momentum I and effective magnetic field H is given by

$$H_D = -g\beta_n \bar{I}.\bar{H} \qquad (1.48)$$

where g is the nuclear gyromagnetic ratio of the nuclear state and β_n, the nuclear magneton. If the magnetic field is acting along z-axis, it becomes

$$H_D = -g\beta_n H I_z \qquad (1.49)$$

The resulting Hamiltonian matrix is diagonal with (2I+1) eigenvalues, given by

$$E_D = -g\beta_n H m_I \qquad m_I = I,(I-1),\ldots(-I+1),-I \qquad (1.50)$$

The sublevels are equally spaced with separation of $g\mu_n H$. For Fe^{57} the ground state ($I_g = 1/2$) is split in two sublevels separated by an amount $\beta = g_0\mu_n H$ and the excited state ($I_e = 3/2$) splits into four sublevels with equal separation of $\alpha = g_e\mu_n H$, (Fig.1.8) where g_0 and g_e are the ground and excited state g factors respectively and the ratio g_0/g_e has been found[93] to be - 1.715. The dipole radiation selection rule, $\Delta m = 0, \pm 1$, restricts the number of allowed transitions to six at the most. The separation between the outermost two lines, $3\alpha + \beta$, or 4.715α, is found[93] to be 10.64 mm/sec. which corresponds to an effective magnetic field H of 330 kG. The relative intensities of those transitions are given by[94]

$$|\langle I_g m_g LM | I_e m_e \rangle|^2 \, F_L^M(\theta) \qquad (1.51)$$

where the first factor is the square of the Clebsch-Gordan coefficients describing the vector coupling of I_g and I_e through the radiation field LM, and θ is the angle between the direction H and the incident gamma rays. The radiation pattern for dipole radiation (L = 1) $F_L^M(\theta)$ is:

$$F_1^0(\theta) = 3/2 \sin^2\theta$$
$$F_1^{\pm 1}(\theta) = 3/4 (1+\cos^2\theta) \qquad (1.52)$$

The relative parameters of the transitions involved are listed in Table 1.2.

Some interesting conclusions from this table are as follows:

For a random orientation of H with respect to the gamma

direction, the radiation is unpolarised and the lines have intensities in the ratio 3:2:1:1:2:3. For a perpendicular magnetic field H ($\theta = 90^0$), the ratios are 3:4:1:1:4:3 with linear polarisation $\parallel, \perp, \parallel, \parallel, \perp, \parallel$. For axial field (i.e., $\theta = 0^0$), the radiation is circularly polarised with $\Delta m = 0$ transition missing and the remaining four lines have intensities 3:1:1:3 with polarisation left, right, left, right.

TABLE 1.2 The relative energies and intensities for various allowed transitions in Fe^{57}.

Sl. No.	Transition	Δm	Relative energy	Relative intensity	Total
1	$-1/2 \rightarrow -3/2$	-1	$-1/2(\beta+3\alpha)$	$3/4(1+\cos^2\theta)$	3
2	$-1/2 \rightarrow -1/2$	0	$-1/2(\beta+\alpha)$	$3\sin^2\theta$	2
3	$-1/2 \rightarrow +1/2$	$+1$	$-1/2(\beta-\alpha)$	$3/4(1+\cos^2\theta)$	1
4	$1/2 \rightarrow -1/2$	-1	$1/2(\beta-\alpha)$	$3/4(1+\cos^2\theta)$	1
5	$1/2 \rightarrow +1/2$	0	$1/2(\beta+\alpha)$	$3\sin^2\theta$	2
6	$1/2 \rightarrow +3/2$	$+1$	$1/2(\beta+3\alpha)$	$3/4(1+\cos^2\theta)$	3

(c) COMBINED ELECTRIC AND MAGNETIC INTERACTION

If a nucleus is in a static nonuniform electric field E and a magnetic field H, the position of the sublevels of the hyperfine structure will depend on the ratio of magnetic to the electric interaction energies, the asymmetry parameter η, the angle between the main axis of the EFG tensor (for a general case), and the direction of the magnetic field H. The combination of these factors makes the determination of the EFG

parameters and effective magnetic field, from a given Mössbauer spectrum, rather involved. For those cases in which the direction of the effective internal magnetic field corresponds to one of the EFG principal axes, closed form mathematical expressions have been derived to locate the peak positions and estimation of their intensities. On the other hand this is not the case for an arbitrary oriented internal magnetic field. Many computer programs[95] have been utilised successfully to combat this problem in which the observed spectrum parameters (line positions, line widths and line intensities) are fitted by the iterative methods to have the best fit EFG parameters and effective magnetic fields. We will only cite here the following special cases:

(i) AXIALLY SYMMETRIC EFG TENSOR WITH SYMMETRY AXIS PARALLEL TO H

This is the simplest case. The energy eigenvalues for the excited and ground state are given by[25]

$$I = 3/2 \quad E_{Q,m} = -G_0/\mu_n H m_I + (-1)^{|m_I|} + 1/2\ e^2qQ/4 \qquad (1.63)$$

and $\quad I = 1/2, \; E_{Q,m} = -G_0/\mu_n H m_I$

All the 4 excited state sublevels of Fig.1.5 are further displaced by an equal amount by the quadrupole interaction. This displacement is of opposite sign for $m_I = \pm 3/2$ and $m_I = \pm \frac{1}{2}$.

(ii) AXIALLY SYMMETRIC EFG TENSOR WITH SYMMETRY AXIS AT ANGLE θ WITH DIRECTION TO THE MAGNETIC AXIS.

Parker[90] has done machine calculations for $I = 1$, $3/2$, 2 etc. For $e^2qQ/\mu_n H \ll 1$, the excited state energy levels can be described[25] by

$$E_{\sigma,\square} = -g_0\mu_n H m_I + (-1)^{|m_I|+1/2}\frac{e^2qQ}{4}\frac{3\cos^2\theta-1}{2} \qquad (1.84)$$

The schematic energy level diagram on the lines of Fig.1.8 and the procedure of the analysis of the observed Mossbauer spectrum has been discussed in Chapter III. We will make few necessary remarks and then will discuss the next case.

It follows from Eq.(1.84) that when angle $\theta = \cos^{-1}(\frac{1}{\sqrt{3}})$, the second term will become zero even for a nonzero EFG. The line splitting will be of the type of Fig.1.8 and an erroneous conclusion of zero field gradient may be inferred. Further if $Q(3\cos^2\theta - 1)/2$ is replaced by Q', Eq.(1.84) becomes formally identical to Eq.(1.83), and the quadrupole moment, Q', which would be deduced, may be in error, both in magnitude and sign; e.g., if $\theta = \pi/2$, Q is in error by a factor of -1/2. Thus Eq.(1.84) is insufficient for the determination of e^2qQ, if θ is unknown. Recently it has been shown[97] that in the case of an axially symmetrical EFG and an arbitrary θ, the energy of the excited state magnetic sublevels ($I = 3/2$) may be written in an exact analytical way for an arbitrary ratio of $|\vec{\mu}\vec{H}|/|e^2qQ|$. In this case

$$\tfrac{1}{2}|e^2qQ| = \Big[\sum_{\square} E^2_{\sigma,\square} - 8(g_0\mu_n H)^2\Big]^{1/2} \qquad (1.85)$$

if $\eta \neq 0$ the Eq. (1.85) becomes[97]

$$\tfrac{1}{2}|e^2qQ|(1+\tfrac{1}{3}\eta^2)^{1/2} = \Big[\sum_{\square} E^2_{\sigma,\square} - 8(g_0\mu_n H)^2\Big]^{1/2} \qquad (1.86)$$

SOME GENERAL FEATURES OF MAGNETIC INTERACTION

The total H_{eff} acting on the nucleus may be represented[98]

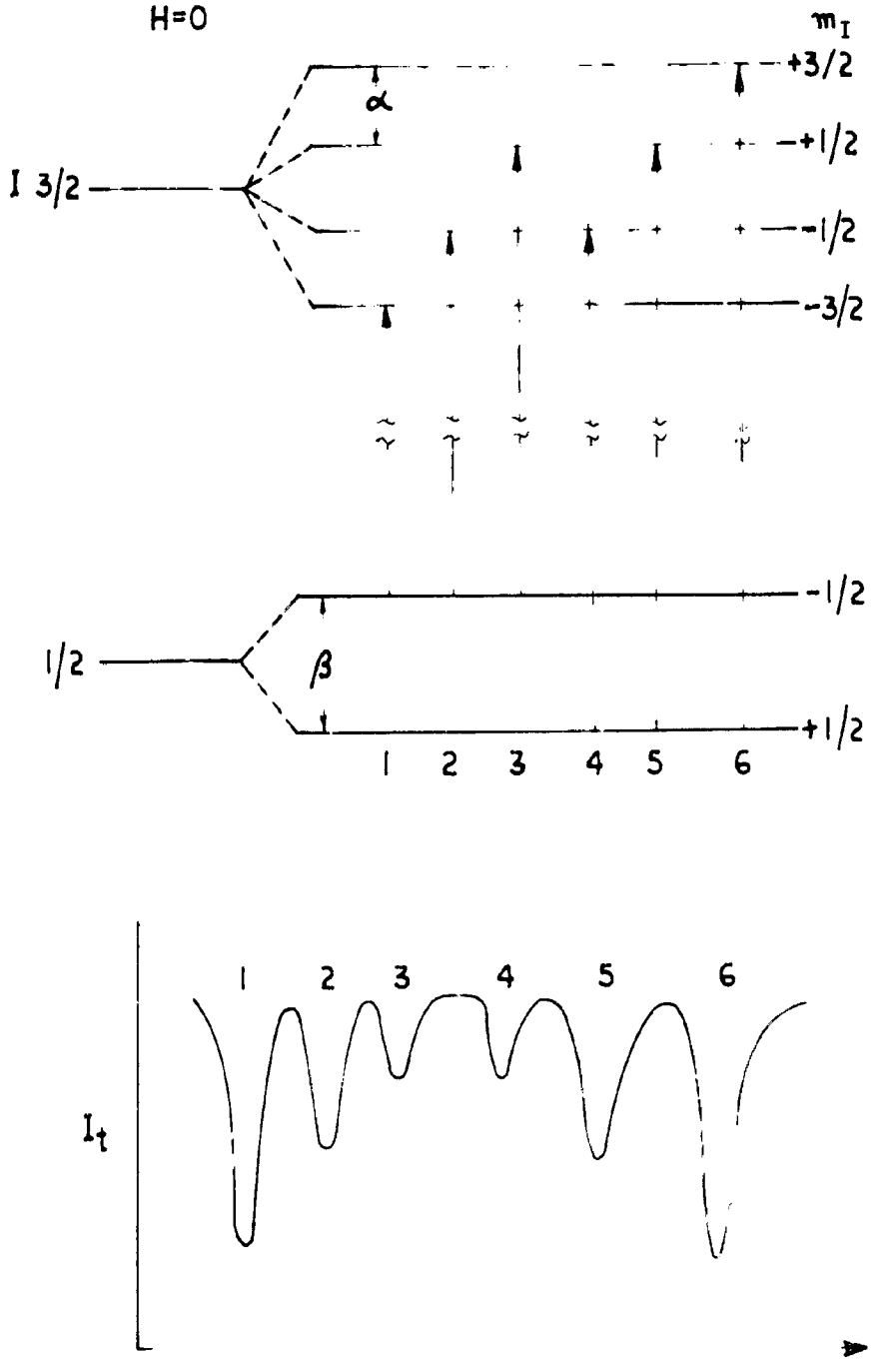

FIG. 1.5 ENERGY LEVELS AND THEORETICAL SPECTRUM OF F_e^{57} WITH MAGNETIC INTERACTION.

as

$$H_{eff} = H_0 + \frac{4}{3}\pi M - DM + H_L + H_D + H_0 \qquad (1.00)$$

The first term H_0, is the externally applied field and its maximum attainable value for all practical purposes is about 60 kG; the second and third terms are the Lorentz and demagnetising fields and are very small. The last three terms are orbital, dipolar and Fermi-contact interaction terms and in fact are the major sources of the observed large magnetic fields. The latter three are discussed in Chapter III.

The conditions for the observability of Zeeman splitting[99] are

$$|e|/\mu_n H_{eff} \gg 2\pi \text{ or } \omega_L \tau_n \gg 1 \qquad (1.01)$$

and $$\omega_L \tau_s \gg 1 \quad \text{or} \quad \omega_L \gg \Omega \qquad (1.02)$$

ω_L is the Larmor frequency, τ_n, the nuclear lifetime, τ_s - the electron spin correlation time and Ω, the spin flip frequency. For Fe^{57}, the first condition requires $H_{eff} > 10^4$ Oe. The second condition (1.02) takes into account the fluctuations in the magnetic field with time (In the first condition, we assumed tacitly that there is a net time averaged magnetic field acting on the nucleus). If the time fluctuation rate which is governed by the electron spin correlation time τ_s is less than the Larmor precession time, then the nucleus will not see any magnetic field. This happens in most of the paramagnetic salts. On the other hand if the Larmor frequency ω_L, is greater than the spin-flip frequency Ω one should expect a Zeeman splitting. That this is indeed the case, has been reported by Northcin and Nozaki among others[81].

This is the reason why most of the discussions of hyperfine splitting in Mössbauer spectra pertain to materials which exhibit spontaneous magnetization or sublattice magnetization.

In the case of Fe^{57} fields varying from 210 to 550 kOe per spin have been observed in various compounds of trivalent iron, the smaller value is characteristic of oxides, the larger one of fluorides. In the case of divalent iron compounds, in contrast to the trivalent, the range of fields which has been reported is much larger. The values range from 200 kOe for Fe^{2+} in CoO to 330 in FeF_2, and to 495 for divalent iron in Fe_3O_4. The reason for this greater diversity lies in the orbital contribution. In case of the covalent trivalent iron compounds the effective magnetic field observed is rather small as quoted above. This decrease may be accounted as follows. Since Fe^{3+} ion is in a spherically symmetric $(3d^5)^6S$ ground state there are no orbital or dipolar contributions to the hyperfine structure and H_{eff} is a measure of the unpaired spin density (spin up-spin down) at the nucleus produced by the 3d electrons (Chapter XII). With increasing covalency, the 3d electron becomes delocalized and admixed with those of the surrounding ligand atoms. This produces a decreased spin density at the nuclei and may also result in some orbital moment. The latter results in a positive contribution to H_{eff} and since the total hyperfine field is negative, both this and the change in spin density, cause a reduction in observed H_{eff}. There will also be dipolar contribution to the hyperfine field.

It appears that the hyperfine field is a more sensitive indication of the degree of covalency than the isomeric shift,

which varies with the total charge density at the nucleus.

A few applications of hyperfine interaction were mentioned earlier. Recently Gonser[10] has enumerated many new and useful applications viz. high pressure physics, occurrence of spontaneous magnetization of thin films, spin density oscillations, penetration of conduction electrons, spin polarisation into non-magnetic films, determination of localised moments, super paramagnetism (the cluster size effect) polarisation of gamma-rays, magnetic 'optic' effects (Faraday effect, magnetic double refraction) etc. Grant[100] also recently discussed the study of magnetic properties of materials using the Mössbauer effect.

It may be remarked that the Mössbauer effect is not the only means to determine the effective magnetic fields acting on the nucleus of a solid. In fact NMR, EPR, nuclear specific heats, angular correlation of gamma rays and interaction of polarised neutrons with polarised nuclei are the other methods employed for this. Compared to all these methods, the Mössbauer method has the advantage of being direct, relatively simple and fast.

1.6 STATEMENT OF THE PROBLEM

The intent of the experimental investigations and the numerical calculations reported in the succeeding chapters of the thesis has been of many fold:

(1) The study of Fe^{2+} Tutton salts, having general formula $Fe(MSO_4)_2.6H_2O$ with M = NH_4^+, K^+, Rb^+, and Cs^+, with the Mössbauer Effect technique may provide.

(b) The extent of charge asphorical distribution leading to the EFG at the Fe^{2+} ion.

(c) The temperature variation of quadrupole coupling constant may yield the change in occupation probabilities of the sixth uncompensated d electron in the Fe^{2+} ion situated in the water octahedron. This in turn will give the estimation of characteristic temperatures of the crystal field split t_{2g} levels.

(d) Comparative studies of quadrupole coupling constants in the series will give the ground state wave function of the other members of the series as MH_4^+ - member has a $|xy\rangle$ ground state wave function.

(e) The effect of the varying cation electronegativity on the I.S. values.

(2) The study of Chalcopyrite ($CuFeS_2$) may provide the conclusive assignment of the so far controversial situation of the valence state of iron through the values of isomeric shifts, quadrupole coupling constant and effective magnetic field and their temperature dependence.

(3) The Mössbauer and magnetic susceptibility studies of Alkali Dithioferrates (III) of the type $AFeS_2$ with A = Na, K, Rb, and Cs, were undertaken with the view

(a) To seek the information of temperature dependent quadrupole splitting in the tetrahedrally bonded Fe(III) ion with a view to compare it to its counterpart Fe(II) and seek the extent of level separation of crystal field split dE and dV levels.

(b) The effect of varying electronegativity on I.S. in view of sp^3 bonding of the Fe(III) ion.

(c) To seek the information of magnetic transition if any.

(d) The molar susceptibility will give the no. of unpaired d electrons; also its temperature dependence will predict the onset of a magnetic transition if any.

(e) The values of isomeric shifts will give the covalent character which in turn will give valence state and type of bonding. The values of I.S. can also give the total s-electron density to seek the effective no. of d-electrons present in the Fe(III) ion.

(f) The point charge-point dipole calculations of EFG tensor in ionic trivalent iron compounds may yield.

(a) The information of the extent to which charge distribution deviates from a spherical symmetry responsible for observed quadrupole coupling constant.

(b) The effective contribution of the permanent and induced dipoles to the EFG acting on an ion.

(c) The re-evaluation of the nuclear quadrupole moment of the Fe^{57} which may remove the existing ferrous-ferric anomaly.

(d) Lastly to assess the adequacy of a point charge-point dipole model calculations for such systems.

CHAPTER II

INSTRUMENTATION AND EXPERIMENTAL TECHNIQUES

2.1 INTRODUCTION

In the event of source and absorber having identical chemical environment, the Mössbauer transition energy from the source will be exactly equal to the energy required to excite the absorber from ground state to the first excited state, and thus there will be resonant absorption. Fortunately this is rarely the case (as otherwise whole wealth of information available would not have been there) and one has to modify the transition energy of the source to get the resonant absorption. The modification which was first employed by Mössbauer in his original experiment and has found almost universal acceptance, is to shift the gamma-ray energies via the first order Doppler shift*. Thus to perform a Mössbauer Experiment, a velocity v is introduced between the source and an absorber so that energy of the emitted gamma-ray, E_γ , is Dopplor shifted by an amount

$$\Delta E = \frac{v}{c} E_\gamma \qquad (2.1)$$

Resonance absorption will occur when the energy of the gamma-ray from the source coincides with a level in the absorber. Thus an energy level or group of levels in an absorber (in absorption geometry) may be traced out by measuring the resonance absorption as a function of velocity. A plot of

---

* In principle, this energy modification, can also be performed by the use of 'drives' based on effects which can be described in terms of second order shift. These drives have special application to narrow line Mössbauer effect spectroscopy.

transmitted (or scattered) gamma-beam intensity versus relative velocity constitutes a Mössbauer spectrum, as it is usually called. The Doppler velocities required, depend upon the natural line width, Γ ; gamma-ray energy, E_γ , and the energy level splittings due to hyperfine interactions. For Fe^{57}, these velocities range from a fraction of a mm/sec. to about 1 cm/sec., the latter gives an energy modification of $\Delta E = 4.8 \times 10^{-7}$ eV. This implies that, with a velocity drive which can be varied within ± 1 cm/sec. energy levels which are within ± 4.8×10^{-7} eV of energy of the 14.4 keV gamma-rays emitted by the source, can be investigated. Thus a very precise way of measuring very small energy differences is provided. It may be remarked that the Mössbauer effect can give this precision only in the relative sense and not in the absolute measurement of the energy.

With the advent of Mössbauer effect a great deal of effort and ingenuity have gone into the development of the apparatus for producing the Doppler shift. Our aim is far from reviewing the existing literature rather to have a casual reference to some of the important developments while detailing the pertinent information about our own experimental set-up.

2.2 MÖSSBAUER SPECTROMETERS

Basically there are three ingredients of Mössbauer spectrometer.

(A) Mössbauer source and absorber (or scatterer)

(B) Drive to provide controlled and well defined relative velocity to source or absorber for Doppler tuning.

(C) A stable counting assembly for detecting the transmitted

compton scattering due to its high atomic number Z, as the latter will make the diffusion requirements for such a source extremely stringent. On the other hand copper matrices, while having large recoilfree fraction at room temperature and a low atomic number, are chemically unstable, since unprotected sources tend to react with atmospheric oxygen and sulphides which may be present in the ambient environment. A reasonable compromise between the various characteristics is provided by palladium host matrix, which in addition also gives a narrower line. Unfortunately this has also one disadvantage of having an X-ray of 21 keV falling near the 14.4 keV Mössbauer gamma-ray level, which may increase non-resonant back ground (in case of scintillation detector).

We on our part, procured commercially certified Co^{57}(Cu) and Co^{57}(Pd) sources each having initial activity of 1 mC. from Nuclear Science and Engineering Corporation, Pittsburg, Pa 15230, Pennsylvania and the Radio Chemical Centre, England, respectively. The first was used in studies of Tutton salts (Chapter IV) and chalcopyrite (Chapter III) while the other was used in studies of alkali dithioferrates(III) (Chapter V).

A passing remark may be made that suitable sources have been found for only a limited no. of radioisotopes and several new techniques using accelerators and reactors have been reported in the literature, most promising being the coulomb excitation and (n,γ) reactions. In these reactions produced sources there is a radiation damage which results into a reduction of recoil free fraction.

(A-ii) ABSORBERS (OR SCATTERERS)

A Mössbauer experiment can be performed either in a

transmitted (or scattered) gamma-beam intensity versus relative velocity constitutes a Mössbauer spectrum, as it is usually called. The Doppler velocities required, depend upon the natural line width, Γ ; gamma-ray energy, E_γ , and the energy level splittings due to hyperfine interactions. For Fe^{57}, these velocities range from a fraction of a cm/sec. to about 1 cm/sec., the latter gives an energy modification of $\Delta E = 4.8 \times 10^{-7}$ eV. This implies that, with a velocity drive which can be varied within ± 1 cm/sec. energy levels which are within ± 4.8×10^{-7} eV of energy of the 14.4 keV gamma-rays emitted by the source, can be investigated. Thus a very precise way of measuring very small energy differences is provided. It may be remarked that the Mössbauer effect can give this precision only in the relative sense and not in the absolute measurement of the energy.

With the advent of Mössbauer effect a great deal of effort and ingenuity have gone into the development of the apparatus for producing the Doppler shift. Our aim is far from reviewing the existing literature rather to have a casual reference to some of the important developments while detailing the pertinent information about our own experimental set-up.

2.2 MÖSSBAUER SPECTROMETERS

Basically there are three ingredients of Mössbauer spectrometer.

(A) Mössbauer source and absorber (or scatterer)

(B) Drive to provide controlled and well defined relative velocity to source or absorber for Doppler tuning.

(C) A stable counting assembly for detecting the transmitted

or scattered gamma beam intensity.

Several additional auxiliary systems (e.g. cryostat, furnace, arrangement for pressure variation etc.) may be necessary to perform a particular experiment.

(A-1) MÖSSBAUER SOURCE

As very precisely pointed out by Herber[16], the preparation of a good Mössbauer source often requires the combined talents of a competent chemist, metallurgist and nuclear physicist as well as a fair amount of good luck. A Mössbauer isotope is incorporated in the host matrix in one of the three usually available fashions: ordinary synthesis of a compound having parent nuclei[101], doping into the matrial under investigation[102] and the diffusion of a Mössbauer isotope in a suitable host so as to give a single unsplit line. It is considered desirable that the source has long half life, a high energy precursor, high f and a γ-ray single unsplit line of natural line width. These requirements are realised by incorporating the Mössbauer nuclei in a highly symmetric (cubic and non-magnetic) lattice site, preferably a conducting material having a small electronic self-absorption coefficient, with a high effective Debye temperature.

Variety of host matrices, mostly of metallic form, have been tried and number of detailed descriptions are available in literature[103]. These studies indicate that Co^{57} in Pt, Pd and Cu are the most suitable cases. A further comparison reveals that platinum[18], which is chemically inert and gives large room temperature recoilless fraction, f, is not well suited because of the large photoelectric and

compton scattering due to its high atomic number Z, as the latter will make the diffusion requirements for such a source extremely stringent. On the other hand copper matrices, while having large recoilfree fraction at room temperature and a low atomic number, are chemically unstable, since unprotected sources tend to react with atmospheric oxygen and sulphides which may be present in the ambient environment. A reasonable compromise between the various characteristics is provided by palladium host matrix, which in addition also gives a narrower line. Unfortunately this has also one disadvantage of having an X-ray of 21 keV falling near the 14.4 keV Mössbauer gamma-ray level, which may increase non-resonant back ground (in case of scintillation detector).

We on our part, procured commercially certified Co^{57}(Cu) and Co^{57}(Pd) sources each having initial activity of 1 mC. from Nuclear Science and Engineering Corporation, Pittsburg, Pa 15230, Pennsylvania and the Radio Chemical Centre, England, respectively. The first was used in studies of Tutton salts (Chapter IV) and chalcopyrite (Chapter III) while the other was used in studies of alkali dithioferrates(III) (Chapter V).

A passing remark may be made that suitable sources have been found for only a limited no. of radioisotopes and several new techniques using accelerators and reactors have been reported in the literature, most promising being the coulomb excitation and (n,γ) reactions. In these reactions produced sources there is a radiation damage which results into a reduction of recoil free fraction.

(A-ii) ABSORBERS (OR SCATTERERS)

A Mössbauer experiment can be performed either in a

transmission geometry or scattering geometry. While most of the investigators have followed the former, very few[104] have opted the latter. The scattering geometry experiments have some outstanding and special advantages over the transmission geometry but require high source strength (as the scattering cross section is less than absorption cross section by a factor of Γ/Γ) and careful attention to geometry and shielding which make this technique less attractive, however, employed the transmission geometry throughout our investigations. It may be pointed out that the absorber mounting materials must be Mössbauer isotope free as otherwise even in traces it may sometimes complicate the whole Mössbauer spectra[105].

(B) THE DRIVE SYSTEM

Mainly there are two types of drives, the mechanical and the electromechanical. The first category includes rotating inclined disc[106], cam[107], lead screw[108], pendulum[109], lathe[110], rotating cylinder[111], linkages, cable or chain[112] and crank[113], to provide a relative velocity to the source and absorber. The electromechanical drives[114] make use of transducers and speakers for providing this motion. In addition to these two distinct types, there are hydraulic drives and variable frequency ultrasonic drives[115] useful only in special cases. However it may be pointed out that these have been classified also as constant velocity[100,116,116] and constant accelaration[114] drives. In principle, any velocity function could be used in the operation of a spectrometer, but in these two modes the data analysis becomes much simplified.

In the constant velocity mode the source is moved

periodically at fixed, equal, positive and negative velocities and the transmitted gamma beam intensity is recorded in two different scalers one for positive and one for negative respectively. Thus on the constant velocity (also called two channel) mode the data is accumulated point by point in sets of periods (determined by the statistics) in systematic way about zero velocity. In electromechanical spectrometers the velocity function appropriate to this mode is a square wave function of time. On the other hand in the constant acceleration mode (also called multiscaler or time mode) the source is given a periodically fixed, equal, positive and negative acceleration and a multichannel analyser is used to record the transmitted gamma beam. Each channel corresponds to an equal velocity interval. Thus the system sweeps repeatedly through the range of velocities of interest, storing the instantaneous counting information in a large no. of channels. The velocity function appropriate to this mode is a triangular wave function of time. The relative merits and demerits of these two modes have been discussed by Flinn[109].

The mechanical drives are the first used in the Mössbauer spectroscopy and are discussed in details[103-12]. We will confine our comments to these only as it is the constant velocity cam driven drive which concerns in our investigations.

In addition to the mechanical drives being very simple straight forward in construction than their counterpart electromechanical drives they also often are less expensive and their associated electronics is also not much complicated. They have special utility when the experimental conditions require the movement of massive objects such as cryostats and

ovens and thus the problem of temperature control for sources or absorbers is considerably eased. They can also be constructed to provide quite high absolute accuracy in velocity. The absolute velocities instead of relative velocities (electromechanical drives) are measured and the velocity calibration can be achieved to a high degree of accuracy. Large massive and powerful drives may be used to ensure reasonably constant velocities at very low vibration level. Thus mechanical drive is potentially a very accurate instrument.

There are also certain disadvantages with these drives. The elimination of extraneous vibrations is a more difficult problem than that usually encountered with electromechanical transducers. Temperature dependence of the performance characteristics of the component mechanical parts may severely limit the long-time stability and reproducibility of such systems. It requires that the complete Mössbauer spectrum must be built up point by point and hence long term changes in the counting rate of the gamma-ray pulses due to the line voltage fluctuation, detector and amplifier drifts etc. become serious. Although it is possible to scan rapidly through a range of velocities by the use of a constant acceleration cam (Boardon, Hauser and Kalkorn Ref.107), but here again the electronic equipment, required to sort and store the data is very similar to that normally used with an electromechanical drive while mechanical problems are considerable. On the other hand the recording of the data point by point requires a lot of time and man hours. The use of automatic devices to vary the velocity sequentially and record the results of large no.

of counting periods at each velocity is of course possible (Flinn Ref.109 and Hanchar and Mullon Ref.110), but the prime importance of simplicity is thereby, largely lost. Bearing noise and friction are the major problems especially in passing through zero velocity where the familiar stick slip problem enters and these produce complicated velocity wave shape generally distorted sinusiodal motion which is of limited utility. Wear and tear of the mechanical parts often causes practical problems. Mechanical drives are useful only where recoilless fraction is sufficiently large for drifts in the counting channel to be unimportant and for a few hours to be sufficient for the plotting of a complete velocity spectrum. This is the reason that the use of mechanical drives is mostly confined to Fe^{57}.

In the following we describe briefly the salient features of our set up which required careful attention for satisfactory operation. A schematic sketch of top plan of the drive is shown in Fig.2.1.

(1) MOTOR AND GEAR BOX

The choice of drive motor is important and one exhibitting very little jitter in motion is necessary. This depends on the no. of segments in its armature and thus one with large no. of segments is preferrable. In addition the speed of the motor should be fairly constant under varying load conditions. We are using a small Dynamotor, D1-83-A2, manufactured by General Electric Company, U.S.A. It operates at 12 volts and 2.0 amp. and has 6000 rpm. A cabinet of lead accumulators was employed to supply a constant input voltage

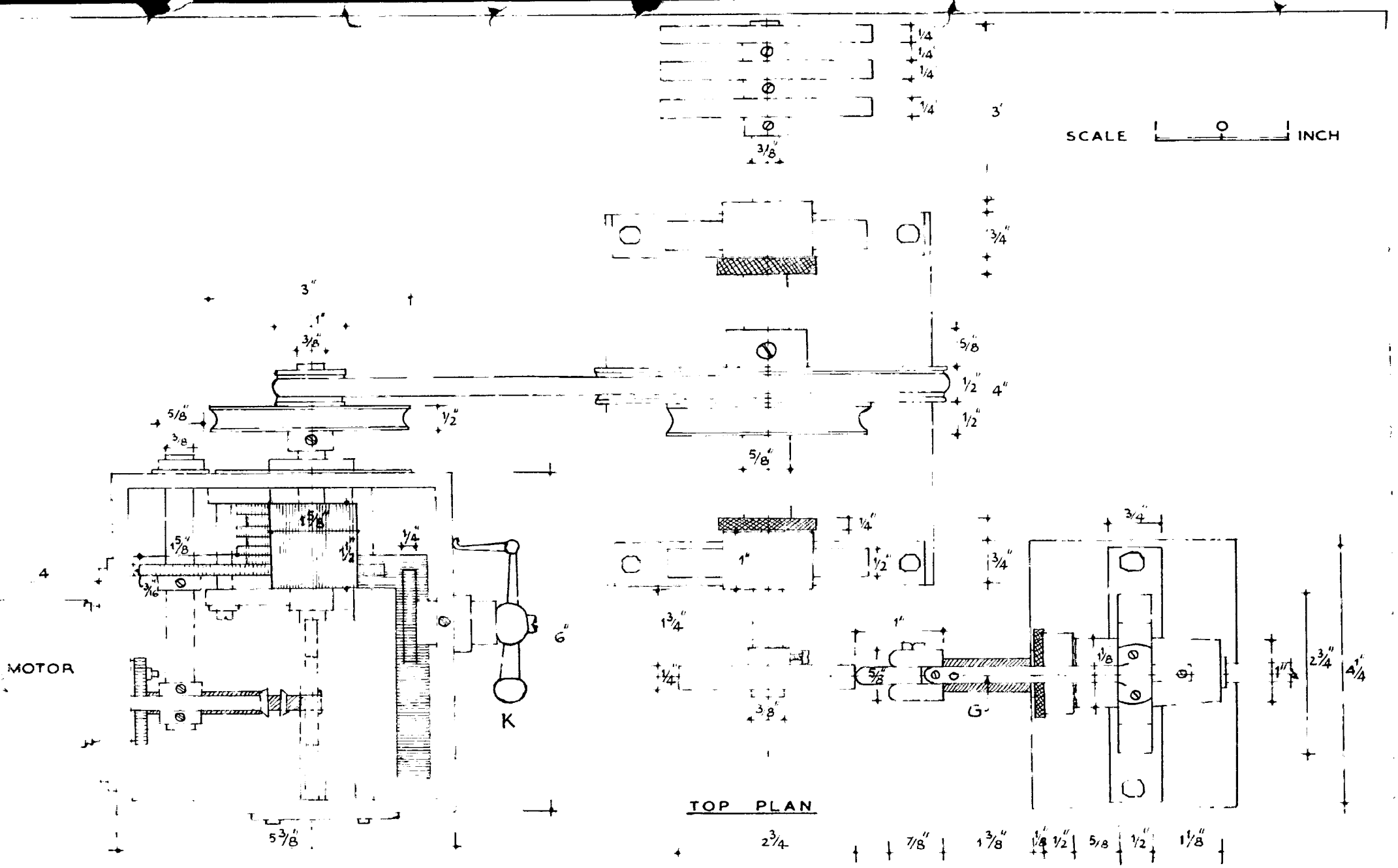

FIG.2-1. TOP PLAN OF THE CONSTANT VELOCITY DRIVE.

of 12 V. A potentiometric device is incorporated for the continuous variation of the velocity. The speed of the motor is reduced by fine toothed gears, with a worm gear at the first stage which brings down the rpm from 6000 to 60. It is further reduced by four sets of spur gears in steps of 1:2.5. The master gear attached with the main shaft can be connected with any of the spur gears with the help of control knob 'K'. Considerable care is taken in reducing the jerks and vibrations arising from the gears. A special grease H(ESSO) was found quite suitable for the purpose. A further reduction of the speed was obtained with the help of the set of aluminum pulleys. The most critical part of the setting up of the apparatus is that of coupling the gear box to cam drive shaft to transmit minimum vibrations from the motor to the source. Elastic 'O' ring belt is used for this coupling. It may be added here that the 'O' ring belt should not be either very tight or very loose as in the first case it may obstruct the uniform motion while in the latter case it may slip, which in turn may vary the velocity (decrease slightly) when the motor or cam system works against it. Therefore the tension of the 'O' ring belt should be loose enough to remove the maximum vibrations without being so loose to affect linear velocity of the source. This adjustment was carried out by sliding the table mounted with motor and gear box. To further ensure the cut in the transmission of motor and gear box vibrations to the cam driving shaft, the two assemblies were mounted on separate tables, also the tables were heavily loaded with lead bricks and were rested on pads of shock absorber cushions to insulate from the floor

vibrations.

(2) CONSTANT VELOCITY CAM

This is the most crucial and also the most difficult part of the drive. The shape of constant velocity cam should obey the curve $r = b\theta$. Cutting of the profile with an accuracy better than 10^{-3} cm/degree was experienced to be quite difficult. A cam cutting jig was designed as suggested by Mössbauer[107], and its plan is shown in Fig.2.2. The diameter of the rollers is chosen according to the total lift required (circumference of the roller is twice the lift of the cam). Six strong springs are used to make the tension greater than the grinding force to avoid slipping while cutting. Preshaped cam of ebonite (as this material requires lesser grinding force) is tightened on one roller and the handle is rotated slowly. Thus as the cam goes forward the grinder cuts the cam according to desired shape. It may be remarked that this machine does not necessitate the constant speed of the handle. Having cut half the cam it is inverted and the remaining half portion was grounded similarly. The profile is finally dressed with a 300 mesh emery paper in order to make it supersmooth. In order to avoid the instantaneous jerks at the two inflection points of the profile these were grounded smooth. One of these two positions was utilized in counting the no. of revolutions required to calculate the velocity of the cam (details of this will be given in the section on calibration).

The checking of the profile is done by mounting the cam on a shaft and noting the lift per degree with a precision dial-gauge (least count 0.002 mm). After a no. of attempts we succeeded in obtaining a profile of accuracy better than

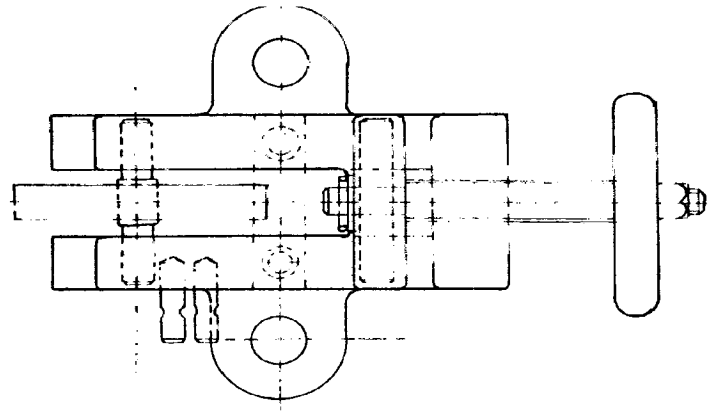

PLAN

SCALE 1 0 1 IN.

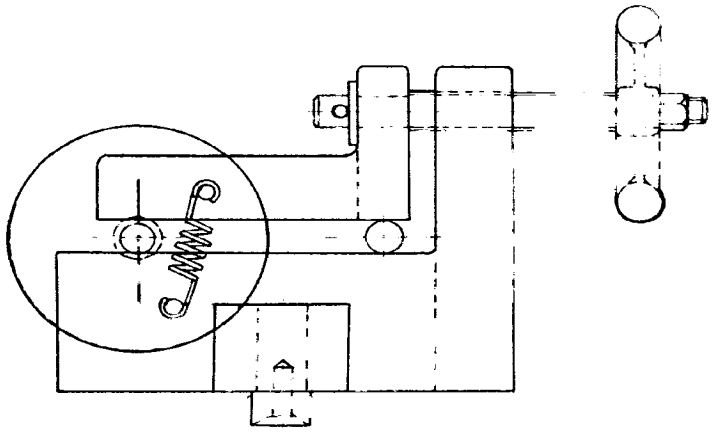

ELEVATION

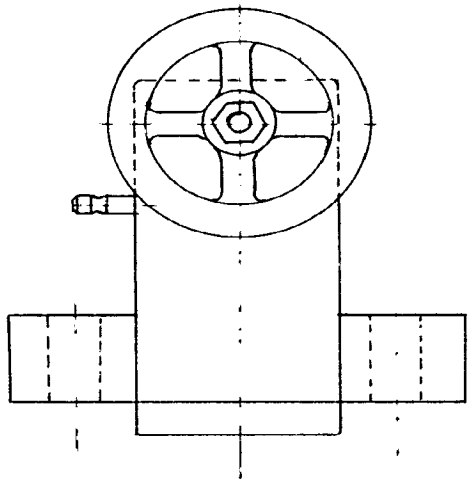

SIDE ELEVATION

FIG. 2-2. CONSTANT VELOCITY CAM CUTTING JIG.

10^{-3} cm/degree.

(3) CAM AND FOLLOWER ARRANGEMENT

The cam is mounted on a shaft supported by two self aligning double row ball bearings housed in two vertical walls. The follower, which is perpendicular to the shaft moves smoothly in a carefully machined perspex sleeve. One end of the follower is fixed with a Teflon bearing and is kept in contact with the cam by means of typewriter springs and on the other the source holder is mounted. The guide G was attached to eliminate any possibility of rotational motion of the follower. For a smooth running of the assembly and to avoid wear and tear with use, the whole system was lubricated with 3 in 1 oil.

(4) CONTROL UNIT

During one complete revolution of the cam, the follower moves to and fro at constant speed (giving both positive and negative velocities) except at the two extremities. The transmitted gamm-beam intensity in these two halves of the cam, was accumulated in two different scalers. Mercury switches were employed to select the proper scalers for positive and negative counts. The storing of pulses by these scalers when the cam is in the two extrimities giving either acceleration or deceleration, was excluded. Three perspex discs with platinum wires fixed in a manner that one end of it is slightly outside the disc's surface and the other in contact with the shaft, are mounted on the latter. These discs dip in the three mercury cups in rotation in one

revolution of the cam. Out of the three connections which are taken from the mercury cups, two connect 'on-off' switches to two scalers and timers, (called negative and positive scalers and timers) coupling one scaler and one timer at a time, and the third one goes to the grid of the power amplifier. The power amplifier in turn drives the revolution recorder, Fig.2.3. The common terminal connected to shaft is grounded. The distances traversed by the follower during these gated parts of these negative and positive motion have been determined with the help of a dial gauge.

(5) ELIMINATION OF VIBRATIONS

As already stated we have used Co^{57} as a Mössbauer isotope which has a natural line width, Γ of the order of 0.1 mm/sec. Thus to make the instrumental broadening negligible, any velocity ripple (vibration) must be kept to a very small fraction of Γ . Mechanical vibrations were eliminated step by step in each of the drive. The final check up is done at the follower stage in the following manner.

The source holder is detached from the follower and and a cylindrical soft iron core is mounted on it which moves in the solenoid having primary and secondary winding (working as differential transformer). The primary is energised by 10 kc/s sinusoidal frequency from an audio-oscillator. The induced voltage produced in the secondary due to the motion of the core is fed to the $(YY)_a$ plates of the double beam cathode ray oscilloscope. An artificial pulse is also applied to the $(YY)_b$ plates through the mercury switch which determines the gated portion of

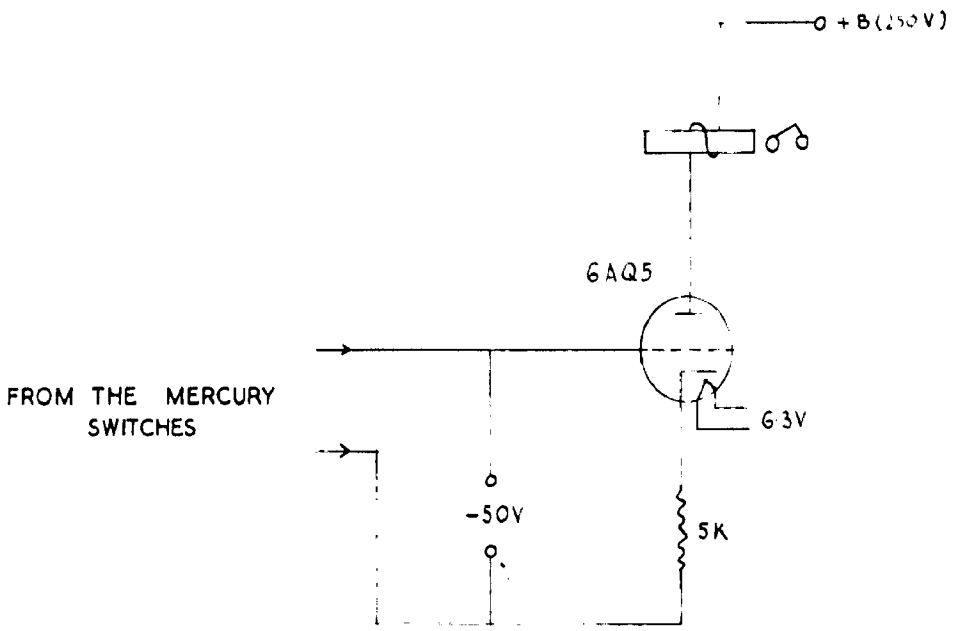

FIG 2·3. CIRCUIT DIAGRAM FOR THE REVOLUTION COUNTER.

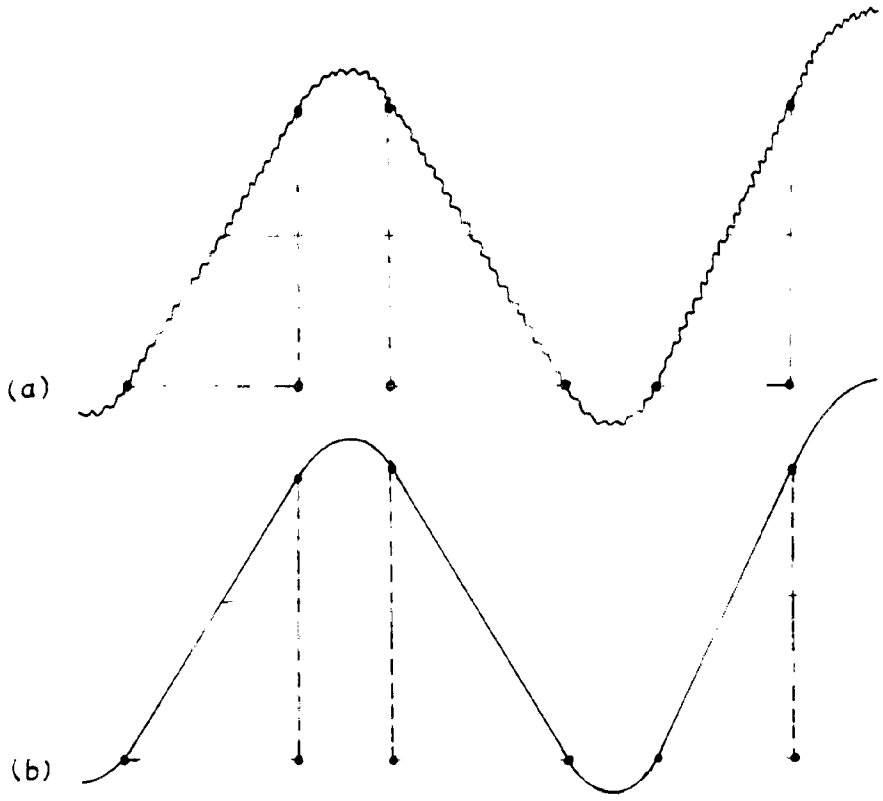

FIG. 2·4. OSCILLOSCOPIC TRACE OF THE PATH OF THE FOLLOWER (a) VIBRATIONS COUPLED (b) VIBRATION FREE AFTER REPLACING METAL-METAL CONTACT TO METAL-FIBRE CONTACT.

the cam during which pulse counting is operative. The shape of the oscilloscope trace is displayed in Fig.2.4(a). Having observed all necessary precautions such as alignment, change of metal-metal contact to metal-fibre contact; Fig.2.4(b) shows the final trace. This corresponds to the vibration free motion within the accuracy of the method.

However we did not get as narrow lines in the spectrum of Fe^{57}(Cu) vs Fe metal as predicted by theory. This happened at velocities more than 2.5 mm/sec and thus the outerlines were some what more broadened. This could be due to the lack of absolute constant motion, poor velocity resolution and or stability of electronic circuitry. The specification of our velocity drive are summarised in Table 2.1

TABLE 2.1: Specifications of the Mechanical drive used for Doppler tuning the source.

(i) Mode of tuning	linear constant velocity
(ii) Velocity limits	Variable in the range -12.5 mm/sec. to + 12.5 mm/sec.
(iii) Velocity accuracy	Constant within ± 0.05 mm/sec.
(iv) Length of the stroke (Lift)	Variable from 0 to 4.5 mm/sec.
(v) The ratio of the spur gears	1:2.5
(vi) Ratio of the pulleys	1:1 and 1:5
(vii) Input voltage for D.C. Motor (DM-53-AZ, GE Co. U.S.A.) with initial rpm after worm gear equal to sixty.	12 volts D.C. at 2.5 amps.

(C) THE DETECTION SYSTEM

To date the Mössbauer effect has not been observed for

γ-ray energies greater than 150 keV and thus the detection of such energies comes under the low energy detection techniques. In practically all the cases, the requirement for energy discrimination to distinguish the Mossbauer radiation from a complex gamma spectrum, coupled with need for maximum available efficiency, dictates the nature of the detector.

Three types of counters are available for this purpose

(i) NaI (Tl) scintillation counter

(ii) Proportional counters , and

(iii) Ge(Li) solid state counters

We have worked with Co^{57}(Cu) and Co^{57}(Pd) sources and for these the NaI(Tl) scintillation is satisfactory. As the energy of the radiation increases, proportionately thick crystals are used. The appropriate thickness is chosen such that the crystal essentially absorbs most of the Mössbauer ratiation, but it remains thin and hence inefficient for the higher energy radiation, e.g., a thick crystal in our case will degrade the 137 and 123 keV γ-rays to lower energies through compton effect so much so that a part of it will be accepted by the Pulse Height Analyser (PHA) window present for 14.4 keV γ-ray (Housley et al. Ref.103). Furthermore, the associated X-rays of 6.5 keV will not be resolved and also unsuitable for 14.4 keV γ-ray due to its self absorption. These considerations lead one to work with a 1 mm or 2 mm thick NaI(Tl) crystals. An energy resolution for 14.4 keV of the order of 45-50/ was attained which is comparable to those reported in the literature. In addition to a thin Al foil at the face of the crystal we have used

a 0.001 thick Al foil as a window in the collimation of the detector which will further suppress the 6.5 keV X-rays and will help to increase the signal to noise ratio.

A block diagram of the circuitry used is shown in Fig.2.5. The 1 cm NaI(Tl) crystal was mounted on a RCA 6342 photomultiplier and the high voltage stabilised power supply (Type HV65A Atomic Energy Establishment Trombay, India) was used. The circuit diagram for photomultiplier head is given in Fig.2.6. The photomultiplier is coupled to a linear amplifier and a single Pulse height analyzer (model 600 B, Eldorado Electronics, Berkeley, California) through a white cathode follower, Fig.2.7. The discriminator setting of the PHA was adjusted so that the photopeak correspondence to 14.4 keV is selected. The output of the analyser is connected simultaneously to two Decade Scalers (DS 325, Electronic Corporation of India, Hyderabad) which store separately the pulses for the negative and positive velocities. Two more scalers are used in the time mode for measuring the time for negative and positive velocities and were connected to each of the counting scalers. A fixed 1kc/sec crystal controlled oscillator was used for timing.

For completeness, the settings of the amplifier and PHA etc. are, H.T. = + 980 V, gain = 1000, channel width = 6 V, and threshold = 12.5 Volts. Input voltage stabilised within ± 1 Volt was used for the electronic assembly.

2.3 CALIBRATION

The source can be mounted in a perspex holder which can easily be screwed with the follower of the velocity drive.

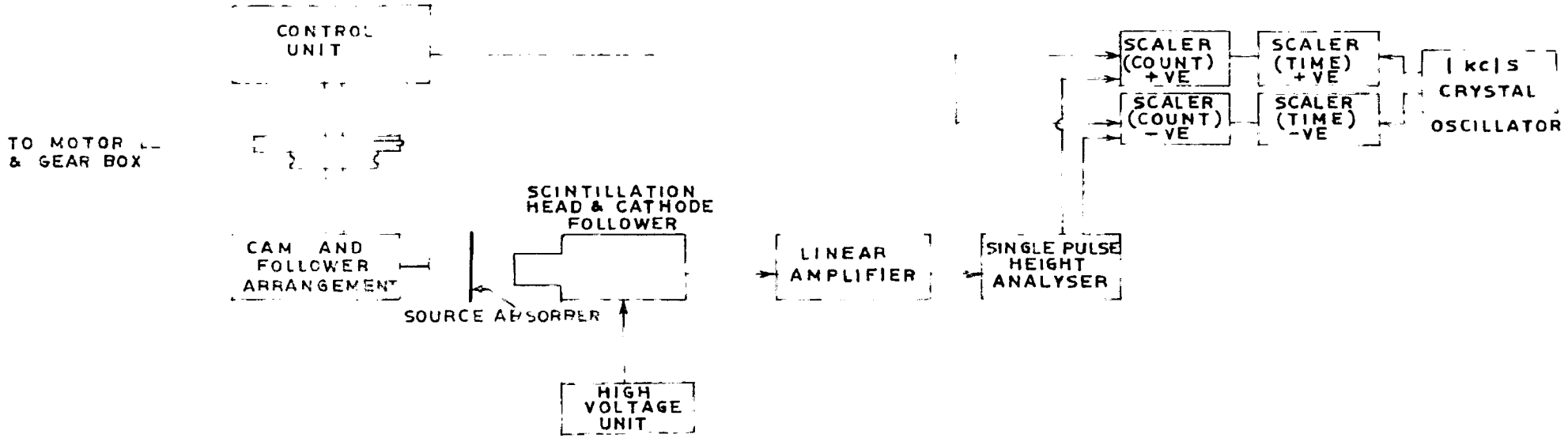

FIG.2·5. BLOCK DIAGRAM OF THE RADIATION DETECTION CIRCUITRY.

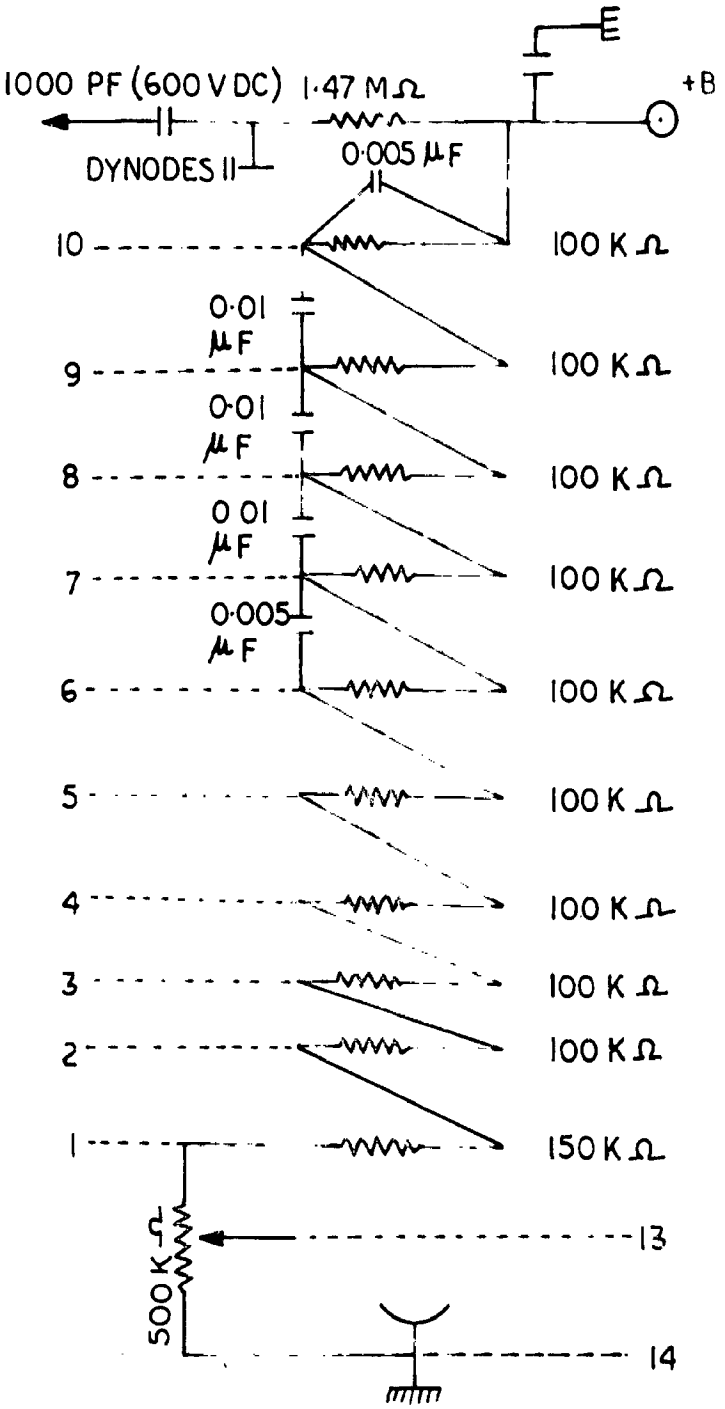

FIG. 2·6 THE CIRCUIT DIAGRAM FOR PHOTO MULTIPLIER(RCA 6342) HEAD

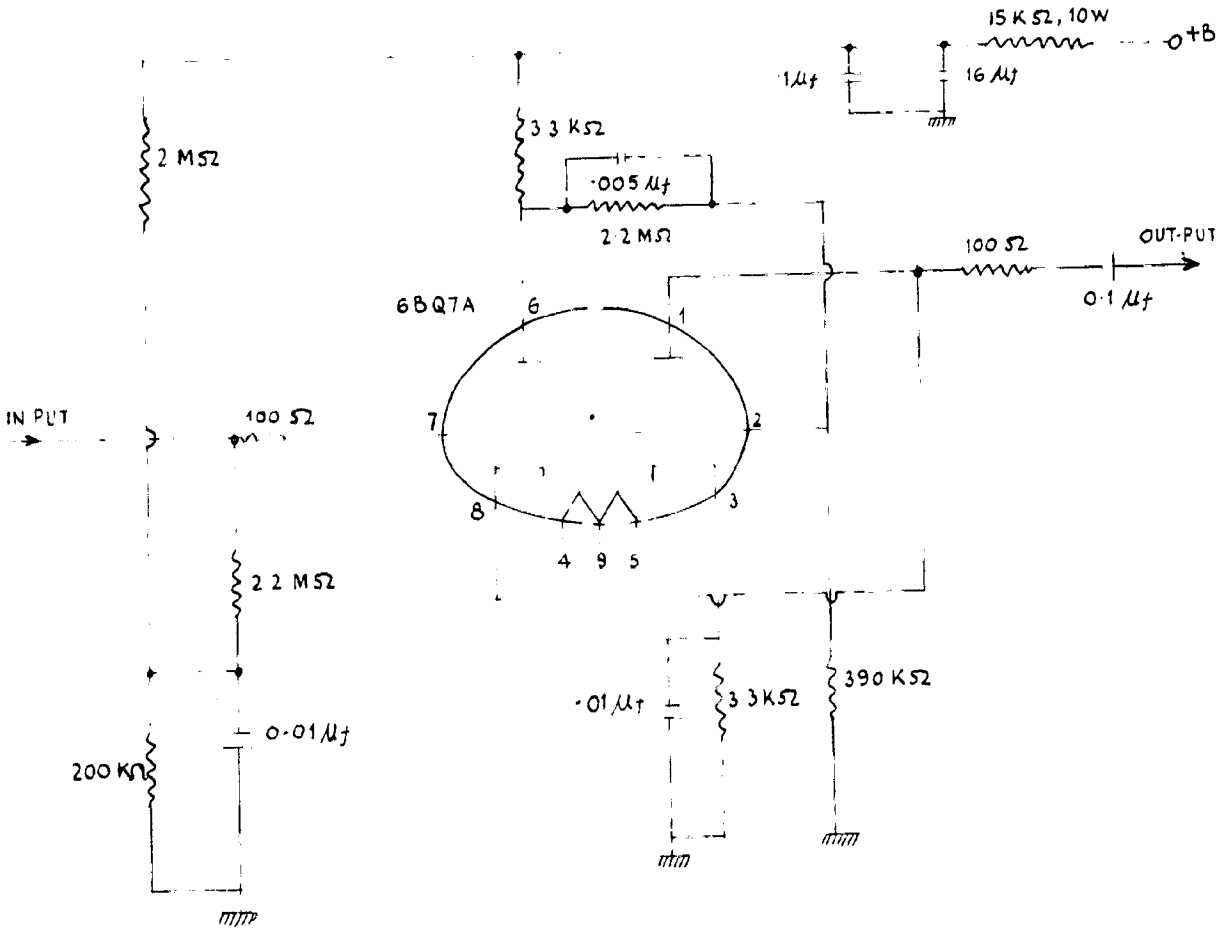

FIG. 2·7. WHITE CATHODE FOLLOWER.

Collination of the γ -ray beam is done by placing lead bricks with a 1/4" hole along the line joining the centres of source and absorber. This is considered essential to eliminate the scattered intensity from entering the detector. The source and detector distance varied during the course of experiments as dictated by the temperature arrangement. At room temperature it was approximately 5" with the absorber placed in the middle.

It has become conventional in the Mössbauer experiments to define positive velocity as the motion of the absorber towards the source, or source towards the absorber. The positive and negative velocities of the cam at any given D.C. voltage to motor and with certain gear ratio is calculated by the no. of revolutions recorded by the revolution counter, the effective lift of the cam follower, predetermined by the dial-gauge (limited by the mercury level settings) and the time recorded by the timer in those revolutions. If L_+ is the lift when the source moves towards the absorber, n the number of revolution and T the time taken, then the positive velocity is

$$V_+ = \frac{L_+}{T} \times n$$

Although absolute measurements of length and time are possible in such mechanical drives it was considered imperative to take few standard sample spectra to calibrate the drive. The Mössbauer spectra with Co^{57} (Cu) source were taken of natural 310 Stainless steel absorber of thickness 0.001" (supplied by Nucl. Sci. Engg. Corp.), $K_4Fe(CN)_6.3H_2O$, $K_3Fe(CN)_6$, $FeSO_4.7H_2O$, and $(NH_4)_2Fe(SO_4)_2.6H_2O$ and iron metal.

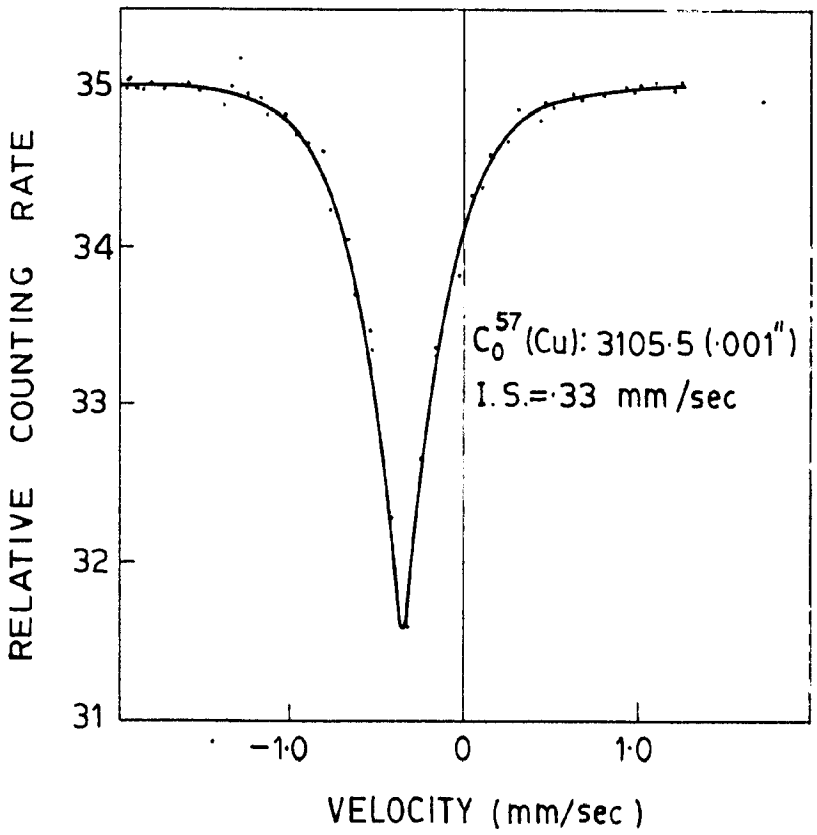

FIG. 2·8 ISOMER SHIFT. THE EFFECT OF ELECTRIC MONOPOLE INTERACTION IS TO SHIFT NUCLEAR LEVELS WITHOUT LIFTING THE SPIN DEGENERACY.

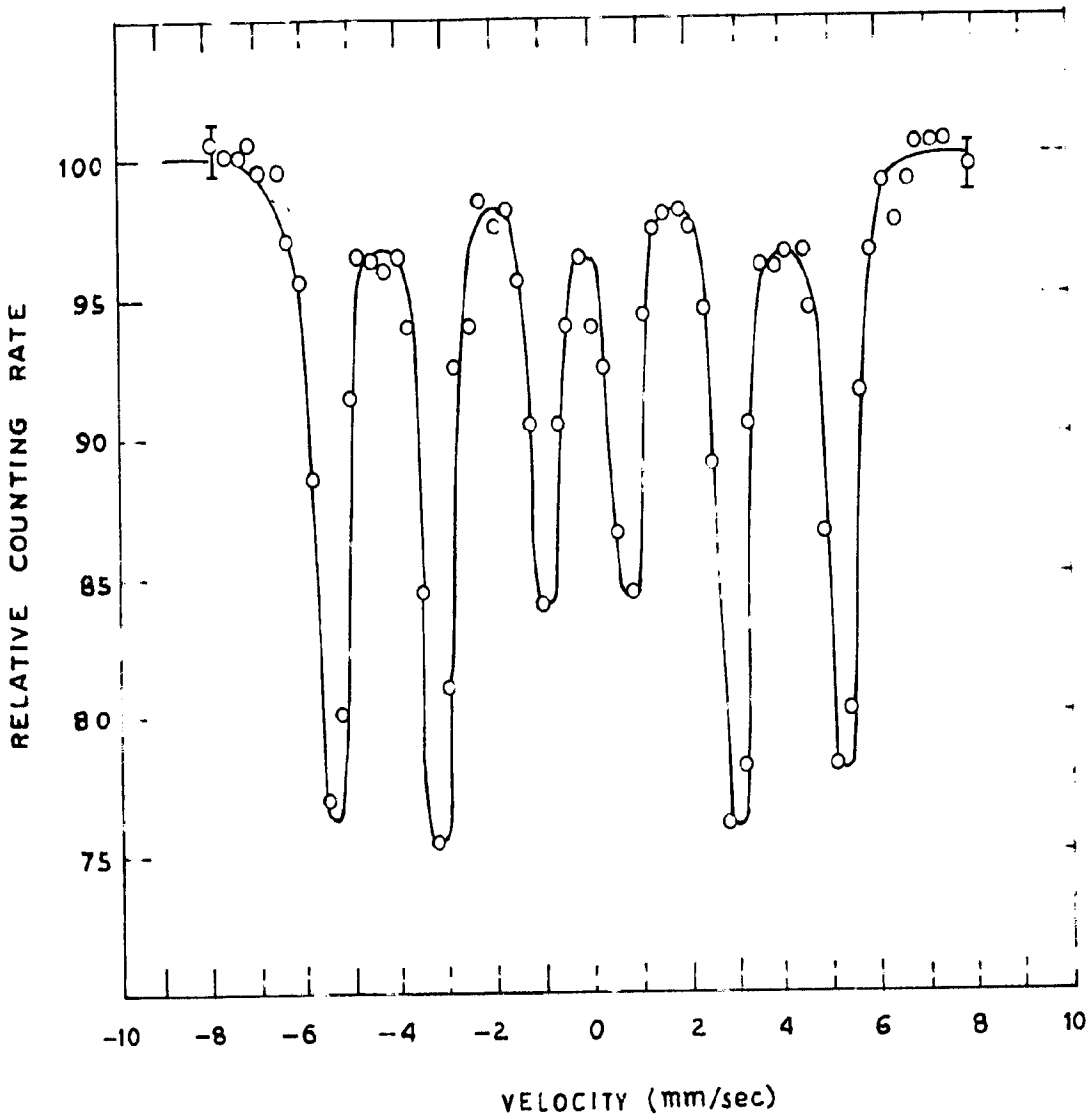

FIG. 2·9. MÖSSBAUER ABSORPTION SPECTRUM OF Fe^{57} IN METALLIC IRON SHOWING THE MAGNETIC HYPERFINE STRUCTURE.

To indicate the quality of the spectra, we give two of these in Fig.2.8 and 2.9. Fig.2.8 shows an unsplit single line Mössbauer spectrum of the stainless steel absorber. The line width (FWHM), = 0.48 mm/sec and I.S. = 0.36 mm/sec (w.r.t. Co^{57} in Cu) agree with those reported in literature[3] within the experimental accuracy. The line width which is more than two times than the natural line width of 0.2 mm/sec. predicted theoretically[5] is because of the unresolved magnetic hyperfine interaction. Fig.2.9 shows the Zeeman split six fingered pattern for a iron metal foil (also obtained from Nuclear Sci.Engg. Corp.). The line width of the internal two lines is 0.3 mm/sec. but the other lines get broadened due to the instrumental vibrations. The intensity ratios of these lines are approximately 3:2:1 and the I.S. = 0.32 ± 0.02 mm/sec., Q.S. = 0.08 ± 0.02 mm/sec and internal magnetic field (H) = -330 ± 5kOe, which are in good agreement with those reported in the literature[93]. It has only recently been pointed out[117] that Fe^{57} enriched iron foils often have reduced splittings and asymmetrical broadened lines and this is explained due to the presence of slight carbon impurities.

2.4 TEMPERATURE VARIATION

To study the temperature dependence of the Mössbauer parameters the low and high temperature arrangements were needed. A good review of the cryogenic arrangements, details of their design and construction and the circuit for their control can be found in the literature[14,31,118]. We worked in our lab only at fixed temperatures viz. freezing mixture = -20°C, solid carbon dioxide-acetone = -78°C and liquid air=-196°C. For this a very simple cryostat, was used and

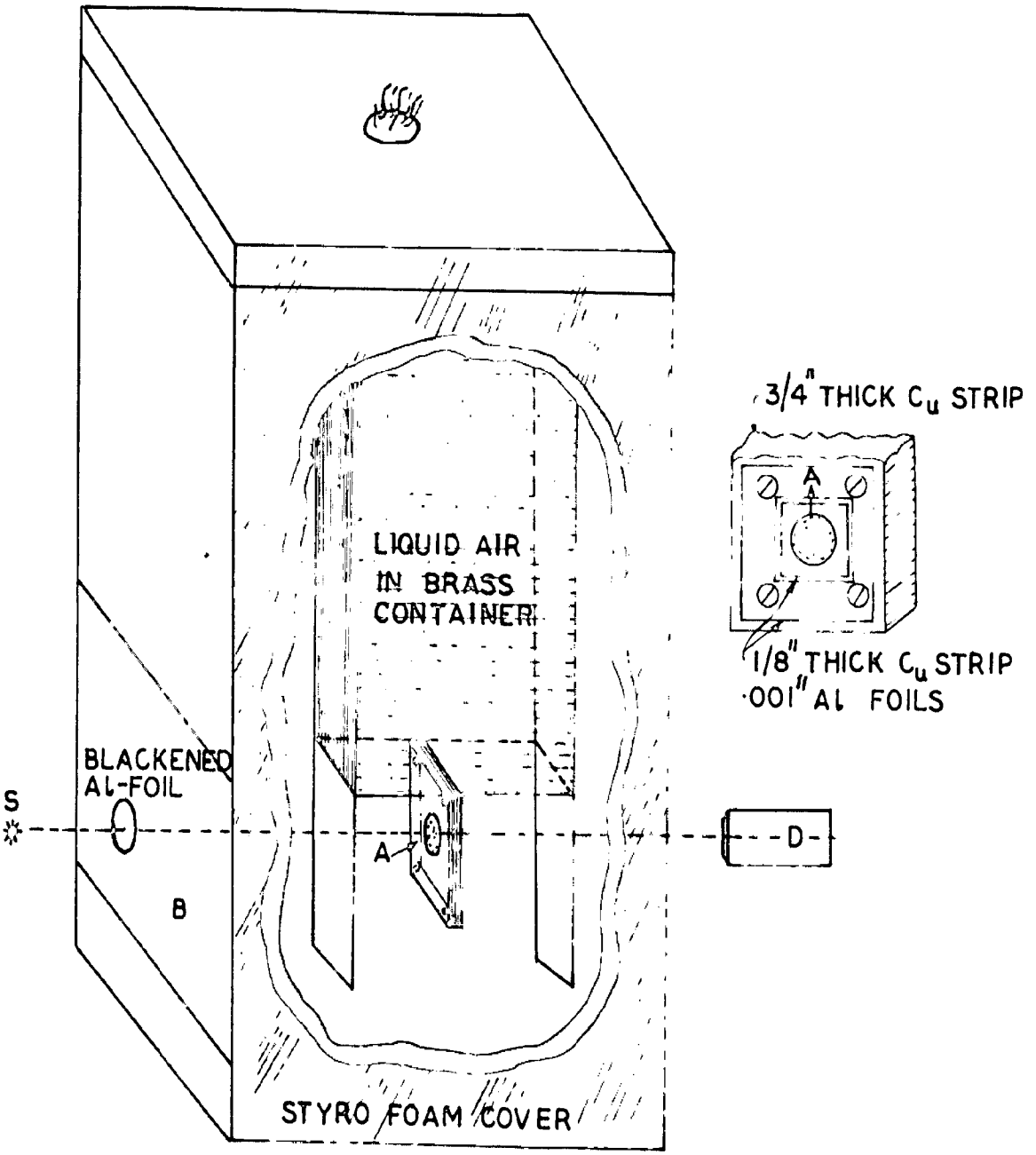

S-SOURCE A-ABSORBER D-DETECTER B-BLACK PAINTED Al FOIL TO AVOID CONDENSATION

FIG. 2·10 LOW TEMPERATURE ARRANGEMENT

relevant details of assembly and arrangement are indicated in the Fig.2.1i. The absorber in the fine powdered form were pressed between two thin mica sheets and was sandwiched in the strip and the absorber holder. The temperatures of interest were obtained by trial and got stabilised for about 10 hours with manual operation of the variac. The temperature monitoring was done by a calibrated thermocouple.

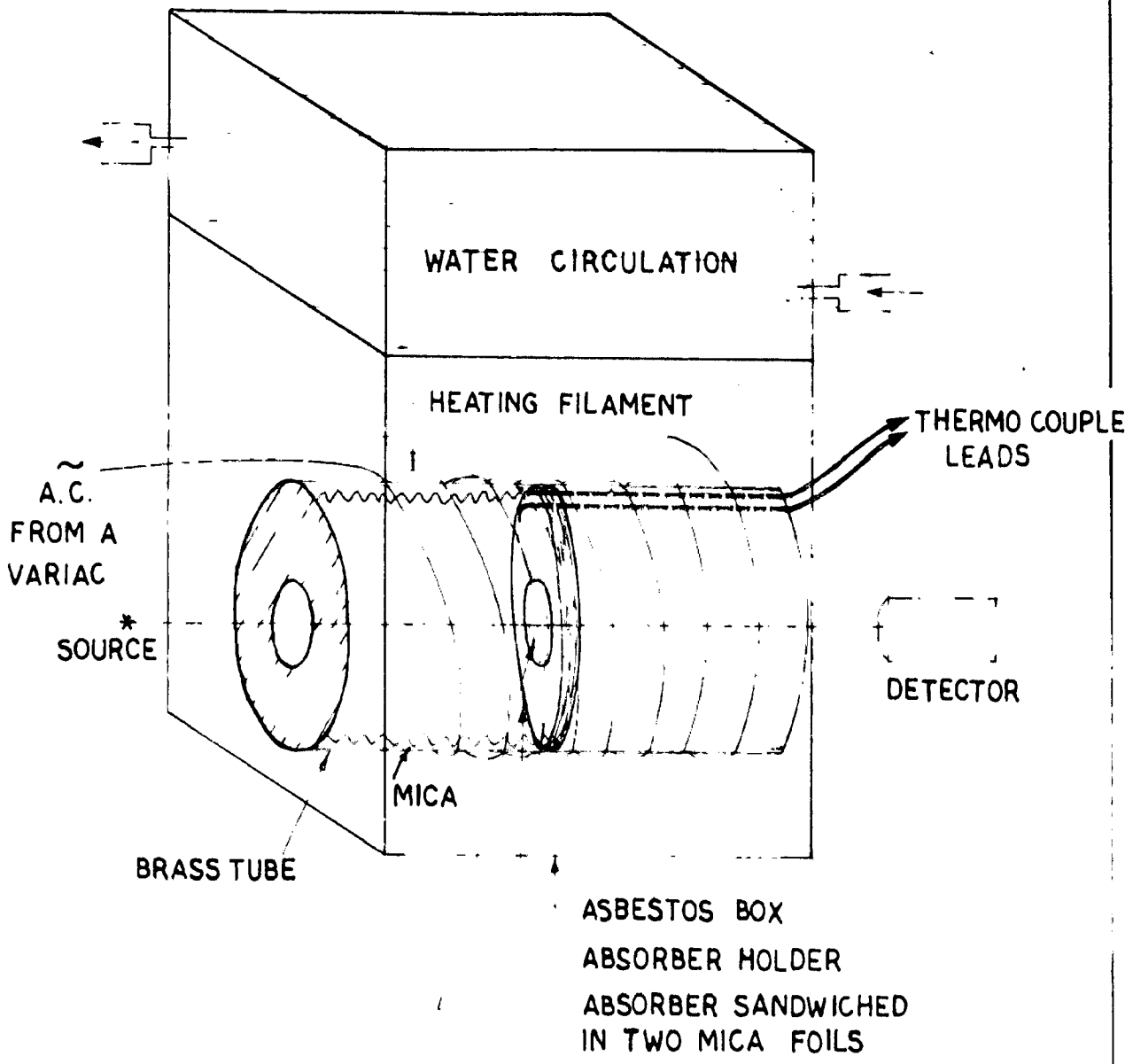

FIG. 2·11 HIGH TEMPERATURE ARRANGEMENTS

CHAPTER III

MÖSSBAUER EFFECT STUDIES OF CHALCOPYRITE

3.1 INTRODUCTION

Chalcopyrite, $CuFeS_2$ (also known as copper pyrite), is a distinct naturally occurring copper mineral in the family of Cu-Fe-S system[119]. It is a semiconductor[120] with ZnS structure and has been a subject of intense study regarding its electric and magnetic properties[121-22]. Neutron Diffraction studies[123] showed it to be antiferromagnetic at least at room temperature, with μ_{eff} values equal to $3.85\mu_B$ for Fe and $0.2\mu_B$ for Cu, and the Neel temperature of 550°C. This confirms to the observation[124] that there is a transition at about 550°C below which the crystal structure is an ordered arrangement of Cu and Fe and above which the structure is that of calcium fluoride. Austin et al.[120] observed the infrared absorption and the Hall effect of natural crystal of chalcopyrite and obtained 0.5 eV as the energy gap and 30 cm^2/volts sec as the mobility of positive holes. Winterberger[121] also made the Hall measurements and determined the sign of the carriers as negative. He observed that the conductivity decreases when copper is partially replaced by silver but increases if copper is replaced by iron or vice versa. These results agree with that of Yoranishi[122] who made observations of Hall effect of natural single crystal and synthetic $CuFeS^{\circ}_{1.9}$ over a temperature range extending from

---

° Chalcopyrite Contains less sulphur than is indicated by the $CuFeS_2$ formula. Its composition is expressed as $CuFeS_{2-x}$. It is yet not known whether this formulation has structural validity.

150°C down to liquid nitrogen. Toranishi has illustrated the temperature dependence of Hall coefficients and number of charge carriers and inferred the sign of Hall coefficient to be negative. Moreover he carried out the room temperature measurements of thermoelectric power of the natural single crystal w.r.to copper and obtained a large value of -450 μV/deg. These thermoelectric power measurements suggest[122] that Fe atom is principally covalently bonded with sulphur atoms in the tetrahedral (sp^3) hybrid orbitals structure. The magnetic torque, powder susceptibility and their temperature dependence of a natural single crystal also suggest[122] that chalcopyrite is a typical antiferromagnet with T_N = 550°C.

In addition thermal stability of chalcopyrite has been studied and the decomposition temperatures as suggested by various workers[121,125] range from 200 to 547 ± 5°C. While Yund and Kullerud[119] give the decomposition temperature as 547 ± 5°C, Vintonberger gives this limit as 200°C only. Fruch[125] predicted this temperature limit to be below 350°C which is the temperature limit for intrinsic conduction.

There has been a confusion in literature about the X-ray structure and the charge states of the copper and iron atoms as varied results have been obtained in attempts to determine the valence states of these atoms. Read[120] et al. titrated a solution of the mineral with potassium permanganate, and considered that iron is present in the ferrous, not ferric state, and they suggested that chalcopyrite is marcasite, with part of the iron replaced by copper. This was in agreement to the earlier works using cryoscopic and electrolytic methods which designated both metals as divalent. Measurements

of X-ray absorption edges[127] suggest that copper is present in two valence states so that resonance between $Cu^{+}Fe^{3+}$ and $Cu^{2+}Fe^{2+}$ may be present. From the considerations of lattice constants and ionic radii of cations, Pauling and Brockway[128] infer that the atoms have fixed valencies but fluctuate between $Cu^{I}Fe^{III}S_2$ and $Cu^{II}Fe^{II}S_2$, the iron atom resonating between Fe^{III} and Fe^{II} states. However, the neutron diffraction studies indicate that iron atom is in the Fe^{III} state. Teranishi[122] has pointed out that by making detailed studies of electric and magnetic properties one cannot obtain the accurate knowledge of the valence state of the transition metals, but has suggested a sp^3 hybrid orbitals structure and d^5 state for iron atom.

To resolve this controversy over the charge state of iron, the Mössbauer effect studies were considered worthwhile because of the following considerations. As the mineral has the desirable features of being semiconductor and antiferromagnetic, these render feasible the detection of the two charge states Fe^{III} and Fe^{II} through the magnetic interaction. Furthermore, the value of isomeric shift and the temperature dependence of quadrupole splitting, under special cases, can also indicate the charge state of an ion. In addition it is desirable to account for the magnitude of the internal magnetic field at the Fe nucleus.

Many workers[129-39] have investigated the Mössbauer effect studies of this mineral. The available data for the hyperfine interaction parameters of some of these workers is compiled in Table 3.1 for the case of comparison and will be discussed in the text latter on. We have studied[129] this

mineral in the temperature range 300° - 448°K. The spectra showed a typical pattern of six absorption lines due to the internal magnetic field at all these temperatures. The quadrupole splitting values are negligibly small and are temperature independent whereas the magnitudes of the internal magnetic field are 325 ± 10, 312 ± 10 and 290 ± 10 kOe at 300°, 373° and 448°K respectively. These features are explained by assuming that Fe atom is in a spin free, trivalent state in weak crystal field configuration. The interanal field is accounted to originate primarily through the Fermi contact interaction, H_c. In the following pages we have given the detailed version of these observations and results. In the end is presented a critique[139] of the paper of Aramu et al.[130]

TABLE 3.1: MÖSSBAUER STUDIES OF CHALCOPYRITE BY OTHER INVESTIGATORS.

Investigator	Temperature °K	Isomeric shift w.r.to Fe) mm/sec.	Quadrupole coupling constant e(mm/sec.	Internal magnetic field H (kOe)
Aramu et al. (Ref.130)	Room	0.32 ± 0.03	0.60 ± 0.03	0.0
	77	0.40 ± 0.03	0.65 ± 0.03	0.0
E. Frank (Ref.134)	295	0.26 ± 0.01	0.0 ± 0.01	352 ± 3
	78	0.28 ± 0.02	0.0 ± 0.02	370 ± 5
Greenwood and Whitfield (Ref.135)	295	0.233	-0.02	356
	77	0.373	-0.03	368
Piekoszewski et al. (Ref.136)	Room	-	-	356 ± 5
Goodman and Cabri (Ref.137)	Room temperature	0.0	-	246

3.2 STRUCTURE

(A) X-RAY AND CHEMICAL

Many compounds, which have the same crystal structure

as chalcopyrite are known[140] . These have the general formula, ABX_2 where A represents monovalent ion Ag^+ or Cu^+ and B is a trivalent ion Al^{3+}, Ga^{3+}, In^{3+}or $Tl^{3+}$and X is S^{2-}, Se^{2-} or in some cases Te^{2-}. Although having apparently the same structure, $CuFeS_2$ is a peculiar member of this series in the sense that both A and B are transition elements which make its properties distinct and interesting.

Chalcopyrite is found in two phases α and β. The β phase, also called the cubic chalcopyrite, refers to a f.c.c. high temperature polymorph of chalcopyrite. We are concerned here with the tetragonal α-phase and will discuss only this.

There are two structure determinations of this mineral: that of Burdick and Ellis[141] and that of Pauling and Brockway[128] (henceforth abbreviated as PB). These two structure determinations differe from each other in atomic positions of copper and iron atoms, magnitude of the axes and the number of molecules per unit cell, Fig.3.1(a) and (b).

Pauling and Brockway[128] using Mo radiation studied a crystal from Joplin, Missouri, by Laue and Oscillation techniques and by studying Laue diagrams showed that the c axis length had to be doubled. They obtained the following cell constants.

$$a = b = 5.24\text{Å} \quad \text{and} \quad c = 10.3\text{Å}$$

and derived the space group $D_{2d}^{12} - I\bar{4}\,2d$.
There are 4 molecules per unit cell. The atomic positions are

$$(0,0,0;\ 1/2,1/2,1/2) +$$

4Cu at(a): $(0,0,0;\ 1/2,\ 0\ ,1/4)$

4Fe at(b): $(0,0,0;\ 1/2,\ 0\ ,3/4)$ and

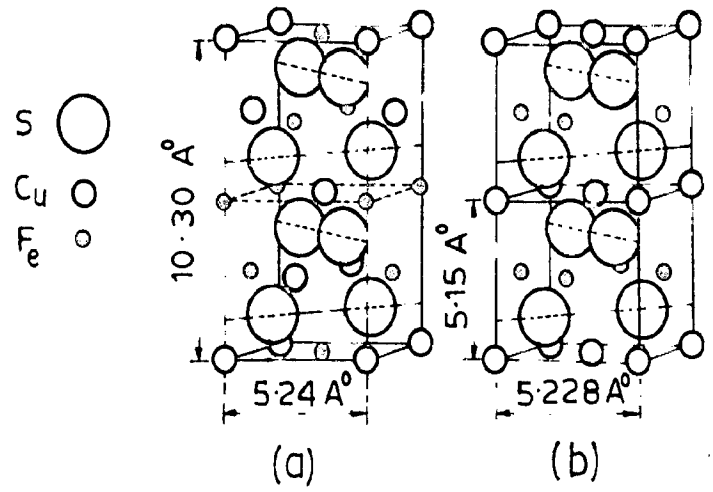

(a) ACCORDING TO PAULING AND BROCKWAY (REF. 128)
(b) ACCORDING TO BURDICK AND ELLIS (REF. 141)

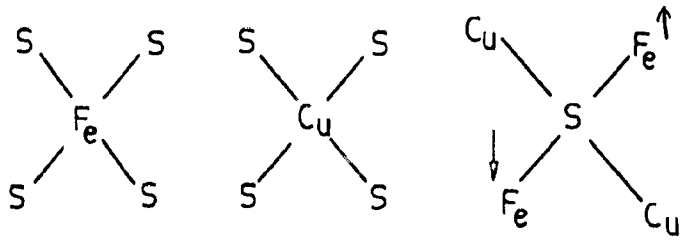

(c)

POINT SYMMETRY OF Fe, Cu & S ATOMS

FIG.3·1 X–RAY STRUCTURE OF CHALCOPYRITE

8S at (d): $(1/4, x, 1/8;\ x, 3/4, 7/8;\ 3/4, \bar{x}, 1/8;\ \bar{x}, 1/4, 7/8)$

with $x = 0.27 \pm 0.01$

Metallic atoms are surrounded, as in ZnS by tetrahedra of sulphur atoms while each sulphur has a tetrahedron of metallic atoms, two of which are copper and two iron, Fig.3.1(c). The significant interatomic distances are

$$Fe - S = 2.20 \pm 0.03\text{Å}$$
$$Cu - S = 2.32 \pm 0.03\text{Å}$$
$$S - S = 3.86 \pm 0.03\text{Å}$$

Such separations are compatible with either ionic or neutral 'covalent' bonds for $CuFeS_2$; if the bonding is considered ionic, this crystal appears as a slightly distorted cubic close packing of large S^{2-} ions with metal ions in the interstices.

In 1944 Boom[142] re-examined the structure of chalcopyrite using Co K radiation in order to increase the effective difference in the scattering powers of copper and iron, thereby enhancing the intensities of those reflections to which copper and iron atoms contribute with opposite phases. He confirmed the FD structure and also that iron is principally covalently bonded. Recently X-ray data of Chalcopyrite is reported by Berry and Thompson[143] with space group $D_{2d}^{12} - I\bar{4}2d$, $a = 5.280\text{Å}$, $c = 10.409\text{Å}$, $z = 4$ and with atomic positions for

4 Cu in (a) (0,0,0)
4 Fe in (b) (0,0,1/2) , and
8 S in (d) (x,1/4, 1/8)

with $x = 0.27$

(B) MAGNETIC STRUCTURE

Donnay et al.[123] in 1959, undertook the neutron diffraction studies of natural chalcopyrite and established that magnetic space group is $I\bar{4}2d$ and confirmed the FD structure. These studies indicate that the structure consists of an arrangement in which the two iron atoms connected to a common sulphur atom have oppositely directed moments, Fig.3.2. The evidence provided by the magnetic structure of $CuFeS_2$ strongly suggests that this interaction is antiferromagnetic. A value of $3.85\mu_B$ is found for the iron moment and $0 \pm 0.20\ \mu_B$ for copper moment. These values led to the assumption that copper is monovalent and that iron is trivalent and are consistent with a simple covalent model in which each atom in the structure is bonded to its nearest neighbours by means of four sp^3 hybrid orbitals. This suggests a value of magnetic moment for Fe as $5.9\mu_B$. They explained this discrepancy, qualitatively, by postulating a further participation of the 3d electrons of iron into covalent bonding. This would be expected to decrease the iron moment and at the same time to strengthen the iron sulphur bonds. This idea is supported by the fact that the sulphur atoms are displaced from the centre of the metal tetrahedra towards the iron atom pairs. Furthermore, the neutron diffraction data ruled out the possible existence of second chalcopyrite modification in nature; suggested by conflicting results on materials of Japanese origin, as specimens from both Ugo, Japan and Joplin, Missouri are found to have the same structure.

3.3 EXPERIMENTAL

The specimen as used was a naturally occuring chalcopyrite

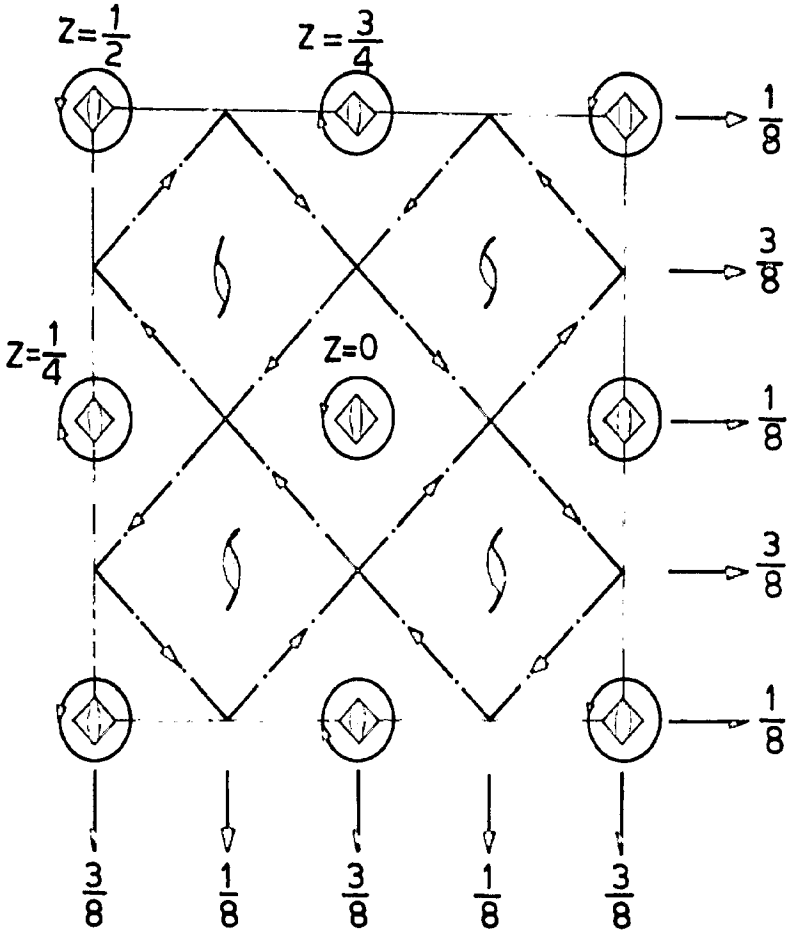

FIG. 3.2 RELATIONSHIP OF IRON MOMENTS TO SYMMETRY ELEMENTS OF SPACE GROUP I $\bar{4}2d$ MOMENTS INDICATED SCHEMATICALLY AS CURRENT LOOPS, ARE LOCATED AT THE INVERSION POINTS OF 4 AXES AND ARE DIRECTED ALONG THE C AXIS. Z COORDINATES GIVE THE FRACTIONAL DISTANCES OF ATOMS ABOVE THE PLANE OF PROJECTION (AFTER DONNAY et al. REF. 123)

crystal°, selected for its purity by the microscope examination. The structure was examined by X-ray diffraction°° and tallied with FD structure. This crystal was powdered to 300 mesh and sandwiched between two thin Al foils (0.01 mm thick), the latter jacketed into two thick copper rings which can move into a miniature oino furnace and can be fixed in its centre. The data were recorded at the three temperatures 300, 373 and 448°K. The typical spectra so obtained are shown in Fig.3.3.

3.4 ANALYSIS

In the presence of electric and magnetic interactions, as discussed in detail in chapter I, the closed form solutions of the Hamiltonian are only possible in special cases. In past few years, computer programs[95] have been made to combat with more general cases with the help of which the data is fitted in an iterative manner to have consistent values of all the unknown parameters. But this procedure takes much of the computational time and requires fast computers. Here we have made use of the symmetry and some approximations to evaluate the unknown hyperfine parameters with ease and simplicity. We know that iron has a regular tetrahedral point symmetry and for a regular tetrahedral disposition of ligands the quadrupole coupling constant C and the asymmetry parameter η both must vanish[12]. On the other hand, in Fig.3.3, we see that compared with a spectrum showing pure magnetic hyperfine interaction, the four inner lines are slightly shifted to the right and the two outer lines are shifted to the left so that

° The author is indebted to Dr. K.K. Singh of Geology and Geophysics Department providing a pure crystal and for useful discussions.

°° The author extends his sincere thanks to Mr. A.K. Chatterjee of C.B.R.I., Roorkee (India) for the X-ray analysis.

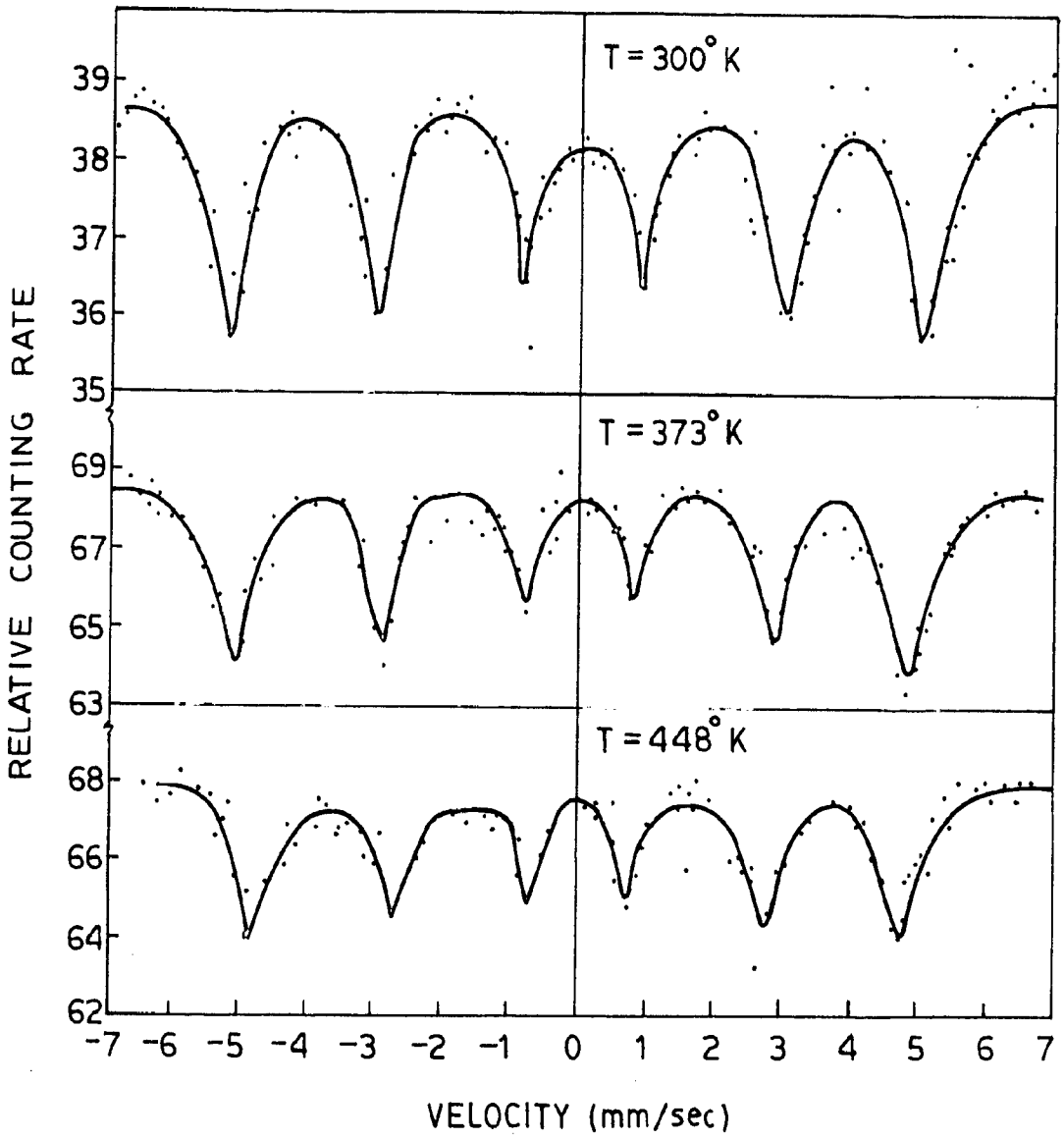

FIG. 3.3 HYPERFINE SPECTRA OF NATURALLY OCCURING CHALCOPYRITE

the spacing of the outer lines to the right and left are no longer equal and show a presence of small quadrupole interaction. This small asymmetrical displacement of the outer lines is due to the distortion caused by the magnetic structure and is discussed in a latter section.

Now if we assume that the distortion caused by the magnetic structure responsible for the quadrupole interaction is still symmetrical i.e., the asymmetry parameter η is zero (even if it is not the case; we know that the inclusion of the asymmetry parameter will only change the value of field gradient, maximum by a factor of 1.10^{5} and in view of the very small interaction it will not incur an appreciable error in our results). Supposing θ is the angle between the internal magnetic field and the symmetry axis of the EFG tensor, the quadrupole interaction energy can be written, considering the quadrupole coupling as perturbation.

$$\epsilon = (-1)^{|m_I|} \pm \frac{1}{2} \frac{e^2qQ}{4} \frac{(3\cos^2\theta - 1)}{2} \qquad (3.1)$$

with usual notations. For a positive EFG, ϵ is positive for $m = \pm 3/2$ and negative for $m_I = \pm 1/2$; which implies that the sublevels with $m_I = \pm 3/2$ will be raised by amount ϵ while those with $m_I = \pm 1/2$ will be lowered with the same amount. In our case vide the schematic diagram, Fig.3.4 the stipulation that the sublevels with $m_I = \pm 3/2$ are lowered by an amount ϵ and those with $m_I = \pm 1/2$ are raised by the same amount make it conform with the observed spectra. This implies a negative EFG.

In Fig.3.4 we have shown the splitting of the excited

---

[5] The asymmetry parameter is defined in such a way that it can have values $-1 < \eta < +1$. Also it effects the value of quadrupole coupling by a factor $(1+\eta^2/3)^{1/2}$ (chapter I) which has the max. value of 1.10 for $|\eta| = 1$.

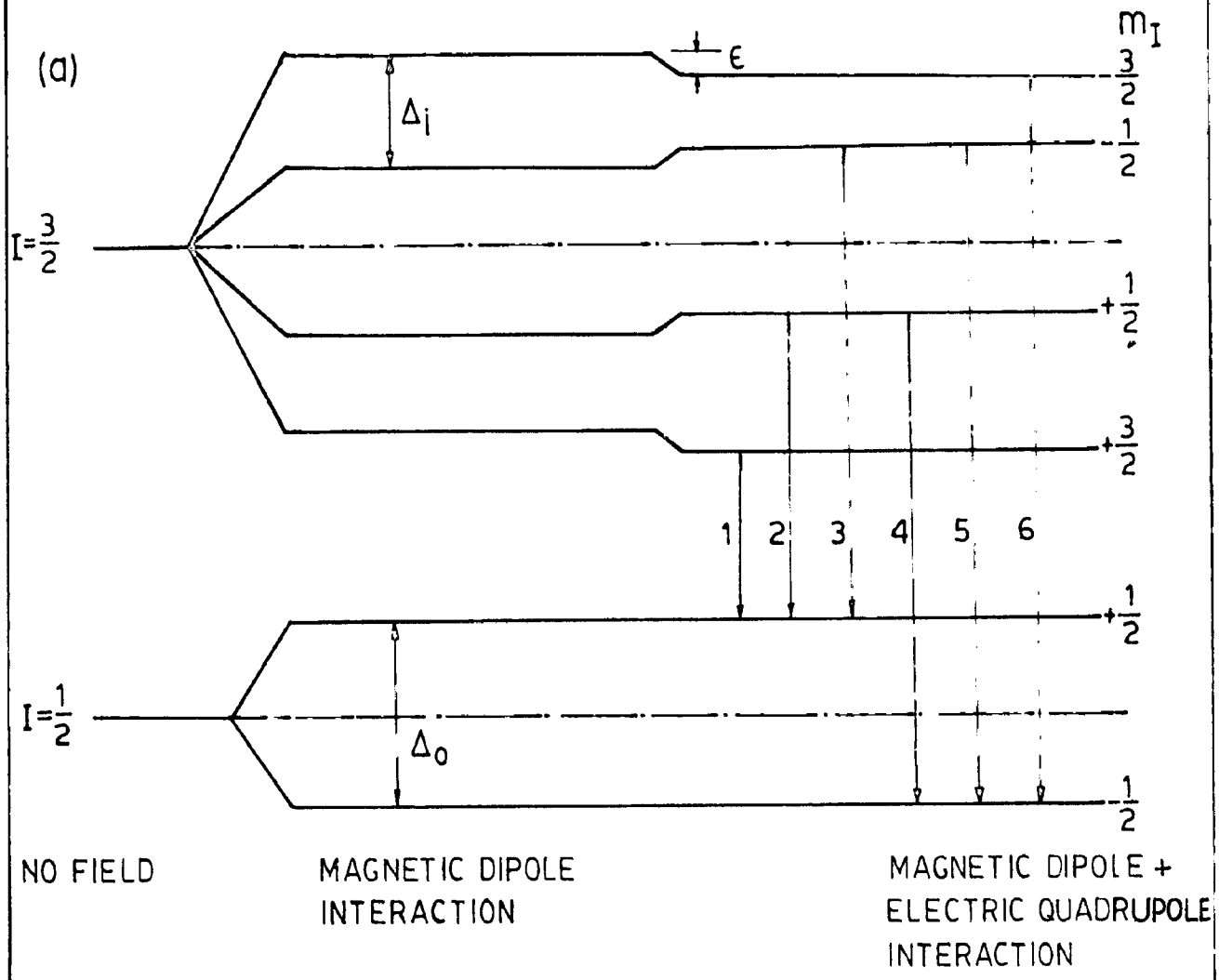

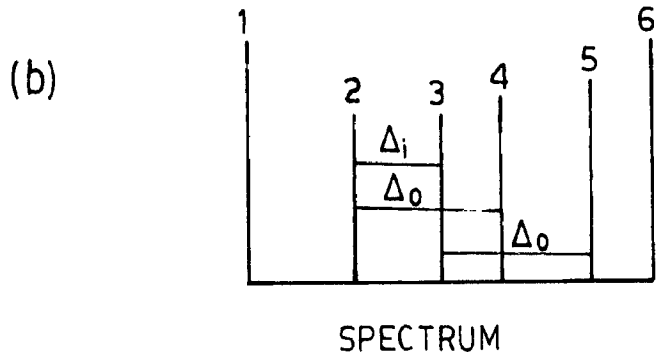

FIG. 3.4 (a) SCHEMATIC SPLITTING OF Fe^{57} LEVELS OF EXCITED & GROUND STATE UNDER THE COMBINED INTERACTION OF MAGNETIC DIPOLE & ELECTRIC QUADRUPOLE.

(b) THE SIX FINGERED SPECTRUM TO A FIRST APPROXIMATION

i.e. ϵ, the quadrupole interaction energy given by Eq. 3.1 is one quarter the difference in splitting of the outer pairs of the six lines spectra. Δ_0, as shown in the Fig.3.4, is the difference in E_n of the lines 2 and 4 or 3 and 5. Similarly Δ_1 is the difference of E_n of lines 2 and 3 or 4 and 5. To determine the value of the internal magnetic field one requires the value of the magnetic moments of ground or excited state. Alternatively the measured value of Δ_0 for the specimen may be correlated with the corresponding Δ_0 for Fe which has been determined from precise measurements related to H_{int} = 330 kOe. We adopted the second procedure as our spectrometer was calibrated by using natural iron as a standard absorber in conjunction with the data of Preston et al.[93]. The values of δ, ϵ and the internal magnetic field so obtained are given in Table 3.2.

TABLE 3.2: ISOMER SHIFT, QUADRUPOLE SPLITTING AND INTERNAL MAGNETIC FIELD IN CHALCOPYRITE AT VARIOUS TEMPERATURES

Source: Co^{57} in Cu matrix

Temperature (^{0}K)	Isomer shift (mm/sec)	Quadrupole splitting (mm/sec.)	Internal magnetic field (Kgauss)
300	-0.03 ± 0.02	0.05 ± 0.02	325 ± 10
373	-0.05 ± 0.03	0.03 ± 0.03	312 ± 10
448	-0.04 ± 0.02	0.04 ± 0.02	290 ± 10

3.5 DISCUSSION

The values of I.S. measured with respect to Co^{57} in Cu are of the order of 0.03 mm/sec. As $CuFeS_2$ is a covalent

compound and in the case of covalently bonded compounds, the values of I.S. for divalent and trivalent iron atom overlap[13] in this region, no unequivocal assignment of valence state is possible on this count. Further it may be mentioned that our values of I.S. when expressed w.r.to iron are in good agreement with those reported in Table 3.1 except with the values of Aramu et al.[130] (the reason of this disagreement is discussed in the next section) and that of Goodman and Gabri[137]. The value reported by the latter authors is zero and is very surprising.

Iron is covalently bonded with S-atoms in a regular tetrahedron as regards the crystallographic structure. But $CuFeS_2$ is an antiferromagnet and the magnetic interactions will make the symmetry lower than cubic as in the case of Dy^{161} in dysprosium iron garnet and Sn^{119} in $SnFe_2$[144]. The covalency between the iron ions and their ligand neighbours plays an important role and the stronger the covalent bonding of iron ions, the small is the value of quadrupole splitting[145]. Thus the magnitude of experimental values might seem to be explicable by considering the iron ion to be Fe^{2+} with covalent bonding, but such a view is untenable when we consider the temperature dependence of splittings in a tetrahedral field. In the tetrahedral ligand field the fivefold degenerate levels of a free Fe ion split[146] into a lower doublet called d_γ orbitals and an upper triplet called d_ε orbitals, Fig.3.3(a). The iron atom in the divalent state will give temperature dependent quadrupole splitting due to the change of Boltzmann factor governing the electron population both in the low as well as high

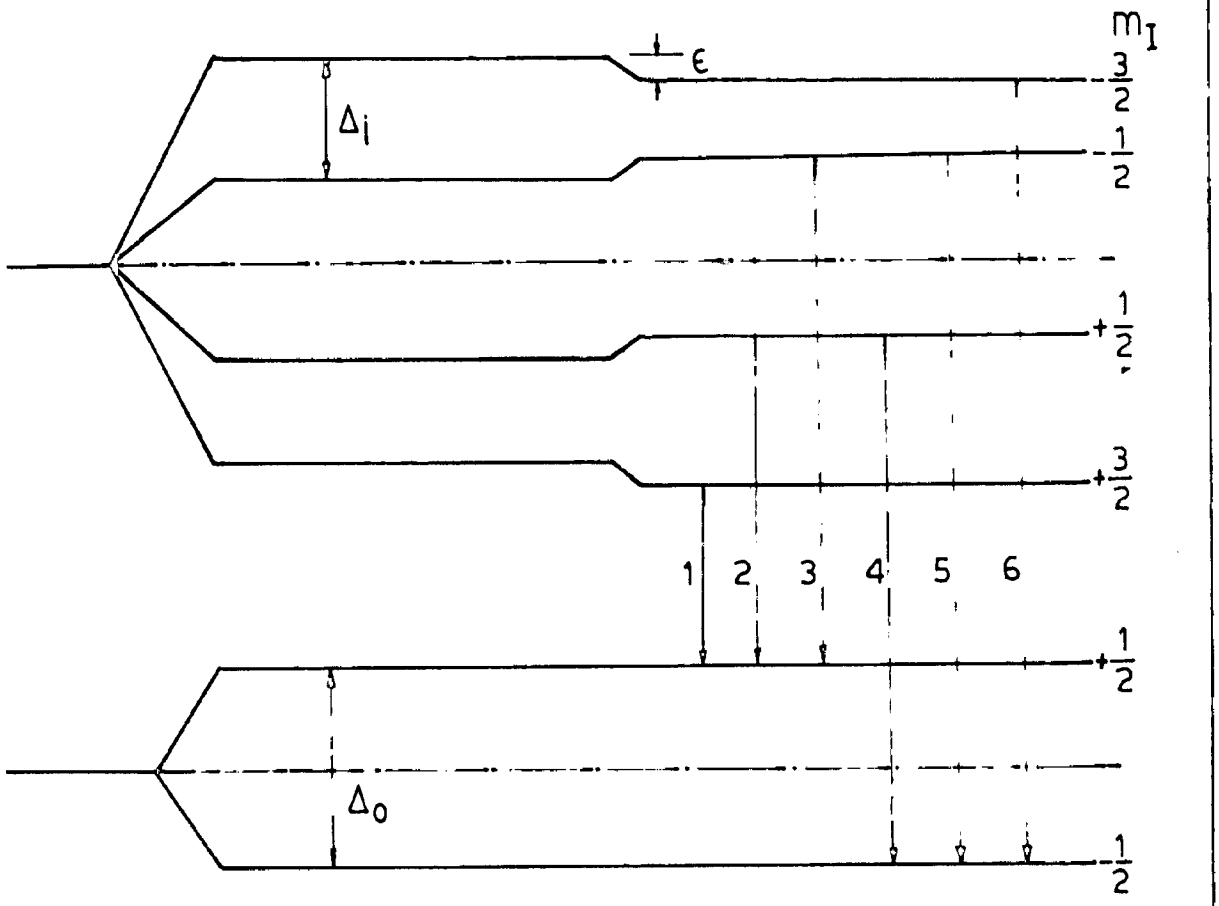

(b)

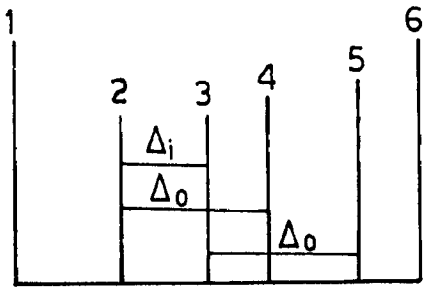

3.4 (a) SCHEMATIC SPLITTING OF Fe^{57} LEVELS OF EXCITED & GROUND STATE UNDER THE COMBINED INTERACTION OF MAGNETIC DIPOLE & ELECTRIC QUADRUPOLE.

(b) THE SIX FINGERED SPECTRUM TO A FIRST APPROXIMATION

and ground state levels in the combined action of internal magnetic field and quadrupole interaction. The magnetic interaction first leads to the splitting of ground state and the first excited state of Fe^{57} characterised by Δ_0 and Δ_1. The substates of the excited state with $m_I = \pm 3/2$ are then displaced to lower and those with $m_I = \pm 1/2$ raised by the electrical quadrupole interaction. The six possible transitions are indicated below with their Doppler energies required to have the observed spectrum.

Sl. No.	Transition	change in m_I	Doppler energy E_n reqd. for resonance.
1	$+3/2 \rightarrow +1/2$	-1	$\delta - \frac{\Delta_0}{2} - \frac{3\Delta_1}{2} - C$
2	$+1/2 \rightarrow +1/2$	0	$\delta - \frac{\Delta_0}{2} - \frac{\Delta_1}{2} + C$
3	$-1/2 \rightarrow +1/2$	+1	$\delta - \frac{\Delta_0}{2} + \frac{\Delta_1}{2} + C$
4	$+1/2 \rightarrow -1/2$	-1	$\delta + \frac{\Delta_0}{2} - \frac{\Delta_1}{2} + C$
5	$-1/2 \rightarrow -1/2$	0	$\delta + \frac{\Delta_0}{2} + \frac{\Delta_1}{2} + C$
6	$-3/2 \rightarrow -1/2$	+1	$\delta + \frac{\Delta_0}{2} + \frac{3\Delta_1}{2} - C$

where δ is the Isomeric shift (I.S.). These Doppler energies E_n are the respective positions of lines in the observed spectra. Now to see that the determination of the parameter δ, C, Δ_0 and Δ_1 is possible in the following manner. δ is obtained as the mean value of the positions of the lines 1,2,5 and 6 or 1,3,4 and 6 as the sum of the energies of interactions E_n for the four excited substates must be zero in the absence of any I.S. Further defining S1 as the difference in E_n for the lines 1 and 2 and S2 as the difference in E_n for the lines 5 and 6 we see that

$$|S1 - S2| = 4C$$

i.e. ϵ, the quadrupole interaction energy given by Eq. 3.1 is one quarter the difference in splitting of the outer pairs of the six line spectra. Δ_o, as shown in the Fig.3.4, is the difference in E_n of the lines 2 and 4 or 3 and 5. Similarly Δ_i is the difference of E_n of lines 2 and 3 or 4 and 5. To determine the value of the internal magnetic field one requires the value of the magnetic moments of ground or excited state. Alternatively the measured value of Δ_o for the specimen may be correlated with the corresponding Δ_o for Fe which has been determined from precise measurements related to H_{int} = 330 kOe. We adopted the second procedure as our spectrometer was calibrated by using natural iron as a standard absorber in conjunction with the data of Preston et al.[93]. The values of δ, ϵ and the internal magnetic field so obtained are given in Table 3.2.

TABLE 3.2: ISOMER SHIFT, QUADRUPOLE SPLITTING AND INTERNAL MAGNETIC FIELD IN CHALCOPYRITE AT VARIOUS TEMPERATURES

Source: Co^{57} in Cu matrix

Temperature (^oK)	Isomer shift (mm/sec)	Quadrupole splitting (mm/sec.)	Internal magnetic field (Kgauss)
300	-0.03 ± 0.02	0.03 ± 0.02	325 ± 10
373	-0.03 ± 0.03	0.03 ± 0.03	312 ± 10
448	-0.04 ± 0.02	0.04 ± 0.02	290 ± 10

3.5 DISCUSSION

The values of I.S. measured with respect to Co^{57} in Cu are of the order of 0.03 mm/sec. As $CuFeS_2$ is a covalent

compound and in the case of covalently bonded compounds, the values of I.S. for divalent and trivalent iron atoms overlap[13] in this region, no unequivocal assignment of valence state is possible on this count. Further it may be mentioned that our values of I.S. when expressed w.r.to iron are in good agreement with those reported in Table 3.1 except with the values of Aramu et al.[130] (the reason of this disagreement is discussed in the next section) and that of Goodman and Gabri[137]. The value reported by the latter authors is zero and is very surprising.

Iron is covalently bonded with S-atoms in a regular tetrahedron as regards the crystallographic structure. But $CuFeS_2$ is an antiferromagnet and the magnetic interactions will make the symmetry lower than cubic as in the case of Dy^{161} in dysprosium iron garnet and Sn^{120} in SnO_2[144]. The covalency between the iron ions and their ligand neighbours plays an important role and the stronger the covalent bonding of iron ions, the small is the value of quadrupole splitting[145]. Thus the magnitude of experimental values might seem to be explicable by considering the iron ion to be Fe^{2+} with covalent bonding, but such a view is untenable when we consider the temperature dependence of splittings in a tetrahedral field. In the tetrahedral ligand field the fivefold degenerate levels of a free Fe ion split[146] into a lower doublet called d_γ orbitals and an upper triplet called d_ε orbitals, Fig.3.9(a). The iron atom in the divalent state will give temperature dependent quadrupole splitting due to the change of Boltzmann factor governing the electron population both in the low as well as high

field configurations, Fig.3.8(a). Furthermore, the Fe^{III} in the case of high field as well as in intermediate field configurations (no intermediate field configuration in the case of Fe^{II} is possible) will also show the temperature dependent quadrupole splitting for the same reason, Fig.3.8(b) and (c). The observed values of quadrupole splitting, Table 3.2, are independent of temperature so it seems plausible that Fe atom is in the spin free trivalent state[122,123] and in weak crystal field; since it is only in this configuration that temperature independent values of quadrupole splitting can be explained. This conclusion is further supported by the observation that in tetrahedral complexes, no 'low spin' complex has so far been substantiated[147], Frank[134] has also reached the same conclusion.

The presence of two charge states will result in producing a complex hyperfine spectrum or much broader lines[140]. $CuFeS_2$ being a semiconductor, will seem to have a longer relaxation time and render feasible the observation of complex spectra due to the presence of two resonating charge states provided these resonate back and forth in a time longer than 10^{-7} sec. But the hyperfine spectra, Fig.3.3, show a typical pattern of six absorption lines, since the observed line width of 0.35 mm/sec. for the inner lines is comparable to the line widths observed in Fe_2O_3[94]. The broadening in the outside wings is of instrumental origin as in the case with the spectrum of natural iron with our spectrometer. The presence of typical six finger pattern and no relaxation broadening do not lend support to the hypothesis of resonating structure and show that Fe atom is

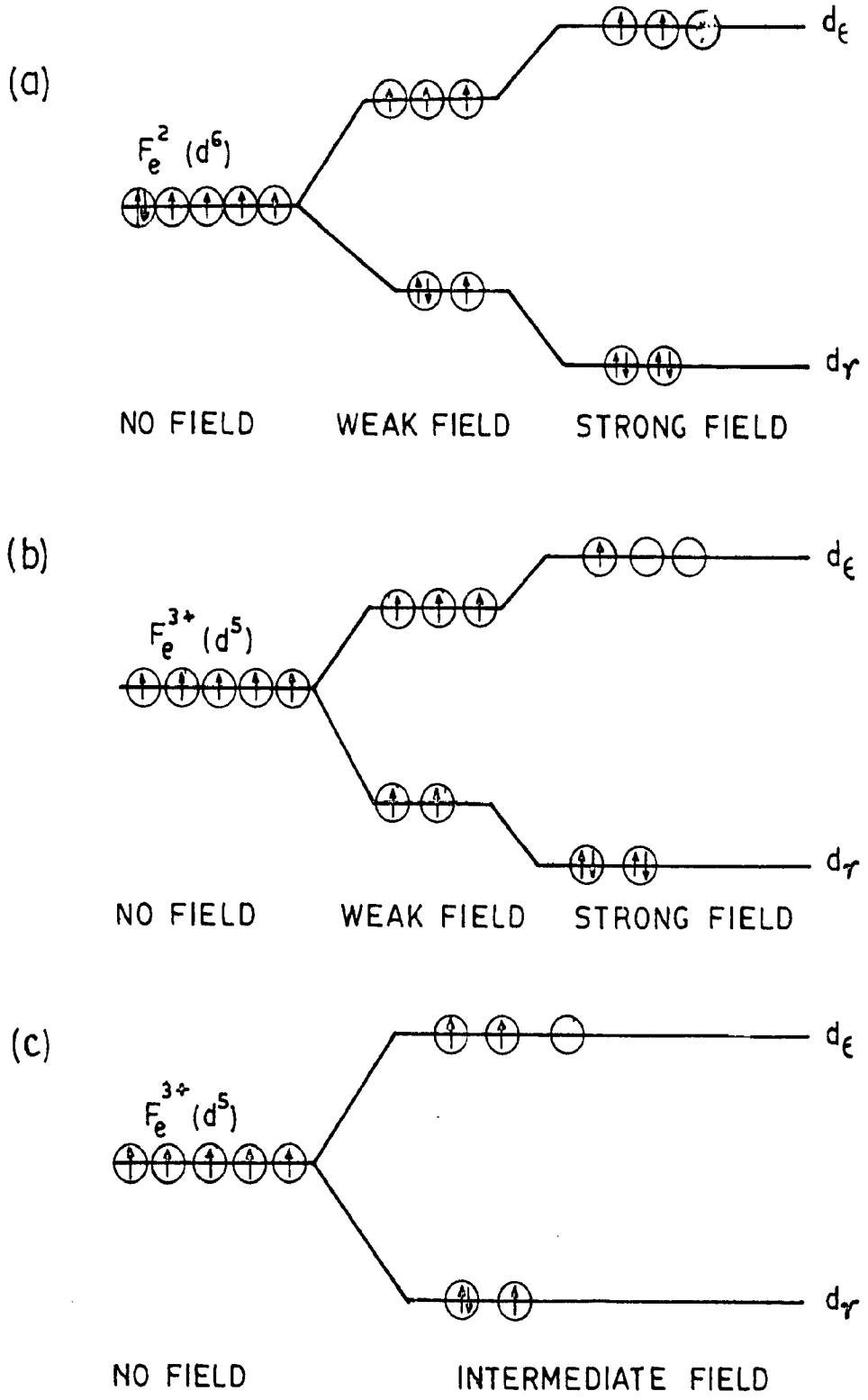

FIG. 3·5 SPLITTING OF THE d LEVELS IN TETRA–HEDRAL LIGAND FIELD

(a) ELECTRON DISPOSITION OF F_e^{2+}

(b),(c) ELECTRON DISPOSITION OF F_e^{3+}

in a single charge state.

Although the observed values of internal magnetic field are smaller than those for Fe^{3+} ionic compounds (550 kOe) but are comparable with that reported by Korlor et al.[103] for $KFeS_2$ where Fe atom is in the trivalent state and bonded covalently with sulphur tetrahedron. It would be interesting to quote at this stage that in bis(III) diethyldithiocarbamate iron (III) chloride, which is a ferromagnet with $S = 3/2$, a magnetic hyperfine field of 329 kOe has been found[149] which is also in very good agreement with the values found on the present sample of Chalcopyrite, as it should be; because the Zeeman splitting on a Mossbauer spectrum is determined, among others, by the average spin value.

The sign and magnitude of the internal field may be accounted as follows[150]. The internal magnetic field H_{exp} arises mainly from three sources:

(i) Fermi contact interaction, H_c

(ii) The inter atomic dipolar interaction, H_{dip} and

(iii) Orbital current, H_{orb}.

The contributions of (ii) and (iii) are given by Okaji and Kanamori[151] as

$$H_{dip} = -(1-\xi)\langle(3z^2 - r^2)/r^5\rangle\langle S_z\rangle(\mu_B/2)$$

$$= -(1-\xi)(\mu_B/2)\, q\langle S_z\rangle \qquad (3.2)$$

and $$H_{orb} = -2\mu_B \langle \bar{r}^3\rangle\langle L_z\rangle \qquad (3.3)$$

where the factor $(1-\xi)$ expresses the covalency effect which mixes the d-orbital with orbitals of surrounding negative ions and consequently reduces the weight of the d-orbitals to some

extent, $\langle S_z \rangle$ is the thermal average value of the z-component of the spin angular momentum, μ_B the Bohr magneton, q the z-component of the electric field gradient, $\langle r^{-3} \rangle$ is the average of the inverse cube of the distance between 3d electrons and the nucleus, and $\langle L_z \rangle$ is the average value of the z-component of the angular momentum. Here μ_B, $\langle L_z \rangle$ and $\langle S_z \rangle$ are defined to be positive. Iron is in the $3d^6$, $^5D_4$ state and lies in nearly cubic environment so from Eq.(3.2) and (3.3) one can conclude that H_{dip} and H_{orb} both will be zero (or negligibly small). So the major contribution comes from H_c, the Fermi contact term which can be expressed as:

$$H_c = - \frac{16\pi}{3} \mu_B \langle \xi(\sigma\uparrow - \sigma\downarrow) \rangle \qquad (3.4)$$

where $\sigma\uparrow$ and $\sigma\downarrow$ are the s-electron spin densities at the nucleus with spin up and spin down respectively. The Fermi contact interaction may arise in three ways: (i) from mixing of excited electronic states containing unpaired s-electrons with the ground state (ii) by a spin-polarisation effect due to different spin-exchange interaction and (iii) by ligand field mixing of the appropriate electronic configuration with the ground state.

The differences in the spin-up and spin-down charge densities appear[25] even in filled s-shells if the atom contains a partially filled magnetic shell e.g., the 3d shell in iron series. The exchange interaction between the spin-up polarised d-shell and the spin-up s-electron is attractive, while that between the d-shell and a spin-down s-electron is repulsive. As a result the radial parts of the two s-electrons wave functions will be different, one being pushed towards the

nucleus other pulled outward. The Fermi contact interaction then causes a local magnetic field at the nucleus which can be of the order of several hundred kOe. In fact this core polarisation, as it is called, is the main mechanism responsible for the large magnetic fields observed in other-wise S-state ions.

Watson and Freeman[152] calculated H_c for Fe^{3+} as - 330 kOe and furthermore, the observed magnetic field H_{exp} depends on the type of ligand neighbour and its bonding. Mn^{2+} is isoelectronic with Fe^{3+} and H_c as estimated by Watson and Freeman[152] is - 700 kOe and for S^{2-} as ligand neighbour is - 490 kOe. Thus the estimated value of H_c for Fe^{3+} covalently bonded with S^{2-} is - 330 x $\frac{490}{700}$ = - 441 kOe. Since the value of μ_{obs} for $CuFeS_2$ at room temperature is not 5.30μ_B(a measured value in $Fe_2(SO_4)_3$ at room temperature where iron is in Fe^{3+}, $3d^5$ state) but 3.85μ_B, as the effective H_c will be - 441 x $\frac{3.85}{5.90}$ = - 287.7 kOe. As already mentioned H_{dip} and H_{orb} are both zero so the estimated H_{exp} is - 290 kOe, the value which agrees with the measured value, Table 3.2. This agreement further supports the contention that iron atom is in the trivalent state. Further the values reported by other investigators Table 3.1, are in agreement with observed values within the experimental accuracy.

As mentioned earlier in Sec.3.2 the observed value of the magnetic moment of the iron atom does not tally with this scheme of results as the room temperature experimental value of μ_{eff} of an iron ion in $3d^5(Fe^{3+})$ state is 5.66 μ_B. It is interesting to note that in the case of intermediate ligand

field, Fig.3.8(b), the spin only formula gives a value of $\mu_{eff} = 3.87\mu_B$ which is in good agreement with the reported value. As in this case one could anticipate such a larger ΔE_Q due to 3d uncompensated electrons and its strong temperature dependence, but as these facts are not born out by experiments this remains just a conjecture, and we prefer our earlier conclusion of weak field configuration.

With a view to corroborate our conclusion further EPR spectra were tried but no absorption did occur probably due to the high dielectric constant of the material. Nor the optical absorption studies were possible since the substance is opaque and does not dissolve in any solvent.

3.6 CRITIQUE OF THE PAPER'ON THE MÖSSBAUER EFFECT OF CHALCOPYRITES' BY ARAMU et al.

Aramu et al.[130] have reported a quadrupole split doublet spectra both at room and liquid nitrogen temperatures and found no evidence for a six-line spectrum characteristic of magnetic interactions. On the basis of experimentally determined I.S., they proposed a new resonant structure $Cu^{+}Fe^{3+}(S^{-2})_2$ $Cu^{+2}Fe^{+1}(S^{-2})_2$, where both the configurations are equally probable. Furthermore, the semiconducting and magnetic properties of the compound were discussed in the light of the new proposed structure and they claimed a success in resolving the controversy of observed value of $5.95\mu_B$ by taking the average of the contribution $1.73\mu_B$ and $5.92\mu_B$ from these two equally probable structures.

A similar study was carried out by us[129] and so the observations are in direct contrast to each other, it was desired to offer the following comments[139] in this regard.

 The specimens studied in both the cases were naturally

occuring chalcopyrite and normally the FeS_2(Pyrite) and FeS_{1+x} (Pyrrhotite) are present as associations in varying proportions (in case of admixture) or fixed proportions (in the case of a solid solution). In view of the vastly varying composition, it is imperative that the structure is examined by X-rays diffraction for identification[170] of the species.

As stated earlier neutron diffraction studies[175] showed the compound to be antiferromagnetic with μ_{eff} for Fe equal to $3.99\mu_B$ and Neel temperature of 823°C. The magnetic ordering due to interlocked sublattices will give rise to magnetic hyperfine splitting thereby giving a six-line Mössbauer spectrum[139]. The values of I.S. (relative to iron) and quadrupole splittings at room and liquid nitrogen temperature for chalcopyrite as reported by Arams et al. agree with those of FeS_2(Pyrite)[163] and for comparison data are tabulated in Table 3.3. The Mössbauer spectra for chalcopyrite and FeS_2(Pyrite) are given in Fig.3.8. It is obvious that spectrum in Fig.3.8(b) seems to correspond to the spectrum of Arams et al.

By comparing the values of I.S. of an ionic compound $CuFeO_2$ (0.40 mm/sec.)[164] with their observed value (0.38 mm/sec) Arams et al. hypothesized the ionic-covalent resonant structure: $Cu^{+}Fe^{3+}(S^{2-})_2$ $Cu^{+3}Fe^{-}(S^{-2})_2$, where both the configurations are equally probable. The covalent bonding in the above structure is regarded to reduce the I.S. If the resonance time of the two structures is less than 10^{-7} sec. (life time of the first excited state of Fe^{57}) the observed spectra will be considerably broadened whereas if it is greater than 10^{-7} sec., it will result either in a complex spectra (if resolved)

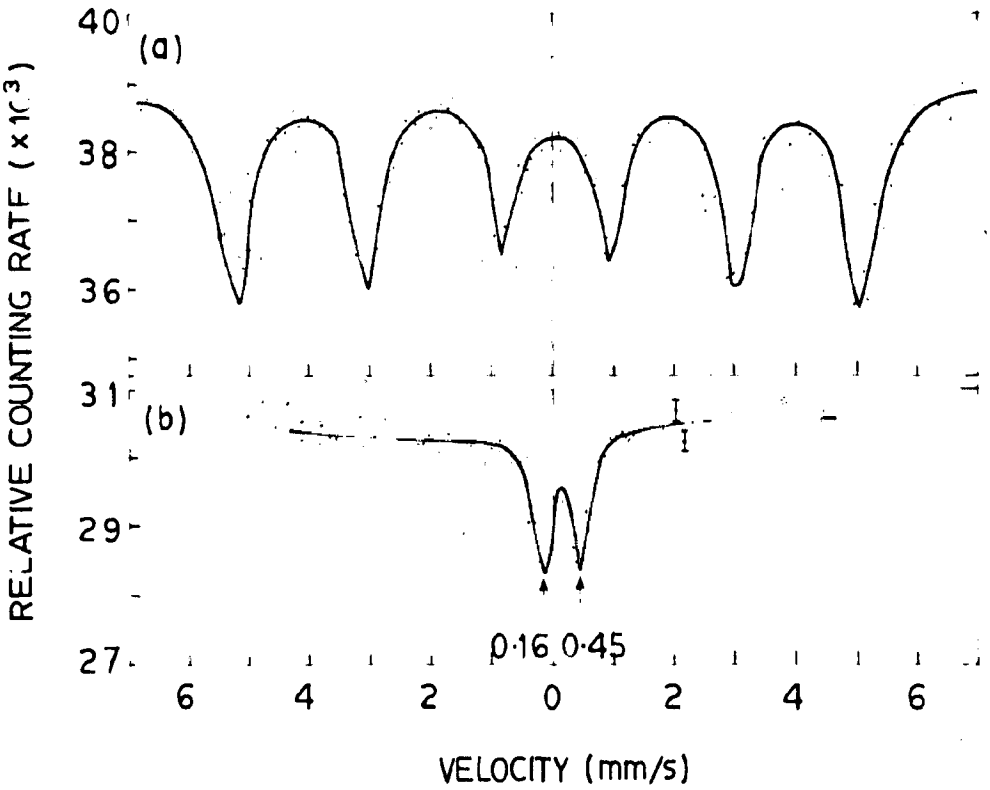

FIG. 3.6: MÖSSBAJER SPECTRA AT ROOM TEMPERATURE OF (a) CHALCOPYRITE ($CuFeS_2$): ^{57}Co (Cu); (b) PYRITE (FeS_2): ^{57}Co(Pd)

or broadened (if unresolved) due to the presence of Fe^{3+} ion in two chemically inequivalent sites. The values of the half width from the spectra[130] are in good agreement to the well resolved spectra of iron compounds[13], and thus the spectra[130] are neither complex nor broadened as one would expect on the plea of the ionic covalent resonating structure.

TABLE 3.3: EXPERIMENTALLY OBSERVED VALUES OF Q.S. AND I.S. WITH RESPECT TO SOURCE IN Fe AT 300°K

Compound	T°K	E_Q(mm/sec.)	δ(mm/sec.)
$CuFeS_2$	300	0.05 ± 0.02	0.190 ± 0.02[a]
	373	0.05 ± 0.02	0.190 ± 0.02[a]
	77	0.650± 0.03	0.400 ± 0.03[b]
	300	0.600± 0.03	0.320 ± 0.03[b]
FeS_2(Pyrite)	81	0.620± 0.009	0.407 ± 0.003[c]
	300	0.614± 0.003	0.314 ± 0.002[c]
	300	0.61 ± 0.02	0.33 ± 0.02[d]
FeS(Pyrrhotite)	90	-0.15 ± 0.14	-
	290	-0.10 ± 0.10	0.640 ± 0.10[a]

(a) Ref.129; (b) Ref.130; (c) Ref.153; (d) Ref.139;
(e) K. Ôno et al.: J. Phys. Soc. Jap. 17, No.10(1962)1618.

Furthermore the assumption of the new proposed structure seems to be untenable when considered from the observed values of quadrupole splitting. It has been shown by Ingalls[153] that the field gradient of a d-electron at the nucleus is given by

$$(1-R)\, q\, e^2\, P$$

where (1-R) is the Sternheimer factor which accounts for the deformation of the inner shells by the electron, α^2 the covalency factor which accounts for the expansion of the electron towards the ligands ($0.6<\alpha^2<0.9$), $q = \frac{4}{7}\langle r^{-3}\rangle_{3d}$ the field gradient calculated from the free ion wave function and P a function of energy level separation, spin orbit coupling, and temperature. For an essentially localised electron as presumably in the ionic configuration $Cu^{+}Fe^{3+}(s^{2-})_2$, $\alpha^2 = 0.9$ whereas in the covalent configuration $Cu^{3-}Fe^{-}(s^{2+})_2(sp^3$ bonding of iron) the covalent bonding will introduce delocalisation of the electron in 3d orbitals reducing the electronic contribution to the field gradient. Assuming (1-R) and P to be nearly the same for both the above configurations, the ΔE_Q values will be different, the difference depending on the degree of delocalisation of the d electrons. In addition with regards to the proposed structure it was assumed that Fe^{3+} ion is spin paired in the ionic form and spin-free in the covalent (sp^3) configuration. There is bound to be a contribution to q from the unecompensated electron in the ionic configuration whereas no such contribution from Fe^{3+} in the spin-free state, resulting inevitably in different values of quadrupole splitting in both the configuration. This will either give rise to additional doublet (if fully resolved) or cause (broadening) of the observed absorption peaks; but neither in the case from the experimental spectra[130].

C H A P T E R IV

MÖSSBAUER STUDIES OF TUTTON SALTS

4.1 INTRODUCTION

Fe^{2+} Tutton salts are a series of hexahydrated isomorphous double sulphates having the general formula

$$M^{2}(M^{1}SO_4)_2.6H_2O$$

where M^1 is a monovalent positive ion like K^+, Rb^+, Cs^+, Tl^+ or NH_4^+, and M^2 is a divalent positive ion like Cd^{2+}, V^{2+}, Mn^{2+}, Cr^{2+}, Fe^{2+}, Ni^{2+}, Co^{2+}, Cu^{2+}, Zn^{2+}, or Mg^{2+}. As we are studying the recoilless emmission or absorption with Fe^{57} our interest will be mainly limited to the Iron series viz.,

$$Fe^{2+}(M^{1}SO_4)_2.6H_2O$$

A great deal of work has been done on these compounds particularly on Ferrous Ammonium sulphate (FAS), also commonly known as Mohr Salt, and which is a well known stable laboratory reagent. Tutton[153] prepared a wide range of these type of series of double sulphates and made exhaustive studies of their optical properties. Tsutsumi[157] measured the wave length values and relative intensities of the X-ray non-diagram lines of $K\beta'$ of $(NH_4)_2Fe(SO_4)_2.6H_2O$ by the fluorescent X-ray method by using two different characteristic X-rays. He concluded that $K\beta'$ line was due, not to the double, but to the single ionisation process, and that it can be derived from the difference of the exchange interactions of the states having different total spins $(S + \frac{1}{2})$ and $(S - \frac{1}{2})$

where S is the total spin of the incomplete 3d shell and $\frac{1}{2}$ is that of the incomplete 3p shell in the final state. The energy separations of the $K\beta^1$ and $K\beta'$ lines calculated from the exchange energies nearly agree with those observed experimentally. Hill and Smith[158] measured the sp. heat of this compound from 2 to 30°K and observed two maxima at 3.8 and 30.3°K respectively, which clearly exhibited an anomaly of the Shottky type. In order to explain this anomaly they proposed a scheme of energy levels indicating that the ground state of ferrous ion is doublet of equal degeneracy having an approximate separation of 6.8 cm^{-1}. Guillien[159], on the other hand, observed an anomaly in its dielectric constant ϵ at -60°C which is its transition point.

The magnetic susceptibilities and anisotropies of Fe^{2+} Tutton Salts had been a subject of considerable investigations[100-07]. These investigations have brought up many interesting results. Chakravarty and Chatterjee[102] worked out a theory of the magnetic susceptibility of DAS on the basis of the Abragam and Pryces[100] method and found that the anisotropic part of the crystal field changes with temperature owing to the thermal expansion of the crystal lattice. They further inferred that the spin orbit coupling coefficient must be decreased by 29% from its free ion value of -130 cm^{-1}, which indicates some amount of overlap between the 3d Fe^{2+} and s-and p-O^{--} charge clouds. Their theoretical values agree well with the experimental values. Richardson and Sapp[162] measured the magnetic susceptibility of this compound at 0.08-4.2°K by both the Faraday and ballistic mutual induction bridge methods. The results were compatible with

available specific heat data in the low temperature region provided that the lowest level is taken to be a singlet and constant susceptibility is ascribed to temperature independent paramagnetism of the lowest level. The low temperature observations of Jackson[100] and also of Ohtsuka[101] et al. have indicated a quenching of the S = 2 spin state at temperatures below 10°K which otherwise is an essentially free S = 2 state at room temperature. Bhattacharyya[109] has worked out the expressions for the magnetic susceptibility and anisotropy of Fe^{2+} Tutton salts ($Fe(NH_4)_2.6H_2O$) employing a more general molecular orbital method of Van-Vleck, Stevens and Bose et al. These results show a good agreement with the experimental values of Bose et al. From these studies he proposed a doublet as the ground state.

Mössbauer spectroscopy has also been employed in the studies of this compound[80,103,155,170,171] and a compilation of all the previous work is presented in Table 4.1. Kerler and Neuwirth[103] measured the line shift and quadrupole splitting in the temperature range 170-339°K. Ingalls[155] has made an extensive study of the electric field gradient (EFG) tensor in ferrous compounds. By making use of crystal field parameters, spin orbit interaction and covalency effects, he has explained the temperature dependence of quadrupole splitting and has concluded that the ground state in FAS is essentially siglet with wavefunction $|xy\rangle$ (this is contrary to Bhattacharyya[100]). In addition he has exhibited a requirement of rhombic rather than tetragonal crystal field symmetry. He has also assigned the characteristic temperatures to the t_{2g} levels. Grant et al.[170] have used

magnetic perturbation technique and concluded that the sign of the nuclear quadrupole coupling constant of FAS is positive.

In view of the interesting investigations of one of the member of the series, it was considered worthwhile to undertake the detailed Mössbauer studies of the whole series to seek information regarding the order and magnitude of crystal field splittings of the levels, the ground state wavefunctions of the individual member and characteristic temperatures of t_{2g} levels. Furthermore, we calculated the sixth electron occupation probabilities of these levels. Moreover effect of varying electronegativity of the alkali cations on the Isomeric shift in these compounds is also of interest. It is expected that such studies of the level parameters from quadrupole splittings will augment the informations from magnetic data and specific heats.

From these studies we have concluded[172] that the ground state wave functions in all the members of the series is a singlet $|xy\rangle$ and that the effect of varying electronegativity of M^1 has negligible bearing on I.S.

4.2 EXPERIMENTAL DETAILS

(A) PREPARATION

Preparation of the Tutton salts is very simple and these were prepared according to methods of Tutton[163] and Thakurata and Mukhopadhyay[166]. High purity (A.R. or E. Merck) component state viz. $FeSO_4.7H_2O$ and the counter part $M_2SO_4.MH_2O$ where M = NH_4, K, Rb, Cs or Tl and x is the water of crystallisation, were taken and their equimolar quantities were dissolved in doubly distilled water. Except in the case of

the Tutton salts were of Hofmann[173], who investigated the lattice constants and space groups of the series $(NH_4)_2M^2(SO_4)_2 .6H_2O$ with M^2 as Mg, Fe and Zn. Very recently Montgomery and Lingafelter[174a] have done a detailed study of the structure of the Tutton salts series $(NH_4)_2M^2(SO_4)_2.6H_2O$ with divalent ion M^2 as Mg^{2+}, Ni^{2+}, Zn^{2+}, Cd^{2+}, and Mn^{2+}; by making use of the three dimensional Fourier and least square refinements of X-ray diffraction data. Their latest paper[174b] gives the information of immediate concern to our work i.e. of FAS. It is a monoclinic crystal, space group C_{2h}^5 ($P_{2\,1/a}$) with lattice constants

$$a = 9.32\ \text{Å}$$
$$b = 12.05\ \text{Å}$$
$$c = 6.24\ \text{Å}$$

and $$\beta = 106.8^0$$

The unit cell contains two molecules and the Fe^{2+} ion is situated at two equivalent site at (0,0,0) and (1/2, 1/2,0). These ions are in a spin free state[8] and are surrounded by a distorted octahedron formed from six water molecules. The bond length and angles of this water octahedron are shown in Fig.4.1(a). All the other members, being isomorphous, have the identical structural properties.

(C) MÖSSBAUER DATA RECORDING

The crystals so obtained were dried and pulverised into a fine powder. An amount of the powdered sample having an equivalent thickness of approximately 10mg/cm^2 of natural iron was sandwiched between two perspex sheets of thickness 1mm for room temperature measurements and between two Al

magnetic perturbation technique and concluded that the sign of the nuclear quadrupole coupling constant of FAS is positive.

In view of the interesting investigations of one of the member of the series, it was considered worthwhile to undertake the detailed Mössbauer studies of the whole series to seek information regarding the order and magnitude of crystal field splittings of the levels, the ground state wavefunctions of the individual member and characteristic temperatures of t_{2g} levels. Furthermore, we calculated the sixth electron occupation probabilities of these levels. Moreover effect of varying electronegativity of the alkali cations on the Isomeric shift in these compounds is also of interest. It is expected that such studies of the level parameters from quadrupole splittings will augment the informations from magnetic data and specific heats.

From these studies we have concluded[172] that the ground state wave functions in all the members of the series is a singlet $|xy\rangle$ and that the effect of varying electronegativity of M^1 has negligible bearing on I.S.

4.2 EXPERIMENTAL DETAILS

(A) PREPARATION

Preparation of the Tutton salts is very simple and these were prepared according to methods of Tutton[186] and Thakurata and Mukhopadyay[106]. High purity (A.R. or E. Merck) component state viz. $FeSO_4.7H_2O$ and the counter part $M_2SO_4.xH_2O$ where M = NH_4, K, Rb, Cs or Tl and x is the water of crystallisation, were taken and their equimolar quantities were dissolved in doubly distilled water. Except in the case of

K salt, the solutions were allowed to evaporate in a dust free airconditioned room, on a vibration proof stand. To avoid the oxidation of ferrous salt from becoming ferric, few drops of sulphuric acid (H_2SO_4) were added to the solutions. K-Tutton salt was obtained by slow crystallisation of the solution in a vacuum desicator. The crystals are liable to efflorosce in vacuum, and as such were removed soon after their formation. The final crystals were obtained by repeated crystallisation.

TABLE 4.1: PREVIOUS MOSSBAUER STUDIES ON FERROUS AMMONIUM SULPHATE (FAS)

Temperature (^oK)	Quadrupole splitting (ΔE) (mm/sec)	Isomeric shift (with respect to iron) (mm/sec)	Ref.
5	2.635 ± 0.002	+ 1.382 ± 0.002	Grand et al.[170]
77	2.74 ± 0.05	-	Lang et al.[171]
	2.70 ± 0.05	+ 1.41 ± 0.05	de Bona dott et al[171]
112	2.64 ± 0.05	-	Lang et al.[171]
170	2.270 ± 0.015	+ 1.282 ± 0.010	Kerlor et al.[103]
195	2.24 ± 0.05	-	Lang et al.[171]
207	2.102 ± 0.015	1.281 ± 0.010	Kerlor et al.[103]
298	1.707 ± 0.015	1.280 ± 0.010	-do-
300	1.73 ± 0.05	-	Lang et al.[171]
Room Temp.*	1.736 ± 0.003	+ 1.240 ± 0.004	Grant et al.[170]
	1.75 ± 0.05	1.31 ± 0.05	de Bonadatti et al.
	1.75 ± 0.05	1.27 ± 0.05	Brady et al.[66]
399	1.68 ± 0.015	1.203 ± 0.010	Kerlor et al.[103]

* Exact temp. not quoted.

(B) STRUCTURE

The first X-ray structure investigations reported for

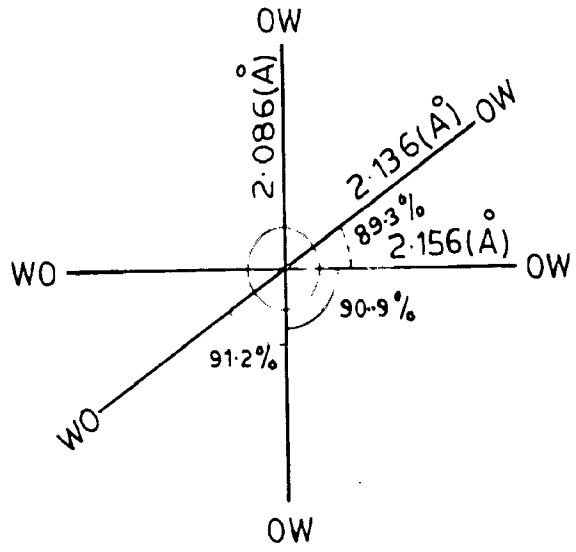

FIG 4.1(a) THE DISTORTED WATER OCTAHEDRON ABOUT THE Fe^{2+} ION IN FERROUS AMMONIUM SULPHATE.

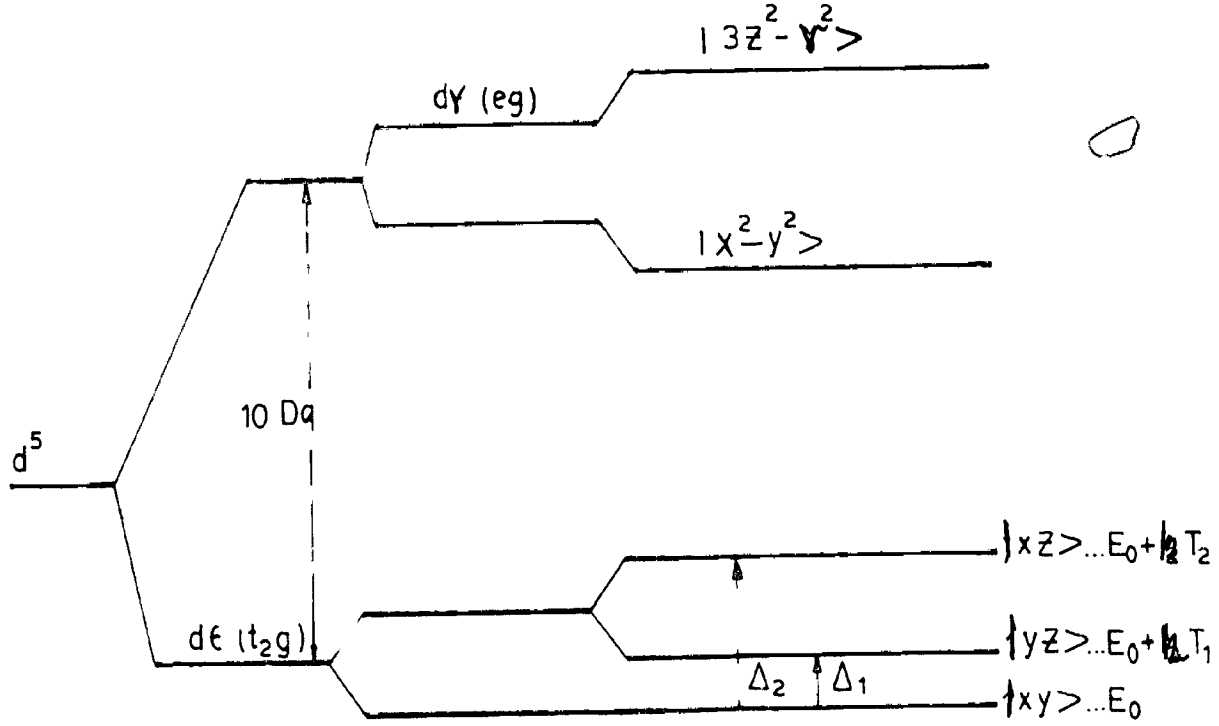

FREE ION + CUBIC FIELD + AXIAL FIELD + RHOMBIC FIELD

FIG. 4.1(b) ENERGY LEVEL SCHEME OF Fe^{2+} ION UNDER THE ACTION OF CRYSTALLINE FIELD ARISING FROM A DISTORED OCTAHEDRON

foils for low temperatures; the latter were again jacketed in two thick copper strips which were fastened to the lower edge of the projected thick-copper plate of the cryostat as described in the second chapter. While recording the data proper care was taken for the counting statistics and for that reason more time was required in the low temperature measurements where attenuation due to cryostat arrangement is inevitable. The counting rate vs relative velocity of the absorber and source was plotted to get the Mössbauer spectrum and typical Mössbauer spectra so obtained are presented in Fig.4.2. The Mössbauer parameters derived from these spectra are given in Table 4.2. Further the temperature dependence of quadrupole splitting is also shown in Fig.4.3. Unfortunately, the data for $Fl_2Fe(SO_4)_2.CH_2O$ could not be recorded with desired accuracy because of the high electronic (atomic) absorption and is not included in the table.

4.3 ANALYSIS

The theory of the quadrupole interaction is discussed in much details in the first chapter and only relevant features will be discussed here.

A nucleus with spin angular momentum $I > 1$ in the presence of an electric field gradient (EFG) gets the $(2I + 1)$ fold degeneracy partially removed due to interaction of the quadrupole moment Q with the EFG which can be expressed by the Hamiltonian[70].

$$H_Q = \frac{eQq}{4I(2I-1)} \left[(3\hat{I}_z^2 - \hat{I}^2) + \frac{1}{2}\eta(\hat{I}_+^2 + \hat{I}_-^2) \right]$$

where $q = \frac{V_{ZZ}}{e}$ and $\eta = \frac{V_{XX} - V_{YY}}{V_{ZZ}}$ (4.1)

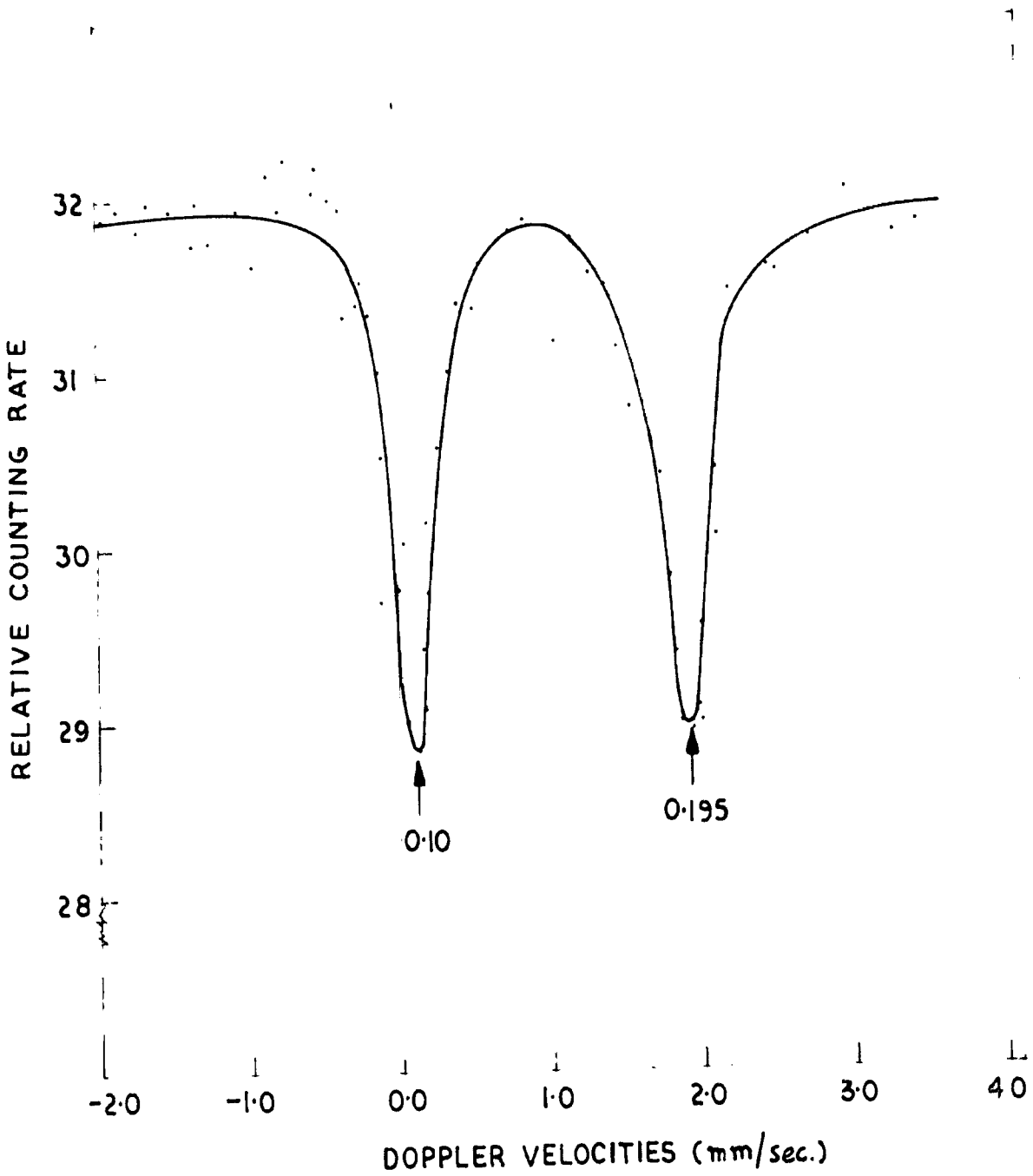

FIG. 4.2 MÖSSBAUER SPECTRUM OF $R_b\ F_e\ (SO_4)_2\ 6H_2O$ AT -20^0C
(SOURCE $C_0^{57}\ (C_u)$)

TABLE 4.2: ISOMER SHIFTS AND QUADRUPOLE INTERACTIONS AT THE IRON NUCLEI IN TUTTON SALTS AT VARIOUS TEMPERATURES

Compound	Temp. ^{o}K	δ^{*} mm/sec.	$e^2qQ/2$ mm/sec.	$\frac{\partial \Delta E_Q}{\partial T}$ mm/^{o}K
$Fe(NH_4SO_4)_2.6H_2O$	293	1.14±0.04	1.76±0.04	4.24×10^{-3}
	253	1.00±0.04	1.90±0.04	
	195	1.07±0.04	2.20±0.04	
	81	1.10±0.04	2.66±0.04	
$Fe(KSO_4)_2.6H_2O$	293	1.16±0.04	1.96±0.04	2.31×10^{-3}
	253	1.00±0.04	2.00±0.04	
	195	1.07±0.04	2.14±0.04	
	81	1.07±0.04	2.45±0.04	
$Fe(RbSO_4)_2.6H_2O$	293	1.05±0.04	1.70±0.04	3.77×10^{-3}
	253	1.03±0.04	1.85±0.04	
	195	1.04±0.04	2.07±0.04	
	81	1.12±0.04	2.50±0.04	
$Fe(CsSO_4)_2.6H_2O$	293	1.04±0.04	1.60±0.04	4.95×10^{-3}
	253	1.05±0.04	1.75±0.04	
	195	1.12±0.04	1.90±0.04	
	81	1.18±0.04	2.65±0.04	

* with respect to Co^{57} in Cu

such that $0 \ll \eta \leq 1$ and keeping in view that for Fe^{57} $I_g = 1/2$, and $I_e = 3/2$, we write Eq.(4.1) in the form

$$H_Q = \frac{1}{4} e^2 |q| Q \left[\hat{I}_z^2 - \frac{5}{4} + \frac{1}{6}(\hat{I}_+^2 + \hat{I}_-^2)\right] \qquad (4.2)$$

The Eq. 4.2 has the eigenvalues

$$E_Q = \frac{e^2|q|Q}{4} (m_I^2 - 5/4)(1 + \frac{1}{3}\eta^2)^{1/2}$$

with $m_I = 3/2,\ 1/2,\ -1/2,\ -3/2$ (4.3)

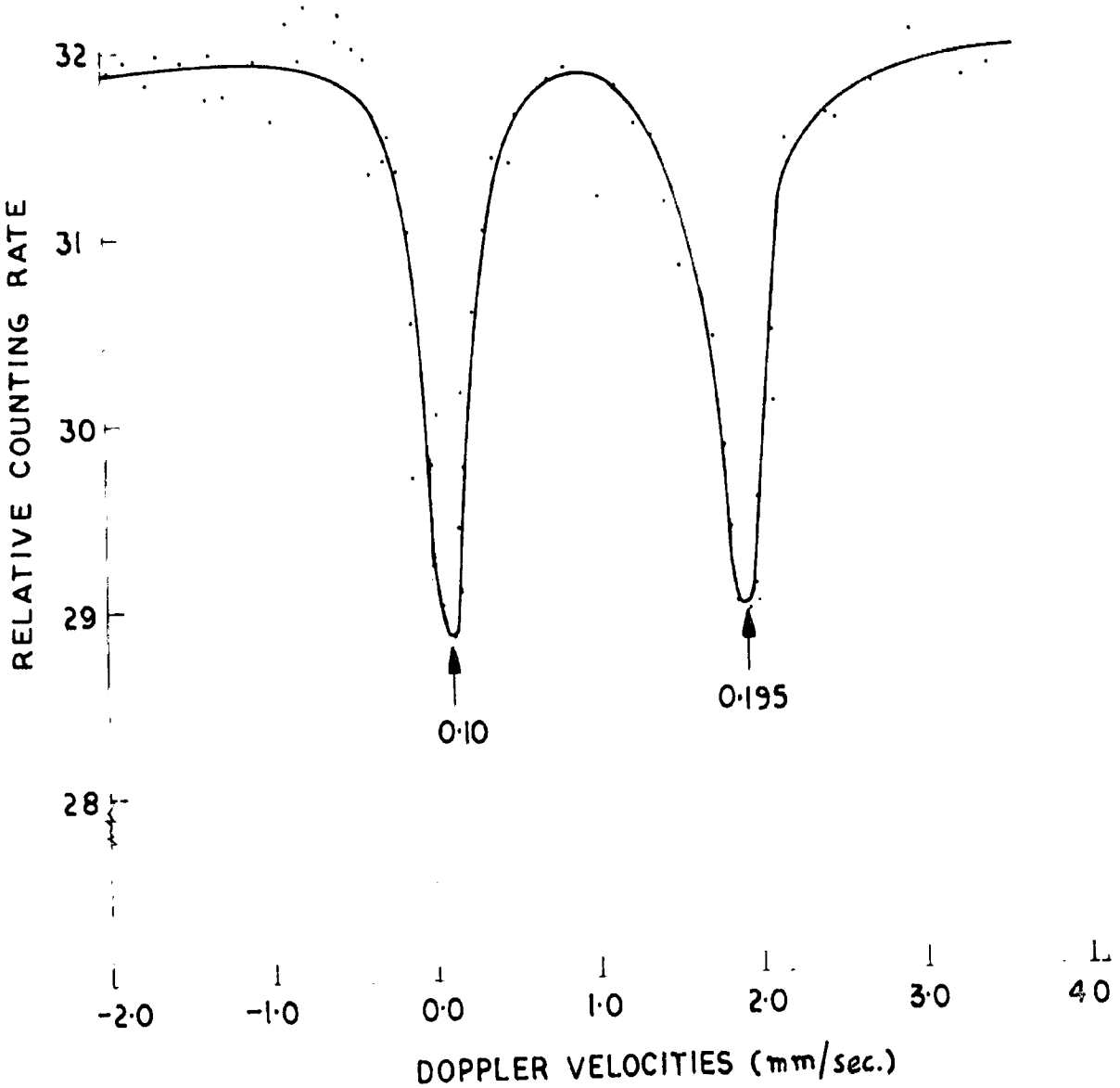

FIG. 4·2 MÖSSBAUER SPECTRUM OF $R_b\ F_e\ (SO_4)_2\ 6H_2O$ AT -20^0C
(SOURCE C_0^{57} (Cu))

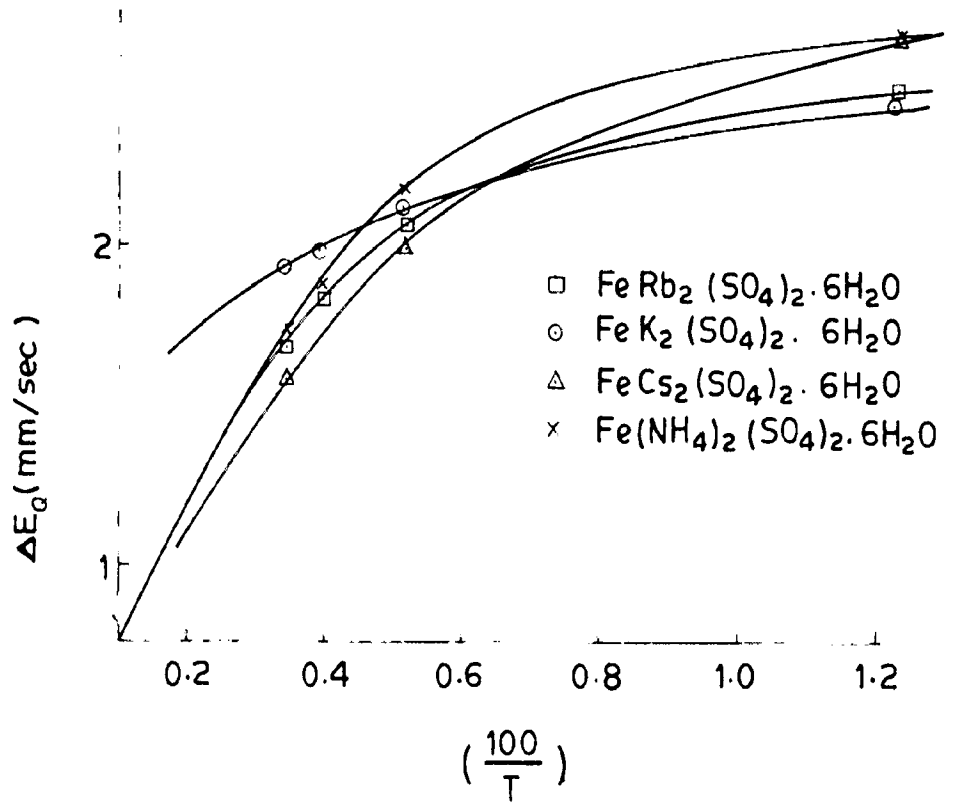

FIG. 4·3. TEMPERATURE DEPENDENCE OF THE QUADRUPOLE SPLITTING IN IRON TUTTON SALTS.

TABLE 4.2: ISOMER SHIFTS AND QUADRUPOLE INTERACTIONS AT THE IRON NUCLEI IN TUTTON SALTS AT VARIOUS TEMPERATURES

Compound	Temp. ^{o}K	δ^{*} mm/sec.	$e^2qQ/2$ mm/sec.	$\frac{\partial \triangle E_Q}{\partial T}$ mm/^{o}K
$Fe(NH_4SO_4)_2.6H_2O$	293	1.14±0.04	1.76±0.04	4.24×10^{-3}
	253	1.00±0.04	1.90±0.04	
	195	1.07±0.04	2.20±0.04	
	81	1.10±0.04	2.66±0.04	
$Fe(KSO_4)_2.6H_2O$	293	1.16±0.04	1.96±0.04	2.31×10^{-3}
	253	1.00±0.04	2.00±0.04	
	195	1.07±0.04	2.14±0.04	
	81	1.07±0.04	2.45±0.04	
$Fe(RbSO_4)_2.6H_2O$	293	1.05±0.04	1.70±0.04	3.77×10^{-3}
	253	1.03±0.04	1.85±0.04	
	195	1.04±0.04	2.07±0.04	
	81	1.12±0.04	2.50±0.04	
$Fe(CsSO_4)_2.6H_2O$	293	1.04±0.04	1.60±0.04	4.95×10^{-3}
	253	1.05±0.04	1.75±0.04	
	195	1.12±0.04	1.90±0.04	
	81	1.18±0.04	2.65±0.04	

* with respect to Co^{57} in Cu

such that $0 \leq \eta \leq 1$ and keeping in view that for Fe^{57} $I_g = 1/2$, and $I_e = 3/2$, we write Eq.(4.1) in the form

$$H_Q = \frac{1}{4} e^2 \left[q|Q \left[\hat{I}_z^2 - \frac{5}{4} + \frac{1}{6} (\hat{I}_+^2 + \hat{I}_-^2) \right] \right] \qquad (4.2)$$

The Eq. 4.2 has the eigenvalues

$$E_Q = \frac{e^2|q|Q}{4} (m_I^2 - 5/4) (1 + \frac{1}{3} \eta^2)^{1/2}$$

with $m_I = 3/2, 1/2, -1/2, -3/2$ (4.3)

This expression contains only the 2nd power of the magnetic quantum number m_I, which means that states whose m_I differ only in sign remain degenerate. In the case of Fe^{57} nucleus the states of $m_I = \pm 3/2$ are degenerate and so are those of $m_I = \pm 1/2$. Putting $m_I = \pm 3/2$ and $\pm 1/2$ in Eq.4.3 one gets

$$E_Q = \pm \frac{e^2|q|Q}{4}\left[1+\frac{1}{3}\eta^2\right]^{1/2} \qquad (4.4)$$

with positive sign for $m_I = \pm 3/2$ and negative sign for $m_I = \pm \frac{1}{2}$ and thus the Mössbauer spectrum gives two peaks with a separation of

$$\Delta E_Q = \frac{1}{2} e^2|q|Q\left[1+\frac{1}{3}\eta^2\right]^{1/2} \qquad (4.5a)$$

or alternatively

$$\Delta E_Q = \frac{1}{2} e^2 Q\left[q^2+\frac{1}{3}\eta^2 q^2\right]^{1/2} \qquad (4.5b)$$

Now q, the Z-component of the EFG at the nuclear site can be split up into two components, the lattice part (arising from ligand disposition) and the valence part (i.e. the uncompensated part of the ion)

$$\frac{V_{ZZ}}{e} = q = (1-R)q_{ion} + (1-\gamma_\infty)q_{lat} \qquad (4.6a)$$

also $$\frac{V_{XX}-V_{YY}}{e} = \eta q = (1-R)\eta_{ion}q_{ion} + (1-\gamma_\infty)\eta_{lat}q_{lat} \qquad (4.6b)$$

The subscripts 'ion' and 'lat' as indicated, stand for the charge distributions of the asphorical 3d-valence electron belonging to the ferrous ion ($^5D_4$, $3d^6$) and the neighbouring ions in the crystalline lattice respectively. (1-R) and $(1-\gamma_\infty)$ are the Sternheimer factors[175-77] which are introduced to correct

Recently this statement has been challenged by Nowik and Kaplan (Phys. Rev. 159(1967)273)who have calculated this part on pt. charge model for some divalent iron compounds. In view of the large 10 Dq values (10400 cm^{-1}) the temperature dependence of the quadrupole splitting is interpreted in terms of the temperature dependent occupation probabilities of the sixth electron in the d_ϵ (t_{2g}) states only. The field gradient parameters of a d electron for the d_ϵ and d_γ orbitals are given in Table 4.3.

TABLE 4.3: THE EFG PARAMETERS OF A d-ELECTRON IN d_ϵ AND d_γ ORBITALS IN AN OCTAHEDRAL SYMMETRY (O_h)

Irreducible representation (energy level label)	Spherical harmonics	Cartesian coordinates	V_{XX} in unit of $\langle r^{-3}\rangle$	V_{YY} in unit of $\langle r^{-3}\rangle$	V_{ZZ} in unit of $\langle r^{-3}\rangle$	η
E (d_γ)	$\lvert Y_2^0\rangle$	$\lvert 3z^2-r^2\rangle$	+ 2/7	+2/7	-4/7	0
	$\sqrt{\frac{1}{2}}\lvert Y_2^2 + Y_2^{-2}\rangle$	$\lvert x^2-y^2\rangle$	- 2/7	-2/7	+4/7	0
T_2 (d_ϵ)	$\sqrt{\frac{1}{2}}\lvert Y_2^1 + Y_2^{-1}\rangle$	$\lvert xy\rangle$	+ 2/7	-4/7	-2/7	+3
	$-\sqrt{\frac{1}{2}}\lvert Y_2^1 - Y_2^{-1}\rangle$	$\lvert xz\rangle$	- 2/7	+4/7	-2/7	+3
	$-\sqrt{\frac{1}{2}}\lvert Y_2^2 - Y_2^{-2}\rangle$	$\lvert xy\rangle$	-2/7	-2/7	+4/7	0

The quadrupole precession times are of the order of 2×10^{-8} sec. which are much greater than the thermal transition times between these levels[161,179], and hence the effective field gradient is the average of the contribution from those states, each of these weighted by Boltzmann factor. Assuming the occupation probabilities of the d_ϵ states as α^2, β^2 and δ^2 and making use of Eqs.4.5 and 4.6 and Table 4.3, we obtain

analysis of the experimental data employed the following values[o].

$$q = 0.20 \text{ barns};\ R = 0.62 \text{ and } \langle r^{-3} \rangle = 9.1/a_0^3$$

The experimental data was analysed by computerising the program to fit the Eq.6.6 and it was found that it is satisfied by several combinations of T_1 and T_2 at an observed temperature T. The choice of the characteristic temperatures assigned to the levels was guided by the observed temperature dependence of the quadrupole splitting and the available results of $Fe(NH_4SO_4)_2.6H_2O$[165]. The characteristic temperatures so assigned are given in Table 6.6.

TABLE 6.6: CHARACTERISTIC TEMPERATURES T_1 AND T_2 OF $^5T_2$ LEVELS OF VARIOUS IRON GROUP SALTS AND THE GROUND STATE ORBITAL HAVE BEEN GIVEN.

Compound	$T_1(^oK)$	$T_2(^oK)$	Orbital case Assigned
$Fe(NH_4SO_4)_2.6H_2O$	230	300	$\|xy\rangle$
$Fe(ZSO_4)_2.6H_2O$	200	260	$\|xy\rangle$
$Fe(RbSO_4)_2.6H_2O$	240	310	$\|xy\rangle$
$Fe(CoSO_4)_2.6H_2O$	220	280	$\|xy\rangle$

In order to decide the ordering of the energy levels it is essential to find the ground state wave function. From Table 6.5 the ratio of 'eq' for the singlet and doublet is

---

[o] The value of ξ ranging from 0.4 to 0.6 have been reported in lit. A detailed discussion is given in chapter VI on DPO calculations. The value of R = 0.62 is recently reported in Ref.170. H Cho and A, Ito have used $\langle r^{-3} \rangle_{3d}$ = 6.6 a.u.(Ref.169)

$$\frac{eq(singlet)}{eq(doublet)} = -2.0 \qquad (4.10)$$

From the Eqs. 4.9a , 4.9b and 4.9c we can determine the sixth electron population of those t_{2g} triplet states for all the members of the series at the observed temperatures after assigning the characteristic temperatures. The values so obtained are tabulated in Table 4.5.

TABLE 4.5: THE PROBABILITIES OF THE SIXTH ELECTRON OCCUPATION IN DIFFERENT t_{2g} LEVELS.

Compound	Temp.	Singlet |xy⟩	doublet |yz⟩	doublet |zx⟩
$Fe(NH_4SO_4)_2.6H_2O$	293	0.550866	0.251205	0.197869
	253	0.586545	0.235829	0.176826
	195	0.656967	0.201978	0.141056
	81	0.929267	0.053970	0.022763
$Fe(KSO_4)_2.6H_2O$	293	0.579079	0.238678	0.181047
	253	0.617790	0.221070	0.161140
	195	0.695774	0.183240	0.121360
	81	0.947513	0.038243	0.014244
$Fe(RbSO_4)_2.6H_2O$	293	0.559295	0.246560	0.194145
	253	0.594905	0.230392	0.174703
	195	0.668420	0.195227	0.136348
	81	0.951587	0.048131	0.020282
$Fe(CsSO_4)_2.6H_2O$	293	0.542406	0.255997	0.201524
	253	0.575718	0.241303	0.182979
	195	0.645318	0.208634	0.146048
	81	0.914073	0.030453	0.029474

4.6 RESULTS AND DISCUSSION

The values of Isomeric shifts at different temperatures

show that it is independent of temperature within the accuracy of measurements for NH_4, K and Rb salts; whereas the slight slope of I.S. vs temperature curve for Cs salt, 2.3×10^{-15} °K is due to the correction of time dilation resulting from the motions of emitting and absorbing nuclei. Further, the Fe^{2+} ion being surrounded by the distorted octahedron formed by $6H_2O$, the varying electronegativity of the alkali cation has no apparent effect on the value of I.S.

The values of the characteristic temperatures T_1 and T_2 are not unique since these are based only on the analysis of the quadrupole splittings (see the nature of Eq.(4.9))..) It is desirable to analyse simultaneously the Mössbauer data, the paramagnetic susceptibilities and the resonance data (if available).

Ingalls[155] taking into account the axial and rhombic crystal symmetry, spin orbit interaction and covalency effects, has shown that the ground state of the $(NH_4)_2.Fe(SO_4)_2.6H_2O$ is a singlet $|xy\rangle$. Keeping in view the Eq.4.10 we see that the order of low temperature values of quadrupole splitting in the rest of the series, Table 4.2, is the same. Hence we infer that the ground state wave function in all these cases is a singlet $|xy\rangle$ like $Fe(NH_4SO_4)_2.6H_2O$. This is further endorsed by the low temperature occupation probabilities of the sixth d electron, Table 4.5.

4.8 COMMENTS

As stated in the text above, the analysis made here neglects (a) the lattice part (b) spin orbit interaction (c) covalency effects and (d) assumes the temperature independence of the characteristic temperature and hence is very elementary.

Thus the inferences arrived at are only approximate. A more general analysis should include all these aspects. We may add here that recently single crystal work on FAS has been done in our laboratory[82b] and by Ingalls et al.[103c] wherein a complete determination of the 5 independent components of the traceless, symmetric EFG tensor has been done. The EFG axes are compared with the susceptibility axes.

C H A P T E R V

MÖSSBAUER STUDIES° OF ALKALI DITHIOFERRATES (III)

5.1 INTRODUCTION

The details of the preparation of a series of compounds of tetrahedrally coordinated Iron (III) having a general formula $AFeS_2$, where the cation A = Na, K, Rb or Cs have been recently reported by Dröngor[180]. Their X-ray studies and magnetic properties of this series, viz., $KFeS_2$ and $NaFeS_2$ are known since long. Preis[182] and Schneider[183] prepared these compounds independently long back in 1809 and studied their structural properties. $NaFeS_2$ has been used as a dyeing compound[184] for homogeneous coloration of glasses. $KFeS_2$ has been used as a catalyst in cracking reactions[185] and it increases its rate by a factor of 100 to 380%.

Mössbauer Studies of $KFeS_2$ have been made extensively by Kerler et al.[108]. In the case of $KFeS_2$ and $KFeO_2$, they have reported that for $KFeS_2$ the magnetic field at the nucleus decreases from 203 Kgauss at -165° to zero at -28°C, but for $KFeO_2$ from 515 Kgauss at -125° only to 400 Kgauss at 78°C. From this they inferred the existence of a low transition point for $KFeS_2$. Further, a plot of I.S. versus temperature showed a deviation from the otherwise normal and approximately linear relationship and thus indicating the transition at -28°C for $KFeS_2$. These studies inspired us to undertake Mössbauer investigation in the other members of the series to look for similar transitions with a view to decide the

---

° Based on paper 'Mössbauer Spectra of Tetrahedral Alkali Dithioferrates (III) D. Nag and S.P. Puri: J. Chem. Phys. 50(1969)3184.

nature of the reported transition in $KFeS_2$.

Edward and Johnson[126] studied iron (II) compounds in tetrahedral coordination and their investigations reveal that, in contrast to the behaviour of high spin Fe(II) octahedral compounds, the Fe(II) compounds in tetrahedral coordination show a markedly greater dependence of quadrupole splitting upon temperature and the isomeric shifts are also considerably lower. In order to seek comparison of hyperfine interactions in the case of iron (III) in tetrahedral coordination and to supplement the relatively fewer reports on such iron compounds, such a study was embarked upon. Furthermore, the bearing of the electronegativity of the cation on the isomeric shift in alkaline ferrocyanides[88] and super complexes[187] having iron in octahedral bonding (d^2sp^3) has been reported. A systematic study of such an effect in the case of compounds with Fe in tetrahedral coordination (sp^3) was considered desirable.

5.2 EXPERIMENTAL

Schneider[183] prepared the compounds $KFeS_2$ and $NaFeS_2$ by fusing the powdered iron with potassium carbonate (sodium carbonate in case of $NaFeS_2$) and sulphur in air, and leaching the cold product with water. A more detailed but similar procedure for preparing the compound $KFeS_2$, alongwith its properties is also reported in literature[188]. The fusion in air[183,184] yields an impure compound and impurity like Fe_3O_4 is not ruled out[181]. We have followed the method* of Brönger[180,181] in preparing** the compounds employing the

---

* The author is very much thankful to Professor Brönger for sending reprints of his papers alongwith the details of the preparation.

** The author is thankful to Mr. Shri Nath, senior analyst of Metallurgy Department of this University for discussion and sparing a furnace for my use.

fusion reaction under a dry, oxygen-free nitrogen atmosphere. All the chemicals used, were of A.R. quality. The reaction temperature in all these cases was 800 to 850°C. The exchange of alkali sulfides with iron and sulfur in closed ampoules also gives the same compounds.

$KFeS_2$ grows in permanganate coloured needle shaped monoclinic crystals whereas $RbFeS_2$, $NaFeS_2$ and $CsFeS_2$ were granular in appearance. X-ray diffractographs were taken which did not reveal the presence of any FeS, FeS_2 or any unreacted iron which ensured the successful completion of the reaction.

The Mössbauer spectra using a standard Co^{57} source in Pd matrix with an initial activity of 1mC. were recorded for polycrystalline powder absorbers in transmission geometry from the room down to the liquid nitrogen temperature. The lines were fitted by least square analysis on 3600 CDC computer making the assumption that the line shapes are Lorentzian.* The values of I.S. and Q.S. so obtained are given in Table 5.1. The representative spectra for $NaFeS_2$ and $CsFeS_2$ are given in Fig.5.1 and 5.2 and the values of Q.S. versus temperature for all the compounds are plotted in Fig.5.3.

Some of the low temperature measurements were taken** at the Tata Institute of Fundamental Research, Bombay and the cryogenic arrangement employed a cryostat fabricated after the design by Wiedermann et al.[118]. Any temperature down to liquid

---

* The computer program of Rhodes et al. Ref.95 was modified by R. Nagarajan and T.S. Radhakrishanan of T.I.F.R. Bombay (India), in order to use it directly for a mechanical drive. The author is thankful to Mr. Nagarajan for this help.

** The author is very much thankful to Dr. R. Patehally and his group for allowing the use of their Mössbauer spectrometer for some low temperature measurements.

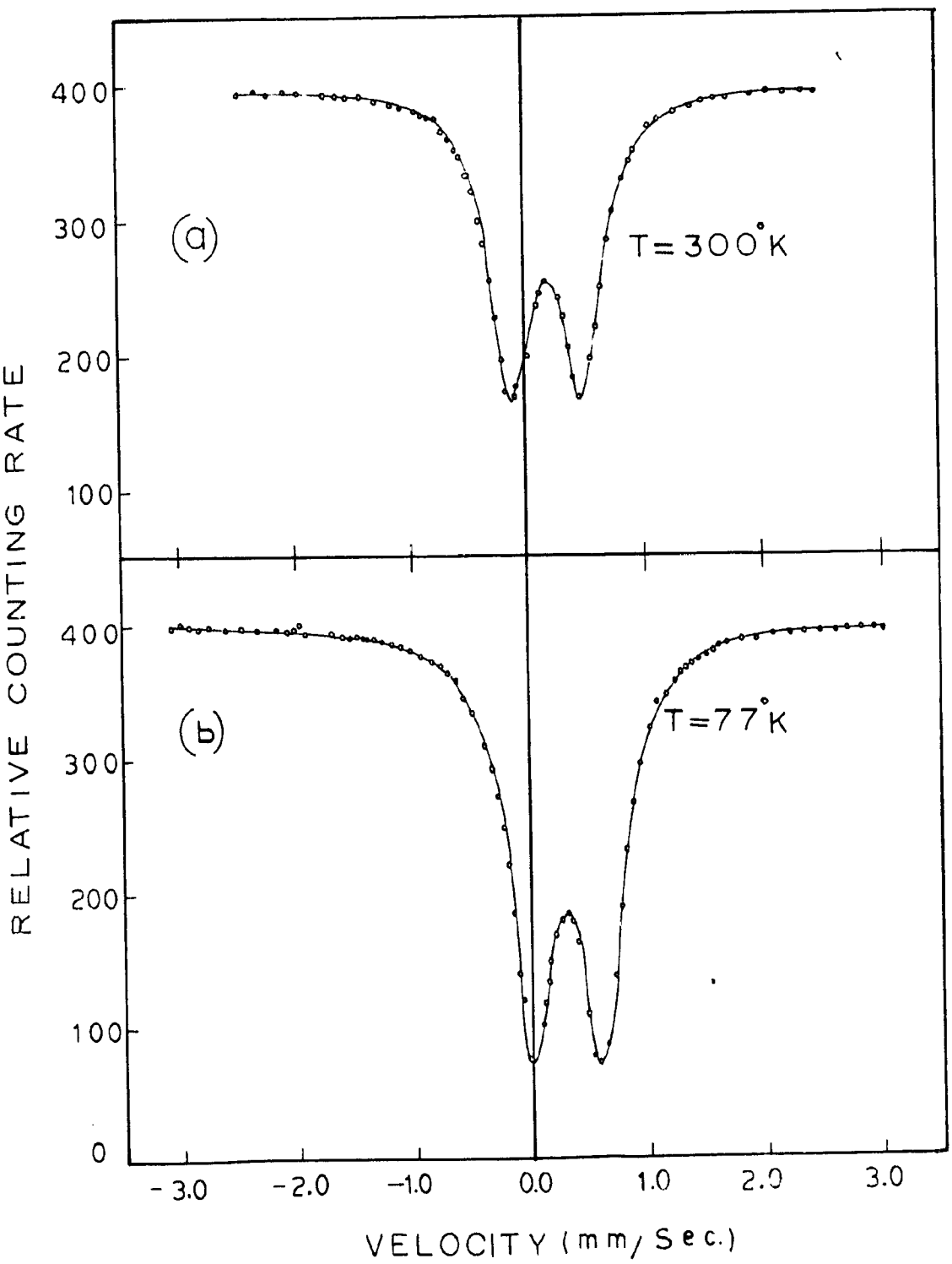

FIG.5.1 LEAST SQUARE FIT MÖSSBAUER SPECTRA FOR Na Fe S_2 (a) AT ROOM TEMPERATURE (b) AT 77°K

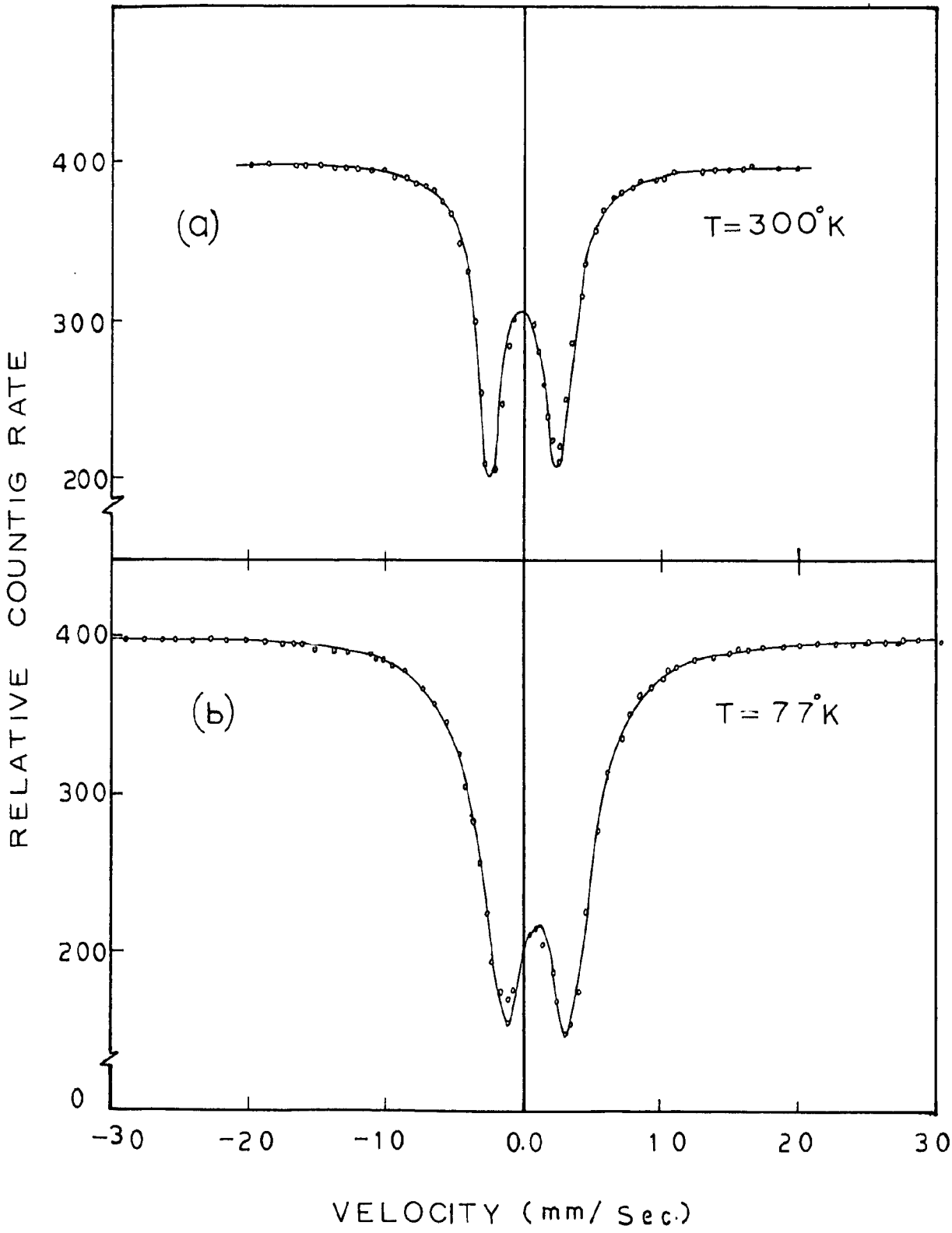

FIG.5.2: LEAST SQUARE FIT MÖSSBAUER SPECTRA FOR $CsFeS_2$ (a) AT ROOM TEMPERATURE (b) AT 77°K.

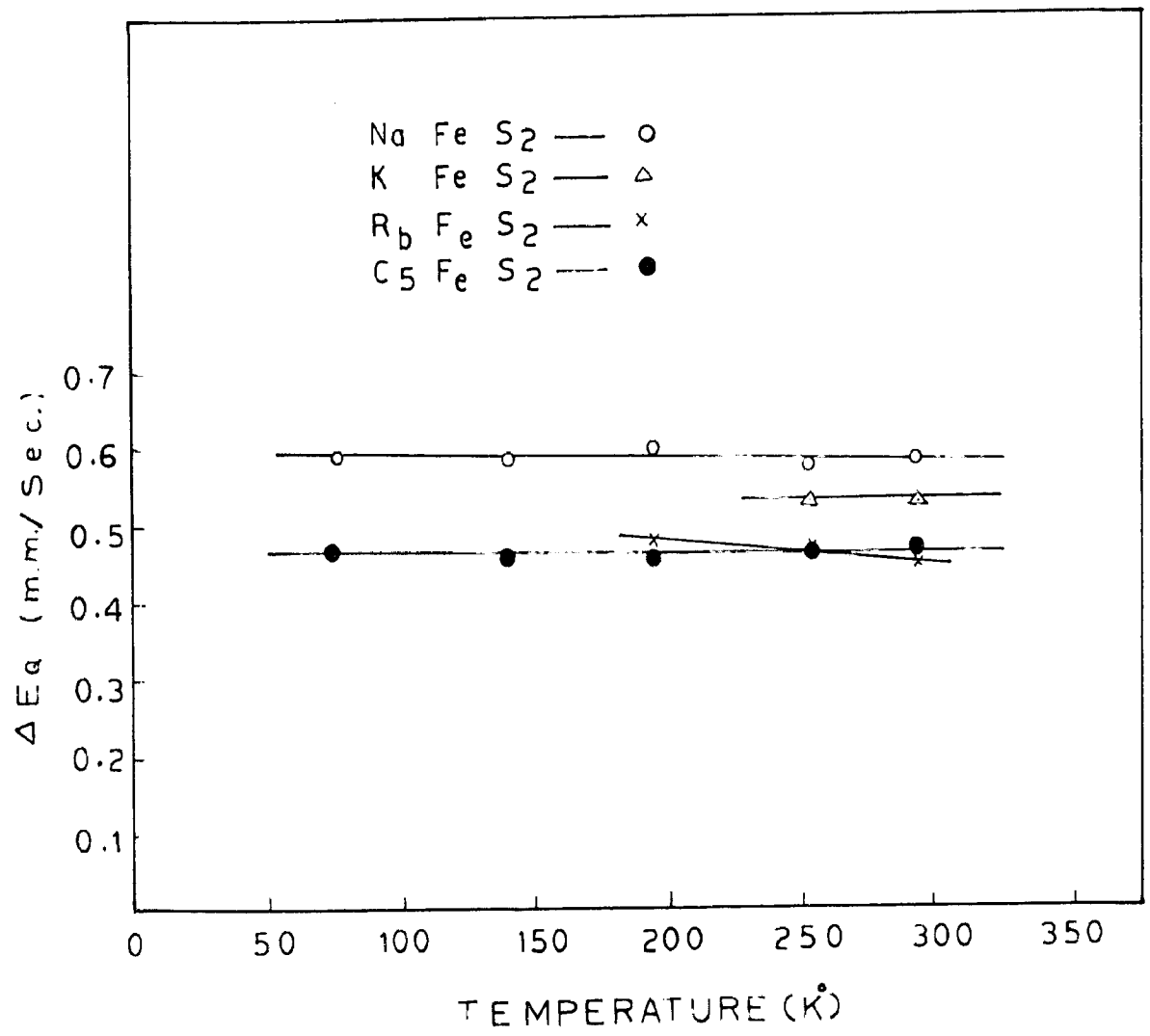

FIG 5.3 : QUADRUPOLE SPLITTING VERSUS TEMPERATURE.

nitrogen could be set within an accuracy of ± 1°C. In addition, the magnetic susceptibility measurements were carred out in the same institute* for all these compounds over the temperature range 77-300°K. The values of μ_{eff} as calculated from molar susceptibilities are listed in Table 5.2.

TABLE 5.1: VALUES OF I.S., ΔE_Q AND LINE WIDTHS FOR ALKALI DITHIOFERRATES(III). THE VALUES OF I.S. ARE RELATIVE TO IRON.

Source: $^{57}Co(Pd)$

Compound	Temp. °K	Isomer shift mm/sec.	Quadrupole Splitting mm/sec.	Line width, and Γ_1 mm/sec.	Γ_2
$NaFeS_2$	295	0.36	0.58	0.35	0.35
	253	0.37	0.57	0.36	0.36
	195	0.39	0.59	0.40	0.40
	140	0.46	0.59	0.38	0.41
	77	0.48	0.59	0.47	0.45
$KFeS_2$	295	0.19	0.53	0.30	0.30
	253	0.21	0.53	0.40	0.40
$RbFeS_2$	295	0.19	0.45	0.30	0.30
	253	0.19	0.47	0.35	0.35
	195	0.27	0.48	0.40	0.40
$CsFeS_2$	295	0.18	0.46	0.30	0.30
	253	0.19	0.46	0.32	0.32
	195	0.25	0.46	0.32	0.32
	140	0.27	0.46	0.30	0.30
	77	0.29	0.47	0.44	0.42

The errors in the values of I.S., Q.S. and line width (assuming a Lorentzian profile) are ± 0.02 mm/sec.

* The author is very much thankful to Prof. Kanekar for allowing to take measurements on his susceptibility measuring apparatus and Mr. Marathe for the assistance in using the equipment.

TABLE 5.2: VALUES OF μ_{eff}, NO. OF UNPAIRED 3d ELECTRONS, TOTAL s-ELECTRON DENSITY AND 4s CHARACTER IN ALKALI DITHIOFERRATES.

Sl. No.	Compound	μ_{eff}	No. of unpaired d-electrons	I.S. Values (mm/sec) w.r.t.Fe	$\Psi_s^2(0)$ (a.u.)	% 4s character (approximate).
1	$NaFeS_2$	4.65	3.77	0.355	11881.80	25
2	$KFeS_2$	4.61	3.72	0.190	11881.85	35
3	$RbFeS_2$	-	-	0.185	11881.86	36
4	$CsFeS_2$	4.38	3.49	0.175	11881.88	38

5.3 STRUCTURE

The first X-ray structure of any member of the series reported was that of $KFeS_2$ by O'Daniel[189], who proposed an orthohexagonal cell with a = 13.04Å and C = 5.40Å. $KFeS_2$ grows in paramagnetic coloured needle shaped monoclinic crystals with space group symmetry C_{2h}^6 with 4 molecules per unit cell[190] having all Fe atoms at equivalent sites. The structure[181] of $RbFeS_2$ is isotopic to $KFeS_2$ whereas $CsFeS_2$ forms orthorhombic crystals with space group D_{2h}^{25} with a tetramolecular unit cell. The crystal structure of $NaFeS_2$ is under investigation[181]. The lattice spacings, space groups, and the significant interatomic distances etc. are reproduced here in Table 5.3 and 5.4 from Brönger's work for ready reference. We see that in $KFeS_2$ and $RbFeS_2$ there is only one short Fe-Fe distance, whereas in $CsFeS_2$ through the Z parameter value of 0.242, two different distances are obtained whose mean is comparable to the distance in $KFeS_2$ and $RbFeS_2$.

In all these compounds the iron atoms are principally

TABLE 5.3: LATTICE CONSTANTS, SPACE GROUP AND NO. OF MOLECULES PER UNIT CELL.

Compound	Lattice constants	Space group	Z
$KFeS_2$	a = 7.09 Å b = 11.27 Å c = 5.39 Å β = 113.2°	C_{2h}^6 - C 2/c	4
$RbFeS_2$	a = 7.22 Å b = 11.70 Å c = 5.42 Å β = 112.0°	C_{2h}^6 - C 2/c	4
$CsFeS_2$	a = 7.13 Å b = 11.92 Å c = 5.42 Å	D_{2h}^{25} - I_{mmm}	4

TABLE 5.4: SIGNIFICANT INTERATOMIC DISTANCES (in Å)

Compound	Fe - Fe	Fe - S	Alkali - S
$KFeS_2$	2.70(2x)	2.18(2x) 2.29(2x)	3.32(2x) 3.34(2x) 3.40(2x) 3.50(2x)
$RbFeS_2$	2.71(2x)	2.20(2x) 2.22(2x)	3.42(2x) 3.48(2x) 3.56(2x)
$CsFeS_2$	2.62 2.81	2.18(2x) 2.28(2x)	3.44(2x) 3.65(2x) 3.85(2x) 4.29(2x)

covalently bonded by slightly distorted sulphur tetrahedra. The $[FeS_2]^-$ ions are arranged in chains of FeS_4 tetrahedra linked by their edges with short Fe - Fe distances, Fig.5.4 (a,b). The Fe - S tetrahedra form the chains,

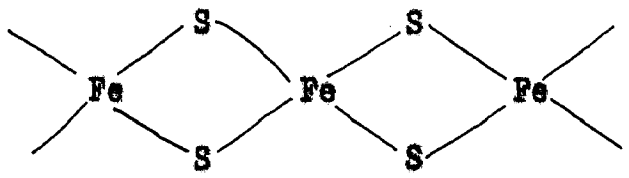

which account for the fibrous character of the substances and suggest a strong covalent bonding for iron atoms which are arranged in chains along the c-axis. The arrangement of the alkali ions in $KFeS_2$ and $CsFeS_2$ type is different; whereas in the former, the alkali and iron ions have the same z parameters with values 0.25 and 0.75, in the latter, Cs ions are 0.0 and 0.5. Thus one obtains for K and Rb ions the coordination number 8 and for Cs number 10.

5.4 DISCUSSION

Under the influence of the tetrahedral ligand field the fivefold degenerate ^6S state of the free Fe(III) ion splits into a lower doublet , containing the orbitals d_{z^2} and $d_{x^2-y^2}$, and a higher triplet d_ϵ, containing d_{xy}, d_{yz} and d_{xz} orbitals. A distortion from the regular tetrahedral symmetry (Tables 5.4, Fe - S distances) will further lift the degeneracy of the d_γ and d_ϵ orbitals and give rise to quadrupole splitting. From the observations that quadrupole splitting. From the observations that quadrupole splitting is almost independent of temperature, Fig.5.3, it is inferred that the level separation is larger or $\sim kT$ with the

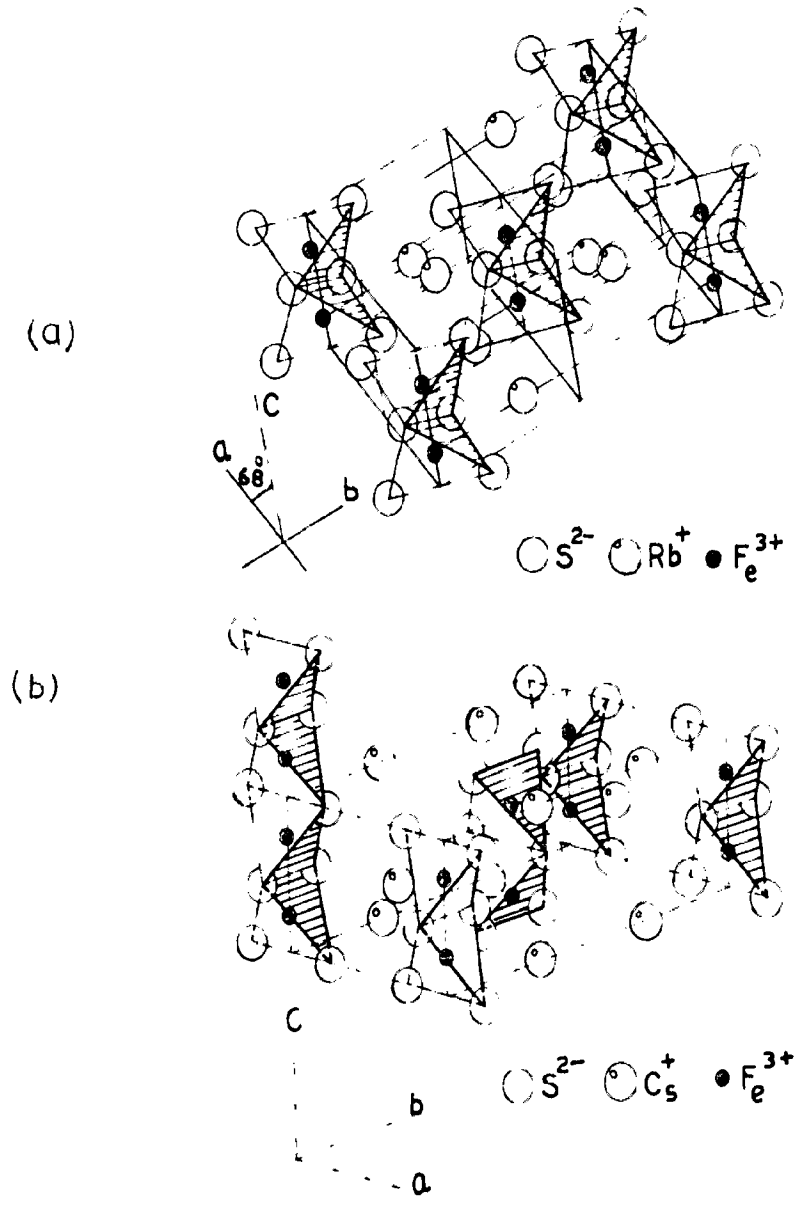

FIG. 5.4 LATTICE STRUCTURES (a) $R_b F_e S_2$, (b) $C_s F_e S_2$

consequence that the electronic population densities do not vary with temperature.

Furthermore, it is observed that the quadrupole splitting decreases with the increase of cationic radius, Fig.5.5. The bigger cation will normally cause greater distortion of the tetrahedral symmetry and thus enhance the electric field gradient (EFG) but this being not the case, there are no solid state effects in these compounds. The increased pairing of the d electrons for the Na to Cs compounds, Table 5.2, implies an increase in the crystal field and decrease in the EFG contribution from the uncompensated electrons.

It has been reported[88] in the case of a series of alkaline ferrocyanides of the type $M_4|Fe(CN)_6|$ where M = H, Li, Na, K, Rb, Cs and NH_4, that the isomeric shift (I.S.) decreases with the increase of electronegativity of the cation. This was explained by the assumption that in the ferrocyanide series from H to Cs the last members with the lowest cation electronegativity are the nearest to the ideal diamagnetic structure of Fe - $3d^{10}4s^2 4p^6$ [191]. Assuming that the octahedral configuration (d^2sp^3) is conserved, in the case of the first few members of this series, with more electronegative cation, the lower number of 3d electrons shields 3s and 4s electrons to a lesser degree, whereas for the last members the transition of the electrons from the electronegative cation is more complete with the consequent higher shielding. This increased shielding will cause more positive isomeric shift. (There is an omission of a negative sign in the I.S. values plotted in Fig.1 of Ref.88). In the case of present compounds the iron(III) is in tetrahedral coordination ($4s4p^3$) involving no d electrons. The increasing

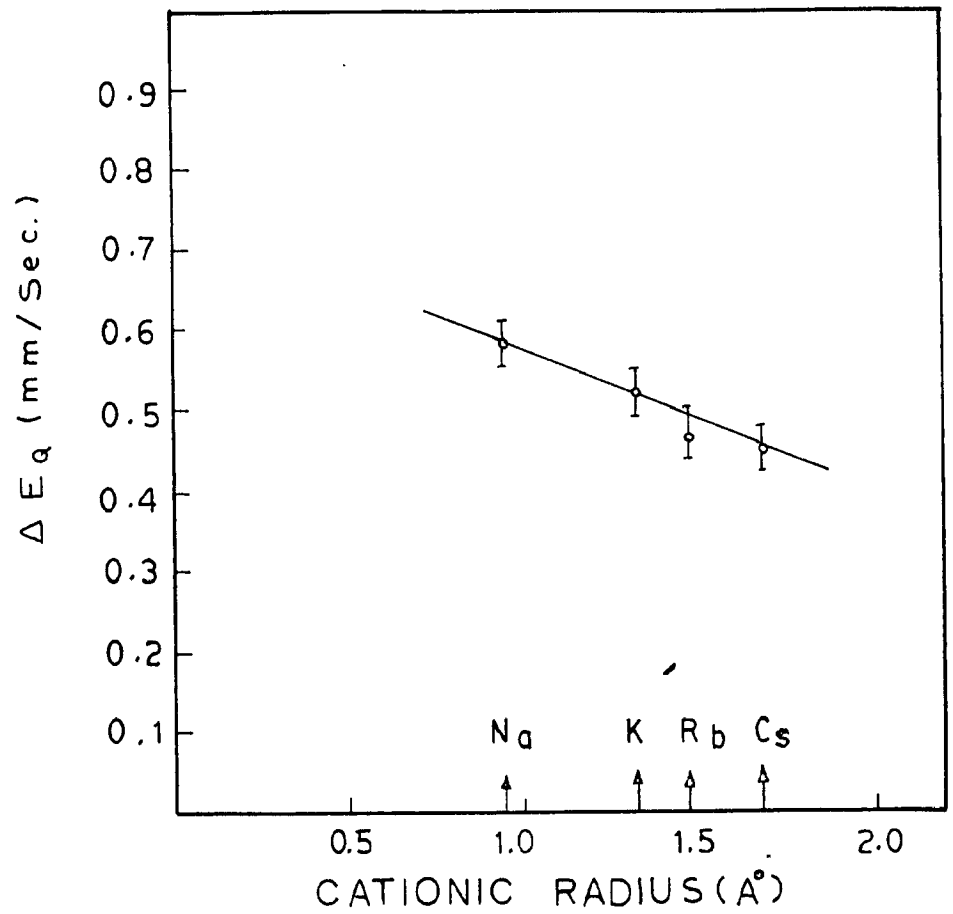

FIG.5 5 : QUARDRUPOLE SPLITTING VERSUS CATONIC RADIUS.

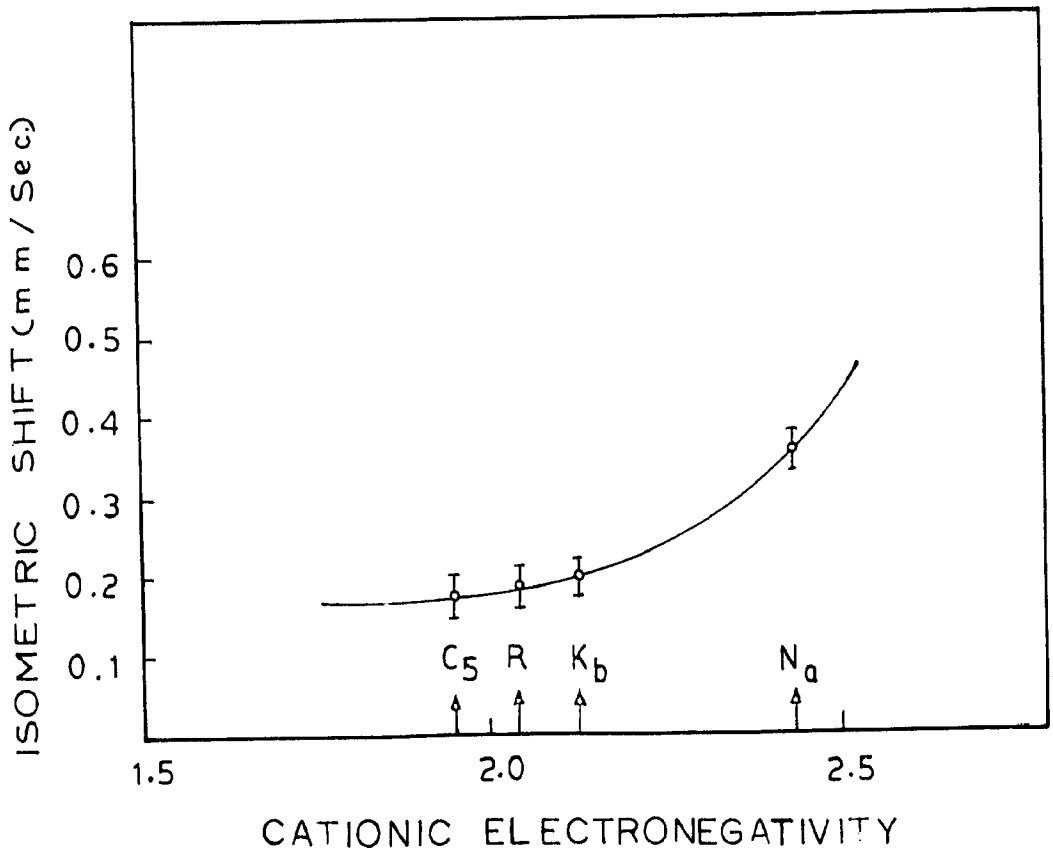

FIG.5.6 I.S. VERSUS ELECTRONEGATIVTY OF THE ALKALI CATION.

electronagativity of the cation will decrease the 4s electron density at the Fe nucleus thereby increasing the I.S. value, which is in agreement with the experiment, Fig.5.6. This conclusion is in contrast to the octahedral case.

The existence of a transition point for $KFeS_2$ at -28°C had been shown by Kerler et al.[103]. All the other compounds give only the quadrupole split doublet spectra with no magnetic hyperfine splitting, down to liquid nitrogen temperature. With a view to decide the nature of transition involved in $KFeS_2$, the magnetic susceptibility vs temperature was studied in all these compounds. Our observations do not indicate any magnetic ordering or magnetic transition throughout the range investigated. It has been shown by Brongor[181] that susceptibility is temperature independent over the range 90-500°K. This rules out the possibility of a magnetic transition in $KFeS_2$ and the internal magnetic field is presumably resulting due to relaxation effects.[52,149] Spin lattice relaxation of paramagnetic ions will give rise to the fluctuating electric and magnetic fields and if the fluctuation rate is rapid compared to the precession frequency of the nucleus, the latter will see a time averaged magnetic field which is zero and hence symmetric quadrupole splitting will be observed. Presumably the internal magnetic field is zero in dithioferrates.

The total s-electron density at the iron nucleus in a complex is due to presence of pairs of electrons in the 1s, 2s, and 3s orbitals and a variable contribution from the 4s orbital. The latter depends on the degree of occupation of this orbital by electrons from the ligands and for this reason

it can change from one complex to another. Furthermore, on the basis of the restricted Hartree-Fock calculations of Watson for iron in different valency states it has been shown that the s-electron density increases when the no. of d electron decreases[71]. This is due to the decrease in shielding of the 3s electrons when the 3d electrons are removed. Thus

$$\Psi_s^2(0) = \sum_{i=1}^{3} \Psi_{is}^2(0) + x\,\Psi_{4s}^2(0) \qquad (5.1)$$

where $\Psi_s^2(0)$ is the total s-electron density at the Fe^{57} nucleus in the host under consideration, first term in the right hand side of the Eq. is the contribution from the inner-shells and x is the fraction of $\Psi_{4s}^2(0)$ of the 4s density arising from the partial occupation of this shell by electrons from the ligands. The inner shells contribution for different d^n configuration has been calculated by Walker et al.[71] and is given as below

d^n	d^8	d^7	d^6	d^5	d^4
$\sum_{i=1}^{3} \Psi_{is}(0)$ (in units of a_0^{-3})	11878.8	11879.2	11879.8	11881.4	11885.4
	11878.8				

The I.S. is related to $\Psi_s^2(0)$ by the relation

$$I.S. = \alpha\,\Psi_s^2(0) + \text{const} \qquad (5.2)$$

The constant of proportionality α depends upon the change in the charge distribution within the nucleus during the nuclear transition. In particular, when relativistic corrections are

neglected, and one assumes a uniformely charged nucleus

$$\alpha \cong (c/E_\gamma)(2\pi/5)\, Ze^2\, (R_{ex}^2 - R_{gd}^2)$$

with symbols having usual meanings. Employing experimental values of I.S. for Fe^{2+} and Fe^{3+} compounds in conjunction with the 3d electron densities at the nucleus calculated using Watson free ion wave functions[73], Ingalls obtained[192] the following value of the calibration constant α*.

$$\alpha = -(0.47 \pm 0.05)\ a_0^3 \ \text{mm/sec.} \qquad (5.3)$$

One can write for any of these compounds from Eq.5.1 and 5.2

$$\Psi_s^2(0)_{Tet.} = \Psi_s^2(0)_{Fe^{3+}} + \frac{1}{\alpha}\left[(I.S.)_{Tet} - (I.S.)_{Fe^{3+}}\right] \qquad (5.4)$$

where $\Psi_s^2(0)_{Fe^{3+}} = 11881.4$ a.u. is the total s-electron density for the free-ion $3d^5$ configuration and the $(I.S.)_{Fe^{3+}}$ is 0.41 mm/sec relative to metallic iron[70].

These are covalent compounds with Fe(III) in tetrahedral coordination (sp^3) and no d electron is being used in bonding. The values of 3d electron spin density as calculated from the molar susceptibilities are given in Table 5.2. In the absence of any pairing, these 3d spin densities will also be the respective 3d charge densities responsible for the observed I.S. values.

The values of $\Psi_s^2(0)_{Tet}$ may be obtained from Eq.5.4 with the experimental I.S. values and are also listed in Table 5.2. Now substituting this value and the value of $\sum_{i=1}^{3} \Psi_{i,s}^2(0)$

---

* J. Danon and L.Iannarella (J. Chem. Phys.47(1967)382) have reported this value as $\alpha = -0.021$ mm/sec. Though there is m much difference in this and Ingall's value, our conclusions remain unchanged even if we use their value.

corresponding to the given number of d electrons in Eq.5.1, one gets the values of x $\Psi^2_{4s}(0)$. The contributions x $\Psi^2_{4s}(0)$ turns out to be negative, which is absurd. This contradicts our assumption about the non-pairing of 3d electrons and points out that rather there is some pairing involved i.e. the number of d electrons responsible for the I.S. value is not equal to that obtained from the μ_{eff} values. We can also interpret this result in the sense that there is no delocalization of the d electrons and that the binding of central iron ion does not involve any d electron as required by the sp^3 hybrid orbitals.

It may be remarked that WWJ[71] plot which is generally used to estimate the 4s character for the ionic compounds is also applicable to the compounds having tetrahedrally bonded (sp^3) iron, since no d electrons of the iron atom are used in its bonding to the ligand. This, however will not hold for iron in octahedral bonding (d^2sp^3). The 4s character of Fe(III) for these compounds from the modified WWJ plot[193] is listed in Table 5.2. This conclusion about a partial pairing of 3d electrons does not contradict the observation about the lack of temperature dependence of ΔE_Q, since the latter merely implies that the relative level separation is very large as compared to kT with the consequence that Boltzmann population does not change.

The line widths (F.W.H.M.) at different temperatures are included in Table 5.1 and are in the range of 3 to 4Γ (Γ is the natural line width of the 14.4 keV transition = 0.095 mm/sec.) Vignall[60] carried out systematic studies of line widths in the case of Fe^{3+} salts and allowed broadening of 4Γ

resulting from instrumental noise, extraneous vibrations, absorber thickness effects[47] etc. It is therefore concluded that the observed line widths do not indicate any pronounced broadening and the electronic relaxation rates are fast[52]. This view is supported both by the short Fe - Fe distances as well as the observed temperature independent paramagnetism[181].

C H A P T E R VI

ELECTRIC FIELD GRADIENT (EFG) CALCULATIONS IN IRON (III) COMPOUNDS

6.1 INTRODUCTION

We know that Fe^{57} has $I_g = 1/2$ and as such no quadrupole moment Q can exist. This unfortunately, precludes the NMR and NQR studies of this nucleus. Nevertheless, there is a quadrupole moment, Q in the excited state and we can study this state by the use of Mössbauer effect.

The experimental values of the nuclear quadrupole coupling constant, e^2qQ/h in the case of divalent and trivalent iron compounds have been extensively utilised to estimate the quadrupole moment $Q(Fe^{57})$ of the first excited state in Fe^{57}. The estimates of Q range between (+0.1b) and (+0.6b), the low value derived from Fe^{2+} in various crystals[68,108,155,178,178,194-201] and the high value derived from Fe^{3+} compounds[202-7]; the variation largely resulting from differences in the calculated values of q, the second derivative of the electrostatic potential along a particular crystal direction. A comparative study of these works is presented in Table 6.1. Ingalls[155] concluded from the analysis of Fe^{57} quadrupole splitting in the ferrous compound $FeSiF_6.6H_2O$ that Q = 0.29 ± 0.02b. In the divalent state ($^5D_4, 3d^6$), the major contribution to the field gradient seen by the nucleus is from the uncompensated 3d valence electron, whereas the gradient contribution arising from the ligand disposition in the lattice is small.

TABLE 6.1: A REVIEW OF THE PREVIOUS ESTIMATIONS OF Q(Fe^{57m})

Sl. No.	Fe^{2+}/Fe^{3+} (Ion investigated)	Q(Fe^{57m}) (barns)	Ref.	Remarks
1	(Fe^{2+}(MgO)	0.20b	201	The Mossbauer effect measurements of Leidor and Pipkorn(Phys. Rev. 105(1958)494) are explained on the basis of strain induced crystal field splitting and is concluded that Q=0.20b and not 0.29b.
2	Fe^{2+}(MgO)	0.21±0.03	200	Magnetic field induced quadrupole splitting employed
3	Fe^{2+}(ferrocene)	0.175±0.02	199	Claimed good agreement with recent calculations of Fe(II) complexes in the solid state.
4	Fe^{3+}(αFe_2O_3)	0.29b±0.03b	207	Most elaborate calculation done, but ignored dipole contribution from Fe^{3+} cations (Previous work reviewed).
5	Fe^{3+}(calcium aluminate ferrite)	0.30	198	The value of Q at tetrahedral site was 0.29b while at the octahedral site it is 0.33b. Only monopolar contribution considered.
6	Fe^{2+}($FeSiF_6.6H_2O$)	0.20	178	Low temperature data used, contribution from lattice included but covalency effects and dipole contribution ignored.
7	Fe^{2+}($FeSiF_6.6H_2O$)	0.16	197	Value derived from the $\langle r^{-3}\rangle_{max}$ value with the assumption that $\langle r^{-3}\rangle$ Q = $\langle r^{-3}\rangle$ L = $\langle r^{-3}\rangle$d.
8	Ferrous and ferric (hemoglobin compounds)	0.17	P13	On separating the data Q(Fe^{3+}), of the order of $Q(Fe^{2+})$

TABLE C.1 continued

1	2	3	4	5
9	-	0.10±0.02	212	Nuclear Model calculation (Coriolis coupling of two rotational bands)
10	Fe^{3+}(α-Fe_2O_3)	0.41	205	Old X-ray data used, induced dipoles on Fe^{3+} ion ignored.
11	Fe^{3+}(α-FeOOH)	0.20	200	Calculated only the monopole contributions, used high temperature e^2qQ data, and assumed that crystallographic special position parameters obtained for α-AlOOH could be used for α-FeOOH.
12	Fe^{3+}(α-Fe_2O_3)	0.277	204	Monopole plus partial dipole (only on O^{-2}) contribution considered Artman(Ref.205, and 207) have reported an error in their calculations.
13	Fe^{3+}(anion of Fe^{3+} garnets)	0.20	203	Do not include dipole contribution and probably more important, they used room temperature structure parameters and high temperature($\sim$ 600°K) measurements of e^2qQ.
14	Fe^{2+}($FeSiF_6.6H_2O$)	0.29±0.02	185	Most elaborate analytical work so far done on Fe^{2+} compounds, with review of the work.
15	-do-	0.15	196	Spin orbit interaction considered but core polarization ignored.
16	Fe^{3+}	0.18	177	Revised downward from 0.23 - 0.18b.
17	Fe^{3+}(α-Fe_2O_3)	0.20	170	Burns value of Q was modified using the newly calculated γ_∞ value.
18	Fe^{2+}($FeSiF_6.6H_2O$)	0.12b	108	Polarized 14.4 keV gamma radiation used, the value reported is Q(1-R) and so is subject to small correction due to (1-R), which will yield a value of R = 0.18.

TABLE 6.1 Continued

1	2	3	4	5
19	Fe^{2+}(divalent compounds)	0.13	175	Value of R = 0.22 calculated and used. This value is further modified to be 0.32 (Ref.155).
20	Fe^{2+}(divalent compounds)	0.16	70	Value of q $=(4/7)\langle r^{-3}\rangle_d = (4/7)\times 0.1/a_0^3$ alongwith R = 0.42 used. Covalency, spin orbit interactions, lattice contributions ignored.
21	Fe^{3+}(YIG and α-Fe_2O_3)	0.40	202	A value of -0.17 calculated for is used. Only monopole contribution used. A recent accepted value of is -0.14(Ref.170).

Furthermore, in the ferric state ($^6S_{5/2}$, $3d^5$), the ions own electron shell does not contribute to the field gradient at the nucleus other than through Sternheimer antishielding. There will be only lattice contribution to the field gradient.

An interpretation made for the isomeric shift for α-Fe_2O_3 on the WMJ plot[71], leads to an admixture of s-character into the $3d^6$ state of about 2% and thus shows that the lattice of α-Fe_2O_3 is ideal for carrying out the lattice summations using a point charge model[209]. Sharma and Das[204] from their field gradient calculations taking into account the monopolar and partial dipolar contributions (from O^{-2} only) interpreted the Mossbauer observations of quadrupole moment, Q of $(Fe^{57m})^{3+}$ in Fe_2O_3, to correspond to +0.27b, in good agreement with Ingalls's result. Later on Artman[205], carrying out an identical lattice sum, showed the value of Q(Fe^{57m}) to be 0.41b and thus bringing out in sharper focus the ferrous-

ferric anomaly. However, now Artman's Q value of 0.41b has been brought down to 0.283 ± 0.03[207], more in accord with the previous data.

Nozik and Kaplan[178] have computed the lattice contributions to the electric field gradient in $FeSiF_6.6H_2O$, $FeSO_4.7H_2O$, $FeCl_2.4H_2O$ and $FeCl_2.2H_2O$ yielding the magnitudes and signs of the lattice effects in these compounds. From the computed electric field gradient in $FeSiF_6.6H_2O$ and the experimentally measured low temperature quadrupole splitting in this crystal, they have re-evaluated the nuclear quadrupole moment of Fe^{57m} to be + 0.20b. They also showed that one cannot, in general, assume the effect of the lattice to be small and in contradiction to the analytic treatment of Ingalls, the lattice contribution in this crystal is very small (as compared to 12 % by Ingalls) and has the same sign as the electronic contribution (need not be always of opposite sign as predicted by Ingalls). Furthermore, they neglected the covalency effects, whereas Ingalls accounts for this by reducing $\langle r^{-3} \rangle$ by the factor $\alpha^2 = 0.8$. The neglect of covalency is considered[178] a good approximation in the case of this crystal as the $Fe(H_2O)_6^{2+}$ complex present in it, is essentially ionic[78, 210-11].

In view of the lack of correspondence between the ferrous and ferric Q values and the importance of lattice contribution to Mössbauer quadrupole splitting, we undertook to study in detail the lattice contribution on a point charge-point dipole model for the compounds $ZnFe_2O_4$, $CuFeO_2$ and α-Fe_2O_3. These compounds have iron in available for them.

We have chosen these compounds with the following considerations. In all these compounds, as will be evident from

the following discussion, the Fe^{3+} ion is essentially bonded ionically and this validates, the appropriateness of the model calculations. In case of Fe^{3+} ion, most of the investigators have studied the α-Fe_2O_3 compound[202,204,208,207] while in the Fe^{2+} case a variety of compounds have been studied Table 6.1. The Sternheimer antishielding factor γ_∞ for Fe^{3+} is recently re-evaluated[176] and a reasonably agreeable value is available. In the case of $ZnFe_2O_4$ and $CuFeO_2$ all the Zn^{2+}, Fe^{3+} and Cu^{+} ions have either inversion or cubic symmetry so that the electric field acting on these ions is zero and hence much of the computation and the possible complications arising due to uncertainties of the polarisability values will be avoided. All these ions do not have permanent dipole moments and this avoids further uncertainties and complications in calculations. A major difficulty which comes in the way of calculating the lattice contribution is the proper assignments of the charges to the lattice site and for this a complete knowledge of covalency is required and in most cases of disagreement between theoretical and experimental results, covalency is held responsible. Inspite of the diffuseness of the O^{--} charge distribution in these compounds, the compactness of the positive ions, as manifested by their small radii, argues against the possibility of much covalent bonding. The structures like ClO_3^-, BrO_3^-, NO_3^-, SO_4^{--} etc. where exact assignment of the charges is not possible are thus also avoided. The charge assignment to different lattice sites were the ionic charges themselves in view of the S-character of their outermost orbits.

$ZnFe_2O_4$ has a typical normal spinel structure and so all octahedral sites are occupied by ferric ions. It is

paramagnetic at room temperature and is favourable for accurate measurements of the quadrupole interactions, since the electron configurations of Zn^{2+} and Fe^{3+} ions do not cause the Jahn-Teller distortion[214]. In $CuFeO_2$ (delafossite), it has been inferred on the basis of crystal ionic radii[215] and on electrostatic calculations of the lattice energy[210], that iron is present in the trivalent and copper in the monovalent state ($Cu^{+}Fe^{3+}O_2^{-2}$). The isomeric shift for Fe^{57} in $CuFeO_2$ is + 0.40±0.15 mm/sec. relative to metallic iron (both at 300°K), and provides conclusive experimental confirmation that the iron is in the Fe^{3+} state[164].

All the ions Zn^{2+}, Fe^{3+}, O^{-2} and Cu^{+} have either half filled or complete filled outer-most orbits and hence have S-character. Therefore a point charge-point dipole model lattice sum calculation is appropriate.

6.2 THE LATTICE SUM CALCULATIONS

As stated in the introduction, the electric field gradient acting on a nucleus of an ion having half filled or complete filled outer electron shells is only due to the crystal or molecular charge distribution and this renders feasible to treat this problem purely as an electrostatic one. Discrete charge distribution (behaving like point charges) is assigned to the infinite perfect lattice and electrostatic potential and its derivatives, are derived by the conventional methods. A detailed treatment of point charge model is given by Hutchings[217]. Many calculations of EFG electric field gradient based on this model have been performed[209,210-22] in ionic crystals. Most of these involve the summing of contributions from the monopole moments of the ions and

information on the degrees of success of such calculations has often been obscured by the presence of structures such as ClO_3^-, BrO_3^-, NO_3^- and others which cannot be adequately described by a monopole moment alone. A few studies such as those of the metal resonance[90,209,221,223] in BeO, Al_2O_3 and Fe_2O_3, the niobium resonance[220] in $KNbO_3$, and the halogen resonance in a number of metal halides, have involved lattice with only monoatomic ions but even in those cases, the sums over monopole contributions, where attempted, have failed to explain the observed coupling constant. On the other hand, calculations[224-26] on the alkali halide molecules indicate that the field gradient at the positive ion nucleus is substantially affected by multipole moments, particularly dipole moments, induced at the negative ion. In several other cases[204, 220-29], the contributions to the electric field gradient from ionic dipoles have been found to be important. Thus, it appears that if the crystal symmetry is such that an electric field and hence a dipole moment can exist at a lattice site, then its contribution to the electric field gradient must be included.

The electrostatic effects of higher multipole moments of ions in a crystal lattice have been discussed theoretically and methods for the calculations of the crystalline potential and its derivatives in lattices of sources having arbitrary multipolar composition are available[230-34].

6.3 ACTUAL COMPUTATIONS°

We detail the procedure adopted for calculations of

° The author is thankful to Dr. R.K. Gupta of Mathematics Dept. for assistance in computer programming in the initial stages.

EFG in these essentially ionic crystals. The lattice sites have been assumed to consist of discrete, deformable and non-overlapping ions with known coordinates and lattice parameters. We have gone upto only dipole contributions. The EFG produced by charges in the crystalline lattice, q_{lat} is given by

$$q_{lat} = \sum_i z_i(3\cos^2\theta_i - 1)/r_i^3 \qquad (6.1)$$

where z_i is the charge and (r_i, θ_i) are the spherical coordinates of the ith ion in the principal-axes system in the lattice and the sum is over all the ions in the lattice. Thus, in an ionic material where iron is in the Fe^{3+} state, the EFG is expressed as

$$q_{Fe^{3+}} = q_{lat}(1-\gamma_\infty) \qquad (6.2)$$

where $(1-\gamma_\infty)$ is the Sternheimer factor which takes into account the polarization of the ions' core electrons by the external EFG. Burns[225] modified the above model by showing that $(1-\gamma_\infty)$ multiplies the contributions of $\ell.g.$ arising from the external moments also. Thus

$$q_{Fe^{3+}} = (q_m + q_d)(1-\gamma_\infty) = q_{total}(1-\gamma_\infty) \qquad (6.3)$$

where $q_m = q_{lat}$ and q_d is the contribution from the effective dipoles at the lattice sites. The effective dipoles at the respective lattice sites are given

$$\mu_{eff} = \mu_{permanent} + \alpha F(\mu_{eff}, \text{charges}) \qquad (6.4)$$

where $F(\mu_{eff}, \text{charges})$ is the electric field arising from the neighbouring charges and effective dipole moments and α is the

polarisability of the ion. The values of q_α and q_β are the negative of the field gradient produced by the charges and dipoles in the lattice sites in a principal axes system. To determine these values the following procedure, which can be divided into four parts for convenience, was adopted.

(i) The field due to charges at all the inequivalent sites was calculated in the first instance.

(ii) Then the field gradient at all these sites was also calculated separately due to other non-equivalent sites and not multiplied by the charges. The f.g. at other sites was needed in the determination of effective dipoles(iii).

(iii) Now effective dipoles were determined using the result of (i)and (ii) in a self consistent manner.

(iv) EFG due to dipoles, so obtained, was calculated at the Fe^{3+} site.

In the following we give some details of these computations in an explicit manner. It may be added here that the ions in all these compounds have the following electronic configurations

$$Zn^{2+} = 1s^2\ 2s^2 2p^6 3s^2 3p^6 3d^{10}$$
$$Fe^{3+} = 1s^2 2s^2 2p^6 3s^2 3p^6 3d^5$$
$$Cu^{+} = 1s^2 2s^2 2p^6 3s^2 3p^6 3d^{10}$$
$$O^{2-} = 1s^2 2s^2 2p^6$$

and thus behave like a charged sphere for which the total charge may be considered as situated at the centre.

The components of the electric field at point (x,y,z) due to an ideal point charge e at $(0,0,0)$ are evaluated using the equation

$$P_x = \frac{\alpha x}{r^3}, \quad P_y = \frac{\alpha y}{r^3} \quad P_z = \frac{\alpha z}{r^3} \tag{6.6}$$

where $r^2 = (x^2 + y^2 + z^2)^{1/2}$. Similarly the components of the electric field at the point (x,y,z) due to an ideal point dipole μ at (0,0,0) with components μ_x, μ_y, μ_z are given by[238]

$$P_x = \frac{3x^2-r^2}{r^5}\mu_x + \frac{3xy}{r^5}\mu_y + \frac{3xz}{r^5}\mu_z$$

$$P_y = \frac{3xy}{r^5}\mu_x + \frac{3y^2-r^2}{r^5}\mu_y + \frac{3yz}{r^5}\mu_z \tag{6.6}$$

$$P_z = \frac{3xz}{r^5}\mu_x + \frac{3yz}{r^5}\mu_y + \frac{3z^2-r^2}{r^5}\mu_z$$

The Eqs. 6.4, 6.5, and 6.6 can be used to determine the effective dipoles in all the lattice sites self-consistently. Let us, for instance, take the case of $CuFeO_2$. There are four atoms in the crystal, Cu, Fe, O_1 and O_2(say). Now let us suppose that μ_{xo}, μ_{yo} and μ_{zo}, are the effective dipole moment components and similarly for other ions also. Let α_O, α_{Cu} and α_{Fe} be the polarisabilities of the O^{2-}, Cu^+ and Fe^{3+} ions, respectively.

Rewritting Eq. 6.4, we get,

$$\mu_{off_x} = \mu_{permanent_x} + \alpha P_x \ (\mu_{off}, \text{charges}) \tag{6.7}$$

as there are no permanent dipoles in our cases this reduces to

$$\mu_{xO_1} = \alpha_O P_{xO_1} \text{ (due to charges)} + \alpha_O P_{xO_1} \text{(due to dipole)}$$

(6.7a)

Now P_{xO_1}(charges) is the x-component of the field acting on oxygen ion O_1 due to all the charges (Cu, Fe, O_1 and O_2 type)

in the lattice sphere selected for computations. Also F_{xO_1} (dipoles) is the x-component of the field acting due to effective dipoles situated at all the Cu, Fe, O_1 and O_2 sites in the same lattice. These can write explicitly as follows:

$$F_{xO_1}(\text{charges}) = \sum_{(\text{all Fe sites})} \left(\frac{3x_1}{r_1^5}\right) + \sum_{(\text{all Cu sites})} \left(\frac{x_2}{r_2^3}\right) -$$

$$\sum_{\substack{(\text{all } O_1 \text{ sites excluding the singularity})}} \left(\frac{2x_3}{r_3^3}\right) - \sum_{(\text{all } O_2 \text{ sites})} \left(\frac{2x_4}{r_4^3}\right) \qquad (3.8)$$

where $r_1 = (x_1^2+y_1^2+z_1^2)^{1/2}$ is the variable distance of all the Fe sites from site of O_1 under consideration. Similarly r_2, r_3, and r_4 are the variable distances of Cu, O_1 and O_2. Similarly F_{xO_1} (dipoles) can be written as

$$F_{xO_1}(\text{dipoles}) = \sum_{\substack{\text{all Fe}\\ \text{sites}}} \left(\frac{3x_1^2-r_1^2}{r_1^5}\right) \mu_{xFe} + \frac{3x_1y_1}{r_1^5}\mu_{yFe} + \frac{3x_1z_1}{r_1^5}\mu_{zFe}$$

$$\sum_{\substack{\text{all Cu}\\ \text{sites}}} \left(\frac{3x_2^2-r_2^2}{r_2^5}\mu_{xCu} + \frac{3x_2y_2}{r_2^5}\mu_{yCu} + \frac{3x_2z_2}{r_2^5}\mu_{zCu}\right)$$

$$\sum_{\substack{\text{all } O_1\\ \text{(sites except}\\ \text{the point of}\\ \text{consideration)}}} \left(\frac{3x_3^2-r_3^2}{r_3^5}\mu_{xO_1} + \frac{3x_3y_3}{r_3^5}\mu_{yO_1} + \frac{3x_3z_3}{r_3^5}\mu_{zO_1}\right)$$

$$\sum_{\substack{\text{all } O_2\\ \text{sites}}} \left(\frac{3x_4^2-r_4^2}{r_4^5}\mu_{xO_2} + \frac{3x_4y_4}{r_4^5}\mu_{yO_2} + \frac{3x_4z_4}{r_4^5}\mu_{zO_2}\right) \qquad (3.9)$$

Similar Eq. for F_{yO_1}, F_{zO_1} and also for Fe, Cu and O_2 sites

are written out. There will be in all 12 Eqs. and will constitute a set. Here all components of the type $\Sigma \frac{x}{r^3}$ and $\Sigma \frac{3x^2-r^2}{r^5}$ are already computed in (i) and (ii) and thus knowing the values of q_0, q_{Cu} and q_{Po}, we can solve this 12x13 matrix to give the effective dipole moment components at the Cu, Po, O_1 and O_2 sites.

We now have a lattice with sites characterised by their respective charges and effective dipole moments, and both these contribute to the electric field-gradient tensor which is a traceless and symmetric second rank tensor with five independent components. The components of q are obtained by differentiation of Eqs.C.8 and C.9, so that

$$q_{xx} = \frac{\partial F_x}{\partial x} \quad \text{and} \quad q_{xy} = \frac{\partial F_y}{\partial x} = q_{yx} \quad \text{etc.}$$

The general formulae[230] can be written as follows

Due to Charges

$$q_{xx} = \frac{e(3x^2-r^2)}{r^5}, \qquad q_{xy} = \frac{3exy}{r^5}$$

$$q_{yy} = \frac{e(3y^2-r^2)}{r^5}, \qquad q_{yz} = \frac{3eyz}{r^5} \qquad (C.10)$$

$$q_{zz} = \frac{e(3z^2-r^2)}{r^5}, \qquad q_{zx} = \frac{3ezx}{r^5}$$

These Eqs. can be summarised in one Eq. as

$$q_{ij} = \frac{e(3x_i x_j - \delta_{ij} r^2)}{r^5} \qquad (C.11)$$

with $i, j = x, y, z$

Due to dipoles

$$q_{xx} = \frac{3(5x^2-r^2)(xm_x+ym_y+zm_z)}{r^7} - \frac{2m_x}{r^5}$$

$$q_{yy} = \frac{3(5y^2-r^2)(xm_x+ym_y+zm_z)}{r^7} - \frac{2m_y}{r^5}$$

$$q_{zz} = \frac{3(5z^2-r^2)(xm_x+ym_y+zm_z)}{r^7} - \frac{2m_z}{r^5}$$

$$q_{xy} = \frac{15xy(xm_x+ym_y+zm_z)}{r^7} - \frac{3(xm_y+ym_x)}{r^5} \qquad (3.12)$$

$$q_{yz} = \frac{15yz(xm_x+ym_y+zm_z)}{r^7} - \frac{3(ym_z+zm_y)}{r^5}$$

$$q_{zx} = \frac{15zx(xm_x+ym_y+zm_z)}{r^7} - \frac{3(zm_x+xm_z)}{r^5}$$

The elements of $q(=q_D+q_Q)$ are obtained by taking into account the effect of all the sites within a selected sphere around the Fe^{3+} ion, which gives convergent values. The 3x3 matrix is formed and diagonalized by a unitary transformation. The eigenvalues represent the principal values of q and the columns of the eigenvector matrix give the orientations of the principal axes with respect to the orthogonal axes of (x,y,z).

The principal values are designated according to the convention that q_{zz} is maximum and $q_{xx}>q_{yy}$. The asymmetry parameter η can then be found by the expression

$$\eta = (q_{xx} - q_{yy})/q_{zz}$$

The experimentally observed quadrupole splitting can be expressed as

$$Q.S. = \frac{1}{2} e^2qQ(1-\gamma_\infty)\ Q\ (1+\frac{1}{3}\eta^2)^{1/2} \qquad (6.13)$$

This expression is only valid when there is no magnetic interaction. In the latter case it is not very easy to extract the value of Q.S. (Chapter I) and in only special cases it can be exactly evaluated. In case of an axially symmetric f.g. (as is evident from the point symmetry in the case of α-Fe_2O_3) if θ is the angle between the magnetic field and the z-direction of EFG then Q.S. can be expressed as

$$Q.S. = \frac{1}{4} e^2qQ\ (1-\gamma_\infty)(3\cos^2\theta-1) \qquad (6.14)$$

Below a temperature of $\sim 260^0K$, α-Fe_2O_3 undergoes the Morin (spin flip) transition in which the spins become aligned parallel and antiparallel to the c-axis, the axis of EFG, and for this case

$$Q.S. = \frac{1}{2} e^2qQ\ (1-\gamma_\infty) \qquad (6.15)$$

which is the same as in a paramagnetic compound with axially symmetric EFG. Above the Morin transition, the spins are perpendicular to c-axis and thus

$$Q.S. = -\frac{1}{4} e^2qQ(1-\gamma_\infty)Q \qquad (6.16)$$

Substituting the values of q, and utilising the experimentally observed values in Eq.(6.13) (or (6.16)} as the case may be), one can obtain the value of Q (Fe^{57}).

It is to be noted that the input data for these

calculations are the exact values of lattice parameters and positions of the lattice sites and precise value of the polarisability of the respective ion. The HFC computations are very sensitive to these parameters[184,207,237].

It may also be noted that all the formulae given in the previous discussion are valid only for an orthogonal set of axes and structure parameters of lattice sites having symmetry lower than cubic should be first transformed into an orthogonal set. Rollett[238] has derived a simple transformation matrix for any general symmetry and we have made use of this while doing calculations for $CuFeO_2$ and α-Fe_2O_3. If we take c-axis of the desired orthogonal coordinate system parallel to c axis and y axis be in be plane then the transformation matrix L can be written as[238].

$$L = \begin{pmatrix} a \sin\beta \sin\gamma^\circ & 0 & 0 \\ -a \sin\beta\cos\gamma^\circ & b \sin\alpha & 0 \\ a\cos\beta & b\cos\alpha & c \end{pmatrix} \qquad (6.17)$$

where α,β and γ are the interaxial angles and

$$\cos\gamma^\circ = (\cos\alpha\cos\beta - \cos\gamma)/\sin\alpha\sin\beta$$

and $$\sin\gamma^\circ = (1-\cos^2\gamma^\circ)^{1/2}$$

since $0<\gamma^\circ<180^\circ$ we have taken the positive value for the sq.root. Thus the coordinates in the desired orthogonal coordinate axis system x are given by the following transformation equation

$$\begin{pmatrix} X \\ Y \\ Z \end{pmatrix} = L \begin{pmatrix} x \\ y \\ z \end{pmatrix} \qquad (6.18)$$

6.4 RESULTS AND DISCUSSION

(a) $ZnFe_2O_4$

It is a normal spinel and the Fe^{3+} ion at the B site is surrounded by six oxygen ions nearly octahedrally, but the point symmetry is trigonal with its axis in the <111> direction. The space group[230] is O_h-Fd3m and there are eight molecules per unit cell. The eight A sites are tetrahedrally coordinated with point symmetry $\bar{4}$ 3m which gives zero field and zero electric field gradient. The 16D sites have trigonal symmetry, 3m and the principal axis of the field gradient tensor is along <111>. All the directions along the four body diagonals of cube occur with equal frequency as the unique axis, thus retaining the overall cubic symmetry. The 32 oxygen sites in a perfect spinel would form a face centred cubic lattice but this is seldom achieved. The size of the ions in the small A sites causes a displacement of the four surrounding oxygen ions along the <111> direction. The cubic symmetry of the A site is retained but the octahedron of oxygen ions around the B site becomes distorted and changes the trigonal component of the e.f.g. The oxygen positions are characterised by a parameter u, ideally equal to 3/8 and have point symmetry 3m. The structure is defined by a parameter u and a, the unit cell length.

For $ZnFe_2O_4$ $\quad a = 8.44\text{Å}$ and $u = 0.388\text{Å}$

The positions of Zn^{2+}, Fe^{3+}, O^{2-} are given as below

Zn^{2+} ions at (8a) positions: $(0,0,0)$; $(\frac{1}{4},\frac{1}{4},\frac{1}{4})$ + F.C.

Fe^{3+} ions at (16d) positions: $(\frac{5}{8},\frac{5}{8},\frac{5}{8})$; $(\frac{5}{8},\frac{7}{8},\frac{7}{8})$; $(\frac{7}{8},\frac{5}{8},\frac{7}{8})$ and $(\frac{7}{8},\frac{7}{8},\frac{5}{8})$ + F.C.

O^{2-} ions at (32b) positions: (u,u,u); $(u,\bar{u},\bar{u})$; $(\bar{u},u,\bar{u})$; $(\bar{u},\bar{u},u)$;

$(\frac{1}{4}+u,\frac{1}{4}-u,\frac{1}{4}-u)$; $(\frac{1}{4}-u,\frac{1}{4}+u,\frac{1}{4}+u)$;

$(\frac{1}{4}+u,\frac{1}{4}-u,\frac{1}{4}+u)$; $(\frac{1}{4}+u,\frac{1}{4}+u,\frac{1}{4}-u)$

+ P.C.

where P.C. means repetition about

$(0,\frac{1}{2},\frac{1}{2})$; $(\frac{1}{2},0,\frac{1}{2})$ and $(\frac{1}{2},\frac{1}{2},0)$

The q_{zz} due to charges was calculated from the direct lattice sums, and the values so obtained are plotted in Fig.6.1 as a function of radius of sphere of calculation. We see that the values converge very satisfactorily and the contribution to q_{zz}, while going from 50Å sphere to 60Å is less than 1%. The value of q_{zz}(charges) at 60Å is 0.105894×10^{24} esu/cm^3. While carrying out these calculations, there appeared a paper by Hudson and Whitfield[203]. They reported the lattice sum calculations and included the dipolar contribution to the field gradient. By taking a slightly different approach to the problem, they calculated these lattice sums as a function of distortion parameter. From the experimental values of quadrupole splitting and assuming $Q(Fe^{57})$ = 0.28b and for two different values of polarisability α of oxygen ions they determined the values of distortion parameter u for $ZnFe_2O_4$ and their extracted values of distortion parameter u for these spinels are:

	monopoles only	monopole + dipole
$ZnFe_2O_4$	0.380	0.381(α for O^{--}=1.51×10^{-24} cm^3)
		0.370(α for O^{--}=2.4×10^{-24} cm^3)
$CdFe_2O_4$	0.393	0.384(α for O^{--}=1.51×10^{-24} cm^3)
		0.382(α for O^{--}=2.4×10^{-24} cm^3)

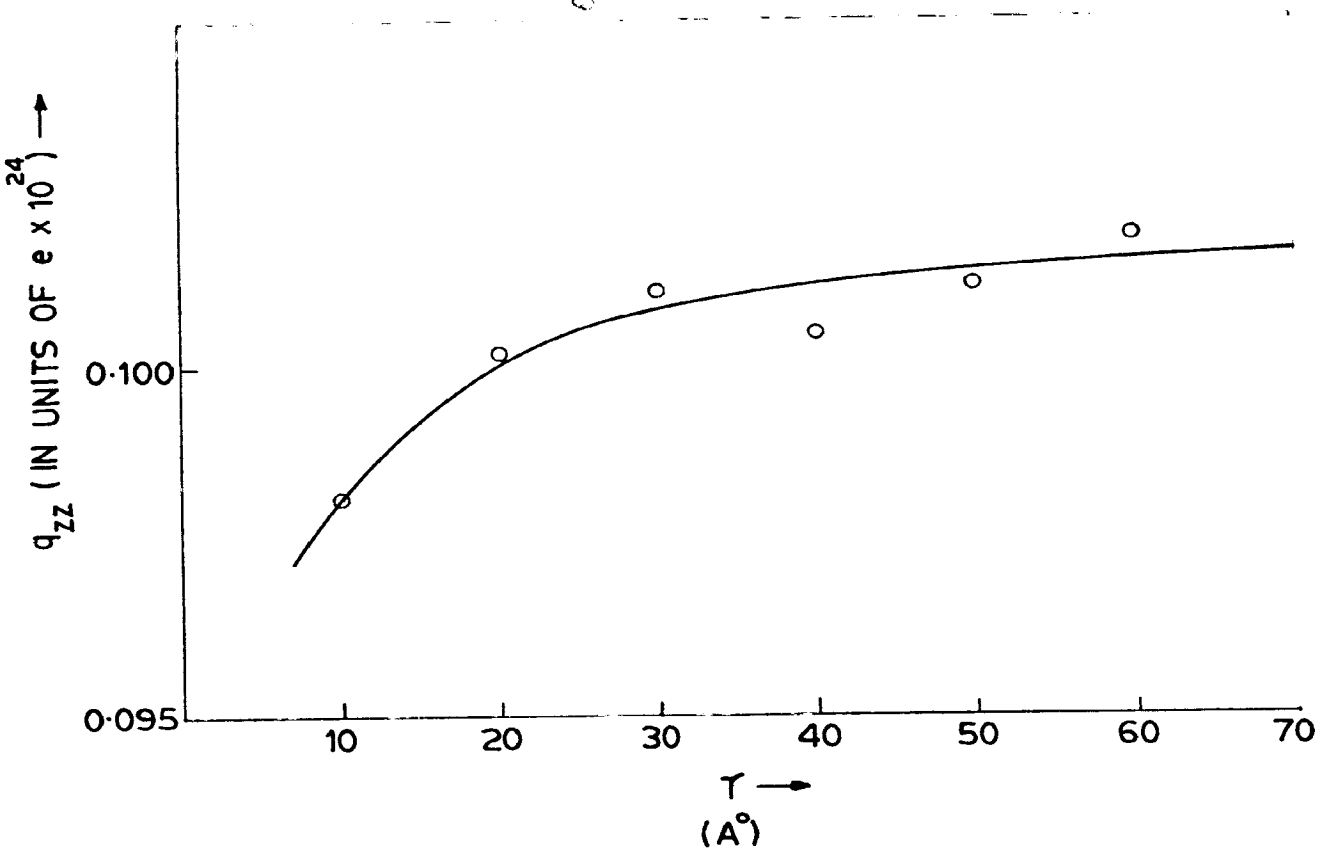

FIG. 6·1 CALCULATED q_{zz} (CHARGES) VS RADIUS OF SPHERE OF CALCULATION

Hudson and Whitfield obtained a good agreement between the values of distortion parameter u obtained by neutron diffraction ($u = 0.3652 \pm 0.002$)[243] and that obtained from the Mössbauer experiment ($u = 0.383$) when the e.f.g. is calculated by taking monopolar contribution only. However, when the dipolar terms are included the agreement becomes poor. They speculate that the dipole terms to a large extent will be cancelled by induced quadrupole moments and covalency, which are not included in their calculations. To support their speculation they have cited the results of quadrupolar contribution calculated by Brun and Hafner[240] in $MgAl_2O_4$ from O^{--} ions and their results show that quadrupolar contribution is positive in comparison to the negative dipolar contribution. In principle contributions from both O^{2-} and Fe^{3+} ions should be considered and consequently, values must be assigned to their quadrupole polarisabilities, β_0 and β_{Fe}. Unfortunately, there is insufficient data available to allow more than a rough estimate of these quantities to be made. Coupled with the uncertainties in the values of α, the numerical results of such calculations are of only limited value at the present time.

In view of this we have not attempted to calculate the dipolar contribution in $ZnFe_2O_4$ and the value obtained for $Q(^{Fe}57)$ is that from the monopolar contribution only.

The value of the electric field gradient q acting[241] on the B site was estimated by Hisoguchi and Tanaka[241] under the point charge model taking the trigonal axis as the principal axis. Taking into account upto the fourth nearest neighbours (a distance of ~10Å) and using the value of antishielding factor $\gamma_\infty = -0.17$, it was concluded that there is

qualitative agreement between the measured (0.30 mm/sec) and the calculated value (0.56 mm/sec) of Q.S. In our calculations, we included all charges within a sphere of 60Å around an Fe^{3+} ion and used the revised value[176] of $\gamma_\infty = -9.14$. $Q(Fe^{57m})$ estimated from the value of EFG due to charges only is 0.220b, and is given in Table 6.2. The values of EFG tensor, the principal values (eigen-values) and the eigen-vectors are given in Tables 6.3 and 6.4.

TABLE 6.2: CALCULATED VALUES OF $Q(Fe^{57m})$ FROM THE EXPERIMENTAL VALUES OF QUADRUPOLE HYPERFINE SPLITTING (Q.S.)

Compound	Q.S. Expt. (mm/sec. (at 300°K)	q_{zz} x 10^{-14} (e.s.u.)		$Q(Fe^{57m})$
$ZnFe_2O_4$	0.30±0.01[a]	0.400393 (charges only)	0.0	0.220b
$CuFeO_2$ (Delafossite)	0.66±0.01[b]	1.043303 (charges only)	0.0	0.190b
		3.010027 (Total)	0.0	0.039b
α-Fe_2O_3	0.30±0.02[c]	0.270902 (charges only)	0.0	0.301b

(a) Ref.241; (b) Ref.184; (c) Ref.207.

TABLE 6.3: COMPONENT OF THE EFG TENSOR DUE TO CHARGES IN $ZnFe_2O_4$ IN THE SPHERE OF 60Å RADIUS. THE VALUES ARE IN THE UNITS OF $e \times 10^{24}$ e.s.u.

0.0	0.05194721	0.05194721
0.05194721	0.0	0.05194721
0.05194721	0.05194721	0.0

TABLE 6.4: THE PRINCIPAL VALUES OF THE EFG TENSOR AND THE DIRECTION COSINES w.r.t. TO CRYSTAL AXES OF $MnFe_2O_4$ AT THE SITES OF (8) NUCLEI.

Principal values (in units of $e \times 10^{24}$ e.s.u)		Direction cosines w.r.t. to a,b,c axes		
q_{xx}	= -0.05194721	0.58456558	0.20140337	-0.78595698
q_{yy}	= -0.05194721	0.57738030	0.57738029	0.57738028
q_{zz}	= +0.10389442	-0.57008593	0.79126696	-0.22121304

(b) α-Fe_2O_3

Cox and Shirane[244] have measured the atomic coordinates of the ions in Fe_2O_3 using the neutron diffraction technique . Their results will be used rather than the previous X-ray work of Pauling and Hendricks[245]. Artman[205] has used the X-ray data of Newnham and V.M. Goldschmidt[246]. The α-Fe_2O_3 is isomorphous to Al_2O_3 and has a rhombohedral structure with two molecules per unit cell. Its space group is D_{3d}^6 or equivalently $R\bar{3}c$ and the atoms are in the following positions

Iron 4(c) $\pm (u,u,u)$; $\pm (\frac{1}{2}+u, \frac{1}{2}+u, \frac{1}{2}+u)$

with Fe site symmetry as C_3

Oxygens(c) $\pm (x, \frac{1}{2}-x, \frac{1}{4})$

with $u = 0.355$; $x = 0.552$ (latter improved to 0.550); $a = 5.424\text{Å}$ and $\alpha = 55^0 17'$

The transformation matrix of Eq.6.17 turns out to be

$$L = \begin{pmatrix} 0.76593 & 0.0 & 0.0 \\ 0.29827 & 0.82196 & 0.0 \\ 0.56052 & 0.53952 & 1.0 \end{pmatrix}$$

where the values are in units of a_0 the lattice parameter. The values of the EFG tensor (from charges only) are computed and diagonalised covering lattice sites in different spheres of radii from 40Å to 80Å and are given in Table 6.5

TABLE 6.5: COMPARISON OF THE VALUES OF Z-COMPONENT OF ELECTRIC FIELD AND FIELD GRADIENT ACTING ON Fe^{3+} SITE IN α-Fe_2O_3 IN THE SPHERES OF DIFFERENT RADII

Sl. No.	Radius of the sphere (R)	E_z in units of $e \times 10^{10}$	q_{zz} $\times 10^{-17}$ e.s.u	η	% change in q_{zz} with an increase of 10Å radius
1	40	0.020612	0.284830	0.0	-
2	50	-0.020303	0.281322	0.0	1.23
3	60	0.001003	0.279257	0.0	0.73
4	70	0.004570	0.277798	0.0	0.52
5	80	-0.012462	0.276987	0.0	0.30

We see that there is only 2.8% increase in the value of q_{zz} while going from 40Å radius sphere to that of 80Å sphere and this reduces to 0.3% only while going from 70Å to 80Å sphere and hence shows a good convergence. Unfortunately the convergence could not be achieved in field acting on Fe^{3+} ions as seen from the Table 6.5. Rather there are much oscillations in E_z values reported in the Table. The same case is with field on O^{2-} ions. To avoid this slow convergence in direct summation, Nijboer and deWette[247] have advanced a more rapidly convergent lattice sum procedure involving in part summation over the inverse lattice. Their

procedure unfortunately usually is not convergent for inverse power of r (radial distance) less than 6. deVotto[248] has also advanced a method of plane-wise summation which he utilised in determining the dipolar contribution to EFG in a dielectric media between the parallel plates of a condenser. Artman[205] has extended the method of Wood[249] of grouping the molecules in the clusters of zero charge and zero dipole moment and has got a very rapid convergence. Ewald's method is a general technique used to overcome this convergence difficulty and we planned to apply this technique. While doing these calculations we received a preprint from Professor Artman°, which was published later in Phys.Rev.[207], in which he has revised his previous calculations[205] in view of recently very accurately determined[250] X-ray data and the elaborate Mössbauer effect measurements of this compound[251]. The value of quadrupole constant was obtained by a non-linear least square fitting of the data at room temperature reported to be[207]

$$e^2qQ = + 0.660 \pm 0.024 \text{ mm/sec}$$

Our values of q_{zz}(charges) are in good agreement to the Artman values[205] but are considerably lower than the values calculated based on the recent X-ray data[250]. The nine components of the EFG tensor, the principal eigen-values and the eigen-vectors are reported in Table 6.6 and Table 6.7.

The values of Q obtained/ are also given in Table 6.2

° The author is thankful to Professor J.J. Artman for this kind help.

The large value in comparison to Artman[207] can be accounted on two counts: firstly a less accurate value of coordinates and secondly non-inclusion of dipolar contribution.

TABLE 6.6: COMPONENTS OF THE EFG TENSOR DUE TO CHARGES IN α-Fe_2O_3 IN THE SPHERE OF 60Å RADIUS. THE VALUES ARE IN THE UNITS OF 0×10^{24} e.s.u.

-0.05531072	-0.00534147	0.02774325
-0.00534147	0.01163870	0.04355961
0.02774325	0.04355961	0.04367804

TABLE 6.7: THE PRINCIPAL VALUES OF THE EFG TENSOR AND THE DIRECTION COSINES w.r.t. THE ARBITRARY ORTHOGONAL AXES SYSTEM IN α-Fe_2O_3 IN THE SPHERE OF 60Å RADIUS.

Principal values $\times 10^{-14}$ e.s.u.	Direction cosines w.r.t. the arbitrary orthogonal axes system		
q_{XX} = -0.138800	0.913398	0.243303	-0.326367
q_{YY} = -0.138483	-0.377760	0.905329	-0.466883
q_{ZZ} = +0.276987	0.151004	0.340800	0.827496

It may be remarked here that neither the metal nor the oxygen ion is at a centre of symmetry so both can have induced dipole moments and a more precise work should inclu

the contribution from both cations and anions and not merely from anions[203,207] Recently Hafner[9] has repeated the EFG calculations of α-Fe_2O_3 and has also included the induced quadrupole contribution. His results marked by differ from those of Artman et al.[207]

(c) $CuFeO_2$

Delafossite ($CuFeO_2$) is rhombohedral[215,282] with $a = 3.90\text{Å}$, $\alpha = 29°26'$; or in the hexagonal description $a_h = 3.03\text{Å}$, $c_h = 17.09\text{Å}$. The unit cell contains 1 $CuFeO_2$ with

Cu at (0,0,0)

Fe at (1/2,1/2,1/2)

and O at $\pm(x,x,x)$ with $x = 0.111$

The iron has octahedral coordination, while the copper has a linear two fold oxygen coordination. The oxygen is surrounded by tetrahedron of 3Fe and 1 Cu. Thus copper as well as iron both have an inversion symmetry and thus field on these sites will be zero.

The transformation matrix in this (rhombohedral) case turns out to be

$$L = \begin{pmatrix} 0.43492 & 0.0 & 0.0 \\ 0.22878 & 0.49161 & 0.0 \\ 0.87093 & 0.87093 & 1.0 \end{pmatrix}$$

Before reporting our results we may point out that there is no general consensus over the value of a_0 to be taken in these nodal calculations. While Sharma and Das[204] has used the value 2.19×10^{-24} cm^3 obtained for O in BeO, Artman[208] has

preferred the value of $2.91 \times 10^{-24} cm^3$ calculated using Clausius-Mossotti relation making use of refractive index value. Recently Romanpolskii and Venevtsev[283] have calculated the EFG in $BiFeO_3$ site and have used the value of α_0 as $2.4 \times 10^{-24} cm^3$. We have used these three values and one more $3.0 \times 10^{-24} cm^3$ to seek the polarisability dependence of q. We see from Table 6.9 that the q_d increases in magnitude with the increase of polarisability value.

The value of field components acting on O^{--} ion and the q_{ss} = (charges) acting on Fe^{3+} ion in three different spheres of radii 61,70 and 80Å are tabulated in Table 6.8.

TABLE 6.8: VALUES OF COMPONENTS OF ELECTRIC FIELD ACTING ON O^{2-} ION AND 5 COMPONENTS OF FIELD GRADIENT ACTING ON Fe^{3+} SITE IN THREE SPHERES OF RADII 61,70, AND 80Å.

Radius Å	Electric field on O^{2-} site in units of $o \times 10^{10}$ e.s.u.			q_{ss} on Fe^{3+} site $\times 10^{-14}$ e.s.u.
	F_x	F_y	F_z	
61	0.03944460	0.00332052	0.24803725	1.042824
70	0.03720040	0.00176321	0.23807514	1.045907
80	0.03744257	0.00336274	0.23107358	1.043345

The values are more or less convergent and we have used the q_{ss} and F_x, F_y, F_z of 80Å sphere to calculate the value of the Q reported in Table 6.2. We have also prepared the Table 6.9 containing values of q_{ss}(charges), q_{ss}(dipoles) and q_{ss}(total) in two different sphere of radii 15Å and 80Å with different polarisability values for comparison.

TABLE 6.9: COMPARISON OF q_{zz}(CHARGES), q_{zz}(DIPOLAR), AND q_{zz}(TOTAL) AND THEIR DEPENDENCE ON (a_0) VALUES IN A DIFFERENT SPHERES OF RADII 15 AND 20Å IN THE COMPOUND ZnO_2O_4.

Sl. No.	Polarisability of oxygen $\times 10^{24}$ cm^3	q_{zz} (charges) $\times 10^{-14}$ e.s.u.		q_{zz} (dipolo) $\times 10^{-14}$ e.s.u.		q_{zz}(Total) $\times 10^{-14}$ e.s.u.	
		15 Å	20 Å	15 Å	20Å	15Å	20Å
1	2.19	1.132019	1.043303	1.892470	1.971638	2.724496	2.714938
2	2.00	1.132019	1.043303	1.870779	1.750279	2.608798	2.802020
3	2.01	1.132019	1.043303	1.948755	2.986410	2.983410	2.989071
4	3.00	1.132019	1.043303	1.970294	3.010914	3.010914	3.018627

We note that thereon there is difference of 0.8% in q_{zz} (charges) of 15Å and 20Å this reduces to almost negligible in q_{zz}(total). This is because that here in this compound the major contribution to the EFG comes from the dipolar term. This predominance of dipolar contribution is not unconventional in the literature. Hundson and Whitfield[203] and Taylor and Dob[227] have reported this situation in $ZnPo_2O_4$ and BeO respectively. In BeO the point charge contribution[221] only one tenth of the total observed EFG. The nine components of the EFG tensor, the principal eigenvalues and the eigenvectors are reported in Table 6.10 and 6.11 respectively.

TABLE 6.10: COMPONENTS EFG TENSOR IN $ZnPo_2O_4$ IN THE SPHERE OF 20Å RADIUS. THE VALUES IN THE BRACKETS ARE DUE TO CHARGES ONLY. ALL VALUES ARE IN THE UNITS OF $X10^{14}$ e.s.u.

-1.38835171 (-0.40371615)	0.18102285 (0.05946730)	0.03722775 (0.22088128)
0.18102286 (0.05946730)	-1.24047307 (-0.42303803)	1.09842125 (0.37031803)
0.03722775	1.09842125	2.62902775

TABLE 6.11: THE PRINCIPAL VALUES OF THE EFG TENSOR AND THE DIRECTION COSINES w.r.t. THE ARBITRARY ORTHOGONAL AXES SYSTEM IN $CuFeO_2$ IN THE SPHERE OF 8Å RADIUS. THE VALUES GIVEN IN THE BRACKETS ARE THOSE DUE TO CHARGES ONLY.

Principal values $\times 10^{-14}$ e.s.u.		Direction cosines w.r.t. the arbitrary orthogonal axes system		
q_{xx} =	-1.484837 (-0.521768)	0.955473 (0.742604)	0.212495 (0.609400)	-0.204738 (-0.277797)
q_{yy} =	-1.533790 (-0.521594)	-0.254921 (-0.662343)	0.943876 (0.752069)	-0.210033 (-0.094031)
q_{zz} =	3.018627 (1.043363)	0.148616 (0. 151620)	0.252873 (0.251046)	0.956017 (0.956027)

A lattice sum calculation of q_{zz}(charges) has been carried out[154] by using a quadrupole moment[205] Q = 0.41b. The calculated value of Q.S. (+1.40 mm/sec) is higher by more than a factor of two than the measured value[154] (0.356 ± 0.15). Our calculated value of q_{zz} (charges) is the same and obviously yields the value of Q(Fe^{57m}) to be +0.20b, Table 6.2. It may be remarked that the lattice sums are very sensitive to X-ray data; a change of value of x coordinate of O^{2-} from 0.111 to 0.108 can satisfy the room temperature value. The value of Q obtained from the q_{total} is very low and we speculate an analogous situation in $MgAl_2O_4$ where quadrupolar contribution and covalency may partially cancel the dipolar contribution thereby increasing the value of Q. The importance of quadrupole term is also pointed out by Das[234] as well as Sholl[236].

6.5 CONCLUSIONS

From the discussion it is clear that the lattice sum

calculations are very sensitive to the precision with which the position coordinates of the ions are determined. It has been very well demonstrated by the change of value of q_{33}(charges) in α-Fe_2O_3 from the papers of Artman[203,207], the variation of distortion parameter[203] u in $ZnFe_2O_4$ and $CdFe_2O_4$ and the change in x parameter of position coordinates of oxygen ions in $CaFeO_2$.

Furthermore these are also sensitive to polarizability of ions and hence an accurate value of this parameter is highly desirable for any meaningful conclusion. As Hudson and Whitfield have pointed out that in some cases (as in $ZnFe_2O_4$) it is possible that the quadrupolar term may cancel the dipolar terms and so higher terms should also be included in a complete treatment of the problem. It is well known that the discrete deformable and non-overlapping point charge model is not real in the proper sense and there is always some overlapping of the ions and thus the effect of covalency should also be taken into account before any meaningful interpretation is made. Furthermore as pointed out by Artman it may be added that the ionic model to the actual interactions in crystals is quite crude in comparison to a complete molecular-orbital treatment. However, carrying out this latter program leads to conceptual and computational difficulties. These calculations which have actually been made to date required approximations with uncertain validity.

The value of γ_∞ is also very large and is decisive factor and so should be very accurately known. Unfortunately, there is insufficient data available to allow more than a rough estimate of these quantities to be made and thus the numerical results

of such calculations are of only limited value at the present time.

The variation in the values of Q obtained here leaves us inconclusive for assigning any definite value to Q. We further conjecture that the point charge-point dipole model is inadequate to give meaningful results in view of the lack of (i) precision X-ray data (to which the calculations are very sensitive) (ii) well-defined values of effective charges, (iii) dipole polarisability, (iv) quadrupole polarisability, and (v) covalency factors accounting for the actual overlapping of the atomic orbitals.

In all the reference unless otherwise stated the (Journal) volume no. is followed by year & then the page.

REFERENCES

1) R.L. Mössbauer: Z. Physik 151 (1958)124; Naturwissenschaften 45 (1958)538; Z. Naturforsch 13a(1959)211.

2) The Mössbauer Effect (Bibliography series) Tech. Rept. Series No.10, International Atomic Energy Agency, Vienna,(1965).

3) A.H. Muir Jr., K.J. Ando, and H.M. Coogan: Mossbauer Effect Data Index, 1958-65. (Inter Science, New York, 1966).

4) H.J. Lipkin: Ann. Phys. (N.Y) 9 (1960) 332; 18(1962)182.

5) H. Lustig: Am. J. Phys. 29(1961)1.

6) V.Weisskopf, The Mössbauer Effect in the U.E. Brittin and B.W. Downs (eds.), 'Lectures in Theoretical Physics Vol.3, (Inter Science, New York, 1961) pp.70-80.

7) D.A. J.F. Boyle and H.E. Hall: Rept. Progr. Phys. 25(1962)441.

8) E.P. Hammel, W.E. Keller and P.P. Craig: Ann. Rev. Phys. Chem. 13 (1962) 295.

9) R.L. Mössbauer: Ann. Rev. Nucl. Sci. 12(1962)123.

10) G.K. Wertheim Am. J. Phys. 31 (1963) 1.

11) V.I. Goldanski: Science and Technology 24(1963)40, Angular Chem. (1967) 844.

12) E. Fluck: Advances in Inorganic Chemistry and Radiochemistry, H.J. Emeleus and A.G. Sharpe, eds., (Acad. Press, New York, 1964), Vol. 6,p.278.

13) J.F. Duncan and R.M. Golding: Quart. Rev. (London)19 (1965)36.

14) R.L. Mössbauer α-,β- and γ-ray spectroscopy, K. Siegbahn, ed., (North Holland Publishing Co., Amsterdam, 1965), p.1293.

15) R.H. Herber: Ann. Rev. Phys. Chem. 17(1966) 261.

16) J.R. DeVoe, J.J. Spijkerman: Anal. Chem. 38(1966)382R; ibid, 40(1968) 472R.

17) N.N. Greenwood: Chem. In Britain 3(1967)56; Rec. Chem. Progr. 28 (1967)181; Endeavour, 27 No.100, Jan.(1968)p.33.

18) U.Gonser Inter. Sci. Eng. 3(1968 69) 1.

19) H. Frauenfelder and H. Lustig, eds., Proc. First Intern. Conf. on the Mössbauer Effect, Univ. of Illinois, Urbana, Illinois, (1960) (published in U.S. Air Force Rept. TN-60-696)

20) D.M. J. Compton and A.H. Schoen, eds., Proc. Second Intern. Conf. on the Mössbauer Effect, Saclay, France, (1961), (John Wiley and Sons, New York, 1962).

21) A.J. Deardon, ed., Proc. Third Intern. Conf. on the Mössbauer Effect Cornell Univ., Itaca, N.Y., (1963), (Rev.Mod.Phys.36 (1964)333).

22) V.P. Alfimenkov and A.V. Strelkov, eds., Proc. of the Conference on the Mössbauer Effect, Dubna, USSR, 1962(Joint Institute for Nuclear Research Dubna, 1963)(In Russian)/ Translation (Consultant Bureau Enterprises, Inc., New York, 1963).

23) N. Frankenfelder: 'The Mössbauer Effect' (W.A. Benjamin, New York, 1962).

24) V.I. Goldanskii, 'The Mössbauer Effect and its Applications'to Chemistry', (Consultant Bureau, New York, 1964).

25) G.K. Wertheim 'Mössbauer Effect: Principles and Applications', (Academic Press, New York, 1964).

26) Applications of the Mössbauer Effect in Chemistry and Solid State Physics, Intern. At. Energy Agency, Tech. Rept. Ser. No.80, Vienna, 1966)(Proc. of the Meeting of the Advisory Pannel on Mossbauer Spectroscopy, Vienna, Austria, April, 1965).

27) I.J. Gruverman, ed., Mössbauer Effect Methodology Vol. 1-4 (Plenum Press, New York, 1965-68)(Proceedings of the annual Symposia, Boston held in New York City, Sponsored by the New England Nuclear Corporation, Boston).

28) A.J. Freeman and R.B. Frankel, eds., Hyperfine Interactions (Academic Press, New York, 1967) (in part, proc. NATO adv. study Inst., Aixon Provence, France, August 8-20, 1966).

29) The Mössbauer Effect and Its Application in Chemistry, Advances in Chemistry Series, No.68, Am. Chem. Soc., (1967).

30) E.Matthias and D.A. Shirley, eds., Hyperfine Structure and Nuclear Radiations North-Holland Publ. Co., Amsterdam, 1968 (Proc. Intern. Conf. on Hyperfine interactions detected by Nucl. Radiations, Asilomar Conf. grand, Pacific grove, California, U.S.A. August 26-30, 1967).

31) V.I. Goldanskii and R.H. Herber, eds., 'Chemical Applications of Mössbauer Spectroscopy', (Academic Press, New York, 1968).

32) A.C.G. Mitchell and M.W. Zemansky, 'Resonance Radiation and Excited atoms', (Cambridge University Press, 1934, Reprinted 1963).

33) P.B. Moon: Proc. Phys. Soc. (London) 64 (1951)76.

34) W. Kuhn: Phil. Mag. 8(1929) 625.

35) K.G. Malmfors: Arkiv Fysik, 6 (1953) 49.

36) E. Pollard and D.E. Alburger: Phys. Rev. 74(1948)926.

37) F.R. Metzger: Progr. Nucl. Phys. 7(1959)53.

38) K.G. Malmfors: Resonant Scattering of gamma rays. In 'Beta and Gamma Ray spectroscopy', K. Siegbahn, ed., Chapt. 18, (North-Holland Publ. Co., Amsterdam, 1955).

39) P.C. Blake: Rev. Mod. Phys. 8(1933), 69; R.W. James: Optical Principles of the Diffraction of X-rays, Bell (1948).

40) W.E. Lamb: Phys. Rev. 55 (1939)190

41) R.H. Dicke: Phys. Rev. 89 (1953)472.

42) W.M. Visscher: Ann. Phys. 9(1960)194.

43) J. Potzold: Z. Physik 163 (1961) 71.

44) D.L. Shapiro: Uspechki Fiz. Nauk.72(1960)685; transl. Soviet Phys. Uspekhi 4(1961) 71.

45) K.S. Singwi and A. Sjolander: Phys. Rev.120(1960)1093; Inelastic scattering of neutrons in solids and liquids Intern. At. Energy Agency, Vienna, 1963), Vol.1, p.3; K.S. Singwi 'Phonons and Phonons Interactions, T.A. Bak (ed.), (W.A. Benjamin, Inc., New York, 1964)p.167.

46) M.K.F. Wong: Proc. Phys. Soc. (London)85 (1965) 723.

47) S. Margulies and J.R. Ehrmann Nucl. Instr. Methods 12(1961) 131.

48) J. Noborio: Nucl. Instr. Meth. 56 (1968) 90.

49) G.K. Wertheim: Physics Today 20(1967)131.

50) J.W.G. Wignall: J. Chem. Phys. 44(1966) 2462.

51) H.H. Wickman and G.K. Wertheim Ref.31,p.366; Phys. Rev. 148 (1966) 211 see also H.H. Wickman: Ref.27 Vol.II (1966) p.39. G.K. Wertheim and J.P. Remeika Nuclear Magnetic Resonance and relaxation in solids L. Van Gerven, ed., North Holland Publ. Co., Amsterdam (1965)p.1.

52) M. Blume: Phys. Rev. Letters 14 (1965)96; ibid 16(1967); Ref.30 p.911 M. Blume and J.A. Tjon: Phys. Rev.165(1968) 446; J.A. Tjon and M. Blume: ibid, 165 (1968)456.

53) P.J. Lynch, R.E. Holland and M. Hamermesh: Phys. Rev. 120 (1960) 513; K. Albrecht and W. Nowitzki: Z. Physik 203 (1967)420.

54) W.Gonser and H. Wiedersich: J. Phys. Soc. Japan 18(1963) Suppl. II, 47.

55) S.M. Harris: Phys. Rev. 103 (1957) 280 see also J.G. Dash and R.H. Nussbaum: Phys. Rev. Letters 16(1966)507.

56) R.M. Housley and H. DeWaard: Phys. Letters: 21 (1966)90.

57) Yu. M. Kagan: Doklady Akad, Nauk SSSR 140(1961)794; S.V. Karyagin ibid 148(1963)1102; V.I. Goldanskii, E.F. Makarov and V.V. Khrapov: Phys. Letters 3(1963)344; V.I. Goldanskii, E.F. Makarov, I.P. Suzdalev, and I.A. Vinogradov: Phys. Rev. Letters 20(1968)137.

58) H.A. Stocklov and H.Sano: Chem. Phys. Letters 2(1968) 448; Phy Phys. Rev. 165(1968)606.

59) S. Margulies, P. Debrunner, and H. Frauenfelder: Nucl. Instr. and Meth. 21(1963)217.

60) M.M. Hack and M. Hamermesh: Nuovo Cimento 19(1961)560; S.L. Ruby and D.I. Bolef: Phys. Rev. Letters 5, 5(1960); see also A. Abragam: Compt. Rend. 250 (1960)4334.

61) A.J. Freeman and R.E. Watson 'Magnetism' G.T. Rado and H. Suhl. eds., (Academic Press, New York, 1965) Vol.IIA p.167.

62) D.O. Patterson, L.D. Roberts, J.O. Thomson and R.P. Lowery: U.S. Atomic energy commission Report ORNL-TM-1665, Jan. 1967)

63) G. Racah: Nature 129(1932) 723.

64) O.C. Kistner and A.W. Sunyar: Phys. Rev. Letters 4(1960) 412.

65) D.A. Shirley: Rev. Mod. Phys. 36(1964)339 (3rd intern. Mossbauer Effect conf. Ref.21).

66) R.V. Pound and G.A. Rebka, Jr.: Phys. Rev. Letters 4(1960) 274.

67) B.D. Josephson: Phys. Rev. Letters 4(1960)341.

68) J.T. Dehn: Phys. Letters 29A(1969)132.

69) M.J. Clauser, E. Kankeleit and R.L. Mössbauer: Phys. Rev. Letters 17(1966)5; M.J. Clauser and R.L. Mossbauer: Phys. Rev. 178(1969)559.

70) S. DeBenedetti, G. Lang, and R. Ingalls: Phys. Rev. Letters 6(1961)60.

71) R.L. Walker, G.K. Wertheim and V. Jaccarino. Phys. Rev. Letters 6(1960)98.

72) J.J. Spijkerman, D.K. Snediker, F.C. Ruegg and J.R. DeVoe: NBS Misc. Publ. 260-13(1967).

73) R.E. Watson: Tech. Rept. No.12, Solid State and Molecular Theory Group, Massachusetts Inst. of Tech. (Unpublished); Phys. Rev.119 (1960)1934.

74) E. Fermi and E. Segre: Z. Physik 82(1933)729; S.A. Goudsmit: Phys. Rev.43(1933)636.

75) J. Danon: Ref.20 pp. 89; J. Danon: J. Chem. Phys.39(1963) 236.

76) N.E. Erickson Ref.29, p.86.

77) R.W. Vaughan and H.G. Drickamer: J. Chem. Phys. 47(1967) 1530; R.V. Pound, G.B. Benedek and R. Drever: Phys. Rev. Letters 7(1961) 405; R. Ingalls, H.G. Drickamer and G. Depasquali Phys. Rev.155 (1967)165.

78) R.M. Housley and F. Hess: Phys. Rev. 154(1967)340.

79) M.H. Cohen and F. Reif: Solid State Phys. 5(1957)321; S.P. Das and E.L. Hahn: ibid Suppl.1(1958).

80) R.L. Collins and J.C. Travis: Rev.27 Vol.3(1967)p.123.

81) P.S.Hion: Soviet Phys. JETP 22(1966) 1080; see also R.U. Grant: Ref.27 Vol.2(1966)23; R.L. Collins and J.C. Travis, ibid.3(1966)123 and R.L. Collins: J. Chem. Phys. 42(1965) 1072.

82a)P. Zory: Phys. Rev. 140(1965)A.1401.

82b)K. Chandra and S.P. Puri: ibid.169(1968)272.

82c)R. Ingalls, K. Ono and L. Chandler: ibid.172(1968)295.

83) W.J. Nicholson and G. Burns: Phys. Rev. 129(1963)2490.

84) G.R. Hoy and K.P. Singh: Phys. Rev. 172 (1968)514; U.Caniol and S. Shtrikman: ibid 167 (1968)288; G.R. Hoy and S. Chandra: J. Chem. Phys. 47(1967)961.

85) M. Tanaka, T. Tokoro, and Y. Aiyama: J. Phys. Soc. Japan 21(1966) 202; P. Imbert: Compt. Rend. 263(1966)707.

86) P.R. Brady, J.P. Duncan and K.P. Mok. Proc. Roy. Soc. 287A(1965)363.

87) R.L. Collins and R. Pettit: J. Am. Chem. Soc. 85(1963)2332; R.H. Rony and H. Pollack: J. Appl. Phys. 36(1965)860; Rev. Mod. Phys. 36(1964)352.

88) J. Mates and T. Zonick: Phys. Letters 19(1965)111.

89) J. Demon: Third Intern. Conf. on Mössbauer, Effect, Ref.21.

90) R.H. Herber, R.B. King and G.K. Wertheim: Inorg. Chem.3 (1964) 101.

91) G.R. Kamokar, K.R.P. Mallikarjuna Rao and V. Udyashankar Rao: Phys. Letters 19(1965)96.

92) S.L. Ruby and P.A. Flinn Rev. Mod. Phys. 36(1964)351; Pl. also see Grant and Collins and Travis ref.81.

93) R.S. Preston, S.S. Hanna, and J. Heberle: Phys. Rev.128 (1962)2207.

94) E.U. Condon and G.H. Shortley, 'Theory of Atomic Spectra', (Cambridge University Press; 1959).

95) W. Kundig: Nuclear Instr. and Meth. 48(1967)219; J.R. Gabrial and S.L. Ruby ibid 36(1965)23; J.R. Gabriel. Ref.27 Vol.1 (1965)p. 121; A.H. Muir, Jr. ibid. Vol.4(1968);G.R. Hoy and S. Chandra: J. Chem. Phys.47(1967)961; W.C. Davidson:ANAL-5900, AECR and D. Rept. (1959); E. Rhodes U O'Neal, and J.J. Spijkerman:NBS Tech. Note 404, Sept.30, 1966).

96) P.H. Parker: J. Chem. Phys. 24(1956)1096.

97) S.V. Karyagin: Soviet Phys. Solid State 8(1966)891,1367.

98) W. Marshall and C.E. Johnson: J. Phys. Radium 23(1962)733.

99) A.J. Dekker and F. Van der Woude: Physica 33(1967)193.

100) R.W. Grant: Ref.20 p.34.

101) G.K. Wertheim, W.P. Kingston and R. Herber: J. Chem. Phys. 37, (1962),687; R.H. Herber and G.K. Wertheim:J. Chem. Phys. 38 (1963)2103.

102) V.G. Bhide and M.S. Multani: Phys. Rev.149(1966)289;V.G. Bhide and G.K. Shenoy: Phys. Rev.143(1966)309;J.D.Siegwarth: Phys. Rev.165(1967)286; H.J. Guggenheim and G.K. Wertheim: J.Chem. Phys. 42(1965)3875; J.G. Mullen:Phys. Rev.131(1963) 1415.

103) J.Stephen: Nucl.Instr.Meth.26(1964)209;J.P. Schiffer,P.H. Parks and J. Heberle:Phys. Rev.133(1964)A1553; T.A. Kitchens, W.A.Steyert, and R.D. Taylor:Phys.Rev.138(1965)A467; R.N. Housley, N.E. Erickson and J.G. Dash:Nucl.Instr.Meth.27 (1964)29; I.Dezsi:Magy.Fud. Akad.Kozp.Fiz Kut Int. Kozlemen 12 (1964)111; W.Kerler et al:Z.Physik 173 (1963)391;W.Kerler and W.Neuwirth:Z Physik 167(1962)178,194; S.M. Qaim, P.J. Black and M.J. Evans: J.PhysC (Proc. Phys.Soc.), 1(1968) 1398.

104) S.Bernstein and B.C. Campbell: Phys. Rev.132(1963)1625; P.Debrunner and H.Frauenfelder: Ref.20 p.53; J.K. Major: Ref.27 Vol.1(1965)p.69; P.Debrunner: Ref.27 Vol.1(1965)p.97.

105) L.May and D.K. Snediker Nucl. Instr. and Meth.53(1967)183.

106) A.J. Boarden, P.L. Mattern and P.S. Noble: Am. J. Phys. 32 (1964)109; C. DePangquali, H. Frauenfelder., S. Margulies and R.N. Peacock: Phys. Rev. Letters 4(1960)71; D.A. Shirley, M. Kaplan, and P1 Axel: Phys. Rev.123(1961)816.

107) K.P. Mitrofanov: Instr. Expl. Tech (USSR) (Eng.Trans)3(1965) 526; A.J. Bearden, M.G. Hauser and P.L. Mattern: Ref.27 Vol.1(1965) p.67; R.L. Mössbauer Ref.20 p.36(1962).

108) R. Booth and C.E. Violet; Nucl. Instr. Method 26(1963)1; R.H. Nussbaum, P. Gerstenfeld, and J.K. Richardson: Am. J. Phys. 34(1966)46.

109) P.A. Flinn: Rev. Sch. Instr. 34(1963)1422; Ref.27 Vol.1 (1965)p.75.

110) S.S. Hanna, J. Heberle, C. Littlejohn, G.J. Perlow, R.S. Preston and J.H. Vincent: Phys. Rev. Letters 4(1964)177.

111) A.D. Adler and M.Hone: Am. J. Phys. 34 (1966)189.

112) J.G. Rush, R.D. Taylor, N.E. Hagle; D.F. Craig and W.M. Visscher Phys. Rev. 122 (1961)1110; R.L. Mössbauer and W.H. Wiedemann: Z. Physik, 159(1960)33.

113) J.G. Mullon: Phys. Rev. 131 (1963)1410.

114) V.Boltran-Lofros and G. Loria.Rev.Sci.Instr. 38(1967)707; K.Clancoll and A.H. Jiggins: J. Sci. Instr. 44(1962)212. E.Kankeloit: Rev. Sci. Instr.38 (1964)195;Ref.27, Vol.1 (1965)p.47; Y.Hanony: Rev.Sci. Instr.38(1967)1760; P.E. Clark, A.V. Nichol and J.S. Carlow J. Sci. Instr.44 (1967)1001; N. Brafman, M. Groenshpan and R.H. Herbor: Nucl. Instr. Meth. 42 (1966)245; R.L. Cohon, P.G. McMullen and G.K. Vorthoim: Rev.Sci.Instr.34(1963)671; J.Lipkin, B.S. Chochtor, S.Shtrikman and D. Trovos: Rev.Sci.Instr.35(1964) 1530; R.L. Cohon: Rev.Sci.Instr.: 37(1966)957;The Phys. Teachor 3 (1965)306; J.D. Cooper and M.M. Groenwood: J. Sci.Instrum.43,(1966)71; P.C. Ruegg, J.J. Spijkerman and J.R. Dovos: Rev.Sci. Inst. 36(1965)380.

115) D.I. Bolef and J. Mishory: Appl. Phys. lettors 11 (1967)321.

116) R.C. Knauer and J.G.Mullon: Rev. Sci.Instr.38(1967)1624.

117) H.Slochtor, U. Ron, S. Niodzwiods and H. Herbor: Nucl. Inst. and Meth. 44(1966)268.

118) M.Kalvius: Ref.27 Vol.1(1965)p.103; P.D. Woodham, J.S. Carlon and R.E. Meads: J. Sci. Instrum.43 (1966)333; A.J. Nozik and M.Kaplan: Anal.Chem.39(1967)864; U.Heidemann, V.A. Mundit, and D.Kullman: Cryogonics 5 (1965)94; D.P.Johnson, G.A. Erickson and J.G. Rook: Rev.Sci.Instr.39(1968)420; B. Sharon and D. Tsovoo: Rev. Scio. Instr. 37(1966)1252.

119) [illegible]; H. Schlogal and A. Schaler: Z. Metallkunde 43(1952)421; H.E. Norvin and H.P. Lombard: Econ. Geol.32(1937)203.

120) C.H.L. Goodman and R.W. Douglas Physica 20(1954)1107; C.H.L. Goodman J. Phys. Chem. Solids 6(1958)305; I.G. Austin, C.H.L. Goodman, and A.E. Pongolly: J. Electrochem. Soc.103 (1956) 609.

121) M. Wintonborgor: compt. Rend 244(1957)1601; Bull. Soc.Franc. Mineral Criot.85(1962)77.

122) T. Toranishi: J. Phys. Soc.Japan 15(1960)1123; ibid 16(1961) 1861; ibid 17(Suppl.) B-1(1962)263.

123) G.Donnay, L.M. Corliss, T.D.H. Donnay, N. Elliott. and J.M. Hastings: Phys. Rev. 112 (1958)1917.

124) J.E. Hiller and K. Probsthain: Z.Kriot 109(1956)109.

125) A.J. Pruch: Am. Min. 44(1959)1010.

126) T.T. Read, L.P. Morgun, and E.F. Smith: Trans.Am.Inst.Min. Eng.37(1907)895.

127) C. Kuzylenko: Bull. Soc. Franc. mineral 65 (1942)59.

128) L. Pauling and L.O. Brockway: Z.Kriot 82(1932)188.

129) Dee Raj, K. Chandra, and S.P. Puri, Nucl. Phys. and Solid State Phys. Symposium I.I.T. Kanpur (India)Feb.1967; J. Phys. Soc. Japan 24(1968)39.

130) P. Aramu, T. Bressani, and P. Manca: Nuovo Cimento 51 B (1967)370.

131) R. Imbert and M. Vintenberger: Bull Soc. Franc. Mineral-Cryst allogr. 90(1967)299.

132) R.H. Goodman: Mossbauer Effect Methodology Vol.3(Ed.Irwin J. Gruverman, Plenum Press, New York,(1967).

133) C.L. Hermenberg: Nuovo Cimento 58 B (1968) 510.

134) H. Frank: Nuovo Cimento 58B (1968) 407.

135) N.N. Greenwood and H.J. Whitfield: J. Chem. Soc.(A)(1968) 1697.

136) J. Piekoszewski, J. Suwalski and S. Ligenza: Phys.Stat. Sol. 29(1968)K99.

137) R.H. Goodman and J. Cabri: Submitted to Science (1968) (The author is thankful to Dr. Goodman for sending his preprint).

138) A.H. Muir Jr. Unpublished data (I am thankful to Dr. C.L. Hermenberg for giving this information in his letter).

139) Dee Raj and S.P. Puri: Nuovo Cimento 60(B) (1968)201.

140) H. Hahn, G. Frank, W. Klinger, A.D. Meyer and G. Storger: Z. anorg. U. Allg. Chem. 271(1953)153.

141) C.L. Burdick and J.H. Ellis: Proc. Natl. Acad. Sci.U.S.3 (1917) 644; J. Am. Chem.Soc.39(1917)2510, It was the first structure to be determined in the U.S.A. and the first of a 'Complex sulphide'.

142) J.W. Beem: Rec. Trav. Chim. 63(1944)69.

143) L.G. Berry and R.M.Thompson: X-ray powder Data for Ore Minerals, The Peacock Atlas, Geol.Soc. Am. Mem.85(1962).

144) S.Ofer, P.Avivi, R. Bauminger, A. Marinov and S.G. Cohen: Phys. Rev. 120(1960)406; R.L. Cohen: Phys. Rev.134(1963)A94.

145) K. Ono and A. Ito: Phys. Solid State 6(1966)391, 1387.

146) L.E. Orgel: 'An Introduction to transition metal Chemistry-ligand Field Theory'(Methuen and Co. London, 1962)p.51; C.P. Boll and H.A.K. Lott: Modern Approach to Inorganic Chemistry(Butter worth and Co.(Publishers) Ltd.London, 1966)Second edn.,p.89.

147) A.K. Barnard: Theoretical basis of Inorganic Chemistry (McGraw Hill Publishing Co.Ltd., New York, 1965)Chap.7 p.245.

148) G.K. Wertheim: Phys. Rev. 124(1961)764.

149) H.H. Wickman, A.M. Trozzolo U.J. Williams, G.N. Hull and F.R. Merritt: Phys. Rev. 155(1967)563; H.H. Wickman, M.P. Klein and D.A. Shirley: Phys. Rev.152 (1966)345.

150) K.Ono, A. Ito, and J. Fujita: J. Phys. Soc. Japan 19(1964) 2129.

151) A. Okiji and J. Kanamori: J. Phys. Soc. Japan 19(1964)908.

152) R.E. Watson and A.J. Freeman: Phys. Rev. 123 (1961)2027.

153) A.A. Tompsrlay and W.H. Lefevar: J. Phys. Chem. Solids 27(1966)85.

154) A.H. Muir and M. Wiedersich: J. Phys. Chem. Solids 28(1967) 65.

155) R.Ingalls: Phys. Rev. 133 (1964) A 787.

156) A.E.H. Tutton: Proc. Roy Soc. A85 (1909) 211, 210; ibid- A88(1913) 72, 301; ibid A94(1918)352; ibid. A101(1922)245; ibid.A100(1925) 240; Phil. Trans. A 217(1917)199; J. Chem. Soc.63(1893)337; ibid.69(1896)344.

157) K. Tsutsumi: J. Phys. Soc. Japan 14(1959)1696.

158) R.W. Hill and P.L. Smith: Proc. Phys. Soc. (London)A66 (1953)226.

159) R. Guillien: Compt. Rend. 209(1939)21.

160) L.C. Jackson: Phil. Trans. Roy. Soc.(London)A224(1924)1.

161) T. Ohtsuka, H. Abe, and E.Kanda: Sci. Rep. Tohku Univ.9A (1957)476.

162) J.R. Richardson and R.C. Sapp: J. Chem. Phys. 29(1958) 337; ibid, 30 (1959)326.

163) A.S. Chakravarty and R. Chatterjee: Indian J. Phys. 34 (1960)10.

164) G.A. Candela and R.E. Mundy: Rev.Sci.Instr. 32(1961)1088.

165) A. Bose A.S. Charkravarty and R. Chatterjee: Proc. Roy. Soc. (London) A262(1961)207.

166) D.G. Thakurta and D. Mukhopadhyay: Indian J. Phys. 40 (1966)68

167) B. Bleaney and K.W.H. Stevens: Rept. Progr. Phys.16(1953)108.

168) A. Abragam and M.H.L. Pryce. Proc. Roy. Soc.A205(1951)175.

169) D.D. Bhattacharya: Indian J. Phys. 38(1964)331.

170) R.W. Grant, H. Wiedersich, A.H. Muir, Jr., U. Gonser, and U.N. Dolgaas: J. Chem. Phys. 45(1966)1015.

171) L.G. Long, S. deBenedetti and R. I. Ingalls: J. Phys. Soc. Japan 17 Suppl.B-I, (1962)131. Also S. de. Benedetti, G. Long and R.Ingalls: Phys. Rev. letters 6(1961)60.

172) Dee Raj, K. Chandra and S.P. Puri: J. Phys. Soc. Japan 24 (1968)35.

173) U.Hofmann: Z. Krist 78(1930) 156; ibid 78(1931)279.

174) H.Montgomery and E.C. Lingafelter: Acta. Cryst. 17(1964) 1295; ibid. 17(1964) 1478; ibid 20(1966)659; ibid.20 (1966) 729.

174b)H. Montgomery, R.V. Chastain, J.J. Natt, A.M. Witkowska and E.C. Lingafelter: Acta. Cryst. 22 (1967)775.

175) R. Ingalls: Phys. Rev. 128(1962)1155.

176) H.M. Foley R.M. Sternheimer and D. Tycko: Phys. Rev. 93 (1954)734; R.M. Sternheimer and H.M. Foley: ibid.102 (1956)731; R.M. Sternheimer: ibid.84(1951)244; ibid.95 (1954)736; ibid.105(1957)158; ibid.150(1963)1423.

177) A.J. Freeman and R.E. Watson: Phys. Rev. 131(1963)2566.

178) A.J. Nozik and M. Kaplan: Phys. Rev. 159(1967)273.

179) M. Tinkham: Proc. Roy. Soc. (London) A236(1956)535.

180) W.Brenger: Naturwissenschaften 52(1965)158; W. Brenger: Z. anorg. allg. Chemie Vol. 359 (1968)15.

181) W. Brenger: Z. anorg. allg. Chemie Vol.359(1968)15.

182) K. Peries: J. Prakt. Chem. 107(1869)16.

183) R. Schneider: J. Prakt. Chem. 108(1839)16.

184) H.J. Hartwedel and K. Dinger: Bull. Inst. Verre No.6 (1946)15.

185) B.S. Khambata and A Wanermann: J. Chem. Soc. (1946)1090.

186) P.R. Edvard and C.E. Johnson: J. Chem. Phys. 47(1967)2074.

187) K. Chandra, Dee Raj, and S.P. Puri: J. Chem. Phys.46(1967) 1686.

188) J.L. Deutsch and H.B. Jonesson: Inorganic Synthesis Vol.VI Chapter VIII page 170(McGraw Hill Book Company, 1960).

189) H. O'Daniel: Z. Krist. 88(1933)192.

190) J.U. Been and C.H. MacGillary: Rec.Trav. Chim. 61(1942)910.

191) B.F. Ormont, Struktury neorganicheskikh vishchestv, GITTL, Moskva (1950)p.205.

192) R. Ingalls: Phys. Rev. 155(1967)157.

218) R.A. Bornhoim and H.S. Gutowsky: J. Chem. Phys. 32(1963) 1072.

219) David H. Adamson: J. Chem. Phys. 35(1961)1353.

220) R.R. Howitt: Phys. Rev. 121(1961)46.

221) J.P. Hon: Phys. Rev. 124(1961)1368.

222) R.G. Barnes, S.L. Segel and W.H. James Jr: J. Appl.Phys. 33 (1962)290.

223) R.V. Pound: Phys. Rev. 79(1950)685.

224) T.P. Das and M. Karplus: J. Chem. Phys. 30(1959)848.

225) G. Burns: Phys. Rev. 115(1959)357.

226) D.K. Ray: Proc. Phys. Soc.82(1963)47.

227) T.T. Taylor and T.P. Das: Phys. Rev. 133(1964)A1327.

228) H.C. Bolton and C.A. Sholl: J. Nucl. Mater. 14(1964)205.

229) G. Burns: J. Chem. Phys. 42(1965)377.

230) F.W. deWette and B.R.A. Nijboer: Physica 24(1958)1105;ibid. 25(1959)1225.

231) R.R. Howitt and T.T. Taylor: Phys. Rev. 128(1962)624.

232) T.T. Taylor: Phys. Rev. 127(1962)120.

233) F.W. deWette and G.E. Schacher: Phys.Rev.137(1965)A78.

234) C.A. Scholl: Proc. Phys. Soc.87(1966)697.

235) C.J.F. Bottcher: 'Theory of Electric Polarisation' (Elsevier Publishing Company Inc., Houston, Texas,1962).

236) D.V.G.L. Narasimha Rao and A. Narasimhamurty: Phys. Rev.132 (1963)961; P. Raj and V. Amirthalingam: Phys. Rev.146 (1966)590.

237) R.W. Vaughan and H.G. Drickamer: J. Chem. Phys. 47(1967) 1530.

238) J.S. Wollott: Computing Methods in crystallography, Edited by J.S. Wollott (Pergamon Press Oxford, 1965)p.22.

239) P.C. Romeijn: Philips Res. Rept. 8(1953)304;R.W.G. Wyckoff 'Crystal Structure'(Interscience Publishers, Inc., New York, 1951) Chapter I, Text p.3.

240) E. Brun and S. Hafner: Z. Krist. 117(1962)63.

241) T. Minoguchi and W. Tanaka : J. Phys. Soc. Japan 18(1963) 1301.

242) G. Burns and E.G. Wikner: Phys. Rev. 121(1961)155.

243) J.M. Hastings and L.M. Corliss: Rev. Mod. Phys. 25(1953) 114.

244) D.E. Cox and G. Shirane quoted by G. Burns Ref.202; G. Shirane S.J. P. Chart, R.Nathans, and Y. Ishikawa: J. Phys. Chem. Solids 10(1959)35.

245) L. Pauling and S.B. Hendricks: J. Am. Chem. Soc. 47(1925) 781.

246) N.E. Newnham and Y.M., deHaan: Z. Krist 117 (1962)235.

247) B.R.A. Nijboer and F.W. deWette: Physica 23(1957)309;ibid. 24(1958)422.

248) F.W. deWette: Phys. Rev. 123(1961)103.

249) R.H. Wood: J. Chem. Phys. 32(1960)1890.

250) R.L. Blake, R.E. Hessevick, T. Zoltai and L.W. Finger. Am. Min. 51(1966)123; R.L. Blake, L.W. Finger and T. Zoltai to be submitted in Am. Min.

251) A.M. Mair, Jr., and H. Wiedersich: Bull. Am. Phys. Soc.11 (1966) 770.

252) W.Soller and A.J. Thompson: Phys. Rev.47(1935)644.

253) Yu. Ya Tomashpolskii and Yu. N. Venevtsev: Soviet Phys. Cryst. 12(1967)24, July-August (Russian).

254) K.C. Das: Proc. Phys. Soc. (London) 87 (1966)61.

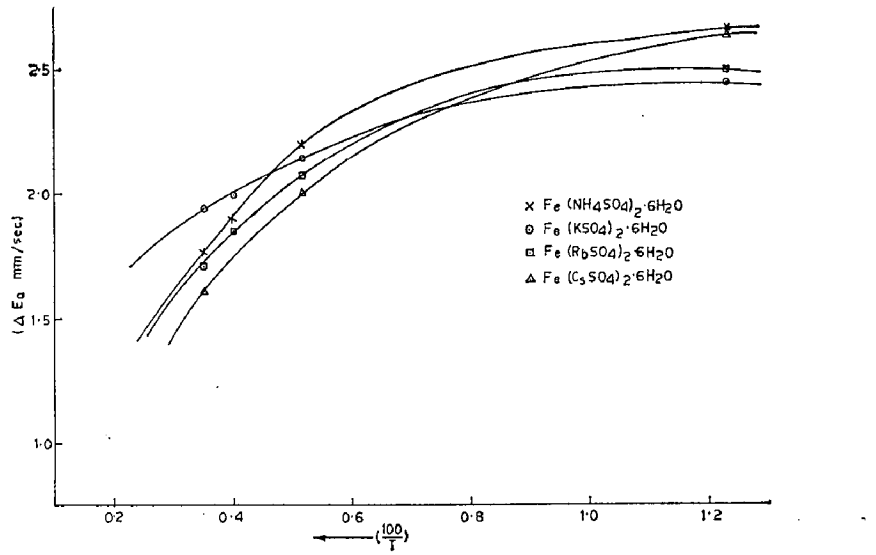

Fig. 1. Temp. Dependence of the quadrupole splitting in iron tutton salts.

a lower energy degenerate triplet $|xy>$, $|xz>$, $|yz>$ called t_{2g} levels and higher energy degenerate doublet $|x^2-y^2>$ and $|3z^2-r^2>$ called e_g levels. Furthermore if the octahedron is a distorted one, a small ligand field of a symmetry lower than cubic such as axial and rhombic[6] will lift the degeneracy of t_{2g} and e_g levels as depicted in Fig. 2.

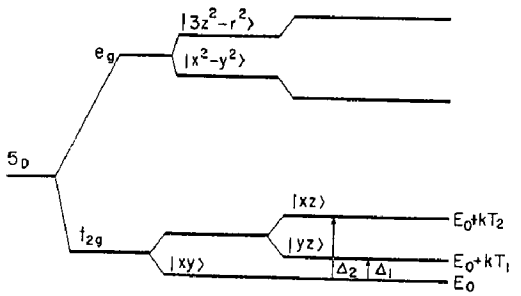

Free ion+cubic field+axial field+rhombic field

Fig. 2. Splitting a d orbital in a crystalline field.

The temperature dependence of quadrupole splitting is interpreted in terms of the temperature dependent occupation probabilities of the t_{2g} states by the sixth electron only. The thermal transition times between the t_{2g} levels ($10^{-9}-10^{-11}$ sec) are shorter than the quadrupole precession times ($\sim 10^{-8}$ sec), hence the effective field gradient is the average of the contributions from these states each of these weighted by Boltzmann factor. Denoting the energies of the t_{2g} triplet by E_0, E_0+kT_1, E_0+kT_2, the substitution of the expressions for q and η in eq. (1) and the insertion of the Boltzmann factors yields the expression for quadrupole splitting[2]

$$\Delta E_Q = \frac{2}{7}e^2Q(1-\gamma) \times \frac{[1+e^{-2T_1/T}+e^{-2T_2/T}-e^{-T_1/T} -e^{-(T_1+T_2)/T}-e^{-T_2/T}]^{1/2}}{[1+e^{-T_1/T}+e^{-T_2/T}]} \langle r^{-3}\rangle_{3d}, \quad (2)$$

The analysis of the experimental data employed the following values:

$Q=0.29$ barn; $\gamma=.42$ and $\langle r^{-3}\rangle_{3d}=5.1/a_0^3$.

The experimental data was analyzed by computerising the program and the eq. (2) was found to be satisfied by several combinations of T_1, T_2 at the observation temperature T, but the final choice of the set was guided by the observed temperature dependence of the quadrupole splitting and the available results of $Fe(NH_4SO_4)_2\cdot 6H_2O$.[2] The characteristic temperatures of the t_{2g} levels are given in Table II.

Table II. Characteristic temperatures T_1 and T_2 of t_{2g} levels of Fe^{2+} in Tutton salts and the ground state orbital wave functions.

Compound	T_1(°K)	T_2(°K)	Ground state orbital wave function
$Fe(NH_4SO_4)_2\cdot 6H_2O$	230	300	$\|xy>$
$Fe(KSO_4)_2\cdot 6H_2O$	260	340	$\|xy>$
$Fe(RbSO_4)_2\cdot 6H_2O$	240	310	$\|xy>$
$Fe(CsSO_4)_2\cdot 6H_2O$	220	290	$\|xy>$

In order to decide the ordering of the energy levels it is essential to find the ground state wave function. The ratio of eq for the doublet and singlet[4] is

$$\frac{\text{eq (singlet)}}{\text{eq (doublet)}} = -2.0 ,$$

By comparing the low temperature (81°K) values of quadrupole splittings with that of $Fe(NH_4SO_4)_2 \cdot 6H_2O$, we infer that the ground wave function assignment in all these cases is the $|xy>$.

§ 4. Discussion of Results

The values of isomer shift at different temperatures show that it is independent of temperature within the accuracy of measurements for NH_4, K and Rb salts, whereas the slight slope of I. S. versus temperature curve for Cs salt: 2.3×10^{-15}/°K is due to the time dilation resulting from the motion of the emitting and absorbing nuclei. The Fe^{2+} ion being surrounded by the distorted octahedron formed by $6H_2O$, the varying electronegativity of the alkali cation has no effect on the value of I. S.

The values of the characteristic temperatures T_1 and T_2 are not unique since these are based only on the analysis of the quadrupole splittings. It is desirable to analyse simultaneously the Mössbauer data, the paramagnetic susceptibilities and the resonance data (if available).

An attempt is being made to calculate the temperature dependence of ΔE_Q in case of spin free Fe^{2+} compounds allowing for the spin-orbit coupling interaction, crystal field interactions of low symmetry and the contribution from the surrounding cations and anions in the crystalline matrix and the results of the calculation will be submitted.

Acknowledgements

Two of the authors (D. R. and K. C.) express their sincere thanks to the Council of Scientific and Industrial Research (India) for grant of a research fellowship. S. P. P. is also grateful to C. S. I. R. for a grant-in-aid for this project which enabled the undertaking of this work.

References

1) M. H. Cohen and F. Reif: *Solid Sfate Physics*, ed. F. Seitz and D. Turnbull, (Academic Press Inc., New York) (1957) Vol. 5.
2) R. Ingalls: Phys. Rev. **133** (1964) A 787.
3) L. G. Lang, S. DeBenedetti and R. I. Ingalls: *the Mössbauer Effect Proc. of the 2nd Conf.* (1962) 168.
4) K. Ôno and A. Ito: J. Phys. Soc. Japan **19** (1964) 899.
5) W. Kerler: Z. Phys. **167** (1962) 194.
6) B. Bleaney and K. W. H. Stevens: Reports Progr. Phys. **16** (1950) 108.
7) A. E. H. Tutton: Proc. Roy. Soc. **88** A (1913) 361.
8) R. S. Preston, S. S. Hanna and J. Heberle: Phys. Rev. **128** (1962) 2207.
9) W. Hofmann: Z. Krist **78** (1931) 279.
10) H. Montgomery and E. C. Lingafeltor: Acta cryst. **17** (1964) 1479.

JOURNAL OF THE PHYSICAL SOCIETY OF JAPAN, Vol. 24, No. 1, JANUARY, 1968

Mössbauer Studies of Chalcopyrite*

Deo RAJ, K. CHANDRA and S. P. PURI
Department of Physics, University of Roorkee, Roorkee, India

(Received July 5, 1967)

Mössbauer spectra of naturally occurring mineral chalcopyrite have been studied over a temperature range 300°–448°K. The spectra showed a typical pattern of six absorption lines due to the internal magnetic field. The Q.S. have values which are independent of temperature whereas the magnitudes of the internal magnetic field are 325±10, 312±10 and 290±10 KOe at 300°, 373° and 448°K respectively. These features are explained by assuming that Fe atom is in a spin free, trivalent state in weak crystal field configuration. The internal field is accounted to originate primarily through the Fermi contact interaction, H_c; both the $H_{dip.}$ and $H_{orb.}$ contributions being zero.

§ 1. Introduction

Chalcopyrite, $CuFeS_2$, a well known semiconducting[1] copper mineral with ZnS structure, has been a subject of intense study regarding its electric and magnetic properties.[2] Neutron diffraction studies[3] showed it to be antiferromagnetic with the $\mu_{eff.}$ for Fe equal to $3.85\,\mu_B$ and Néel temperature of 550°C. Furthermore thermoelectric power measurements[2] suggest that Fe atom is principally covalently bonded with sulfur atoms in the tetrahedral (sp^3 hybrid orbitals) structure. But there exists a controversy regarding the valence state of iron atom. From considerations of lattice constants and ionic radii of cations, Pauling and Brockway[4] considered that chalcopyrite is a mixture with two states $Cu^{I}Fe^{III}S_2$ and $Cu^{II}Fe^{II}S_2$, the iron atom resonating between Fe^{III} and Fe^{II} states. However, the neutron diffraction studies indicate that iron atom is in the Fe^{III} state.[3] This mineral has the desirable features of being a semiconductor and an antiferromagnet, which render feasible the detection of two charge states Fe^{III} and Fe^{II} through the magnetic interactions. In addition it is desirable to account for the sign and magnitude of internal magnetic field at the Fe nucleus.

§ 2. Experimental Procedure and Results

The specimen was naturally occurring chalcopyrite crystal selected for its purity by ore microscope examination. The structure was examined by *X*-ray diffraction and tallied with that given by Pauling and Brockway.[4]

The spectrometer employed a constant velocity cam and was calibrated by using natural iron as a standard absorber in conjunction with the data of Preston *et al.*[5]

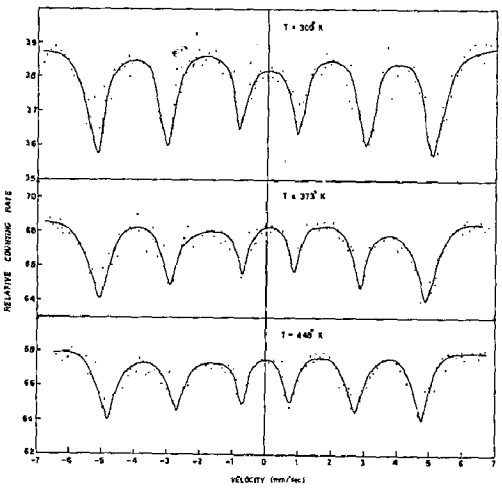

Fig. 1. Hyperfine spectra of naturally occurring Chalcopyrite.

Table I. Isomer shift, quadrupole splitting and internal magnetic fields in Chalcopyrite at various temperatures. Source: Co^{57} in Cu matrix.

Temperature °K	Isomer Shift mm/sec	Quadrupole splitting mm/sec	Internal Magnetic Field Kgauss
300	−0.03±0.02	0.05±0.02	325±10
373	−0.03±0.02	0.05±0.02	312±10
448	−0.04±0.02	0.04±0.02	290±10

The spectra were taken at temperatures 300°K, 373°K and 448°K and are shown in Fig. 1. The values of isomer shift, quadrupole splitting and internal field are given in Table I. The data at higher temperatures could not be taken as the compound starts decomposing before 300°C.[6]

* A preliminary report was presented in the Solid State and Nuclear Physics Symposium held at I. I. T. Kanpur (India) in Feb. 1967.

§ 3. Discussion

The values of I.S. measured with respect to Co^{57} in Cu are of the order of 0.03 mm./sec. As $CuFeS_2$ is a covalent compound and in the case of covalently bonded compounds, the values of I.S. for divalent and trivalent iron atoms overlap[7] in this region, no unequivocal assignment of valence state is possible on this account.

Iron is covalently bonded with S-atoms in a regular tetrahedron as regards the crystallographic structure. But $CuFeS_2$ is an antiferromagnet and the magnetic interaction will make the symmetry lower than cubic as in the case of Dy^{161} in dysprosium iron garnet and Tm^{169} in $TmFe_2$.[8] The covalency between iron ions and their ligand neighbours plays an important role and the stronger the covalent bonding of iron ions, the smaller is the value of quadrupole splitting.[9] Thus the magnitude of experimental values might seem to be explicable by considering the iron ion to be Fe^{2+} with covalent bonding, but such a view is untenable when we consider the temperature dependence of splittings in a tetrahedral field. In the tetrahedral ligand field the fivefold degenerate levels of free Fe ion are split into a lower doublet called $d\gamma$ orbitals and an upper triplet called $d\varepsilon$ orbitals. The iron atom in the divalent state will give temperature dependent quadrupole splitting both in the low as well as high field configuration. Furthermore the Fe^{III} in the case of high field configuration will also show the temperature dependent splittings. The observed values of quadrupole splitting, Table I, are independent of temperature, so it seems plausible that Fe atom is in the spin free[2,3] trivalent state and in weak crystal field, since it is only in this configuration that temperature independent values of quadrupole splitting can be explained. This conclusion is further supported by the observation that in tetrahedral complexes, no 'low spin' complex has so far been substantiated.[10]

The presence of two charge states will result in producing a complex hyperfine spectrum or much broader lines.[11] $CuFeS_2$, being a semiconductor, will seem to have a longer relaxation time and render feasible the observation of complex spectra due to the presence of two resonating charge states provided these resonate back and forth in a time longer than 10^{-7} sec. But the hyperfine spectra, Fig. 1, show a typical pattern of six absorption lines, since the observed line width of 0.35 mm/sec for the inner lines is comparable to the line-widths observed in Fe_2O_3.[12] The broadening in the outside wings is of instrumental origin as is the case with the spectrum of natural iron with our spectrometer. The presence of typical six finger pattern and no relaxation broadening do not lend support to the hypothesis of resonating structure and show that Fe atom is in a single charge state.

Although the observed values of internal magnetic field are smaller than those for Fe^{3+} ionic compounds (550 KOe) but are comparable with that reported for $KFeS_2$[13] where Fe atom is in the trivalent state and bonded covalently. The sign and magnitude of the internal field may be accounted as follows.[14]

The internal magnetic field $H_{exp.}$ arises mainly from three source, (i) Fermi contact interaction, H_c, (ii) the intra-atomic dipolar interaction, $H_{dip.}$ and (iii) orbital current, $H_{orb.}$. The contributions of (ii) and (iii) are given by Okiji and Kanamori[15] as

$$H_{dip.} = -\langle(3z^2-r^2)/r^5\rangle\langle S_z\rangle(\mu_B/2) = (\mu_B/2)q\langle S_z\rangle \quad (1)$$

$$H_{orb.} = = -2\mu_B\langle r^{-3}\rangle\langle 1_z\rangle \quad (2)$$

where the symbols have their usual meanings.

Fe^{+++} is in the $3d^5$, ^6S state and the major contribution is from H_c, Watson and Freeman[16] calculated H_c for Fe^{+++} as -630 KOe and furthermore the observed magnetic field $H_{exp.}$ depends on the type of ligand neighbour and its bonding. Mn^{++} is isoelectronic with Fe^{+++} and H_c as estimated by Watson and Freeman is -700 KOe and for S^{--} as ligand neighbour is -490 KOe. Thus the estimated value of H_c for Fe^{+++} covalently bonded with S^{--} is $-630\times\frac{490}{700}=-441$ KOe. Since the value of $\mu_{obs.}$ for $CuFeS_2$ at room temperature is not 5.86 μ_B (a measured value in $Fe_2(SO_4)_3$ at room temperature where iron is in Fe^{3+}, $3d^5$ state) but 3.85μ_B, so the effective H_c will be $-441\times\frac{3.85}{5.86}=-289.7$ KOe.

$H_{dip.}$ is zero because in a cubic environment there can be no dipolar contributions. Since the ground state of Fe^{3+} is ^6S, the $H_{orb.}$ is also zero. Hence the estimated $H_{exp.}$ is -290 KOe, the value which agrees with the measured value. This agreement further supports the contention that iron atom is in the trivalent state.

With a view to corroborate our conclusion further EPR spectra was tried but no absorption did occur probably due to the high dielectric constant of the material. Nor the optical absorption studies were possible since the substance is opaque

and does not dissolve in any solvent.

Acknowledgements

Our sincere thanks are due to Dr. K. K. Singh of Geology Department for supplying the compound and Mr. A. K. Chatterjee of Central Building Research Institute for *X*-ray analysis. We are also grateful to Council of Scientific and Industrial Research (India) for the financial assistance. We acknowledge refree's help in pointing out the use of correct value of μ_B for Fe^{3+} ion at room temperature.

References

1) C. H. L. Goodman and R. W. Douglas: Physica **20** (1954) 1107; I. G. Austin, C. H. L. Goodman and A. E. Pengelly: J. Electrochem. Soc. **103** (1956) 609.
2) T. Teranishi: J. Phys. Soc. Japan **15** (1960) 1123; **16** (1961) 1881; **17** (1962) Suppl. B-1 263.
3) G. Donnay *et al*: Phys. Rev. **112** (1958) 1917.
4) L. Pauling and L. O. Brockway: Z. Krist. **82** (1932) 188.
5) R. S. Preston, S. S. Hanna and J. Heberle: Phys. Rev. **128** (1962) 2207.
6) A. J. Frueh: Am. Min. **44** (1959) 1010.
7) J. F. Duncan and R. M. Golding: Quart. Rev. **19** (1965) 36.
8) S. Ofer, P. Avivi, R. Bauminger, A. Marinov, and S. G. Cohen: Phys. Rev. **120** (1960) 406; R. L. Cohen: Phys. Rev. **134** (1964) A94.
9) K. Ôno and A. Ito: J. Phys. Soc. Japan **19**, (1964) 899.
10) A. K. Bernard: *Theoretical basis of Inorganic Chemistry* (McGraw Hill Publishing Co. Ltd., New York, 1965) Chap. 7 p. 245.
11) G. K. Wertheim: Phys. Rev. **124** (3) (1961) 764.
12) O. C. Kistner and A. W. Sunyar: Phys. Rev. Lett. **4** (1960) 412.
13) W. Kerler, W. Neuwirth, E. Fluck, P. Kuhn and B. Zimmerman: Z. fur Phys. **173** (1963) 321.
14) K. Ôno, Atsuko Ito and Toshizo Fujita: J. Phys. Soc. Japan **19** (1964) 2119.
15) A. Okiji and J. Kanamori: J. Phys. Soc. Japan **19** (1964) 908.
16) R. E. Watson and A. J. Freeman: Phys. Rev. **123** (1961) 2027.

PUBLISHED IN NUOVO CIMENTO 60B(1969) 261.

ON THE MÖSSBAUER EFFECT OF CHALCOPYRITE

DEO RAJ AND S.P.PURI
Department of Physics, University of Roorkee, Roorkee, India.

Summary:

The reported Mössbauer spectra of the ^{57}Fe 14.4 keV γ-rays in $CuFeS_2$ of Aramu et al. are criticized and shown to originate from FeS_2 (pyrite) association of the studied sample. In addition, the hypothesis of the iono-covalent resonant structure as advanced by them is shown to be untenable considering the observed values of quadrupole splitting.

The Mössbauer absorption of the ^{57}Fe 14.4 keV γ-rays in $CuFeS_2$ was studied by ARAMU et al.(1). They reported a quadrupole split doublet spectrum both at room and liquid-nitrogen temperatures and found no evidence for a six-line spectrum characteristic of magnetic interactions. On the basis of an experimentally derived isomeric shift, they proposed a new resonant structure $Cu^{+}Fe^{+3}(S^{-2})_2 \longleftrightarrow Cu^{-3}\ Fe^{-}(S^{+2})_2$ where both the configurations are equally probable. Furthermore the semi-conducting and magnetic properties of the compound were discussed in the light of the new proposed structure. A similar study has been carried out by us and others(2) and as the observations are in direct contrast to each other, it is desired to offer the following comments in this regard.

The specimens studied in both the cases(1,2) were naturally occurring chal-copyrite and normally

the FeS_2 (pyrite) and $FeS_{1\pm x}$ (phyrrhotite) are present as associations in varying proportions (in case of admixture) or fixed proportions (in case of a solid solution). In view of the vastly varying composition, it is imperative that the structure be examined by X-ray diffraction ([3]) for identification of the species.

Neutron-diffraction studies([4]) showed the compound to be antiferromagnetic with μ_{eff} for Fe equal to $3.85\mu_B$ and Neel temperature of 550 °C. The magnetic ordering due to interlocked sublattices will give rise to magnetic hyperfine splitting thereby giving a six-line Mössbauer spectrum ([3]). The values of I.S. (relative to iron) and quadrupole splittings at room and liquid-nitrogen temperature for chalcopyrite as reported by ARAMU et al. ([1]) agree with those of FeS_2 (pyrite) ([5]) and for comparison are tabulated in Table I. The Mössbauer spectra for chalcopyrite and FeS_2 (pyrite) are given in Fig.1. It is obvious that the spectrum in Fig. 1 b) seems to correspond to the spectrum of ARAMU et al.([1]).

TABLE I. - Experimentally observed values of Q.S. and I.S. with respect to source in iron at 300 °K.

Compound	T (°K)	ΔE_Q (mm/s)	δ (mm/s)
$CuFeS_2$	300	0.05 ± 0.02	0.196±0.02 (a)
	373	0.05 ± 0.02	0.196±0.02 (a)
	77	0.650± 0.03	0.400±0.03 (b)
	300	0.600± 0.03	0.320±0.03 (b)
FeS_2 (pyrite)	81	0.620± 0.009	0.407±0.003 (c)
	300	0.614± 0.006	0.314±0.002 (c)
	300	0.61 ± 0.02	0.33 ±0.02 (d)

Table contd.

Compound	T(°K)	ΔE_Q (mm/s)	δ (mm/s)
FeS(pyrrhotite)	90	-0.15 ± 0.14	-
	290	-0.16 ± 0.10	0.648±0.10 (e)

(a) Reference (3).
(b) Reference (1).
(c) Reference (5).
(d) This work.
(e) K. ONO, et al.:Journ. Phys.Soc.Jap., 17,1617(1962)

By comparing the values of I.S. of an ionic compound $CuFeO_2$ (6) (0.40 mm/s) with their observed value (0.32 mm/s) ARAMU et al. (1) hypothesized the ionocovalent resonant structure: $Cu^{+}Fe^{+3}(S^{-2})_2 \longleftrightarrow Cu^{-3}Fe^{-}(S^{+2})_2$, where both the configurations are equally probable. The covalent bonding in the above structure is regarded to reduce the I.S. If the resonance time of the two structures is less than 10^{-7} s (lifetime of the first excited state of ^{57}Fe) the observed spectrum will be considerably broadened, whereas if it is greater than 10^{-7} s it will result either in a complex spectrum (if resolved) or broadened (if unresolved) due to the presence of the Fe^{+3} ion in two chemically inequivalent sites. The values of half-width from the spectra (1) are in good agreement with the well-resolved spectra of iron compounds(7) and thus the spectra (1) are neither complex nor broadened as one would expect on the plea of the ionocovalent resonating structure.

Furthermore the assumption of the new proposed structure seems to be untenable when considered from the observed values of quadrupole splitting. It has

been shown by INGALLS ([8]) that the field gradient of a d-electron at the nucleus is given by

$$(1-R)q\,\alpha^2 F,$$

where (1-R) is the Sternheimer factor which accounts for the deformation of the inner shells by the electron; α^2 the covalency factor which accounts for the expansion of the electron towards the ligands ($0.6 < \alpha^2 < 0.9$); $q(= 4/7\langle r^{-3}\rangle)$ the field gradient calculated from the free-ion wave-function and F a function of energy-level separation, spin orbit coupling and temperature. For an essentially localized electron as presumably in the ionic configuration $Cu^{+}Fe^{+}(S^{-2})_2$, $\alpha^2 = 0.9$, whereas in the covalent configuration $Cu^{-3}Fe^{-}(S^{+3})_2$ (sp^3 bonding of iron) the covalent bonding will introduce delocalization of the electron in 3d orbitals, reducing the electronic contribution to the field gradient. Assuming (1-R) and F to be nearly the same for both the above configurations, the ΔE_Q value will be different, the difference depending on the degree of delocalization of the electrons. In addition, with regards to the proposed structure, it was assumed that the Fe^{+3} ion is spin-paired in the ionic form and spin-free in the covalent (sp^3) configuration. There is bound to be a contribution to q from the uncompensated electron in the ionic configuration, whereas there is no such contribution from Fe^{+3} in the spin-free state, so resulting inevitably in different values of quadrupole splitting in both the configurations. This will either give rise to an additional doublet(if fully resolved) or cause

broadening of the observed absorption peaks; but neither is the case from the experimental spectra ([1]).

REFERENCES:

(1) F.ARAMU, T.BRESSANI and P.MANCA: Nuovo Cimento, 51 B, 370 (1967).

(2) D.RAJ, K.CHANDRA and S.P.PURI: Journ. Phys. Soc.Japan, 24, 39 (1968); C.L.HERZENBERG: Nuovo Cimento, 53 B, 516 (1968); R.H.GOODMAN: Mossbauer Effect Methodology, vol. 3 (Ed.I.J.GRUVERMAN) (New York, 1967).

(3) L.PAULING and L.O.BROCKWAY: Zeits. Krist., 82, 188 (1932).

(4) G.DONNAY, L.M.CORLISS, J.D.DONNAY, N.E. ELLIOT and J.M.HASTINGS: Phys.Rev., 112, 1917(1958).

(5) A.A.TEMPERLEY and H.W.LEFEVRE: Journ. Phys. Chem.Solids, 27,85 (1966).

(6) A.H.MUIR and M.WIEDERSICH: Journ.Phys. Chem. Solids, 28, 65 (1967).

(7) W.KERLER and W.NEUWIRTH: Zeits. Phys., 167, 176 (1962); W.KERLER, W.NEUWIRTH,E.FLUCK, P.KUHN and B.ZIMMERMANN: Zeits. Phys., 173, 321(1963); J.F. DUNCAN and R.M.GOLDING: Quart. Rev., 19,36(1965).

(8) R.INGALLS: Phys.Rev., 133, A 787 (1964).

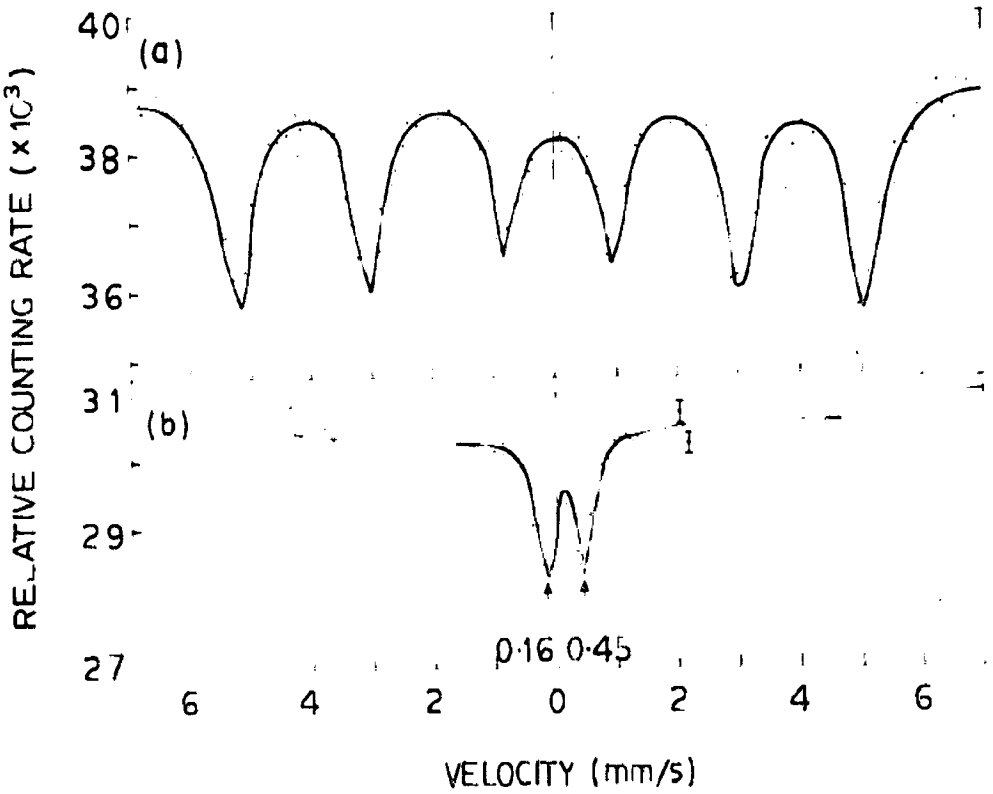

FIG.1 MÖSSBAJER SPECTRA AT ROOM TEMPERATURE OF (a) CHALCOPYRITE ($CuFeS_2$): ^{57}Co(Cu); (b) PYRITE (FeS_2):^{57}Co(Pd)

Published in J.Chem Phys. 50 (1969) 3184.

MOSSBAUER SPECTRA OF TETRAHEDRAL ALKALI DITHIOFERRATES(III)

Deo Raj and S.P.Puri
Department of Physics, University of Roorkee, Roorkee (India)

Mossbauer spectra were taken of a series of compounds, with tetrahedrally coordinated (sp^3) Iron (III), having a general formula $AFeS_2$ where A = Na, Rb, K C_s; over a temperature range 77-300°K. The molar susceptibilities were also examined over the same range of temperatures. The almost temperature independence of ΔE_Q indicates that level separation is larger or $\sim kT$. In contrast to the observations in the case of octahedral compounds, the increasing electronegativity of the cation increases the I.S.value. This is explained by the fact that the decreasing electronegativity of the cation increases the partial 4s character at Iron in the compound. Furthermore it is pointed out that WWJ plot is applicable to the compounds having tetrahedrally bonded (sp^3) iron.

The internal magnetic field in $KFeS_2$ at - 28°C is considered to result not from any magnetic transition but from relaxation effects, whereas in the case of Na, Rb and Cs dithioferrates it is getting averaged to zero.

MÖSSBAUER SPECTRA OF TETRAHEDRAL ALKALI DITHIOFERRATES(III)

INTRODUCTION :

A series of compounds of tetrahedrally coordinated iron (III) having a general formula $AFeS_2$ where the cation A is Na, K, Rb or Cs has been studied by Mössbauer effect. In contrast to the behaviour of high spin Fe(II) octahedral compounds, the Iron (II) compounds in tetrahedral coordination show a markedly greater dependence of quadrupole splitting upon temperature and the isomer shifts are also considerably lower[1]. In order to seek comparison of hyperfine interactions in the case of Iron (III) in tetrahedral coordination and supplement the relatively fewer reports on such iron compounds, such a study was embarked upon.

In the case of $KFeS_2$ and $KFeO_2$, Kerler et al[2] reported that for $KFeS_2$ the magnetic field at the nucleus decreases from 206 killogauss at -145^0 to zero at -28^0C, but for $KFeO_2$ from 515 killogauss at -123^0 only to 400 killogauss at 75^0C. They inferred the existence of a low transition point for $KFeS_2$. A plot of I.S. versus temperature showed a deviation from the otherwise normal and approximately linear relationship and thus indicating the transition at -28^0C for $KFeS_2$. Mössbauer investigation was undertaken to look for similar transitions in the other members of the series with a view to decide the nature of the reported transition in $KFeS_2$.

Furthermore the bearing of the electronegativity of the cation on the isomer shifts in alkaline ferrocyanides[3] and supercomplexes having Iron in octa hedral bonding (d^2sp^3) has been reported[3,4]. A

systematic study of such an effect in the case of compounds with Fe in tetrahedral coordination (sp^3) was considered worthwhile.

STRUCTURE AND EXPERIMENTAL :

$KFeS_2$ grows in paramanganate colored needle shaped monoclinic crystals with space group symmetry C_{2h}^6 with 4 molecules per unit cell[5], having all Fe atoms at equivalent sites. The structure 6) of $RbFeS_2$ is isotopic to $KFeS_2$ whereas $CsFeS_2$ forms orthorhombic crystals with space group D_{2h}^{25} with a tetramolecular unit cell. The crystal structure of $NaFeS_2$ is under investigation[6]. In all these compounds the Iron atoms are principally covalently bonded by nearly regular sulphur tetrahedra. The FeS_2 ions are arranged in chains of FeS_4 tetrahedra linked by their edges with short Fe-Fe distances. In $KFeS_2$ and $RbFeS_2$ both K and Rb are surrounded by 6 sulphur atoms whereas in $CsFeS_2$ Cesium by 8.

The specimens were prepared from A.R. quality chemicals, following the method by Bronger[6]. X-ray diffractographs were taken which did not reveal the presence of any FeS, FeS_2 or any unreacted iron.

The Mössbauer source was a standard Co^{57} in Pd matrix with an initial activity of 1 mC. The spectrometer employed a constant velocity cam, 1 mm NaI(Tl) crystal detector and a single pulse height analyzer. The spectra were recorded for polycrystalline powder absorbers in transmission geometry from the room down to the liquid nitrogen temperature. The lines were fitted by least square analysis on computer, making the

assumption that the line shapes are Lorentzian. The values of I.S., quadrupole splitting and line widths so obtained are given in Table I. The representative spectra for $NaFeS_2$ and $CsFeS_2$ are given in Figs.1 and 2 and the values of ΔE_Q versus temperature for all the compounds are plotted in Fig.3.

The low temperature measurements were taken at Tata Institute of Fundamental Research, Bombay and the cryogenic arrangement employed a cryostat fabricated after the design by Wiedemann et al[7]. Any temperature down to liquid nitrogen could be set within an accuracy of $\pm$ 1°C.

The magnetic susceptibility measurements were carried out for all these compounds over the temperature range 77-300°K. The values of μ_{eff} as calculated from molar susceptibilities are listed in Table II.

DISCUSSION :

Under the influence of the tetrahedral ligand field the five fold degenerate ^6S state of the free Fe (III) ion splits into a lower doublet d_γ, containing the orbitals d_{z^2} and $d_{x^2-y^2}$, and a higher triplet $d\epsilon$, containing d_{xy}, d_{yz} and d_{xz} orbitals. A distortion from the regular tetrahedral symmetry will further lift the degeneracy of the d_γ and $d\epsilon$ orbitals and give rise to quadrupole splitting. From the observation that quadrupole splitting is almost independent of temperature Fig.3, it is inferred that the level separation is larger or $\sim kT$ with the consequence that the electronic population density does not very with temperature.

Furthermore it is observed that the quadrupole splitting decreases with the increase of cationic radius, Fig.4. The bigger cation will normally cause greater distortion of the tetrahedral symmetry and thus enhance the EFG but this being not the case, there are no solid state effects in these compounds. The increased pairing of the d electrons for the Na to Cs compounds, implies an increase in the crystal field and decrease in the EFG contribution from the uncompensated electrons.

It has been reported[3] in the case of a series of alkaline ferrocyanides of the type $M_4[Fe(CN)_6]$ where M=H, Li, Na, K, Rb, Cs, NH_4 that the I.S. decreases with the increase of electronegativity of the cation. This was explained by the assumption that in the ferrocyanide series from H to Cs the last members with the lowest cation electronegativity are the nearest to the ideal diamagnetic structure of Fe - $3d^{10}4s^2 4p^6$ [8]. Assuming that the octahedral configuration (d^2sp^3) is conserved, in the case of the first few members of this series, with more electronegative cation, the lower number of 3d electrons shields 3s and 4s electrons to a lesser degree, whereas for the last members the transition of the electrons from the electronegative cation is more complete with the consequent higher shielding. This increased shielding will cause more positive isomer shift[9]. In the case of present compounds the iron (III) is in tetrahedral coordination ($4s4p^3$) involving no delectrons. The increasing electronegativity of the cation will decrease the 4s electron

density at the Fe nucleus thereby increasing the I.S. value, which is in agreement with the experiment, Fig.5 This conclusion is in contrast to the octahedral case.

The existence of a high transition point for $KFeS_2$ at -28^0 had been shown by Kerler et al[2]. All the other compounds gave only the quadrupole split doublet spectra with no magnetic hyperfine splitting, down to liquid nitrogen temperature. With a view to decide the nature of transition involved in $KFeS_2$, the magnetic susceptibility vs temperature was studied in all these compounds. Our observations do not indicate any magnetic ordering or magnetic transition throughout the range investigated. It has been shown by Brönger[10] that susceptibility is temperature independent over the range 90-500°K. This rules out the possibility of a magnetic transition in $KFeS_2$ and the internal magnetic field is presumably resulting due to relaxation effects[11]. The spin lattice relaxation of paramagnetic ions will give rise to the fluctuating electric and magnetic fields and if the fluctuation rate is rapid compared to the precession frequency of the nucleus, the latter will see a time averaged magnetic field which is zero and hence symmetric quadrupole splitting will be observed. Presumably the internal magnetic field is getting averaged to zero in the case of Na, Rb and Cs dithioferrates.

The total s-electron density at the Fe^{57} nucleus in the compound may be written as the sum of the inner-shell contribution and a fraction $\psi^2_{4s}(0)$ of 4s density arising from the partial occupation of this shell by

electrons from the ligands[12].

$$\psi^2_s(0) = \sum_1^3 \psi^2_{is}(0) + x\,\psi^2_{4s}(0) \qquad (1)$$

The I.S. is related to $\psi^2_s(0)$ by the equation

$$I.S. = \alpha\,\psi^2_s(0) + \text{const.} \qquad (2)$$

where α is a calibration constant. Employing experimental values of I.S. for Fe^{2+} and Fe^{3+} compounds in conjection with the 3d electron densities at the nucleus calculated using Watson free ion wave functions[13], Ingalls[14] obtained the following value of the calibration constant :

$$\alpha = -(0.47 \pm 0.05)\ a_0^3 \text{ mm/sec} \qquad (3)$$

One can write for any of these compounds from (1) and(2)

$$\psi^2_s(0)_{Tet} = \psi^2_s(0)_{Fe^{3+}} + \left[\{(I.S.)_{Tet} - (I.S.)_{Fe^{3+}}\}/\alpha\right] \qquad (4)$$

where $\psi^2_s(0)_{Fe^{3+}} = 11881.4$ a.u. is the total s-electron density for the free-ion $3d^5$ configuration[13] and the $(I.S.)_{Fe^{3+}}$ is 0.41 mm/sec relative to metallic iron[15].

These are covalent compounds with Fe(III) in tetrahedral coordination (sp^3) and no delectron is being used in bonding. The values of 3d electron spin density as calculated from the molar susceptibilities are given in Table II. In the absence of any pairing, these 3d spin densities will also be the respective 3d charge densities responsible for the observed I.S. values.

The values of $\psi^2_s(0)_{Tet}$ may be obtained from Eq.(4) with the experimental I.S. values and are listed in Table II. The $\sum_{i=1}^{3} \psi^2_{is}(0)$ term corresponding to the given number of d electrons is obtained from Watson[13] and so $x\,\psi^2_{4s}(0)$ values are given by equation(1). The contribution $x\,\psi^2_{4s}(0)$ turns out to be negative, which is absurd. This contradicts our assumption about the non-pairing of 3d electrons and points out that rather there is some pairing involved i.e. the number of d electrons responsible for the I.S. value is not equal to that obtained from the μ effective values. It may be remarked that WWJ[12] plot which is generally used to estimate the 4s character for the ionic compounds is also applicable to the compounds having tetrahedrally bonded (sp^3) iron, since no d electrons of the iron atom are used in its bonding to the ligand. This, however, will not hold for iron in octahedral bonding (d^2sp^3). The 4s character of Fe(III) for these compounds from the modified WWJ plot[16] is listed in Table II. This conclusion about a partial pairing of 3d electrons does not contradict the observation about the lack of temperature dependence of ΔE_Q since the latter merely implies that the relative level separation is very large as compared to kT with the consequence that Boltzmann population does not change. The above discussion of partial pairing of 3d electrons is also applicable to the case of Chalcopyrite[17].

The line widths (F.W.H.M.) at different temperatures are included in Table I and are in the range of 3 to 4 Γ_o (Γ_o = natural line width of the 14.4 keV

transition = 0.095 mm/sec). Vignall[18] carried out systematic studies of line widths in the case of Fe^{3+} salts and allowed broadening of 4% resulting from instrumental noise, extraneous vibrations, absorber thickness effects[19] etc. It is therefore concluded that the observed line widths do not indicate any pronounced broadening and the electronic relaxation rates are fast[11]. This view is supported both by the short Fe-Fe distances[10] as well as the observed temperature independent paramagnetism[10].

ACKNOWLEDGEMENTS :

We feel great pleasure to convey our gratitude to Dr. C.R.Kanekar and Dr.P.Fatehally, both of T.I.F.R., (Bombay), for allowing the use of the magnetic susceptibility apparatus and Mössbauer spectrometer for work at liquid nitrogen respectively; to Dr. K.Chandra for his collaboration in the initial stages of the investigation. Furthermore we express our thankfulness to Incharge, Computer Centre, T.I.F.R. for working on CDC 3600.

One of the authors (D.R.) expresses his gratitude to Atomic Energy Commission, Trombay (India) for the award of Senior Research Fellowship.

REFERENCES :

1. P.R.Edwards and C.E.Johnson, J.Chem. Phys.47, No.6,2074-2082(1967).

2. W.Kerler et al, Z.Physik 173, 321-346 (1963).

3. J.Matas and T.Zemick, Phys.Letters 19, 111 (1965).

4. K.Chandra, Deo Raj and S.P.Puri,J.Chem. Phys.46, 1466 (1967).

5. J.W.Boon and C.H.MacGillavry, Rec.Trav. Chim.61 , 910(1942).

6. W.Bronger, Naturwissenschaften, 52(7), 158 (1965).

7. W.Wiedemann, W.A. Mundt and D.Kullmann, Croyogenics 94, April (1965).

8. B.F.Ormont, Struktury neorganicheskikh veshchestv, (GITTL, Moskva 1950) p.203.

9. There is an omission of a negative sign in the I.S. values plotted in Fig.1 in Ref.3.

10. W.Bronger, Z.Anorganische und Allegemeine Chemie 359 , No.5-6, 225 (1968).

11. M.Blume, Phys. Rev. Letters 14(4),96 (1965), 18(9),305(1967)

12. L.R.Walker, G.K.Wertheim and V.Jaccarino, Phys.Rev.Letters 6, 98 (1961).

13. R.E.Watson, Technical Report No.12,Solid State and Molecular Theory Group, MIT (Unpublished); Phys.Rev.119, 1934 (1960).

14. R.Ingalls, Phys.Rev.135, No.2, 157(1967).

15. S.D.Benedetti,G.Lang and R.Ingalls,Phys. Rev.Letters 6, 60 (1961).

16. J.Danon, Technical Report Series No.50, (International Atomic Energy Agency, Vienna,1966).

17. Deo Raj, K.Chandra and S.P.Puri, J.Phys. Soc. Jap.24, 39 (1968).

18. J.W.G. Wignall, J.Chem.Phys. 44 , No.6, 2462 (1966).

19. S.Margulies and J.P.Ehrman,Nucl.Instr. Methods 12, 131 (1961),

TABLE I

Values of I.S., ΔE_Q and line widths for alkali dithioferrates (III). The values of I.S. are relative to iron.

Compound	Temperature ^oK	Isomer shift mm/sec.	Quadrupole splitting mm/sec.	Line width, and , mm/sec.	
$NaFeS_2$	295	0.36	0.58	0.35	0.35
	253	0.37	0.57	0.36	0.36
	195	0.39	0.59	0.40	0.40
	140	0.46	0.59	0.38	0.41
	77	0.48	0.59	0.47	0.45
$KFeS_2$	295	0.19	0.53	0.30	0.30
	253	0.21	0.53	0.40	0.40
$RbFeS_2$	295	0.19	0.45	0.30	0.30
	253	0.19	0.47	0.35	0.35
	195	0.27	0.48	0.40	0.40
$CsFeS_2$	295	0.18	0.46	0.30	0.30
	253	0.19	0.46	0.32	0.32
	195	0.25	0.46	0.32	0.32
	140	0.27	0.46	0.30	0.30
	77	0.29	0.47	0.44	0.42

The errors in the values of I.S., Q.S. and line width (assuming a Lorentzian profil) are $\pm$ 0.02 mm/sec.

TABLE II

Values of μ_{eff}, no. of unpaired 3d electrons, total s-electron density and 4s character in alkali dithioferrates.

No.	Compound	μ_{eff}	No. of unpaired d electrons	I.S. Values (mm/sec)	$\psi^2_s(0)$ (a.u.)	% 4s character (approx.)
1	$NaFeS_2$	4.65	3.77	0.355	11881.50	25
2	$KFeS_2$	4.61	3.72	0.190	11881.85	35
3	$RbFeS_2$	-	-	0.185	11881.86	36
4	$CsFeS_2$	4.38	3.49	0.175	11881.88	38

CAPTIONS OF THE DIAGRAMS

Fig.1 Mössbauer spectra for $NaFeS_2$ at; (a) room temperature (b) 77°K (The source used is Co^{57} in Pd matrix and the points plotted on the curves are the least Sq.ft. values corresponding to the experimentally observed values).

Fig.2 Mössbauer spectra for $CsFeS_2$ at; (a) room temperature (b) 77°K (The source used is Co^{57} in Pd matrix and the points plotted on the curves are the least Sq.ft. values corresponding to the experimentally observed values).

Fig.3 Quadrupole splitting versus temperature.

Fig.4 Quadrupole splitting versus cationic radius.

Fig.5 I.S.versus electronegativity of the alkali cation.

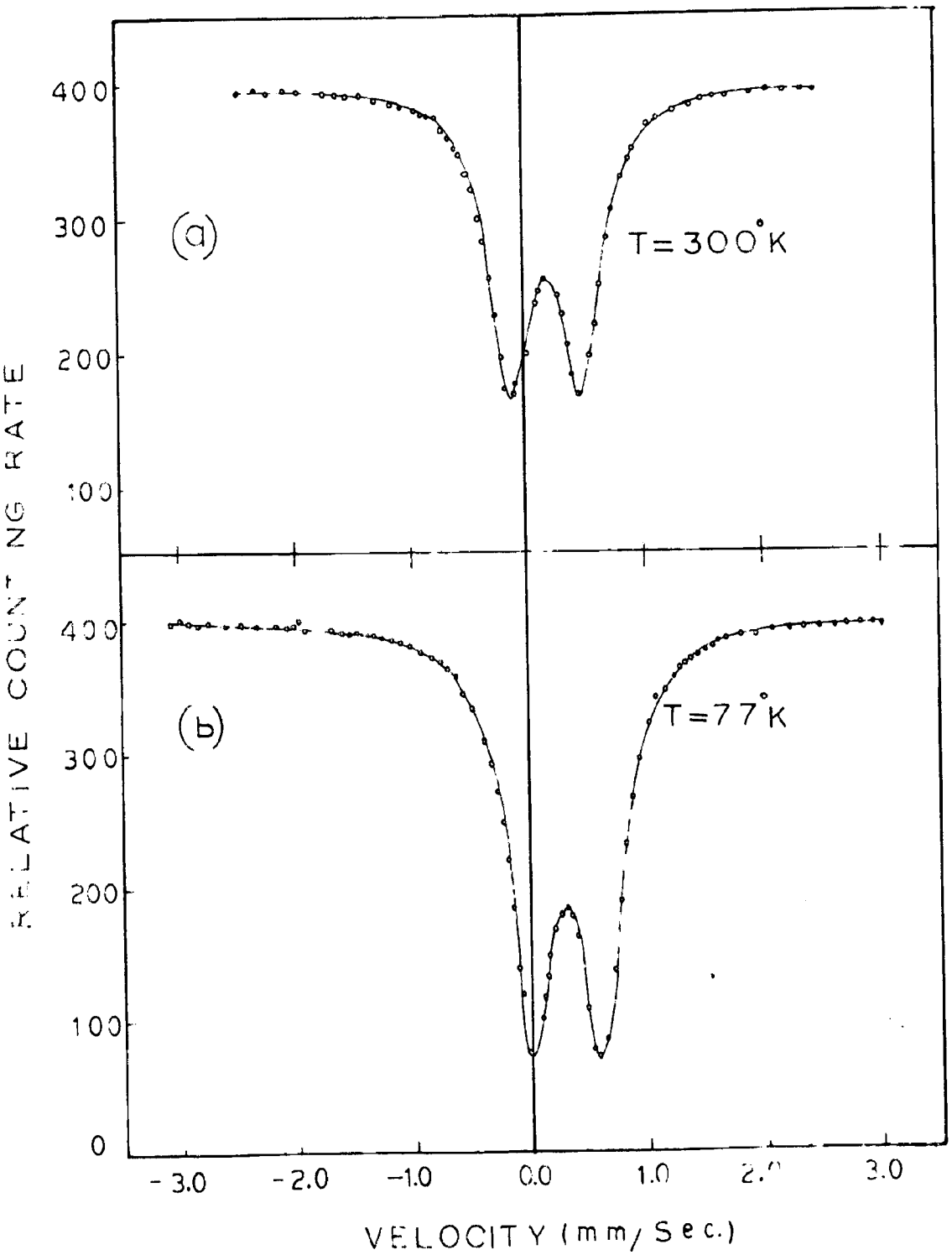

FIG. 1 LEAST SQUARE FIT MÖSSBAUER SPECTRA FOR Na Fe S_2 (a) AT ROOM TEMPERATURE (b) AT 77°K

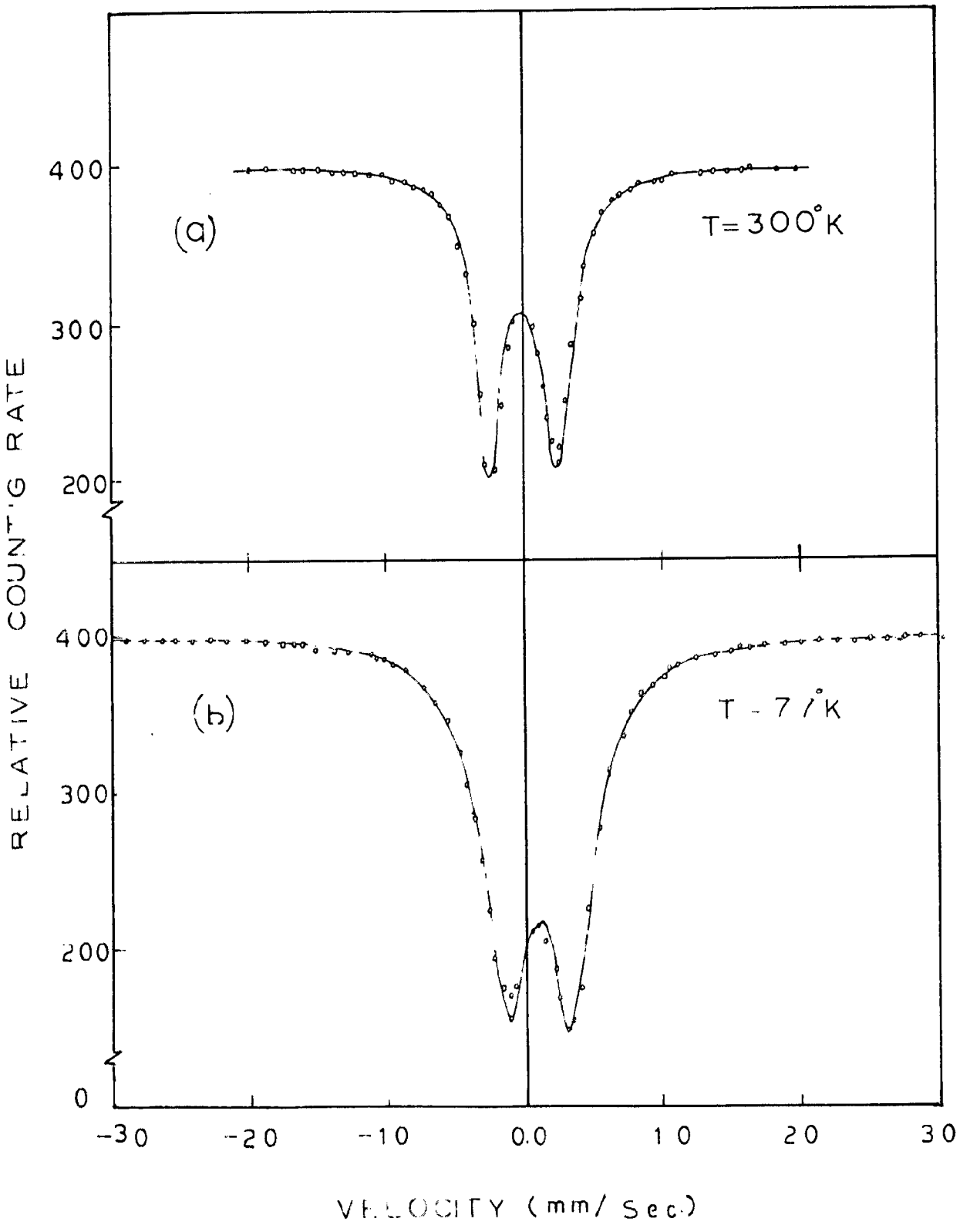

FIG. 2 LEAST SQUARE FIT MÖSSBAUER SPECTRA FOR $CsFeS_2$ (a) AT ROOM TEMPERATURE (b) AT 77°K.

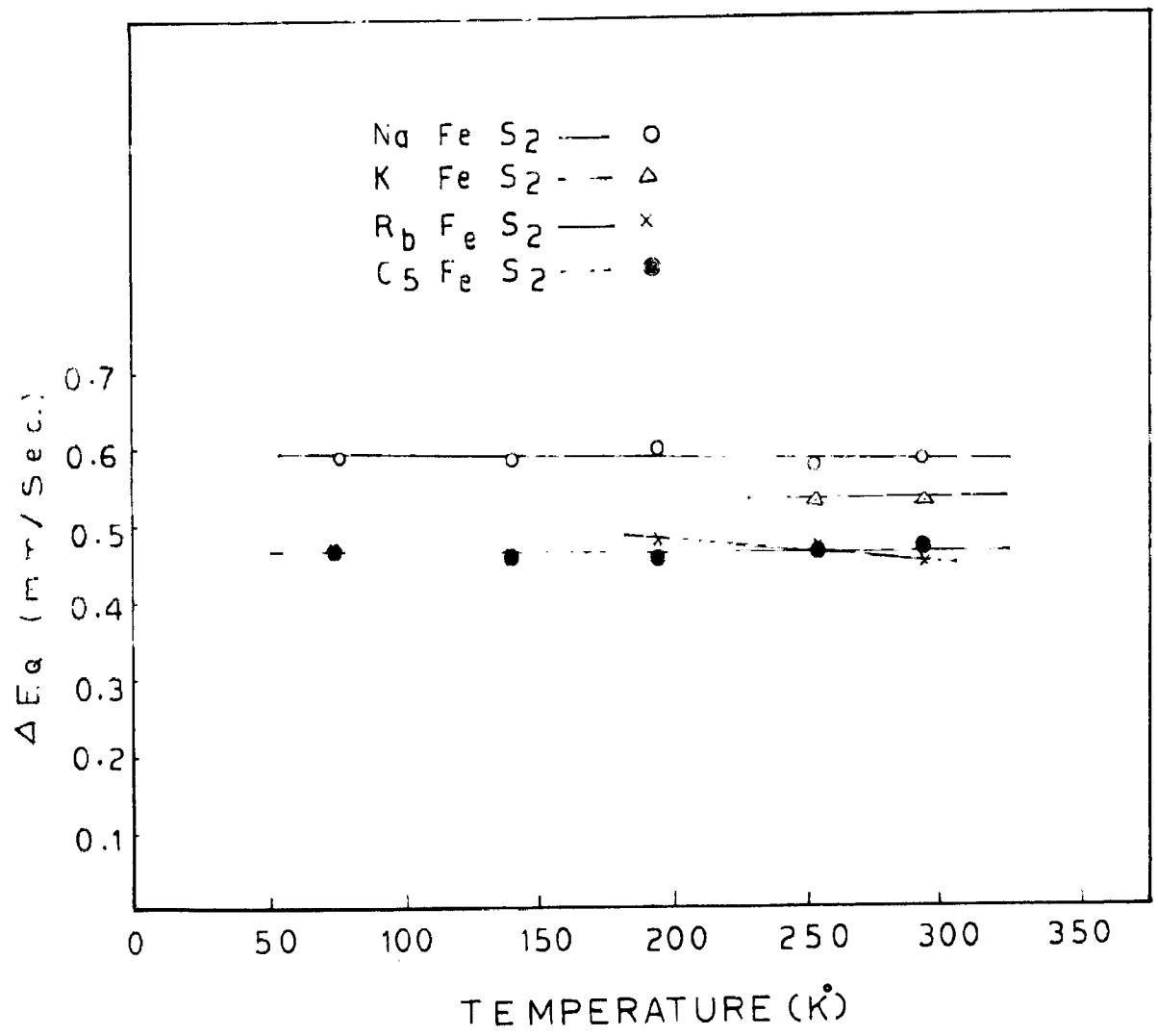

FIG 3 : QUADRUPOLE SPLITTING VERSUS TEMPERATURE.

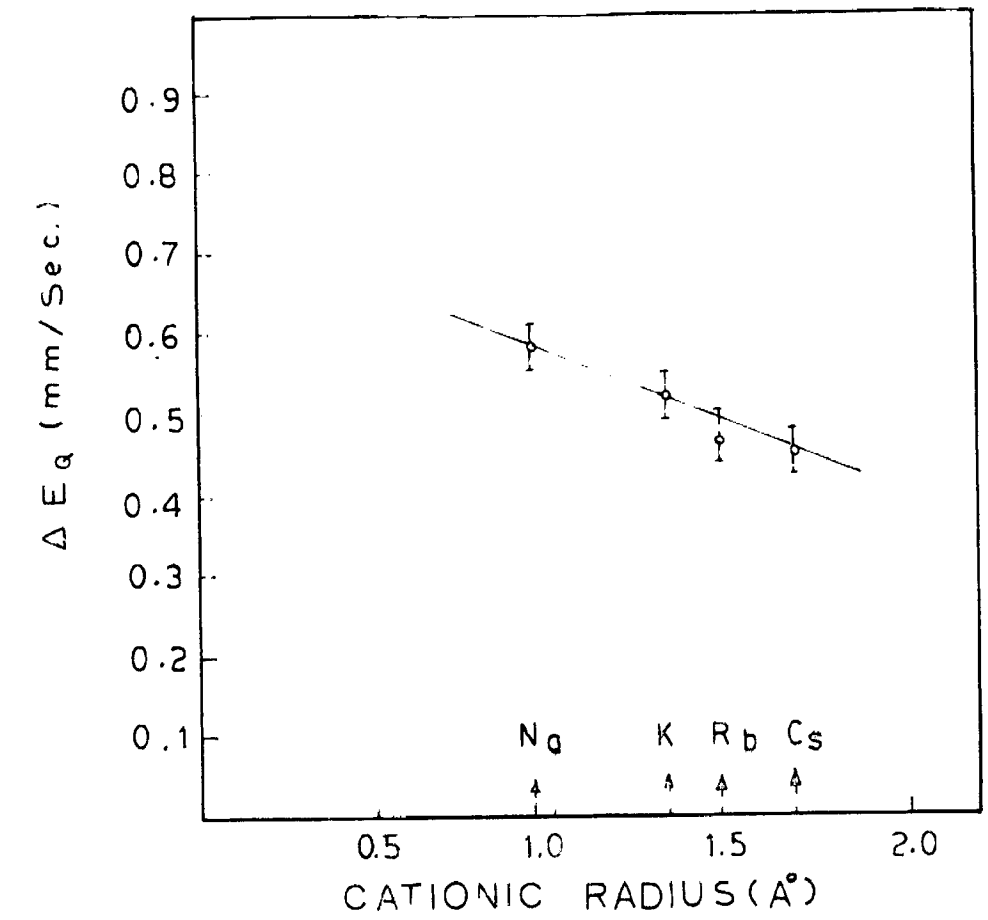

FIG. 4 QUARDRUPOLE SPLITTING VERSUS CATONIC RADIUS.

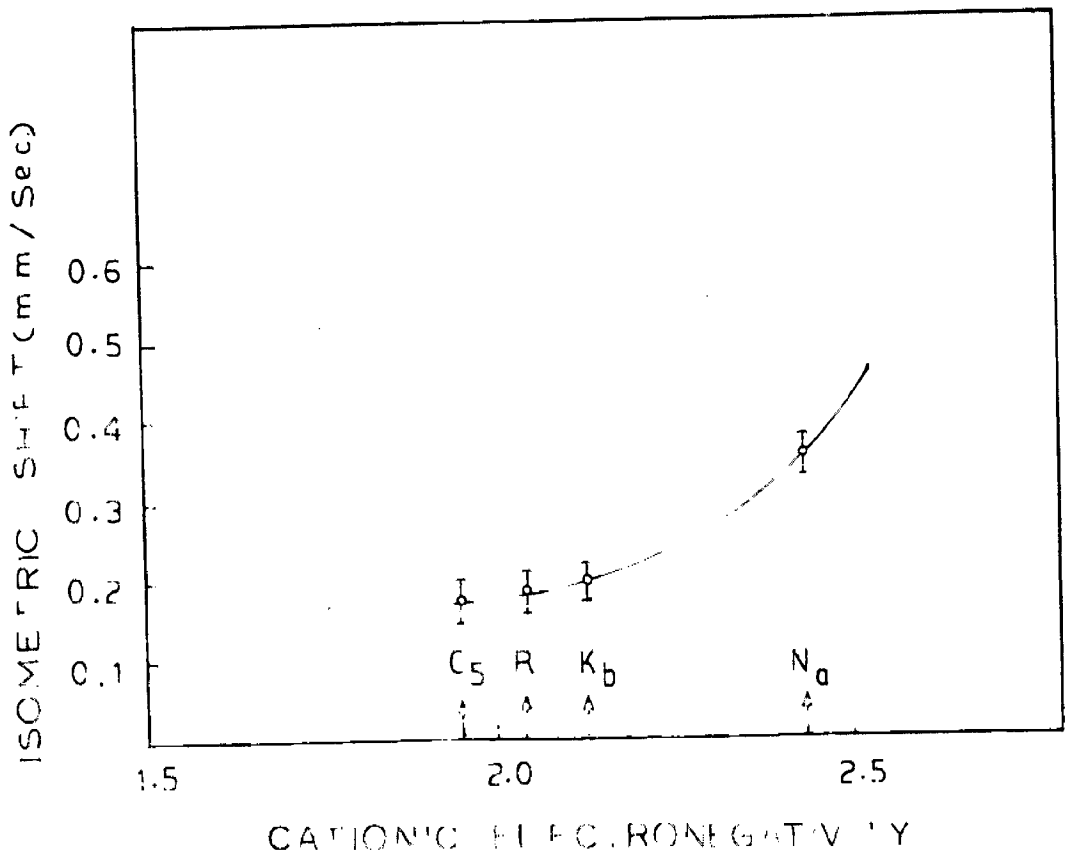

FIG. 5 [illegible] VERSUS ELECTRONEGATIVITY OF THE ALKALI

Published in Phys.Letters
Vol.30(A),July'69

RECOILLESS FRACTION AND THERMAL SHIFT OF W^{182} AND W^{183}

Deo Raj and S.P.Puri
Physics Department, Roorkee University, Roorkee (India)

The recoilless fractions of W^{182} and W^{183} are calculated over the temperature range 4-300 °K on the basis of experimentally determined phonon frequency distribution function as well as the one on Krebs' model. There is reasonable agreement between the experimental values and calculations. In addition, the thermal shift values for these isotopes, have also been computed.

Recoilless emission and absorption of gamma radiation from the 46.5 keV ($\frac{3^-}{2}$) first excited state of W^{183} has been investigated by a host of workers [1-6]. Furthermore the 100.09 keV state of W^{182} has also been studied by Mossbauer technique [1,7-8]. Sumbaev et al.[1] assuming the conventional Debye approximation obtained $\theta_W = 320 \pm \frac{70}{40}$ °K which is the same as obtained from other data [9].

Chen and Brockhouse [10] measured the phonon dispersion relations for Tungsten from the momentum and energy changes in the inelastic scattering of slow neutrons. They also calculated the phonon frequency distribution function (p.f.d.f.) using the 23 force constants obtained from the 8th. neighbour best fit [11]. In addition, the calculations based on Krebs' model of p.f.d.f. for Tungsten including the third nearest neighbour central force interactions [12] have also been reported. The probability for the Mossbauer effect and the temperature shift like the specific heat are integral quantities in the phonon spectrum but the temperature dependence of the latter is governed by a different moment of the p.f.d.f., favoring the higher frequencies.

On the contrary the spectral density of the squared displacement of the radiating (or absorbing) nucleus is determined mainly by the low frequency portion of the phonon spectrum and the temperature independent zero point vibrations. The experimentally determined phonon spectrum [11] was used to calculate the recoilless fraction f, and second order Doppler shift (S.O.D.) over the temperature range 4-300°K. These were repeated for the phonon spectrum calculated on Krebs' model [12] for the sake of comparison.

Tungsten has a B.C.C. lattice and for a monoatomic lattice of cubic symmetry, the f and S.O.D. are

$$f=\exp\left[-\frac{E^2}{2Mc^2k}\cdot\frac{1}{3N}\int_0^{\omega_{max}}\frac{g(\omega)}{\omega}\cdot\coth\left(\frac{k\omega}{2k_BT}\right)d\omega\right]$$

and $$\text{S.O.D.} = \frac{3k}{4Mc}\cdot\frac{1}{3N}\int_0^{\omega_{max}} g(\omega)\coth\left(\frac{k\omega}{2k_BT}\right)d\omega$$

where $g(\omega)$ is the phonon frequency distribution function; 3N is the normalizing factor; M is the mass of the gamma-ray emitting (or absorbing) nucleus, E is the γ-ray energy. The calculated values of f and S.O.D. using the $g(\omega)$ of ref [11] are shown in Table I.

The f for 100.09 keV γ-ray of W^{182} was measured with a source of metallic Tantalum irradiated with thermal neutrons and an an absorber of a foil of metallic Tungsten and its value is $f = 0.083^{+0.060}_{-0.030}$ at 101°K [1] It compares with our calculated value of f = 0.093 within experimental error. The recoil free fraction for 46.5 keV γ-ray of W^{183} was investigated by Mossbauer technique in small Tungsten particles[13] They obtained f (77°K) = 0.57 for the microcrystals

with average diameter of 30 ^{o}A and f (77°K) = 0.61 for the 1 micron powder (large crystals). These are the only available experimental values and are stated to be within ± 20% accuracy. Our calculated value of f (77°K) = 0.64 for 46.5 keV transition in W^{183} agrees reasonably with the experimental one. The corresponding Krebs' model values of f (101 °K) = 0.120 for W^{182} f (77°K) = 0.67 for W^{183} are slightly higher than the ones from experimental g( ).

Hardy et al 6 also investigated the Mossbauer effect by populating the 46.5 keV level of W^{183} by Coulomb excitation and obtained f_s (77°K) = 0.10±0.02 for the source. The reduced recoilless fraction in Coulomb excited Mossbauer target was explained by the author on the lines suggested by Czjzek et al 14 . This only confirms that the method of preparation of the source has a marked bearing on f values 15,16 . No experimental observations are available for thermal shifts (S.O.D.) for any of the Tungsten isotopes for comparison.

Table 1: The calculated values of Mössbauer Recoilless fraction and thermal shifts in W^{182} and W^{183} at various temperatures

Temperature °K	W^{182}		W^{183}	
	f	S.O.D x 10^{-2} (cm/sec)	f	S.O.D. x 10^{-2} (cm/sec)
4.0	0.19988297	0.26340527	0.70803498	0.26196590
20.0	0.19519240	0.26355631	0.70443864	0.26211611
50.0	0.16688647	0.27082151	0.68116439	0.26934161
77.0	0.12695323	0.29403058	0.64236327	0.29242385
101.0	0.09277151	0.32578657	0.60057467	0.32400631
150.0	0.04395213	0.40891745	0.51167425	0.40668293
195.0	0.02080835	0.49628793	0.43586711	0.49357597
200.0	0.01911011	0.50637037	0.42798161	0.50360332
250.0	0.00804138	0.60981707	0.35547430	0.60648474
293.0	0.00376596	0.70140211	0.30210510	0.69756930
300.0	0.00332564	0.71646854	0.29415624	0.71255341

REFERENCES

1. O.I.Sumbacv, A.I. Smirnov and V.S.Zykov, Soviet Physics JETP 15 (1962) 92.

2. M.Drosg and E.Ujlaki, Acta Phys. Austriaca, 20 (1965) 171.

3. M.Drosg and E.Ujlaki, Acta Phys. Austriaca, 23 (1966) 47 .

4. N.Shikazono, H.Takekoshi and T. Shoji, J.Phys.Soc. Japan 21 (1966) 829.

5. D.Agresti, E.Kankeleit and B.Persson, Phys. Rev.155 (1967). 1342.

6. K.A.Hardy, D.C.Russel and R.M.Wilenzick, Phys.Letters 27A (1968) 422.

7. A.Bussiere De Nercy, M.Langewn and M.Spighel, Compt. Rend. 250 (1960) 1031.

8. L.L.Lee, L. Meyer-Schutzmeister, J.P.Schiffer and D.Vincent, Physics Rev. Letters 3 (1959) 223.

9. J.S.Kasper and K. Lousdale, eds. International tables of X-ray crystallography, Vol.III (The Knock Press, Birmingham, 1959).

10. S.H.Chem. and B.N.Brockhouse, Solid State Comm.2 No.3 (1964) 73.

11. S.H.Chen, Ph.D. thesis (1964), McMaster University (unpublished) Private communication from Prof.B.N. Brockhouse.

12. P.S.Mahesh and B.Dayal, Phys.Rev. 143 (1966) 443.

13. S.Roth and E.M.Horl, Phys. Letters 25A (1967) 299.

14. G.Czjek, J.L.C. Ford Jr., F.E.Obenshain and D.Seyboth, Phys. Letters 19 (1966) 673.

15. J.G.Mullen, Phys. Letters 15 (1965) 15.

16. Deo Raj and S.P.Puri, Phys. Stat. Solidi (In press).

Published in Phys. Stat. Sol. Vol. 34
No. 1 July 1, '69

RECOILLESS FRACTION AND THERMAL SHIFT FOR 29.4 keV TRANSITION IN REACTION PRODUCED K^{40}

Deo Raj and S.P.Puri,
Physics Department, University of Roorkee, Roorkee
(India)

The Mössbauer investigations of 29.4 keV γ-ray of K^{40} have been reported by three groups who produced the isotope by (n, γ) (1,2) and (d,p) (3) nuclear reactions. The recoilless fraction f measured at $4^{o}K$ for potassium used as source is 3.6% (1). The Debye temperature $\theta_f = 60^{o}K$ and $\theta_D = 98^{o}K$ were derived from experimental values of f and specific heat data respectively and it was inferred that thermal neutron beam does not cause target heating and the (n, γ) reaction does not substantially diminish the recoil free fraction in insulators or metals (1). In connection with the lattice dynamical studies from Mössbauer effect it was pointed out that estimates of mean square displacements at room temperatures in sources or absorbers, based on Debye temperatures from specific heat measurements and using the Debye model for the phonon frequency, should not be taken too seriously (4,5). This is due to the reason that $\langle x^2 \rangle$ and the lattice specific heat are determined by different weighted averages over the frequency spectrum. In view of the availability of the theoretical phonon frequency distribution functions for potassium, it was decided to have an estimate of the reduction of f by the method of formation of the source. Moreover the thermal shift S.O.D. values are calculated over the range $2-28^{o}K$.

Cowley et al.(6) measured the dispersion curves of potassium at 9°K by inelastic neutron scattering technique, and the measured normal mode frequencies have been analyzed by fitting them to a Born-Von Karman model (7). The interatomic force constants (in real space) between near neighbour atoms were employed to calculate the density of phonon states $g(\omega)$ and thermodynamic properties such as the heat capacity. The equivalent Debye temperature obtained from the calculated and observed heat capacity (8) agree to better than 2% over the range 0 to 30°K. Furthermore the frequency distribution function for potassium calculated on de Launay's model (9) was employed to calculate the f and S.O.D. values. However it may be stated that the agreement between the theoretical and experimental values of C_v(9) has been found to be very good down to 10°K and at lower temperatures the deviations were ascribed to the presence of phase transformation.

Potassium has a b.c.c. lattice and for a monatomic lattice of cubic symmetry, the f and S.O.D. are

$$f = \exp\left[-\frac{E_\gamma^2}{2Mc^2\hbar}\,\frac{1}{3N}\int_0^{\omega_{max}}\frac{g(\omega)}{\omega}\coth\left(\frac{\hbar\omega}{2k_BT}\right)d\omega\right]$$

$$\text{and S.O.D.} = \frac{3\hbar}{4Mc}\,\frac{1}{3N}\int_0^{\omega_{max}} g(\omega)\omega\coth\left(\frac{\hbar\omega}{2k_BT}\right)d\omega$$

where $g(\omega)$ is the frequency distribution function; 3N is a normalising factor; M is the mass of the γ-ray recoiling nucleus; E_γ is the γ-ray energy. The frequency distribution functions $g(\omega)$ calculated by Cowley et al (6) and Dayal and Sharan (9) have been used in evaluating f and S.O.D. The values are tabulated in Table.I.

Hafemeister and Shera (10) by extending Lang's (11) calculation of absorption areas to large values of absorber thickness, obtained f = 0.036 for potassium used as source at 4°K. However in the absence of an experimental measurement of internal conversion coefficient of the 29.4 keV transition, they used α = 0.35 derived from Rose (12) for a pure M1 transition and due to this uncertainty, no errors were assinged to the value of f. Our calculated values of f(4°K) = 0.1039 (using the $g(\omega)$ values from Ref.(6)) and f(4°K) = 0.0773 (using the $g(\omega)$ from Ref.(9)) are higher than the experimental value. The values of θ_f from the theoretical values of f are 89°K and 79°K from references 6 and 9 respectively. We will prefer the value of f = 0.1039 due to the better agreement of predictions of this model (6) with the specific heat data.

The disagreement between the observed and theoretical values is not surprising (13,14) keeping in view that the formation of the 29.4 keV level is preceeded by the emission of energetic photons and leaves the K^{40} nucleus with a distribution of recoil energies upto a maximum of 800 eV. Alternatively it may be argued that the heat generated by the slowing down of the recoiling excited nucleus causes local, heating. It is estimated that the temperature due to recoil heat is around 20°K, at which the theoretical value of f(6) equals the experimental value . Further, it may be stated that contrary to the conclusion of Hafemeister and Shera (1) the (n,γ) reactions do cause substantial reduction of the recoil free fraction, Such a reduction of f is also obtained

for Ni^{61} produced by (p,α) reaction (15). No experimental observations of thermal shift of K^{40} are available at present.

Table 1 : The calculated values of Mossbauer fractions and thermal shifts of 29.4 keV K^{40}.

T (^{o}K)	with g(ω) of Cowley, Woods and Dolling (Ref.6)		with g(ω) of Dayal and Sharan (Ref.9)	
	f	S.O.D. x102 cm/sec	f	S.O.D. x 10^{2} cm/sec.
2	0.11016	0.38724	0.08570	0.37035
4	0.10390	0.38730	0.07727	0.37054
6	0.09651	0.38763	0.06699	0.37111
8	0.08820	0.38850	0.05645	0.37234
10	0.07928	0.39021	0.04649	0.37446
12	0.07020	0.39293	0.03758	0.37762
14	0.06132	0.39678	0.02990	0.38195
16	0.05294	0.40184	0.02347	0.38752
18	0.04524	0.40810	0.01822	0.39431
20	0.03833	0.41554	0.01401	0.40228
22	0.03222	0.42410	0.01069	0.41137
24	0.02691	0.43370	0.00809	0.42150
26	0.02235	0.44426	0.00609	0.43256
28	0.01847	0.45569	0.00456	0.44447

REFERENCES

1. D.W.Hafemeister and E.B.Shera, Phys.Rev.Letters 14 593 (1965); Mössbauer Effect Methodology Vol.3. Ed. Irwin J. Gruverman (Plenum Press New York) 231(1967).

2. P.K. Tseng, S.L.Ruby and D.H.Vincent, Phys.Rev.172 (2), 249 (1968).

3. S.L.Ruby and R.E.Holland, Phys.Rev. Letters 14 591 (1965).

4. H. Frauenfelder, The Mössbauer Effect (W.A.Benjamin, New York, 1962).

5. A.J.F.Boyle and H.E.Hall, Rept.Progr.Phys.25, 441 (1962).

6. R.A.Cowley, A.D.B.Woods and G. Dolling, Phys. Rev. 150(2)487 (1966).

7. M.Born and K.Huang, Dynamical Theory of Crystal Lattices (Clarendon Press, Oxford, England, 1954).

8. D.L. Martin, Phys. Rev. 139, A150 (1965).

9. B.Dayal and B.Sharan, Proc. Roy. Soc. A262, 136 (1961)

10. D.W.Hafemeister and E.B.Shera, Nucl.Instr.Methods 41, 133 (1966).

11. G. Lang, Nucl.Instr. Methods 24, 425 (1963).

12. M.E.Rose, Internal Conversion coefficients (North-Holland Publishing Company, Amsterdam, 1958).

13. G.Czjzek, J.L.C.Ford Jr., F.E.Obenshain and D.Seyboth, Phys. Letters 19, 673 (1966).

14. K.A. Hardy, D.C.Russel and R.M.Wilenzick, Phys. letters 27A, 422 (1968).

15. Deo Raj and S.P.Puri (to be published)

Published in Phys.Soc.Japan Vol.27(1969) August/September

MÖSSBAUER FRACTION AND THERMAL SHIFT FOR 67.4 Kev γ-ray in Ni^{61}

Deo Raj and S.P.Puri,
Department of Physics, University of Roorkee, Roorkee (India)

The Debye-Waller factor f of Ni^{61} was calculated by Gleiss[1] in harmonic approximation, employing the moments of the lattice frequency spectrum both calculated from the two neighbour lattice model as well as from the experimental values of specific heat. It was claimed that the calculations agree with the experimental values within the accuracy of the measurements. The extraction of values of f by assuming that $f_{abs} \sim f_{source}$[2] varies approximately as f^2 for Ni^{61} in Ni^{61} host, is however not free from objection; when the source is reaction produced.[3] In the event of directly available experimental $g(\omega)$ curve[4] for Ni from inelastic Neutron scattering, it is advisable to use this as a basis of calculation rather than model calculations or the moments from the specific heat data; since the $\langle x^2 \rangle$ and the lattice specific heat are determined by different weighted averages over the frequency spectrum.

Nickel is a fcc lattice and the recoilless fraction f and second order Doppler shift, D.O.D., are given by the expressions

$$f = \exp\left[- \frac{E_\gamma^2}{2Mc^2} \frac{1}{3N} \int_0^{\omega_{max}} \frac{g(\omega)}{\omega} \coth\left(\frac{\hbar\omega}{2k_BT}\right) d\omega \right]$$

and $$S.O.D. = \frac{3\hbar}{4Mc} \frac{1}{3N} \int_0^{\omega_{max}} g(\omega) \coth\left(\frac{\hbar\omega}{2k_BT}\right) d\omega$$

respectively; where the symbols have their usual meanings. The calculated values are given in Table I, after applying

the mass correction; which was considered necesary since the $g(\omega)$ curve is for natural Ni (average atomic wt. 58.7) whereas we require it for Ni^{61}. Taking account of the mass dependence of frequency from the harmonic theory; the ω in the above formulae was replaced, in first approximation, by $\omega(61) = \omega(58.7)\left(\frac{58.7}{61}\right)^{\frac{1}{2}}$. The value of f_{source}, Table I, was extracted from the measured value of f_{source}, $f_{abs.}$[3] by assuming that $f_{calc.} = f_{abs.}$ The value of f_{source} so obtained are consistently lower than the $f_{calc.}$, pointing thereby that the (p,α) reaction causes substantial reduction of the recoil free fraction. The calculated value of parameter B = 0.30±0.008 at 300°K in the Debye-Waller factor[5] compoares with our calculations of B = 0.359 at 300°K, this discrepancy of 5% is not unexpected since two different $g(\omega)$ curves have been employed. No experimental observations of thermal shift of Ni^{61} are available at present.

REFERENCES :

1) R.Gleiss: Phys.Stat. Sol.17 (1966) 761.

2) F.E.Obenshain and H.H.F. Wegener: Phys. Rev. 121(1961) 1344.

3) Deo Raj and S.P.Puri: Phys. Stat. Sol. 34(July,1969); G.Czjzek et al. Phys. Letters 19(1966) 673.

4) N.A. Tschernoplekov et al; Soviet Phys. - JETP 17 (1963) 585.

5) H.W.T. Barron and T.Smith: J.Phys. Chem. Solids 27 (1966) 1951.

TABLE I. The temperature dependence of $f_{calc.}$ f_{source} and S.O.D. for Ni^{61} (67.4 keV transition).

Temperature ^{o}K	$f_{calc.}$	f_{source}	S.O.D. (cm/sec.
83	0.139471	0.054084	0.011736
92	0.128728	0.051979	0.011967
101	0.118134	0.047791	0.012233
109	0.108993	0.047393	0.012496
117	0.100211	0.047296	0.012781
123	0.093901	0.039340	0.013010
130	0.086870	0.044391	0.013289
134	0.083018	0.033770	0.013456
141	0.076577	0.032460	0.013756
146	0.072213	0.019090	0.013978
157	0.063300	0.018841	0.014486
172	0.052627	0.010742	0.015216

Phys.Letters(Communicated)

EVIDENCE OF FORCE CONSTANT CHANGE FROM MÖSSBAUER FRACTION OF Sn^{119} IN VANADIUM

DEO RAJ and S.P.PURI
Department of Physics, University of Roorkee, Roorkee (India)

Reanalysis of the V: Sn^{119} Mössbauer system has been carried out to seek evidence for the force constant change. It turns out that the force constant ratio, λ'/λ is about 1.67; contrary to the conclusion of Bryukhanov et al.

When a Mossbauer atom with atomic mass M' is introduced as an impurity into the Debye type crystal lattice composed of atoms with the atomic masses M; the change in mass at the defect site and the change in the force constant for the impurity-host atoms will influence the mean square displacement $\langle x^2 \rangle$ of the impurity atom. This is turn will influence the recoilless fraction of Mössbauer radiation and its temperature dependence.[1] The Debye-Waller factors for the 14.4 keV γ-rays of Fe^{57} atoms as a dilute impurity have been measured at constant temperature for different crystal lattices.[2] Further the temperature dependence of the recoilless fraction, f for Fe^{57} introduced into a definite crystal lattice has been reported over a wide temperature range[3,4]. Both these measurements were considered to be consistent with the calculations of Visscher[5] and Maradudin and Flinn[6] and both the groups inferred independently that the impurity-host coupling constant is about the same as the host-host coupling constant.

Bryukhanov et al[7] from similar studies of f and its temperature dependence for Sn^{119} atom introduced into Vanadium, Thallium, Gold and Platinum and their

comparison with the calculations of Kagan and Iosilevskii[8] could claim satisfactory fit, obtained by ignoring the force constant change. Mannheim[9] derived closed expression for $\langle x^2 \rangle$ for the central force bcc cubic crystal model, in which there are changes in the nearest forces around the defect site inaddition to the change in mass at the impurity site. By analysing the temperature dependence of f for the V: Fe^{57} Mössbauer system, Mannheim and Simopoulos[10] obtained a good fit to the experimental data for an increase in force constant ratio of about 2.5. We undertook the reanalysis of the V: Sn^{119} system for any change in the force constant in the light of above facts for the V: Fe^{57} system, making use of the experimental $g(\omega)$ curve for Vanadium[11].

Sn^{119} is an impurity in the bcc Vanadium lattice considering the changes in forces between the defect and its 8 nearest neighbour host atoms in the harmonic approximation Mannheim[9] derived the following expression for $\langle x^2 \rangle$ for the central forces only

$$x^2 = \frac{\hbar}{2M}\left(\frac{M}{M'}\right)^2 \int_0^{\omega_{max}} \frac{\coth(1/2\,\hbar\beta\omega)\,g(\omega)\,d\omega}{\omega\left\{\left[1+\rho(\omega)S(\omega)\right]^2 + 1/4\,\pi^2\omega^2 g^2(\omega)\right\}}$$

$$+ \frac{\hbar}{2M}\left(\frac{M}{M'}\right)^2 \frac{\coth(1/2\,\hbar\beta\omega_L)}{\omega_L}\left[\rho^2(\omega_L)\,T(\omega_L) + \frac{M}{M'} - \left[1+\rho(\omega_L)\right]^2\right]^{-1}$$

where $\beta = \frac{1}{kT}$ and the functions $\rho(\omega)$, $S(\omega)$, $T(\omega)$ are defined in Ref.(9), M and M′ are the masses of Vanadium and Sn^{119} atoms respectively. The second expression contributes only if there is a localized mode with frequency and the localized modes are obtained if

$$1+\rho(\omega)\;S\;(\omega) = 0$$

The calculated values of f over a temperature range

20-700°K, for a set of values of the force-constant ratio $\frac{\lambda'}{\lambda}$; are shown in Fig.1 alongwith the experimental absolute values of f.[12] It appears that the value of $\frac{\lambda'}{\lambda}$ about 1.67 gives the best fit to the data within the accuracy of the observations, while a good fit can be obtained for $\frac{\lambda'}{\lambda}$ from 1.4 to 2.0. The position of the localized mode is at = 2.86 x 10^{13} cycles/sec and its contribution to f (corresponding to $\frac{\lambda'}{\lambda}$ = 1.67) varies from 1.6% at 50°K to 8.4% at 600°K and is included in the curve. In view of the large experimental errors in f, no attempt was made to account for anharmonicity at high temp ratures. In the model independent classical limit, we calculated the value of f at 663°K from the first term of the formula given by Maradudin and Flinn[6], neglecting the other terms containing $\frac{\lambda'}{\lambda}$; and it gives f = 0.171. This value is lower than the experimental value of 0.186 and corroborates the necessity for $\frac{\lambda'}{\lambda}$ to be greater than 1. This evidence for change of force constant in V: Sn^{119} system seems plausible and does not substantiate the conclusion of Bryukhanov et al.[7] This conclusion is augented by similar analysis carried out in W: Fe^{57} and Mo: Fe^{57} systems.[13]

REFERENCES :

1. A.A.Maradudin, Solid State Physics, edited by F.Seitz and D.Turnbull (Academic Press Inc., New-York, 1966), Vol.18, p.273.

2. J.Bara and A.Z.Hrynkiewicz, Phys.Stat.Sol. 15, 205(1966).

3. J.Bara, H.U.Cholewa, A.Z.Hrykiewicz and T. Matlak, Report No.459/PL(Feb.1966).

4. M.A.Steyert and R.D.Taylor, Phys. Rev.134

3A, 1716(1964).

5. W.M.Visscher, Phys. Rev. 129, 28(1963).

6. A.A.Maradudin and P.A.Flinn, Phys. Rev.126 2059 (1962).

7. V.A.Bryukhanov, N.N.Debyagin and Yu Kagan, Soviet Physics JETP 18, 945 (1964); ibid 19, 563(1964).

8. Yu Kagan and Ya A. Iosilevskii, Soviet Physics JETP 15, 182 (1962); ibid 17, 195 (1963).

9. Philip D. Mannheim, Phys.Rev. 165, No.3 1011 (1968).

10. Philip D. Mannheim and A.Simopoulos, Phys. Rev. 165, No.3, 845, (1968).

11. C.M.Eisenhauer, I.Pelah, D.J.Hughes, and H. Palevsky, Phys. Rev. 109, 1046 (1958).

12. Private communication from N.N.Delyagin.

13. Deo Raj and S.P.Puri, (unpublished).

CAPTION :

Fig.1: Temperature dependence of Mossbauer Fraction of Sn^{119} in Vanadium for different values of foreeconstant ratio.

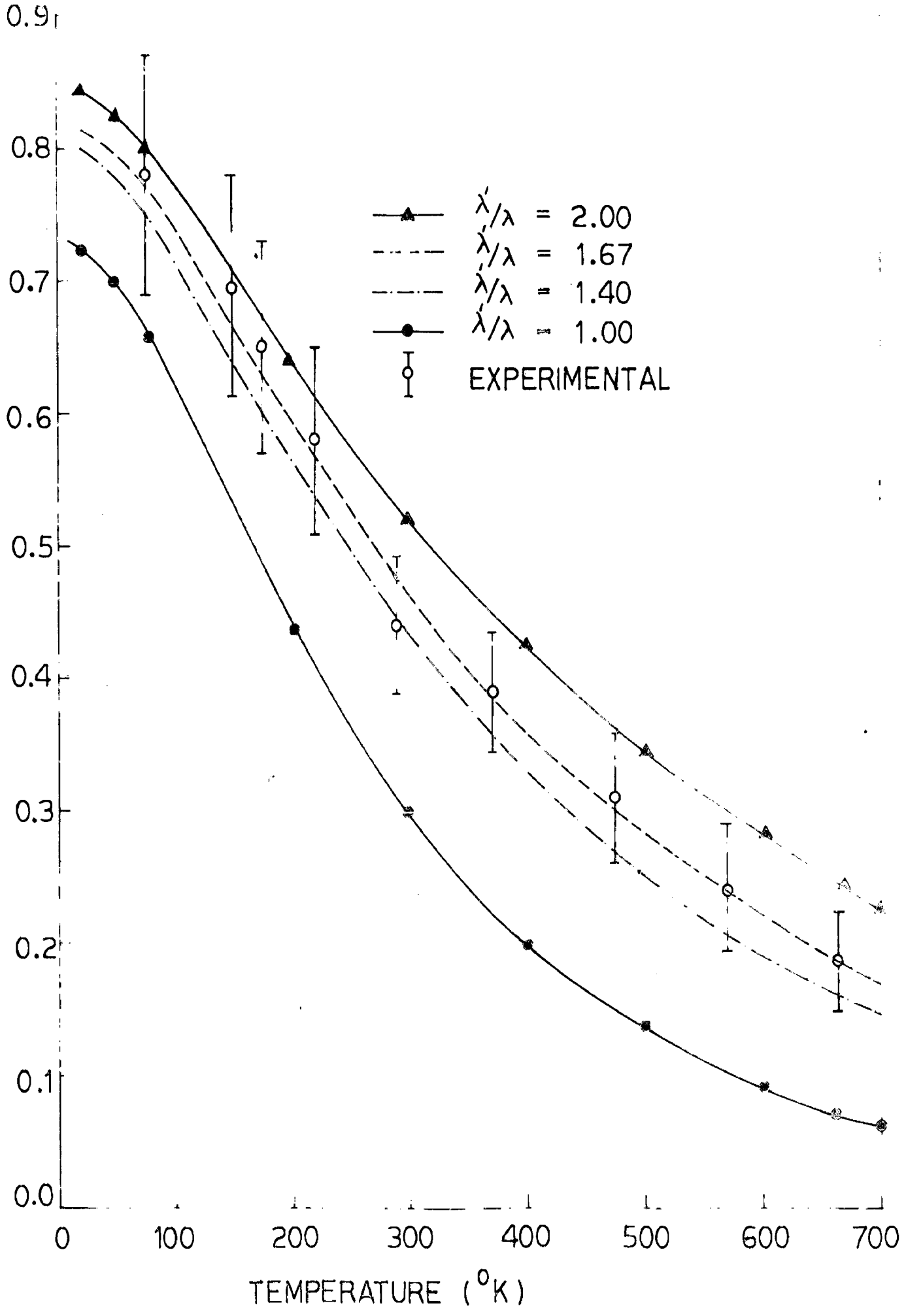
0.9
0.8
0.7
0.6
0.5
0.4
0.3
0.2
0.1
0.0
λ'/λ = 2.00
λ'/λ = 1.67
λ'/λ = 1.40
λ'/λ = 1.00
EXPERIMENTAL
0
100
200
300
400
500
600
700
TEMPERATURE (°K)